Order Number 8924894

Development and evaluation of a fluorescence emission ratio-based fiber optic pH measurement system for use in monitoring changes in tumor pH during clinical hyperthermia

McCarthy, John Francis, Ph.D.

University of Illinois at Urbana-Champaign, 1989

U·M·I
300 N. Zeeb Rd.
Ann Arbor, MI 48106

DEVELOPMENT AND EVALUATION OF A FLUORESCENCE EMISSION RATIO BASED FIBER OPTIC pH MEASUREMENT SYSTEM FOR USE IN MONITORING CHANGES IN TUMOR pH DURING CLINICAL HYPERTHERMIA

BY

JOHN FRANCIS MCCARTHY

B. A., Boston University, 1976
M. S., University of Connecticut, 1978

THESIS

Submitted in partial fulfillment of the requirements
for the degree of Doctor of Philosophy in Biophysics
in the Graduate College of the
University of Illinois at Urbana-Champaign, 1989

Urbana, Illinois

UNIVERSITY OF ILLINOIS AT URBANA-CHAMPAIGN

THE GRADUATE COLLEGE

DECEMBER 1988

WE HEREBY RECOMMEND THAT THE THESIS BY

JOHN FRANCIS MCCARTHY

ENTITLED DEVELOPMENT AND EVALUATION OF A FLUORESCENCE EMISSION RATIO BASED FIBER OPTIC pH MEASUREMENT SYSTEM FOR USE IN MONITORING CHANGES IN TUMOR pH DURING CLINICAL HYPERTHERMIA

BE ACCEPTED IN PARTIAL FULFILLMENT OF THE REQUIREMENTS FOR

THE DEGREE OF DOCTOR OF PHILOSOPHY

Director of Thesis Research

Head of Department

Committee on Final Examination†

Chairperson

† Required for doctor's degree but not for master's.

ABSTRACT

The pH of the tumor microenvironment may be important in assessment of response to hyperthermic therapy. Little clinical *in vivo* data is available during such therapy due to the inherent limitations of the microelectrode technique in the presence of a microwave field. A fiber optic pH measurement system, due to its dielectric nature, provides a method for overcoming such limitations. Optrodes sensitive to pH have been studied based on absorption and fluorescence. Absorption based optrodes are difficult to fabricate due to the complex nature of the required optical geometry. Fluorescence based optrodes have been developed based upon either a single emission intensity measurement at a specific wavelength or the ratio of two emission intensities, at the same wavelength, following sequential excitation. Single intensity measurements are prone to substantial errors introduced by differences in the ionic strength and temperature of the samples as well as by fluorophore leakage, photobleaching, and fluctuations in the intensity of the excitation source. The ratio technique minimizes the above sources of measurement error, but the need for a sequential excitation results in instrumentation that may be too complex and expensive for routine use. Using the dual emission pH sensitive fluorophore 1,4-dihydroxyphalonitrile (1,4-DHPN), a simple ratio based optical pH measurement system was constructed. Optrodes were fabricated using glass capillary tubes < 1 mm in diameter with a Cuprophan membrane fixed at one end. The 1,4-DHPN was encapsulated in 4:1 DPPC/DPPG containing LUV in order to limit fluorophore loss and extend the sensor lifetime. A 2 mole percent quantity of gramicidin was added to the lipid phase, during preparation of the LUV, in order to insure rapid equilibration of hydrogen ions across the lipid bilayer. A flashlamp excitation source was used in conjunction with a single optical fiber to excite the fluorophore and to collect its fluorescence. Emission wavelengths of 488 and

434 nm were detected using narrowband interference filters in the optical subsystem. The electronics subsystem was used to electronically process the resultant signals before digitization. Ratios were computed digitally in real time using an Apple 2E microcomputer. This ratio based fiber optic pH measurement was able to to measure pH values in the 6.5-7.5 range with a standard deviation of better than 0.1 pH unit. Over this range a maximum standard deviation of 0.007 pH units / °C was measured. The time constant of these optrodes was determined to be 3.2 minutes when measured in 305 mOsm phosphate buffer. The time constant in whole blood increased to 10.0 minutes due to a decrease in the hydrogen ion permeability of the LUV membrane. This is most likely due to the blockage of gramicidin channels by divalent cations in the blood plasma.

ACKNOWLEDGEMENTS

I am deeply grateful for the help of the many people who have assisted me throughout the course of this research project. Without their help an undertaking of this magnitude would not have been possible.

First, I would like to thank my main thesis advisor, Dr. Richard Magin, for his many helpful suggestions during the course of this project. His friendship, patience and encouragement throughout this endeavor helped in easing the burden of an otherwise formidable task. I would also like to thank Dr. Floyd Dunn for his guidance and help in overcoming many of the problems associated with the completion of this thesis.

I am grateful to Dr. Enrico Gratton for the use of his fluorescence laboratory as well as his many helpful technical discussions. Several of the experiments and ideas discussed in this thesis have come about as consequence of these discussions.

The help of several of my fellow students Tom White, Kevin Ehlert, Jay Alameda, and Francis Jatico was indispensable in completing this research project. Tom's theoretical noise study and Kevin's prototype hardware and software helped establish the foundation upon which the current system is built. Jay's expertise and help in preparing liposomes played a significant role in the successful fabrication of a practical sensor. Francis was directly responsible for acquiring much of the sensor data presented in this thesis.

I would like to extend a sincere note of thanks to several members of the Bioacoustics Research Laboratory for their contributions to this research project. Without the expert technical assistance provided by Joe Cobb and Bob Cicone much of this thesis would not have been possible. I am especially grateful to Billy McNeill for his help in turning many crude ideas and sketches into workable systems. His mechanical expertise was instrumental in making the optical subsystem a reality. A

special thanks is extended to Wanda for her help in getting this manuscript into final form. Her dedication and experience made this task far easier than it otherwise might have been.

Finally, I would like to thank the countless other faculty, staff, students and friends who have assisted me in some fashion during either the research or preparation phase of this thesis.

TABLE OF CONTENTS

CHAPTER		PAGE
1	INTRODUCTION	1
2	BACKGROUND	5
	2.1. Hyperthermia	5
	2.1.1. Introduction	5
	2.1.2. Cellular Mechanisms of Heat Injury	6
	2.1.3. Biochemical and Physiological Modulating Factor	8
	2.1.3.1. Perfusion	9
	2.1.3.2. pH	10
	2.1.3.3. Oxygen Level	13
	2.1.3.4. Nutrient Levels and Metabolism	14
	2.2. Fiber Optic Chemical Sensors	16
	2.2.1. Introduction	16
	2.2.2. pH Sensors	17
3	PHYSICAL CHEMICAL STUDIES OF 1,4-DHPN	21
	3.1. Introduction	21
	3.2. Potentiometric Titration	25
	3.2.1. Procedure	25
	3.2.2. Results and Discussion	25
	3.3. Ultraviolet and Visible Absorption Measurements	27
	3.3.1. Procedure	27
	3.3.2. Results and Discussion	28

3.4. Fluorescence Measurements 29
3.4.1. Lifetime 29
3.4.1.1. Procedure 29
3.4.1.2. Results and Discussion 29
3.4.2. Excitation and Emission 33
3.4.2.1. Procedure 33
3.4.2.2. Results and Discussion 33
3.5. Conclusions 36
4 INSTRUMENT DESIGN 54
4.1. Introduction 54
4.2. Overall System Design 56
4.3. Excitation Source 58
4.4. Optical Subsystems 60
4.5. Photodetectors 61
4.6. Electronics Subsystem 63
4.7. Software 65
5 INSTRUMENT PERFORMANCE 90
5.1. Introduction 90
5.2. Subsystem Evaluation 91
5.2.1. Excitation Source 91
5.2.1.1. Procedure 91
5.2.1.2. Results and Discussion 92
5.2.2. Optics 93
5.2.2.1. Procedure 93
5.2.2.2. Results and Discussion 94

5.2.3. Photodetectors 95
5.2.3.1. Procedure 95
5.2.3.2. Results and Discussion 95
5.2.4. Electronics 96
5.2.4.1. Procedure 96
5.2.4.2. Results and Discussion 97
5.2.5. Conclusion 97
5.3. Measurement System Evaluation 98
5.3.1. Solution Studies 98
5.3.1.1. Procedure 98
5.3.1.2. Results and Discussion 100
5.3.2. Optrode Studies 106
5.3.2.1. Procedure 106
5.3.2.2. Results and Discussion 107
5.3.3. Conclusion 115
5.4. Animal Testing 116
5.4.1. Procedure 116
5.4.2. Results and Discussion 116
5.4.3. Conclusion 118
6 SUMMARY AND RECOMMENDATIONS FOR FURTHER STUDY ... 150
APPENDIX A PHYSICAL CONTROL LINE CONNECTIONS 155
APPENDIX B SYSTEM INITIALIZATION PROGRAMS 156
APPENDIX C APPLESOFT BASIC CONTROL PROGRAM 157
APPENDIX D ASSEMBLY (6502) CONTROL PROGRAM 182
BIBLIOGRAPHY 221
VITA 230

CHAPTER 1
INTRODUCTION

The effects of elevated temperatures on physiological functions has fascinated researchers for many years [55]. The history of mammalian hyperthermia (temperatures ≥ 42 °C) as a means of treating malignant disease can be traced back several centuries [78]. Recently, there has been a revival of interest in the the use of hyperthermia as a clinical modality in the treatment of certain types of malignant tumors [41]. This has been primarily due to advent of new heating methods which make the induction of elevated temperatures, either locally or over the whole body, clinical feasible.

Today, the three physical modalities that are most often employed for power deposition in local and regional clinical hyperthermia are ultrasound at frequencies of about 0.3-3 MHz, electromagnetic fields at radio frequencies of less than 300 MHz, and electromagnetic radiation at microwave frequencies of 300-2,450 MHz [70]. Use of these physical heating modalities, however, introduce difficulties in the monitoring of tissue parameters during the course of treatment.

Tissue temperature is usually monitored through the use of conventional thermistor or thermocouple probes. While these probes permit accurate data acquisition under normal conditions, interaction between the metallic leads of the probe and the applied electromagnetic field present complications during therapy. These complications result from a current density in the probe leads, as a consequence of an induced electric field along their length [70]. This current density can cause perturbations in different ways.

The electromagnetic field in the surrounding tissue can be perturbed by the reradiated fields from the probe leads. This would lead to nonuniform power deposition in the vicinity of the probe. In addition, probe heating and noise caused

by electromagnetic interference could cause errors in the accuracy and precision of the measurements obtained.

In order to circumvent these type of problems, fiber optic temperature measurement techniques were developed. Fiber optic probes, made of glass or plastic, are dielectric in nature and as such, their interaction with electromagnetic fields is considerably less than that seen with probes of conventional design. All optical temperature probes measure changes in some temperature-dependent interaction with light [70]. In a fluorescence based sensor, light is absorbed and reemitted at longer wavelengths. Many chemical and physical processes can effect the efficiency of optical energy transfer, as well as the observed emission wavelengths. One of the most widely used optical temperature sensors in hyperthermia is a fluorescence sensor made from a mixture of two phosphors [99]. The two phosphors employed have fluorescence intensities that are quenched at widely different temperatures with emission wavelengths that can easily be spectrally separated. A calibration curve, based on the ratio of these two wavelengths as a function of temperature, can be constructed and used to determine unknown temperatures from ratio data. Luxtron Corporation (Mountain View, CA) markets an optical temperature measurement system based on this concept.

As a result of the growth in the use of hyperthermia in cancer therapy, increased interest was generated in defining physiological parameters that could be used as prognostic indicators of response [91]. Such information is necessary in order to develop effective treatment protocols which could be used to optimize the therapeutic potential of hyperthermia.

Many *in vitro* studies and a limited number of *in vivo* studies (Chapter 2), suggest that the tumor microenvironmental values of pH, pO_2, pCO_2 and perfusion may play a significant role in the response tumors to hyperthermia. The pH of the tumor microenvironment has been suggested as a good candidate for a

prognostic factor in predicting the response of tumors to hyperthermia. A decrease in extracellular pH within tumors has been shown to result in hyperthermia sensitization relative to normal tissue [92]. Furthermore, pH not only affects hyperthermic sensitivity but also may be expected to influence the cellular transport, metabolism, and cytotoxicity of chemotherapeutic drugs [31].

To date, limited data has been obtained on the *in vivo* correlation between tumor pH and hyperthermic response. Furthermore, no data exists on the dynamic pH response of tumors to induced clinical hyperthermia using current heating techniques. This situation is principally due to the lack of suitable pH measurement techniques and instrumentation.

Nearly all *in vivo* measurements of tumor pH have been made with microelectrodes. Due to the electrical nature of this measurement technique, it suffers from the same difficulties as conventional thermometry when used in an applied electromagnetic field. For this reason, clinical measurements of tumor pH are performed, before and after therapy only, by removal and reinsertion of the microelectrode using an in-dwelling catheter. This technique precludes the acquisition of dynamic pH data. Such data has only been obtained during water bath heating experiments [82]. Furthermore, such techniques make exact relocation of the microelectrode difficult, so the two measurements may not be obtained from the same location. Given the heterogeneous pH distribution found within tumors (Chapter 2), large errors in pH measurement and subsequent data interpretation could result.

In order to help overcome the above difficulties, the development of a fiber optic, fluorescence emission ratio based pH measurement system was undertaken. The pH sensor was developed and evaluated using solutions of fluorophore dissolved in buffers at various values of pH. Suitability of both the measurement system and fluorophore, for use within the temperature range employed in clinical

hyperthermia, was demonstrated. In addition, miniature optical sensors, suitable for *in vivo* use with minimum tissue destruction, were developed and tested. Finally, the ability of both the sensors and measurement system to make accurate and precise pH measurements, in a physiologically relevant medium, was demonstrated.

Through the use of optical measurement techniques, for monitoring important hyperthermic parameters during therapy, planning and control of an optimal treatment strategy for a given tumor should one day be possible.

CHAPTER 2
BACKGROUND

2.1. Hyperthermia

2.1.1. Introduction

Many studies, some of which go back at least 100 years, have suggested that intrinsic differences in survival occur between normal and neoplastic cells when treated at hyperthermic temperatures [15, 88, 90, 91]. However, Hahn [38] concludes that although studies demonstrating increased heat sensitivity of malignant cells clearly exist, there are enough contradictory reports to suggest that this sensitivity is not a general characteristic of all malignant cells. In some *in vitro* studies, either no difference in heat sensitivity between normal and neoplastic cells was found, or neoplastic cells were found to be more heat resistant. In the older literature the data obtained were from experiments in which the assay procedures used, such as dye exclusion or morphological criteria, are no longer considered reliable. Thus, it is not surprising that earlier studies produced results that were extremely variable. In more recent experiments, the diversity of results obtained are more difficult to explain. Using *in vitro* studies, Chen and Heidelberger [16] clearly showed that mouse prostate cells, on being transformed by carcinogenic hydrocarbons, acquired a pronounced heat sensitivity. On the other hand, Harisiadis [42] compared survival of "normal" liver cells *in vitro* with those from a closely associated hepatoma. The hepatoma cells were found to be slightly more resistant to heat than normal liver cells.

With respect to *in vivo* studies, a slightly different picture appears. In early *in vivo* studies Overgaard [68] observed that hyperthermic exposures between 41.5 and 43.5 °C caused little histological damage in normal mouse mammary tissue, but

resulted in severe damage to mammary carcinoma tissue. However, Sapareto [78] has pointed out that temperature differences between tumor and adjacent normal tissue complicate the interpretation of this study.

Kang [49] has studied the response of SCK mammary adenocarcinoma, growing subcutaneously in the leg of A/J mice, to both *in vivo* and *in vitro* hyperthermia. He found that the number of clonogenic cells in tumors excised immediately after heating was significantly less than that in the *in vitro* culture treated with the same heat doses. This result suggests that factors in the tumor microenvironment may play an important role in modulating the effects of *in vivo* heat treatment.

Despite the lack of convincing evidence that neoplastic cells are intrinsically more sensitive to heat than normal cells *in vitro*, Song [85] suggests that clinical experience as well as studies with animal tumors would indicate that tumors are more heat sensitive than normal tissue *in vivo*.

To understand why *in vivo* results do not always agree with *in vitro* observations, it is necessary to study the mechanisms of heat injury, and their potential for modulation by physiological and biochemical factors present in the tumor microenvironment [9].

2.1.2. Cellular Mechanisms of Heat Injury

Due to the ubiquitous nature of heating effects on cellular components, as well as on physiological and biochemical variables, its is impossible to establish a single mechanism for all heated induced cell injury. According to Sapareto [78], three major mechanisms of heat injury at the cellular level have been proposed.

The first mechanism involves a direct effect on the cell membrane, changing its permeability, composition or fluidity, and ultimately leading to the death of the cell. In Chinese hamster ovary (CHO) cells, hyperthermia inhibits thymidine uptake

by facilitated diffusion [7]. Also, heat causes the plasma membrane to become permeable to polyamines, such as putrescine, spermidine, and spermine [32, 59]. Heat effects on membrane fluidity have been implicated by the observed interaction of heat with membrane modifying drugs. Both alcohols [57] and local anesthetics [102] have been shown to cause increased sensitivity to heat. As far as membrane composition is concerned, Cress [19] has shown an inverse relationship between cholesterol to phospholipid ratio and heat sensitivity. Evidence against the membrane hypothesis is that activation energies for most types of membrane damage are low. For example, the activation energy required to induce permeability changes is 20 kcal/mol for ascites tumor cell membranes, and the activation energy for loss of adenyl cyclase activity is 27 kcal/mol [81]. These values are far lower than the observed activation energies for cell killing of 150 and 300 kcal/mol above and below 43 °C, respectively. Another argument against membrane damage being solely responsible for heat induced cell death is that membrane turnover and replacement occurs to a greater extent in plateau phase cells, which have been found to be more heat sensitive than in exponentially growing cells.

The second mechanism of cellular heat injury was suggested by the histological observations of Overgaard [67]. These observations show an increase in lysosomes in the cellular cytoplasm after heat exposure. It has been suggested that disintegration or damage of these lysosome vesicles may release digestive enzymes leading to cellular death. Biochemical evidence of increased lysosomal enzyme activity during hyperthermia by several investigators [45, 69] lends support to this theory. However, because lysosomes are involved in the destruction of dead cells, this evidence may reflect tissue response to other physiological changes caused by heat, and thus be a secondary effect of cell death. Evidence against the lysosome

theory is the observation that agents which modify lysosomal membranes (trypan blue, retinol, and hydrocortisone) did not affect heat induced cell killing [44].

The third mechanism for cellular heat injury involves thermal damage to proteins. The evidence for the idea that protein denaturation is involved in cell killing is that the activation enthalpy for cell killing above 45 °C is 150 kcal/mol, which is similar to that observed for protein denaturation. Several investigators implicate heat in affecting a number of protein functions such as DNA synthesis, RNA synthesis, protein synthesis, and respiration. However, Roti-Roti [76] maintains that the protein denaturation hypothesis is untestable unless the proteins responsible for cell killing are specified.

A possible fourth mechanism of heat injury, at the nuclear level, has also been suggested. Tomasovic [93] and Roti-Roti [76] both have reported an increased, nonspecific attachment of nonhistone nuclear proteins to DNA following hyperthermia. They have subsequently demonstrated that this increased chromatin protein mass impairs chromatin function and is also highly correlated with heat induced cell killing.

2.1.3. Biochemical and Physiological Modulating Factors

Regardless of the actual mechanisms involved in heat induced cell killing, from the differences observed between *in vitro* and *in vivo* studies, it is reasonable to postulate the existence of physiological and biochemical factors in the tumor microenvironment which modulate the underlying mechanisms in ways that result in increase thermal sensitivity. Current research has found at least four significant factors which modify cellular heat response. These factors are perfusion, pH, oxygen consumption, and nutrient or metabolic levels. However, in spite of the importance of these factors for clinical hyperthermia, little *in vivo* information is

available about either their temporal or spatial variation, their relationship to one another, or their relationship to any of the previously proposed mechanisms.

2.1.3.1. Perfusion

Tumor blood flow, or perfusion, is emerging as the major mediator in tumor response to heat, since it governs not only the local tumor environment (nutrient supply, oxygen level, pH) but is also the key link in the host-tumor relationship [23]. While tumor blood flow is influenced by heat, it is also affected by the local tumor microenvironment. Constituents of the microenvironment that are influenced by blood flow have in turn been found to exert some degree of reciprocal control on the flow itself. Thus, it could well be that a tumor's blood flow response to heating could be a secondary manifestation of a more direct effect on a primary microenvironmental variable.

There is considerable controversy about whether or not the blood perfusion of tumors is greater than that of normal tissue under normothermic conditions. The flow response to hyperthermic conditions in both tissues is even more controversial. LeVeen [56] states that tumor blood flow from surgically excised material was 2-15% of normal tissue. On the other hand, Bierman [13] found that in 12 patients with metastatic, neoplastic lesions, the blood flow through the tumors was greater than that through normal tissue. Song [86] concludes that tumor blood flow varies significantly depending on the type, age, and size of the tumors. He also concludes that due to the heterogeneous distribution of perfusion in tumors, blood flow may or may not be greater than the surrounding tissues at normothermic temperatures. At hyperthermic temperatures, Song [86] found that tumor blood flow either remains unchanged or increases less than a factor of two, when heated at 41-43 °C. In contrast he found that the blood flow to normal tissue increase by a factor of 3-20 on heating at 42-45 °C. Meanwhile, Bicher [10] found that a rise in

temperature up to 41 °C leads to a significant increase in tumor blood flow, while a further rise in temperature up to 42 °C results in a marked breakdown of this flow to below the initial value. He also found similar results for normal tissue, however, the break point occurs at a much higher temperature (approximately 46 °C).

The actual mechanisms responsible for the variations in tumor blood flow observed during hyperthermia remain the subject of much controversy. Virtually all the blood flow measurements that have been done to date either measure blood flow at a single point or measure average blood flow rate throughout the tumor. Hahn [39] has pointed out that the inherent biological variability and heterogeneity of tumors make the description of blood flow rates by one number not very meaningful. To characterize the role of blood flow during hyperthermia, a means of determining its temporal and spatial variation must be found. Since blood flow is responsible for almost all convective heat transfer in tissue, its importance in the development of successful hyperthermia treatment planning is clear.

2.1.3.2. pH

There is now a large amount of evidence [92] indicating that exposure of cells *in vitro* to a low pH environment sensitizes them to hyperthermia. It has also been established that the intratumor environment is acidic relative to normal tissue and that its pH further decreases during hyperthermic treatment [83].

Most of the *in vitro* studies in this area were carried out by Gerweck and Overgaard. Gerweck [29] showed that the pH sensitizing effect took place over a temperature range of 41-44 °C and increased with decreasing pH; the effect was particularly pronounced at 42 °C and became less evident at 43 and 44 °C. Gerweck [30] also found that maintaining tissue culture cells at low pH after heating increased the cytocidal effects of hyperthermia and inhibited the onset of thermal tolerance. Overgaard [65, 66] studied the ability of L182 ascities tumor cells

suspensions, heated *in vitro* at 42.5 °C for 60 minutes at either pH 7.2 or 6.4, to form tumors when injected into mice immediately after the incubation period. He found that cells that had been heated at pH 7.2 were able to form tumors in 100% of the hosts, while those heated at pH 6.4 were incapable of initiating tumors. The major change occurred between pH values of 7.2 and 7.0 where the percentage of successful tumor growths was reduced from 100 to 33%. Overgaard also found on ultrastructural examination that the number of cells having lesions in their plasma membranes, as well as those showing increased lysosomal activity, increased when heating and incubation took place at low values of pH.

Dickson and Calderwood [23] measured the extracellular pH values both in tumors and in normal tissue. They found the extracellular pH range for tumors (7.19-6.99) to be slightly lower than that for normal liver (7.32) or normal muscle (7.21). Several other studies have also shown that the extracellular pH of tumors is consistently lower than that of normal tissue. However, Bicher [10] has shown that, as in blood flow, extracellular pH values differed considerably between different parts of tumors. The data of Eden et al. [25] indicate that hydrogen ion concentration in some areas of tumors may be more than 10 times those in areas of neutral pH.

The effective of hyperthermia on pH has been studied by several investigators. Song [82] observed that the pH in control SCK tumors of mice was 7.05. On heating at 43.5 °C, it temporarily increased and then rapidly decreased reaching 6.67 at the end of 30 minutes of heating. When the heating was terminated, the pH rose to 6.78, but it decreased to 6.5-6.6 when the tumors were heated again. He also found similar decreases in pH in Walker tumor 256 heated at 43 or 46 °C. However contrary to the behavior of tumor pH, the pH in the muscle tissue of rats increased when heated at temperatures up to 46 °C, but decreased at temperatures above 46 °C. Bicher [10] reported extracellular pH decreases in human tumors of

0.5 to 1 unit at temperatures above 42 °C. It seems that the extracellular pH change observed after heating varies according to tumor type and heating conditions. In general, the higher the temperature and the longer the heating the greater the decrease in tumor pH.

The cause of the extracellular decrease in tumor pH during hyperthermia is not clear. Changes in blood flow and oxygen level have been suggested. Also, changes in nutrient level and a metabolic shift to a higher level of glycolytic activity may cause lactic acid accumulation resulting in decreased extracellular pH. Von Ardenne [95] found that hyperglycemia by itself selectively reduces tumor pH to near 6.0 while heating further reduces the pH. The influence of blood flow and other microenvironmental changes on pH has yet to be unravelled. Song [82], while measuring temporal variation in pH and temperature, did not measure simultaneous temporal variations in blood flow. His use of average blood flow measurements did not allow him to resolve the issue of whether changes in blood flow caused the observed changes in pH or whether the change in pH was the dominant factor in modifying blood flow. Bicher [10] , while able to measure blood flow, pH, and temperature simultaneously with some degree of temporal resolution, did not use a hyperthermic range of temperatures for those measurements (< 40 °C). Also, his failure to measure the simultaneous spatial variation of these variables made it impossible to determine their relationship to each other, given the known heterogeneity of tumor microenvironments.

From a clinical perspective a knowledge of extracellular pH and the ability to modulate it are extremely important. Hahn et al. [40] have demonstrated the enhanced cytotoxicity of some chemotherapeutic drugs in regions of decreased extracellular pH. Knowledge of the relationship between blood flow and pH may allow for selective modulation of the appropriate factors, during hyperthermia, in order to achieve maximal therapeutic effect.

2.1.3.3. Oxygen Level

Most reports in the literature indicate that *in vitro* hypoxic cells are as sensitive or more sensitive to heat when compared to oxic cells. The early reports of Hahn [37] on the response of CHO cells to heating at 43 °C found survival to be independent of the presence or absence of oxygen during heating. Bass [8] found a slight protective effect of hypoxia against the killing of HeLa cells exposed to 43 °C. Kim [50] found that oxygen depleted HeLa cells were appreciably more heat sensitive than their well oxygenated counterparts. Hahn [38] points out that since the roles of pH and nutritional factors were not appreciated at the time of these experiments, the response of the cells may not be simply the result of their hypoxia but may be due to a combination of factors. In fact, Adams et al. [2] found that cells cultured in suspension at pH 7.4 show substantial heat resistance in air after chronic exposure to hypoxia. These results cast some doubt on the concept of hypoxia enhanced heat sensitivity *in vitro*.

There is no data directly linking hypoxia with thermal sensitivity *in vivo*, although there is a considerable body of indirect evidence. Crile [20] and Suit [89] found that clamping the tumor blood supply increases thermosensitivity, and this sensitizing effect increases with the duration of clamping before heating. This seems to indicate that chronic hypoxia is more important than acute hypoxia in gaining increased thermosensitivity. However, Dickson et al. [23] point out that increased heat sensitivity with duration of clamping indicates that the effect involves more than just increased uniformity of heating or decreased oxygen levels. Nutrient level, pH, catabolite level, and other biochemical parameters may be altered. During hyperthermia, Bicher [10] has shown that tumor pO_2 closely follows changes in tissue temperature. The response is very fast , with tumor pO_2 increasing shortly after the rise in temperature and then decreasing as the tumor

cools off. This effect was always seen when heating took place below 41 °C. At higher temperatures, there was an initial increase in tumor pO_2 which was followed by a decrease to low levels as the temperature was held constant at 46 °C. The same pattern of pO_2 variations was found when normal tissue was heated, only the temperature of pO_2 fall off was always significantly lower in tumors. A strong correlation between decreases in tumor pO_2 and blood flow was found as the temperature was increased to 45 °C. Furthermore, Bicher noted widely differing values of pO_2 even within a single tumor [11].

When hyperthermia is used as an adjuvant to radiotherapy, the tumor pO_2 could be a major factor in determining the outcome of this treatment. It is well known that oxygen sensitizes cells to radiation. If hypoxic cells are truly more sensitive to heat, then the ability to modulate tumor pO_2 may have significant impact in treatment planning when using these combined modalities. To resolve this question, however, the relationship of pO_2 to blood flow, pH, and nutrient level must first be established.

2.1.3.4. Nutrient Levels and Metabolism

Several investigators have postulated that low levels of nutrients found in the microenvironment of many tumors, as a result of their low levels of perfusion, aid in increasing their thermosensitivity. Warburg [46] demonstrated that unlike normal cells, malignant cells are generally capable of aerobic glycolysis and thus use glucose at a rapid rate. He also demonstrated that lactic acid production by malignant cells, contrary to normal cells, increases as a function of extracellular glucose concentration. These facts led Von Ardenne et al. [38] to speculate that glucose infusions could lead to hyperacidification of tumors with a resultant increased thermosensitivity. Other researchers, such as Song [84] demonstrated by use of 5-thio-D-glucose, an inhibitor of glycolysis, that since hypoxic cells depend

on glycolytic pathways for energy metabolism, the increased cytotoxicity seen in hypoxic versus oxic cells in this experiment was not due to glucose deprivation alone but due to a complex interrelationship between the availability of both oxygen and glucose. Kim [51] showed that the selective effect of this glucose analogue on hypoxic cells was greatly magnified at elevated temperatures. In these studies, however, no data on extracellular pH were presented.

Thus, again evidence is seen of the complex interrelationship of one microenvironmental variable with others. It should also be noted that Song (unpublished results) suggests that insufficient nutrient levels, along with decreased pH, may also be a contributing factor to the reduced thermotolerance seen in heated tumors *in vivo*, but he is unable to separate their combined influences.

There is considerable controversy regarding the effect of hyperthermia on metabolism. This is partly due to the fact that metabolism is once again regulated by two microenvironmental variables, pH and pO_2. Mondovi [59] reported a decrease of the respiration rate when Novikoff hepatoma cells were incubated at 38 °C with glucose and succinate after a preincubation of 3.5 hours at 43 °C. Glycolysis was only slightly reduced under the same conditions. However, no effect was observed when the assay and preincubation were performed without oxygen. Dickson et al. [24] investigated the metabolism of Yoshida sarcoma in rats. They found that heating of the tumor for 1 hour at 40 °C had no influence on the respiration or on anaerobic glycolysis, both measured *in vitro* at 38 °C. However, after preincubation of the tumors *in situ* at 42 °C, both parameters were depressed, with a greater depression for aerobic glycolysis. Furthermore, if the rats were made hyperglycemic by glucose injections given before hyperthermia, than even a temperature of 40 °C caused a marked inhibition especially on aerobic glycolysis. Extracellular pH decreased after glucose loading but the correlation between lactate accumulation and decrease of extracellular pH was poor. These results are at odds

with the theory of Song. Streffer [87] measured glycolytic metabolites in liver and in transplanted adenocarcinoma E0771 in mice after heat treatment. He found that both respiration and glycolysis were enhanced during hyperthermia but decreased immediately afterwards. Furthermore, he found that lactate was only slightly increased whereas two acidic metabolites, acetoacetate and B-hydroxybutyrate were increased considerably. However, if the hyperthermic treatment was combined with a glucose load given before hyperthermic exposure, an increase in lactate accumulation was observed. These findings do not agree with those of the similar glucose loading experiments of Dickson et al. [24] previously mentioned.

Again many widely varying and confusing findings have been reported. As in the past, much of this variability can probably be attributed to significant differences in the state of the experimental tissues used. Only when the complete state of the cellular system is known, can any valid conclusions be drawn regarding the possibility of metabolically or nutritionally modulating cellular heat response for more effective therapy. One step in this direction lies in the development of fiber optic sensors to measure the microenvironmental variables of interest during actual clinical hyperthermic treatments.

2.2. Fiber Optic Chemical Sensors

2.2.1. Introduction

Early fiber optic sensors relied on the physical property of the medium being sampled to cause a change in the light transmitting properties of the optical fiber. By using such methods, acceleration, strain, position, magnetic field, and other physical properties could be monitored [4]. Later, optical transducers were used at the distal end of an optical fiber to provide enhanced sensitivity or chemical specificity. These optical transducers (optrodes) were classified as physical

(responding to such parameters as temperature and pressure) or chemical (responding to chemical concentration), depending on what was being measured [4]. All chemical optrodes involve a reagent phase coupled to an optical fiber, and measure concentrations through a change in the optical properties of the reagent [63]. Light from a suitable source travels along an excitation fiber and is returned from the reagent phase by either scattering or luminescence stimulated by the excitation source. Either the same or different fibers can be used to collect and transmit the returned optical signal to an appropriate photodetector.

According to Angel [4], optical sensors have many advantages over the use of potentiometric electrodes. These include electromagnetic immunity, low cost, small physical size, physical separation of the sample and the instrument, and the ability to easily multiplex many sensors to a central instrument. In addition, optrodes are not as sensitive to surface contamination because they respond to actual concentrations rather than concentration gradients.

Several disadvantages of fiber optic chemical sensors have also been noted [63]. Since ambient light will interfere with the sensors, they must be used in the dark or the optical signal must be modulated. In addition, the response time of such sensors is limited by the necessity of a mass-transfer step before a constant response can be reached. The limited dynamic range of most chemical sensors also tends to limit their applicability.

2.2.2. pH Sensors

Fiber optic pH sensors have principally been developed for biomedical or biological applications. Consequently, the pH range of such sensors always includes the physiological range (7.0-7.5) [79]. All fiber optic pH sensors developed to date have used a pH sensitive indicator dye immobilized on a solid support matrix which is then affixed in some fashion maner to the end of an optical fiber. In most cases a

semipermeable membrane is used to prevent dye leakage and allow for easy diffusion of hydrogen ions into the dye matrix. Both absorption and fluorescence techniques have been used to monitor the pH dependent behavior of these dyes.

Recently, techniques have been developed which allow the indicator dye to be directly fixed to the fiber end surface rather than to a solid support [61]. This improvement has resulted in further probe miniaturization, reduction in response time, since the membrane envelope is no longer necessary, and high mechanical stability.

Since pH is defined in terms of activity, while optical techniques measure the number of molecules (i.e. concentration), significant errors can occur in the optical measurement of pH if the matrix of the sample differs substantially from that of the calibration solution [48]. The solute-solvent and solute-solute interactions, which determine the value of activity, show up as second-order effects which are frequently ignored [47]. Unfortunately, this omission can only be tolerated for very dilute aqueous solutions where the activity coefficients tend to unity. In real measurement situations, the effect of ionic strength differences on the indicator dye must be taken into account in arriving at the correct value of pH for an unknown sample.

The first fiber optic pH sensor was developed by Peterson [73]. This sensor was based on the spectral changes of the indicator phenol red with pH. This indicator dye was immobilized on polyacrylamide microspheres (5-10 μm in diameter) which contain small light scattering polystyrene microspheres (approximately 1 μm in diameter). These microspheres are confined to the tip of the optical fiber by using hydrogen ion permeable cellulose dialysis tubing. Light of wavelengths 558 and 600 nm is used. The 558 nm light signal is a function of pH, while the 600 nm light serves as a pH independent reference signal. This probe can measure pH in the physiological 6.8-7.4 range. It had an accuracy and precision of

±0.01 pH unit and a temperature coefficient of 0.017 pH units / °C. This probe had a reported diameter of about 0.4 mm, a length of 3 mm and a time constant of approximately 0.7 minutes. A significant dependence of the pH response on the ionic strength of the sample was noted for this sensor.

The first fluorescence based fiber optic pH sensor was developed by Saari and Seitz [77]. It was based on fluoresceinamine immobililized on cellulose or porous glass. Excitation was at 480 nm with a single wavelength fluorescent emission measured at 520 nm. The working pH range of this sensor was 3-6. A bifurcated optical fiber was used for making the optical measurements. Steady state fluorescent response was achieved by this sensor in about 15-30 seconds. The accuracy and precision of this sensor are not good. This is mainly due to a poor SNR resulting from a reduction in the fluorescence signal intensity as a consequence of the dye immobilization procedure employed. In addition, high levels of background signal, as a result of light scattering by the substrate, caused further degradation of the SNR.

More recently the development of a fluorescence sensor for quantifying pH values in the 6.5-8.5 range has been based upon the electrostatic immobilization of the trisodium salt of 8-hydroxyl-1,3,6-pyrene trisulfonic acid (HOPSA) on an anion exchange membrane [103]. A bifurcated optical fiber was again employed. The pH values were obtained from the ratio of two fluorescent emissions measured at 520 nm following a sequential excitation at wavelengths of 405 and 470 nm. For a pH change from 6 to 8, the measured response time was 2 minutes and the standard deviation of the final pH was ±0.03 units. A temperature coefficient of 1.1% / °C was measured. No measurable influence on the calculated pH by the ionic strength of the sample could be observed while using this sensor.

Lastly, a fluorescence sensor for pH in the 6.4-7.7 range was recently developed based upon the glass-immobilized fluorescent pH indicators

1-hydroxypyren-3,6,8-trisulphonate (HPTS) and 7-hydroxycoumarin-3-carboxylic acid (HCC) [64]. Again a bifurcated optical fiber was used. However in this study, only single excitation and emission wavelengths were employed due to the complexity of the instrumentation required for the sequential wavelength excitation method. Analytical excitation and emission wavelengths were, respectively 410 and 455 nm for the HCC-based sensor, and 465 and 520 nm for the HPTS-based sensor. These sensors were reported to have a precision of ±0.01 unit and a response time in the order of 1 minute. Effects of ionic strengths on the optically determined pH values were small.

With the introduction of the pH sensitive dual emission fluorophore 1,4-dihydroxyphalonitrile (1,4-DHPN), an optical pH measurement system can be built in order to take advantage of the benefits of the dual wavelength ratio technique, without the additional complexity of the instrumentation usually associated with this method. Furthermore, since only a single broad band excitation is required, simultaneous acquisition of the fluorescence emission intensities adds to the short term stability and precision of this technique.

The research effort described in the following chapters focuses on the development and evaluation of a fluorescence emission ratio based fiber optic pH measurement system utilizing the above technique. This system was designed specifically for use in monitoring changes in tumor pH during clinical hyperthermia.

CHAPTER 3
PHYSICAL CHEMICAL STUDIES OF 1,4-DHPN

3.1. Introduction

In fabricating a simple pH sensitive optrode, it is desirable to use the same optical fiber for both exciting the fluorophore and collecting its fluorescence emissions. This single fiber design simplifies instrument development by avoiding the difficulties associated with multiple fiber alignment at the sensor interface. Reduction in overall size and bulk of the resulting optrode is also achieved by using this type of design. With such an optrode, fluorescence emission spectroscopy following a single excitation offers many of the same advantages for optical sensors that it does for flow cytometry.

Due to the similarity in requirements of fluorophores for both optical sensors and flow cytometry, 1,4-DHPN was chosen as the pH sensitive component of the optrode. Further studies of 1,4-DHPN were undertaken to both confirm and extend the existing base of knowledge with regard to the physical chemical properties of this compound. In particular, studies designed to measure the pK values of 1,4-DHPN were carried out and the sensitivity of several physical chemical properties of this compound to shifts in both pH and temperature were examined. Finally, consideration was given to the variety of ways in which this compound might be used for measuring pH. The advantages and disadvantages of each of these techniques, with regard to optical sensor design, is discussed.

The pH sensitive fluorescent probe 1,4-dihydroxyphalonitrile (1,4-DHPN), also known as 2,3-dicyano-1,4-hydroquinone, was purchased from Molecular Probes, Inc. (Eugene, OR), and forms the core of the proposed pH sensitive optrode.

The chemical forms of this compound (Fig. 3.1) in solution are dependent upon the pH of the solution with respect to the pK values of the fluorophore. Since the optical properties of each form are distinct, several spectroscopic techniques may be used to discern the fractional contribution of each form to the chemical characteristic being measured, and thus uniquely determine the pH of the solution under a standard set of conditions.

Until recently, the acid-base properties of hydroquinones, especially cyano-substituted hydroquinones, have received relatively little attention. Since the purpose of any spectroscopic probe is to be able to discover information about its surroundings from a study of the properties of its absorption or emission, it is essential that a thorough knowledge of the properties of the isolated probe be acquired. Only then can alterations in its spectroscopic behavior, caused by the properties of a new environment, be analyzed with certainty.

The fluorescent probe 1,4-DHPN can be prepared by the addition of two moles of hydrogen cyanide to one mole of benzoquinone, followed by recrystallization from distilled water [18]. This results in a yellow leaf shaped crystal with a molecular weight of 160.16 Daltons and a melting point of 230 °C. These crystals are very soluble in ethyl alcohol or diethyl ether and only slightly soluble in water, benzene, and chloroform [96]. Since hydroquinones are highly conjugated structures, they are rather closely balanced energetically against the corresponding quinones [60]. This results in a ready interconversion of 2,3-dicyano-1,4-hydroquinone to 2,3-dicyano-1,4-benzoquinone in the presence of molecular oxygen (Fig. 3.2). This process is made apparent by a change in color of the solution of 1,4-DHPN from pale yellow to rust brown and occurs over the course of several days, at room temperature. Changes in both absorbance and fluorescence have also been noted during the course of this interconversion.

The acid-base and spectroscopic properties of 1,4-DHPN were first measured in 1977 by Brown et al.[14]. Absorption spectra of 1,4-DHPN solutions between pH 10.0 and pH 3.5 were analyzed as a sum of contributions from three species with two equilibria. From this analysis, pK values of 8.0 ±0.2 (dianion/monanion equilibrium) and 5.5±0.3 (monoanion/neutral species equilibrium) were obtained. The absorption maximum for the three species involved were found to occur at 405 nm for the dianion, 380 nm for the anion, and 345 nm for the neutral species.

The fluorescence lifetime and emission properties of 1,4-DHPN were also measured by Brown et al. Lifetime measurements were made using single-photon counting and were evaluated by computer convolution. Lifetimes of 7.7 ns for the dianion, 10.0 ns for the anion, and 14.0 ns for the neutral species were obtained. Computer convolution of the emission spectra at various values of pH yielded emission maxima of 480 nm for the dianion, 450 nm for the anion, and 400 nm for the neutral species.

The first biophysical utilization of 1,4-DHPN did not occur until 1981 when Valet [94] realized its unique potential for determination of the pH of single cells in flow cytometry. Most fluorescent pH indicators, including fluorescein, have maximum emission at a fixed wavelength with an intensity that is pH dependent. This makes a sequential dual-wavelength excitation necessary for reliable pH determination with such indicators. The disadvantage of this sequential method is that it allows only the mean pH value of a cell suspension to be determined by flow cytometry, since the measurement of the pH of any single cell would require two passes of that same cell through the flow cytometer. Valet was able to measure the pH of individual cells in a flow cytometer by taking advantage of the fact that 1,4-DHPN shows a pH dependent shift of its peak emission wavelength. By using a 300-400 nm broadband excitation, and a simultaneous measurement of the ratio of

fluorescence emission in two distinct bands (420-440 nm and 500-580 nm), he was able to determine the pH of a single cell in a one-step measurement.

In a subsequent study by Kurtz et al. [54], 1,4-DHPN was used in conjunction with a microspectofluorometer to measure the topographical variation of intracellular pH within cultured A6 monolayers derived from toad kidney cells. A broad band excitation from 375-407 nm was used and the 512 nm / 455 nm emission ratio was determined. This ratio was then taken as a gauge of the wavelength of the fluorescence emission maximum, which in turn was a measure of the intracellular pH. Since the two emission intensities were determined simultaneously, Kurtz et al. found that measurements made in this fashion were independent of dye concentration, photobleaching, and intensity fluctuations of the excitation source. All three of these complications introduce measurement errors when sequential excitation spectroscopy was used. Kurtz et al. also established that the value of the ratio obtained was not altered by varying the concentrations of Na^+ (20-130 mM), K^+ (30-130 mM), Ca^{++} (0-1 mM), Mg^{++} (0-1 mM), PO_4^{-3} (0-10 mM), and albumin (0-10 g/l).

In a recent study [62], the physiological pH sensitive indicators 2,3-dicyano-hydroquinone (1,4-DHPN), 4-methyl-umbelliferone (4MU), and 2',7'-bis(carboxyethyl)-5,6-carboxy fluorescein (BCECF) were evaluated in terms of resolution, range, and stability of cellular fluorescence. In each case, the ratio of two emission wavelengths following a single excitation was taken as a measure of pH. It was found that 1,4-DHPN exhibited the best resolution of the three indicators tested over a useful range of greater than 1.5 pH units. The greater pH resolution of 1,4-DHPN, when measured by the ratio technique using fluorescence emission spectroscopy, is probably due to the fact that both of the emission wavelengths used in the ratio are pH sensitive and change in opposite directions as the pH of the sample is varied. This is in sharp contrast to the other two dyes in which only one

emission wavelength is sensitive to pH shifts, while the other remains at a constant value independent of the sample pH being measured. Reports of an accuracy of ±0.02 pH units have been reported where 1,4-DHPN emission spectroscopy has been employed during flow cytometric measurement of pH [33].

3.2. Potentiometric Titration

3.2.1. Procedure

One liter of 17.5 mM NaOH was prepared and standardized against the primary standard, potassium acid phthalate, according to a modification of a published procedure [27]. This resulted in a mean calculated NaOH molarity of 17.3 mM with a standard deviation of 0.4 mM for three separate determinations. The pH of all titrations was monitored using a Beckman Model 71 pH meter with a combination electrode. The volume of NaOH consumed at the equivalence point was determined graphically from the titration curves.

A 2 mM solution of 1,4-DHPN was prepared using a 50/50, by volume, ethanol/water solvent. This mixed solvent was necessary due to the limited solubility of 1,4-DHPN in water at acidic pH values. This solution was then titrated against the previously standardized NaOH. The pH during the entire course of the titration was monitored, using a Beckman Model 71 pH meter, and the total volume of NaOH consumed at each pH was recorded. The pK values of 1,4-DHPN were then determined from a computer aided analysis of the titration curve.

3.2.2. Results and Discussion

The titration curve for 1,4-DHPN (Fig. 3.3) is typical for a weak polyprotic acid titrated with a strong base. The actual shape of any given curve depends on the absolute ionization constants of the acid being titrated, the relative strengths of the ionizable groups, and the concentrations of the solutions used [27]. As the acid

becomes progressively weaker, the distinctness of the inflection at the equivalence points diminishes and the pH at these points shifts to higher values. In addition, for a polyprotic acid, difficulty in locating distinct inflection points occurs when the ratio of the first to the second dissociation constant approaches values of 100 or less. To give sharp inflection points, the ratio of the first to the second dissociation constant must be greater than 10^5. Furthermore, it has been determined that for an uncertainty of 0.1% or less in aqueous solution, the product $K_a[HA]$ should exceed 10^{-8}, assuming the titrant is completely dissociated and 0.1 N in strength [100].

From the above, it is clear that obtaining accurate pK values from a visual inspection of the depicted 1,4-DHPN titration curve shows little promise. At the concentrations of organic acid and titrant used in this experiment, the first pK approaches the limit of detectability and the second pK far exceeds this limit. The situation is further complicated by the fact that a 50% ethanol solvent was used in this experiment. Thus, both the pH values and ionization constants obtained directly from this curve are "apparent" and may not agree with the values obtained in water alone.

In order to locate more accurately the equivalence points for the experimentally obtained 1,4-DHPN titration curve, two different techniques were employed. First, titration of a blank solution was performed. This solution was prepared and titrated like the sample itself, but without the addition of the organic acid 1,4-DHPN. The volume of titrant used to achieve a specific blank pH was subtracted from the volume of titrant used to achieve the same value of pH in the sample solution. This procedure has been described by Parke et al. [71]. The resultant titration curve (Fig. 3.4) has now been corrected for errors introduced by solvent impurities, as well as any volume errors that may have been caused by the acid-base properties of the solvent utilized. The equivalence points for this corrected titration curve are then obtained by numerical differentiation, in order to

locate the volumes of NaOH required to make the second derivative of the titration curve equal to zero as the value of the ordinate rapidly changes from a positive to a negative number. The pH values corresponding to these volumes can be read directly from the corrected titration curve and correspond to the pK values of the acid being titrated. Using this procedure in the case of 1,4-DHPN, the pK values of 5.59 ±0.05 at 2.25 ml of titrant and 7.95 ±0.2 at 9.74 ml of titrant were obtained. The first pK can be read very accurately using this technique, while the second value bears a slightly higher degree of uncertainty. These values agree with the 5.5 ±0.3 and 8.0 ±0.2 results previously obtained by Brown et al. [14].

3.3. Ultraviolet and Visible Absorption Measurements

3.3.1. Procedure

Stock solutions of 122 mM $Na_2HPO_4 \cdot 7H_2O$ (Solution A) and 122 mM KH_2PO_4 (Solution B) were prepared in distilled water. Phosphate buffers covering the pH range of 6.0-8.0, in 0.5 unit pH steps, were prepared by mixing together appropriate volumes of the stock solutions A and B while observing the final pH value of the mixture using a Beckman Model 71 pH meter with a combination electrode. Using a 50/50 mixture of stock solutions A and B resulted in a phosphate buffer of approximately 305 mOsm, with a pH of about 7. This procedure resulted in a maximum of ±20% osmotic error, occurring at the extremes of the useable range (pH 5.0 and 9.0) of this buffer.

A 10 mM stock solution of 1,4-DHPN was prepared in distilled water. The pH of this solution was adjusted using 0.1 N NaOH so that a slightly alkaline solution resulted. This led to an increase in dye solubility as a result of a shift in equilibrium favoring the more water soluble basic forms of this molecule. All

subsequent concentrations of 1,4-DHPN required during the course of this experiment were made by appropriate dilution of this stock solution.

Absorption measurements were preformed using a Perkin-Elmer Lambda 4 uv/vis spectrophotometer. Concentrations studies were made using a pH 7.0 phosphate buffer over a concentration range extending form 10 mM to 1 μM. The pH studies were performed, using the appropriate phosphate buffer in the 6.0-8.0 pH range, at a dye concentration of 0.1 mM.

3.3.2. Results and Discussion

Absorbance spectra of 1,4-DHPN at pH 7.32 (Fig. 3.5) show a broad absorption band centered around a maximum at 381 nm with a full width at half maximum (FWHM) of approximately 57 nm, as measured with a dye concentration of 0.1 mM. For concentrations of this compound exceeding 0.5 mM, spectral distortion and a departure form the linear dependence of absorbance upon concentration, as would be anticipated from the application of Beer's law, were observed (Fig. 3.6). The behavior, in these concentrated solutions, may result from both a high degree of light scattering and differential absorption by a variety of polymeric forms of 1,4-DHPN which may be present. The value of the molar extinction coefficient (ε), at 381 nm and pH 7.32, can be determined from the slope of the concentration versus absorbance curve for concentrations of 1,4-DHPN below 0.5 mM. This value was found to be ε=5885 M^{-1} cm^{-1}. The pH sensitivity of the molar extinction coefficient (Fig. 3.7) makes accurate experimental determinations of dye concentration difficult.

As the pH of a solution of 1,4-DHPN is made more alkaline, its absorbance band shifts to longer wavelengths (Fig. 3.8). This can more easily be shown by plotting the peak absorption wavelength against solution pH (Fig. 3.9). This

calibration curve, easily fit by a cubic equation, can be used to determine solution pH if the peak absorption wavelength is known.

3.4. Fluorescence Measurements

3.4.1. Lifetime

3.4.1.1. Procedure

Phosphate buffers extending over the pH range 5.0-9.0, in 0.5 pH units, were prepared according to the procedure described in Section 3.3.1. Dilutions were made from a 10 mM stock solution of 1,4-DHPN so that the final dye concentration in each sample was 1.0 μM.

Lifetime measurements were preformed in the lab of Dr. Enrico Gratton using an I.S.S. GREG1 multifrequency cross-correlation phase and modulation fluorometer. Excitation was achieved using the 325 nm line of a helium-cadmium laser at a power level of approximately 1 mW. The full emission spectrum of each sample was collected and analyzed for phase shift and demodulation with respect to a known reference. Measurements were taken at temperatures of 31.4, 41.2 and 50.8 °C, and frequencies of up to 160 MHz were employed for an effective resolution of 6.25 ns. Lifetimes were computed from this data using a nonlinear least-squares method for minimizing the value of Chi square in the fitting of a multiexponential decay.

3.4.1.2. Results and Discussion

Since the decay time of a fluorophore is often sensitive to its environment, the effect of both pH and temperature on the fluorescence lifetime of 1,4-DHPN was studied in order to determine the feasibility of using this parameter to quantitatively determine the pH of a given sample.

Lifetime data may be obtained using either pulsed or harmonic methods. In the pulse method, a brief pulse of light is used for excitation and the time-dependent decay of fluorescence intensity is measured. The lifetime of each component can then be directly determined by using a multiple exponential fit to the decay curve.

In the harmonic method, the sample is excited with sinusoidally modulated light. The fluorescence emission will also be sinusoidally modulated at the same frequency but, since the lifetime of the excited state is finite, it will be delayed in phase and less modulated than the excitation. Measurement of the phase delay and the modulation ratio provides independent determinations of the fluorescence lifetime [34]. Furthermore, if a wide range of modulation frequencies are available, the information contained in the phase and modulation values is equivalent to that obtained from the more direct pulse measurements [36]. The primary advantages of the phase-modulation method are the ability to measure short nanosecond lifetimes with good resolution and the speed (seconds) with which the measurement can be carried out [28].

A plot of phase delay, as a function of modulation frequency (Fig. 3.10), shows that this delay is a function of both pH and modulation frequency. The phase delay increases as the modulation frequency is increased, and is greater at more acidic values of pH for all frequencies measured. A similar behavior (Fig. 3.11) is expected and found when the modulation ratio is plotted as a function of modulation frequency and pH. The amount of demodulation increases as the modulation frequency increases and is greater at more acidic values of pH for all frequencies considered. These data suggest that the measured lifetime of this fluorophore is strongly pH dependent and decreases with increasing deprotonation of the sample.This is in sharp contrast to 2-naphthol, the most widely studied model of a simple fluorophore, and has been attributed to the inductive effect of the cyano groups [14].

After application of nonlinear least-squares curve fitting techniques to the experimentally acquired modulation and phase information, it was found that a double exponential fit was adequate to describe the data over the pH range considered. The largest fraction (>90% at all pH values) had lifetimes that ranged from 8.73 ns at pH 5.12 to 5.48 ns at pH 8.87 (Fig. 3.12). This fraction can best be thought of as a lifetime averaged over a weighted contribution from all species present at any given pH, rather than the lifetime of any individual species. Experiments conducted over a more extensive pH range, as well as use of higher modulation frequencies, would be required in order to determine species specific lifetimes. A second minor fraction (<10% at all pH values) with an average lifetime of 10 ps was found to be required to give an acceptable fit to the experimental data. Due to the small fractional contribution from this component, as well as its short highly variable lifetime, it is reasonable to conclude that this component is most likely an artifact introduced to account for errors in the experimental measurements. Given the above limitations on this study, the lifetimes determined using this technique are in reasonable agreement with those reported in the literature [14].

While the above experimental data does not allow accurate determination of species specific lifetimes, it does provide the basis for a fast and accurate method of pH determination in the physiological range. If the modulation/phase versus frequency curve for pH 8.0 is subtracted from the corresponding curve for pH 6.0, the maximum change in modulation/phase with pH occurs at a frequency of 30 MHz. By plotting the modulation/phase at this frequency versus pH (Fig. 3.13) an accurate calibration curve can be constructed. An error analysis of the experimental data, acquired with the previously described laboratory based system, suggests that a precision of ±0.04 pH units can be achieved throughout a 6.0-8.0 pH

range at a temperature of 31.4 °C, using either modulation ratio or phase information.

The effect of temperature on both the modulation ratio and phase delay at 30 MHz was explored using solutions of 1,4-DHPN dissolved in phosphate buffers of known pH when measured at 25 °C. From this data (Figs. 3.14 and 3.15), it appears that lifetimes of solutions of 1,4-DHPN at acidic values of pH are more temperature sensitive then those that are slightly alkaline. Furthermore, temperature sensitivity reaches a minimum at pH 7 and in addition, seems to undergo a sign reversal at this point. A possible explanation for this phenomena is that each species of 1,4-DHPN has a distinct temperature sensitivity with regard to its fluorescence lifetime. As the pH of the environment changes, so does the fractional distribution of the different forms of this dye. The measured temperature sensitivity at a given pH would then be a weighted average of the sensitivities of the particular species involved. If this explanation is correct, it suggests that neutral species interacts with its surroundings in a very different manner from that of the dianion, especially in the excited state.

The change in hydrogen ion activity with temperature has been reported to be -0.0028 pH units / ° C for standard phosphate buffers [97]. From the experimental data, an average pH error of approximately +0.05 pH units / °C can be calculated over a pH range of 6-8. This error is smallest at pH 7 and increases the greater the deviation from this value in either direction. Since this pH error is more than an order of magnitude greater than that introduced by the buffer, as well as being of the opposite sign, it can be seen that a significant error can be introduced when using this technique to measure pH over an extended temperature range. Since acid dissociation constants are known to be temperature dependent, this is the most likely explanation for these temperature dependent pH errors.

3.4.2. Excitation and Emission

3.4.2.1. Procedure

Phosphate buffer of approximately 305 mOsm was prepared spanning the 6.0-8.0 pH range, in 0.5 unit steps, according to the procedure detailed in Section 3.3.1. Each of these samples was prepared from a 10 mM stock solution of 1,4-DHPN, achieving a final dye concentration of 10 μM. All measurements were preformed using an early prototype of an I.S.S. microprocessor controlled photon-counting spectrofluorometer [35]. An Apple IIE microcomputer was used for both instrument control and data acquisition.

All excitation spectra were obtained by scanning the excitation monochromator form 250 to 450 nm with the emission monochromator fixed at 455 nm. The emission spectra were obtained by scanning the emission monochromator from 400 to 600 nm with the excitation monochromator fixed at 387 nm. The fixed wavelengths were chosen to be near to either emission or excitation maxima, as determined from a prescan of the pH 7.0 sample. Spectra were taken at temperatures of 30.6, 39.0, and 49.4 °C.

3.4.2.2. Results and Discussion

Like most pH sensitive fluorophores, 1,4-DHPN can be used to measure pH by calculating the fluorescence emission ratio at a fixed wavelength, after a sequential excitation at two different wavelengths. For maximum sensitivity however, it is best if both excitation wavelengths chosen are sensitive to sample pH. Furthermore, the emission change should be in opposite directions following excitation at each of these wavelengths. Where this is not possible, one wavelength can be chosen at an isosbestic point with some resultant loss in sensitivity.

The overall excitation spectra of 1,4-DHPN is strongly dependent on sample pH (Fig. 3.16). When a difference spectrum (pH 6.0-pH 8.0) is taken (Fig. 3.17), it

is observed that the maximal change in emission, upon excitation, occurs at wavelengths of 365 and 414 nm. The ratio of these two wavelengths (Fig. 3.18), as a function of pH, gives a calibration curve which, given the limited number of data points, can be fit exactly by a fourth order polynomial.

When the temperature of the sample is increased (Fig. 3.19), the emission decreases slightly for excitation at 365 nm and increases slightly for excitation at 414 nm. The peak of the excitation spectrum, however, is seen to remain fixed across the temperature range considered in this study. This results in an increased ratio (414 nm /365 nm) with temperature (Fig. 3.20), for any given pH value. The degree of increase in the value of the ratio appears to be a linear function of temperature. The slope of this function is generally found to increase with pH over the pH interval examined in this study. The average amount of error introduced into pH measurements, by this technique, is again found to be on the order of ±0.05 pH units / °C.

By calculating the temperature difference spectrum (30.6 - 49.4 °C), it is seen that maximal temperature sensitivity tends to occur at approximately the same wavelengths as maximal pH sensitivity (Figure 3.21). This result precludes use of this dye for simultaneous pH independent temperature measurements by simple selection of another pair of excitation wavelengths.

Unlike most pH sensitive fluorophores, this indicator dye can also be used to measure pH by using dual wavelength emission spectroscopy following a broadband excitation. The peak emission is shifted to longer wavelengths as the sample pH increases in alkalinity (Fig. 3.22). A difference spectra (pH 6.0 - pH 8.0) shows that the maximal change with pH occurs at wavelengths of 435 nm and 486 nm, respectively (Fig. 3.23). By plotting the ratio of emission wavelengths (486 nm /435 nm) as a function of pH, a calibration curve can be obtained which can be exactly fit, given the sparse data, by a fourth order polynomial (Fig. 3.24).

As in the case of the excitation spectra, the wavelength of peak emission remains constant with temperature (Fig. 3.25), while the intensities of fluorescence at 435 and 486 nm, as well as their ratio (486 nm /435 nm), appear to be a function of temperature. Unlike the temperature behavior of the emission spectrum, however, the functional form of the relationship among the variables of ratio, temperature and pH appears to be considerably more complex (Fig. 3.26).

The behavior of the emission ratio, with respect to temperature, parallels closely the behavior of fluorescence lifetime. A minimum sensitivity is seen to occur at pH 7.0, with increased temperature sensitivity the greater the departure from this pH in either direction. Also, as in the lifetime experiments, the temperature sensitivity changes sign as neutral pH is approached. At acidic pH, the ratio increases with increasing temperature, while it tends to decrease, with increasing temperature, at more alkaline pH. The average pH error introduced by temperature over range of this study was ±0.02 pH units / °C. In a more restricted pH range (pH 6.5 - pH 7.5), a maximum error of ±0.03 pH units / °C occurred at the pH extremes. Unfortunately, as was discussed above with regard to the excitation spectrum, the emission wavelengths chosen in order to optimize pH sensitivity are also those that possess a high degree of temperature sensitivity (Fig. 3.27).

The behavior of the dual emission ratios as a function of temperature seem to be largely dependent upon the 486 nm component. This wavelength is approximately that of the peak emission wavelength of the dianionic species. A plot of the temperature difference spectrum (49.4 - 30.6 °C) illustrates the change in sign and magnitude of the 486 nm fluorescence as the sample pH is altered (Fig. 3.28). This result is probably due to the effect of temperature on this systems complex equilibria. The sample pH determines the fractional contribution of each equilibrium constant to the overall temperature sensitivity of the resultant ratio.

3.5. Conclusions

The studies described above suggest that the pH sensitive fluorophore 1,4-DHPN can be employed in many different ways as the basis of a pH sensitive optrode for use in the physiological pH and temperature ranges. Each approach presents advantages as well as disadvantages with respect to instrument design, accuracy, and precision.

A simple absorption technique could be used near the peak absorption wavelength. Changes in pH could then be measured by measuring the changes in absorbance at this wavelength. This technique, while affording simplicity in instrument design, requires the use of complex sensor geometry for acceptable measurement sensitivity. Furthermore, changes in indicator concentration will manifest themselves as pH measurement errors. On the other hand absorbance peak detection while not suffering form concentration dependent problems, still requires complex optrode designs, as well as sophisticated optical and electronic processing in order to be able to detect the absolute position of the peak wavelength. Use of a scanning diode array may make this approach more feasible. It should be noted however, that this technique exhibits extremely poor pH sensitivity in the physiological (pH 6.5 - pH 7.5) range.

The measurement of pH using the fluorescence lifetimes of 1,4-DHPN has several attractive features, especially when frequency domain techniques are employed using either phase delay or modulation ratio at a fixed frequency. The measurement is fast, has good precision, and minimum temperature sensitivity near physiological pH. In addition, the maximum pH sensitivity occurs at slightly acidic values of pH (pH 6 - 7). This is most likely due to the larger difference in lifetimes observed between the neutral and anionic species (4 ns) than between the anionic and dianionic species (2.3 ns). This increased sensitivity at acidic values of pH make this technique attractive for hyperthermia studies since the microenvironment of

most tumors is slightly acidic. Disadvantages of this technique are its dependence on sophisticated and expensive instrumentation. Extremely stable frequency synthesizers, as well as light sources capable of being modulated at frequencies as high as 1 GHz are usually required. Another disadvantage is the complex shape of the pH calibration curve obtained using this technique. Obtaining a pH value from a measurement of phase or modulation would impose a considerable processing burden, resulting in the need for fast microprocessors in order to achieve a reasonable real time data acquisition rate.

Fluorescence excitation spectroscopy is a poor choice for a pH measurement technique when utilizing 1,4-DHPN. Its maximum pH sensitivity is in the 7-8 pH range. However, useable sensitivity is exhibited down to pH 6. The need for sequential excitation makes for complex instrumentation, as well as poor precision due to the nonsimultaneous acquisition of the data needed to compute the desired ratio. In addition, the large temperature sensitivity of this technique makes temperature correction necessary at almost all pH values.

Dual wavelength emission spectroscopy appears to offer the most promise for use in making physiological pH measurements with a 1,4-DHPN based optrode. Sensitivity in the 7-8 pH range is ≥ 1, with sufficient sensitivity down to pH 6. Simple instrumentation can be employed to acquire simultaneous dual wavelength intensity data, following a single broadband excitation. This makes the computed ratio relatively independent of parameter fluctuations in either the measurement system or the sample. Furthermore, a single fiber can be used for both excitation and emission. In addition, the temperature sensitivity is the smallest of all the techniques studied across the physiological 6.5-7.5 pH range, with an absolute minimum temperature sensitivity occurring at pH 7.

For the above reasons, a pH sensitive optrode using 1,4-DHPN was constructed and instrumentation was built in order to take advantage of its unique dual emission wavelength characteristics.

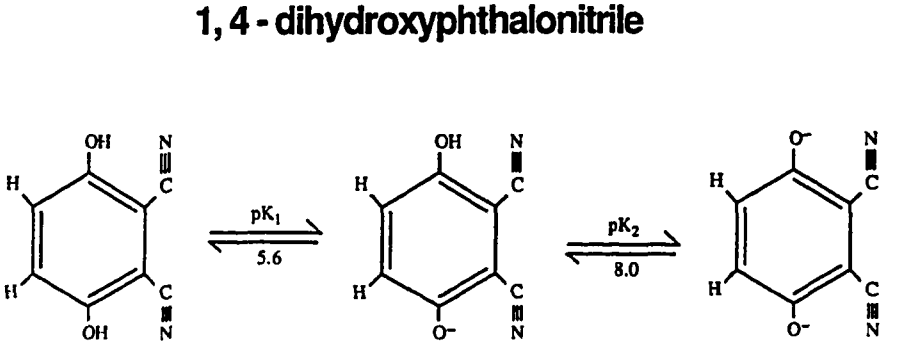

Figure 3.1. Three forms of the fluorescent probe 1,4-DHPN in solution.

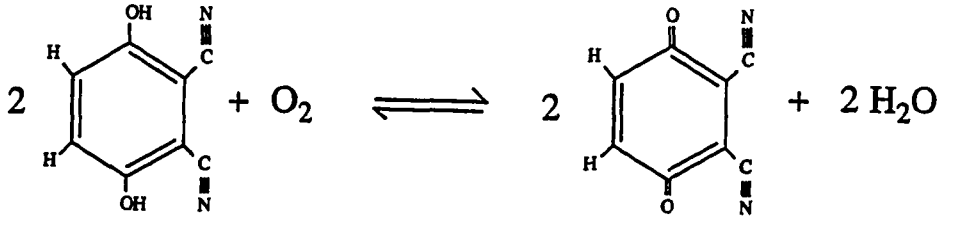

Figure 3.2. Oxidation of the fluorescent probe 1,4-DHPN in solution.

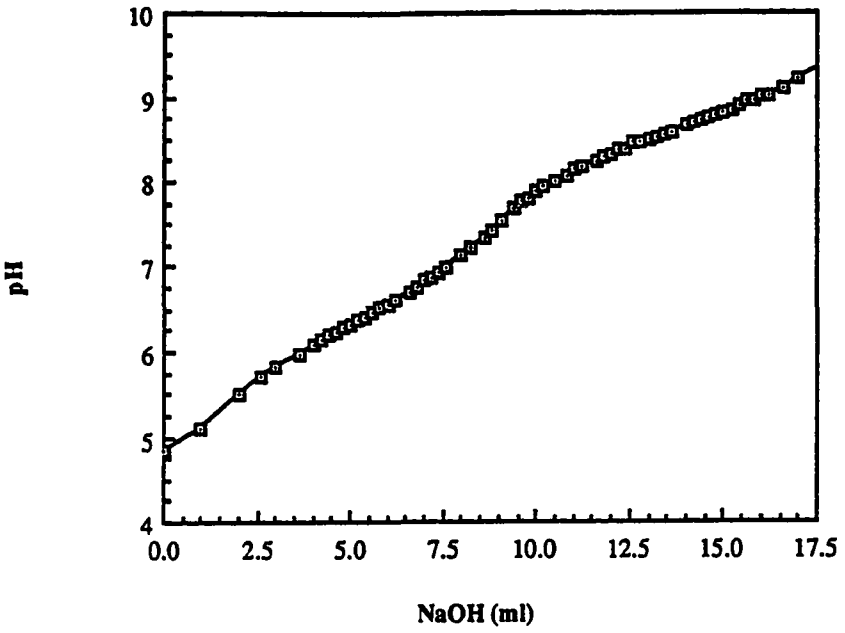

Figure 3.3. Uncorrected titration curve for a 2 mM solution of 1,4-DHPN in a 50/50 ethanol/water solvent.

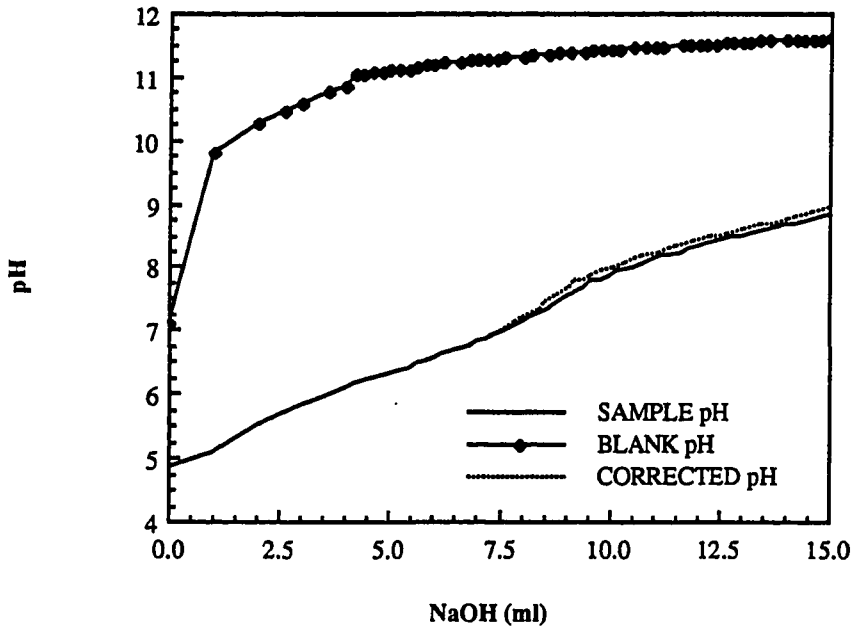

Figure 3.4. Blank corrected titration curve for a 2 mM solution of 1,4-DHPN in a 50/50 ethanol/water solvent.

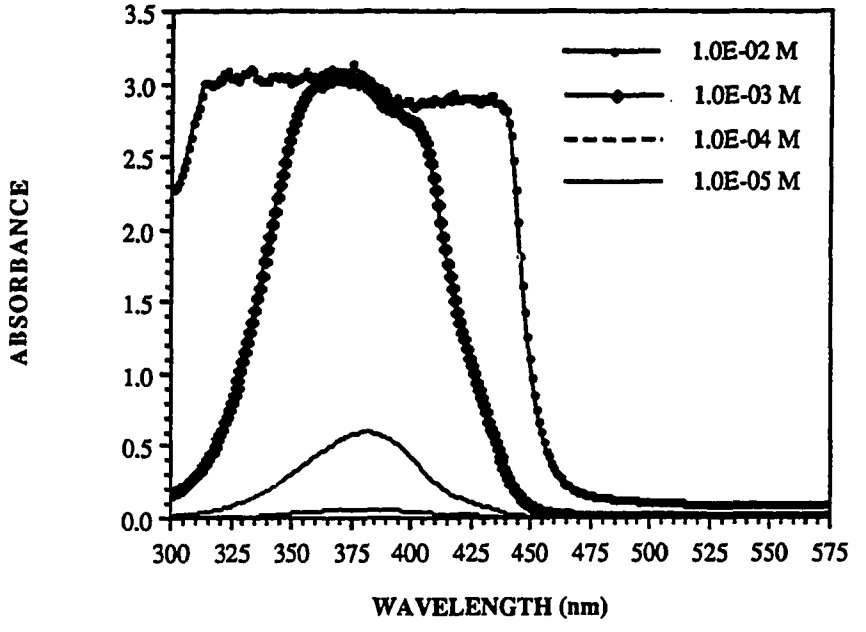

Figure 3.5. Concentration dependence of the absorption spectrum of 1,4-DHPN in 305 mOsm phosphate buffer at pH = 7.32.

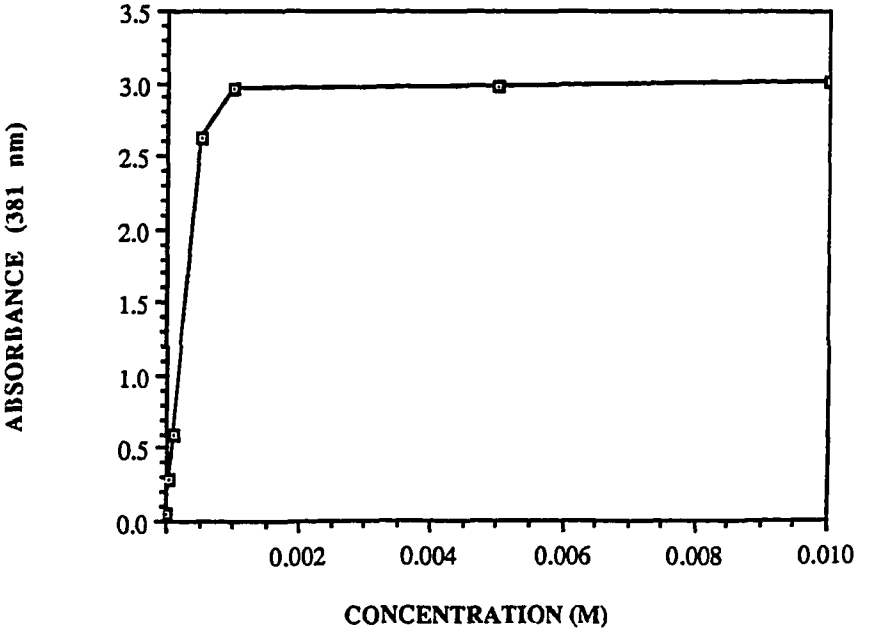

Figure 3.6. Concentration dependence of the absorbance of 1,4-DHPN measured at a peak wavelength of 381 nm, in 305 mOsm phosphate buffer at pH = 7.32.

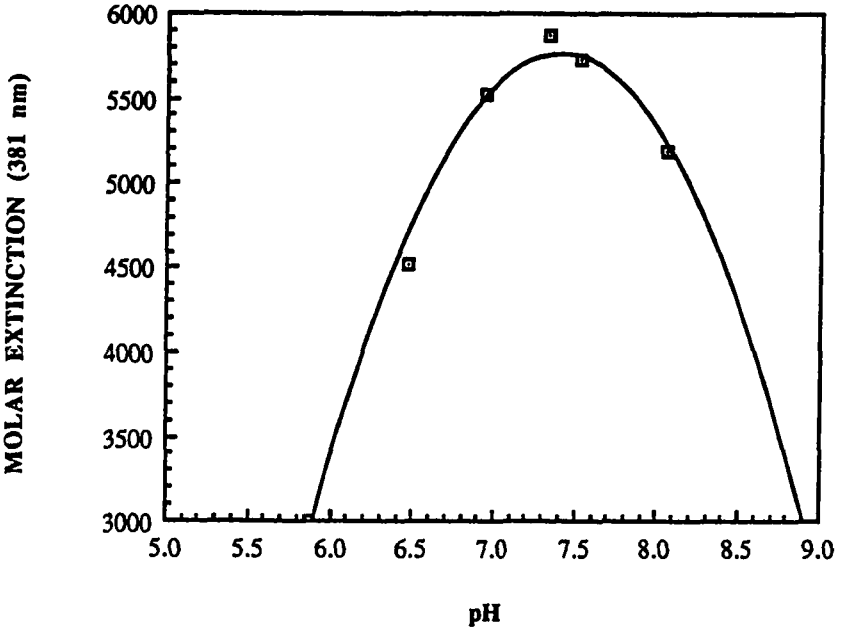

Figure 3.7. The pH dependence of the 381 nm extinction coefficient of a 0.1 mM solution of 1,4-DHPN.

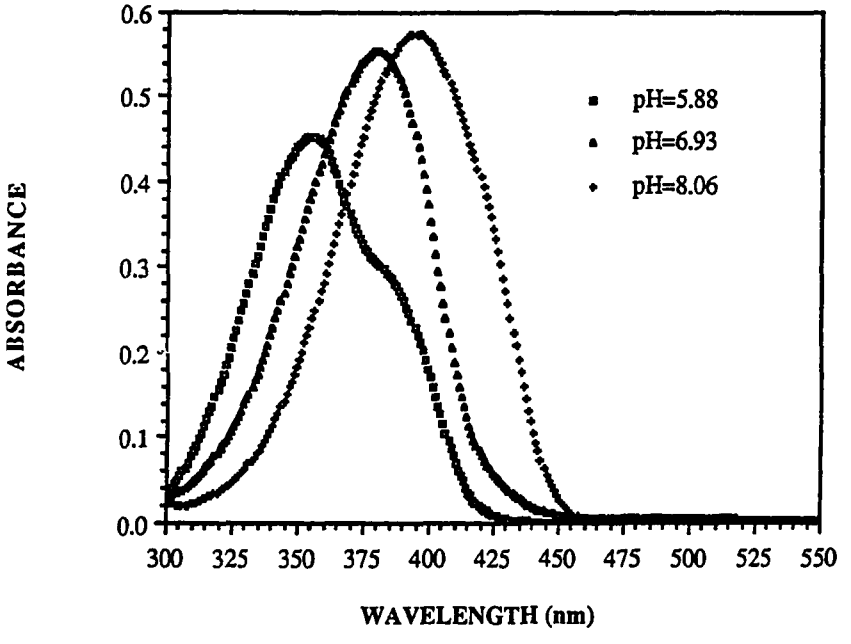

Figure 3.8. The pH dependence of the absorption spectrum of a 0.1 mM solution of 1,4-DHPN.

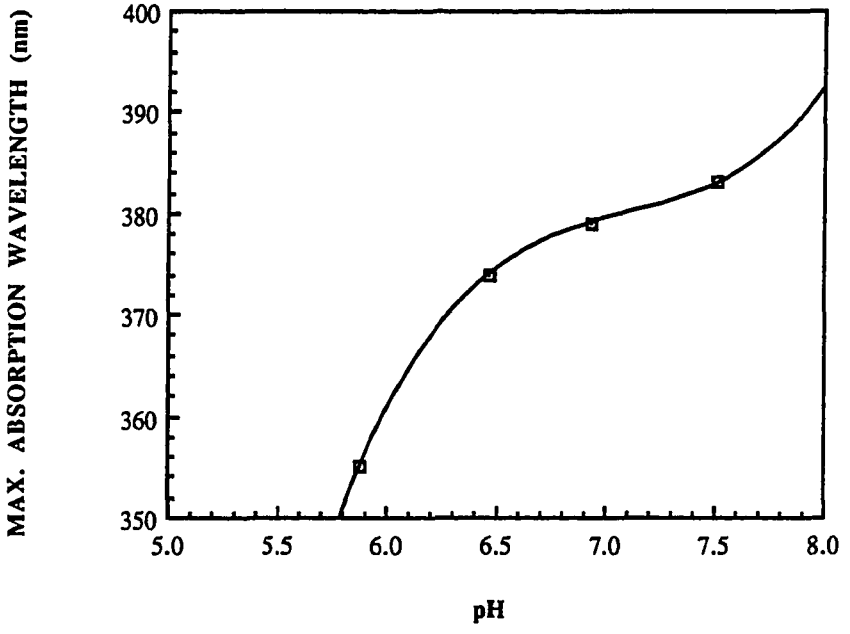

Figure 3.9. The pH dependence of the peak absorption wavelength of a 0.1 mM solution of 1,4-DHPN.

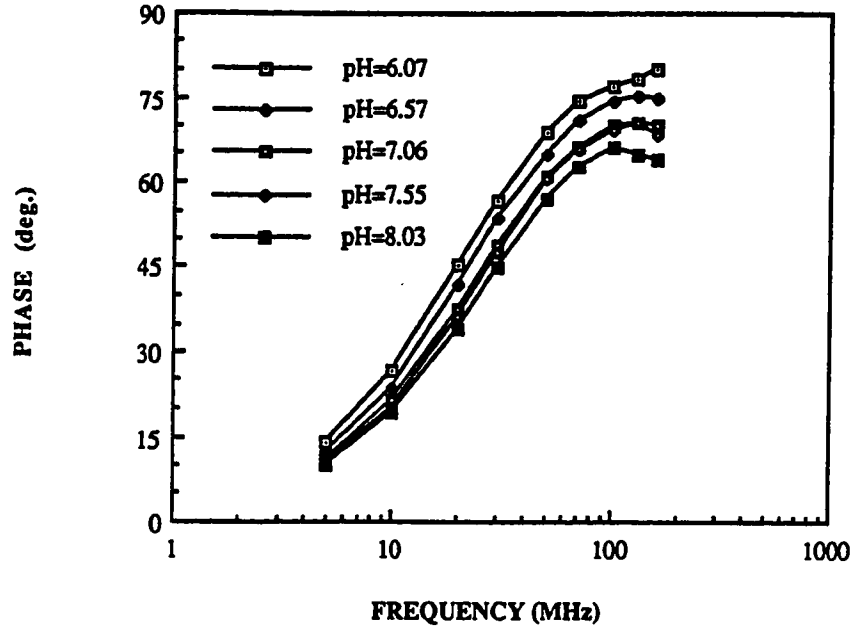

Figure 3.10. Frequency dependence of the fluorescence phase of a 0.002 mM solution of 1,4-DHPN in 305 mOsm phosphate buffer as a function of pH.

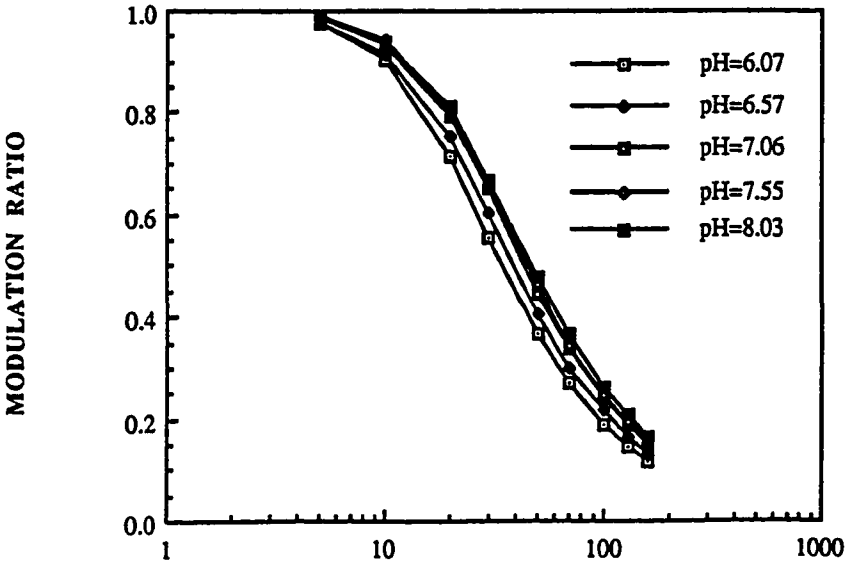

Figure 3.11. Frequency dependence of the fluorescence modulation ratio of a 0.002 mM solution of 1,4-DHPN in 305 mOsm phosphate buffer as a function of pH.

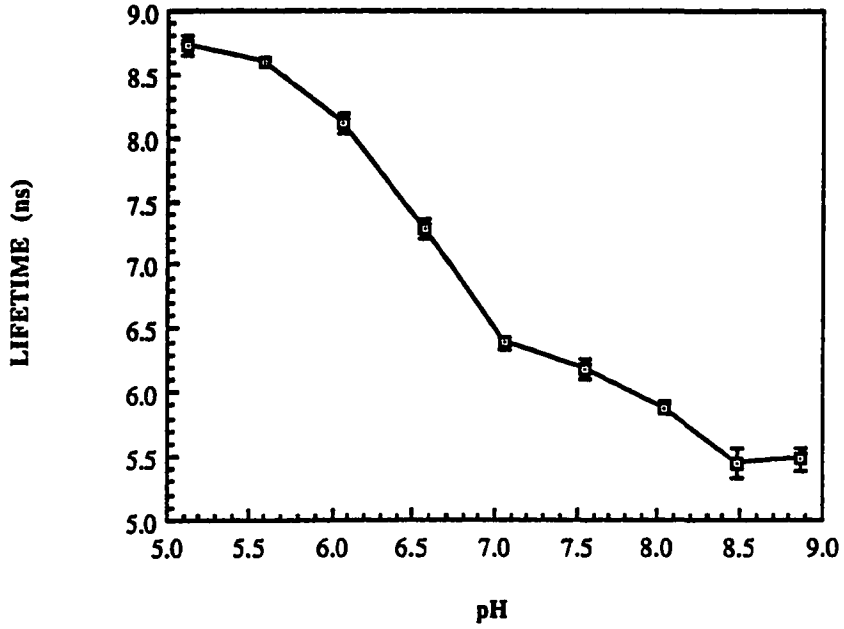

Figure 3.12. Calculated fluorescence lifetime of a 0.002 mM solution of 1,4-DHPN in 305 mOsm phosphate buffer as a function of pH.

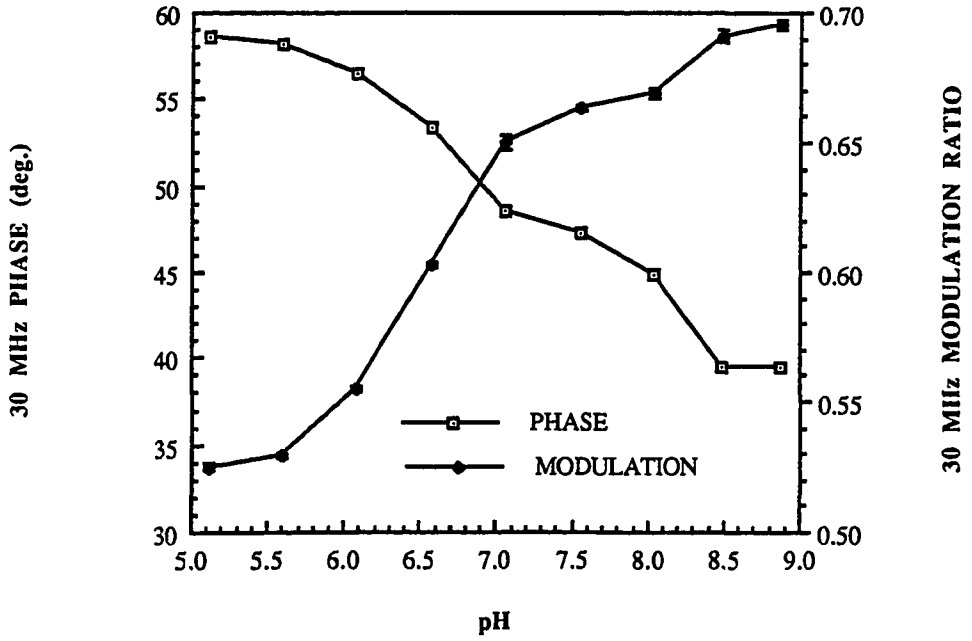

Figure 3.13. Fluorescence modulation ratio and phase of a 0.002 mM solution of 1,4-DHPN in 305 mOsm phosphate buffer as a function of pH. Measurements were taken at a frequency of 30 MHz.

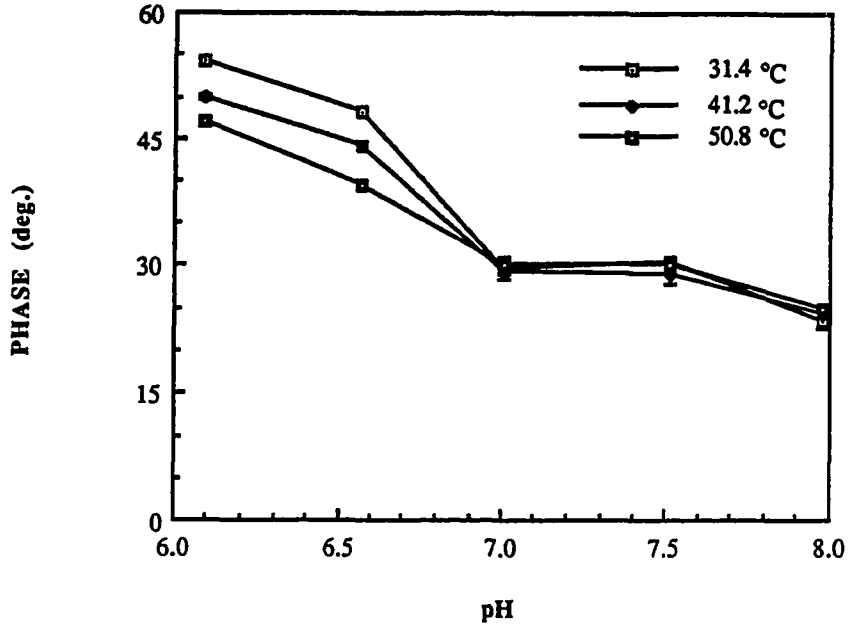

Figure 3.14. Temperature dependence of the fluorescence phase of a 0.001 mM solution of 1,4-DHPN in 305 mOsm phosphate buffer as a function of pH. Measurements were taken at a frequency of 30 MHz.

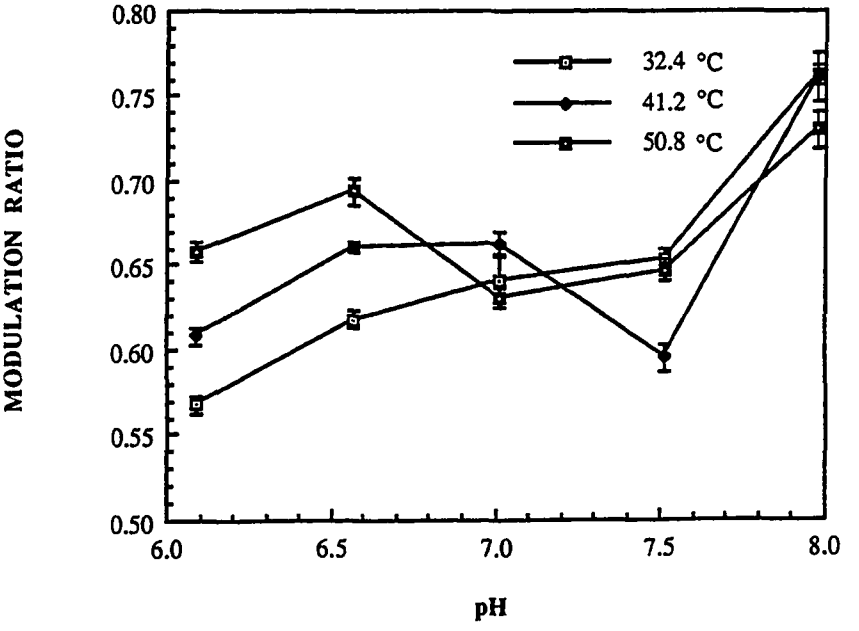

Figure 3.15. Temperature dependence of the fluorescence modulation ratio of a 0.001 mM solution of 1,4-DHPN in 305 mOsm phosphate buffer as a function of pH. Measurements were taken at a frequency of 30 MHz.

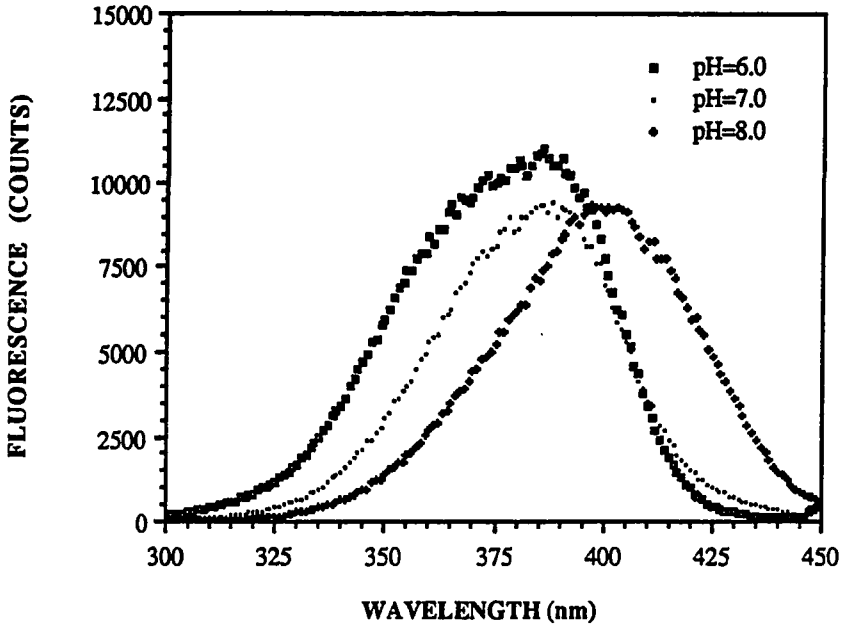

Figure 3.16. The pH dependence of the excitation spectrum of a 0.001 mM solution of 1,4-DHPN in 305 mOsm phosphate buffer. Emission measurements were taken at 455 nm.

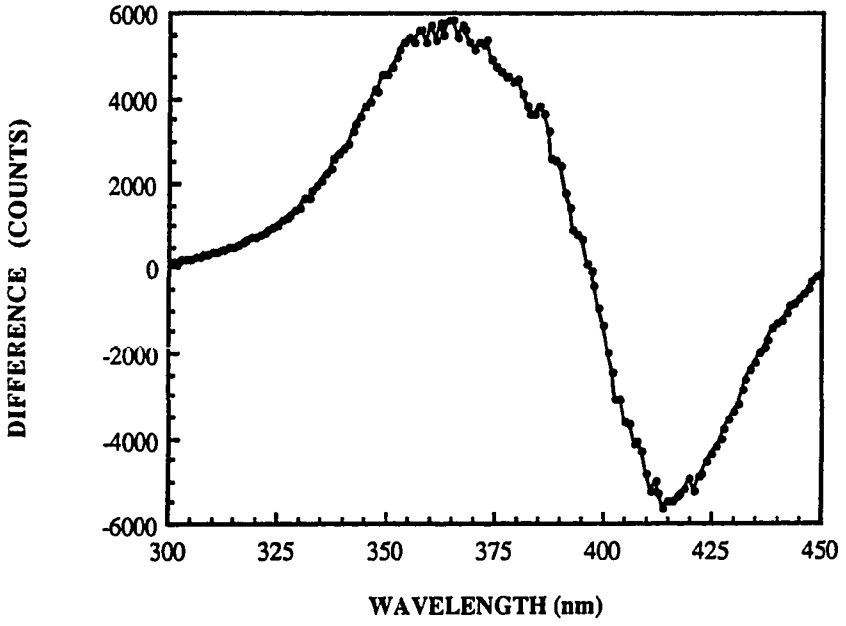

Figure 3.17. Excitation pH difference spectrum (pH 6 - 8) of a 0.001 mM solution of 1,4-DHPN in 305 mM phosphate buffer. Emission measurements were taken at 455 nm.

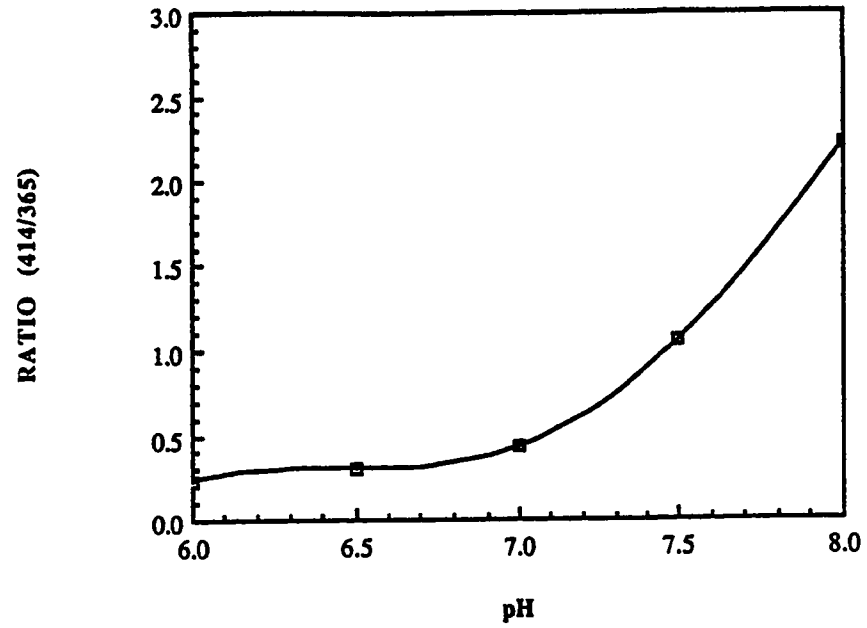

Figure 3.18. The pH dependence of the excitation ratio (414 nm / 365 nm) of a 0.001 mM solution of 1,4-DHPN in 305 mOsm phosphate buffer. Emission measurements were taken at 455 nm.

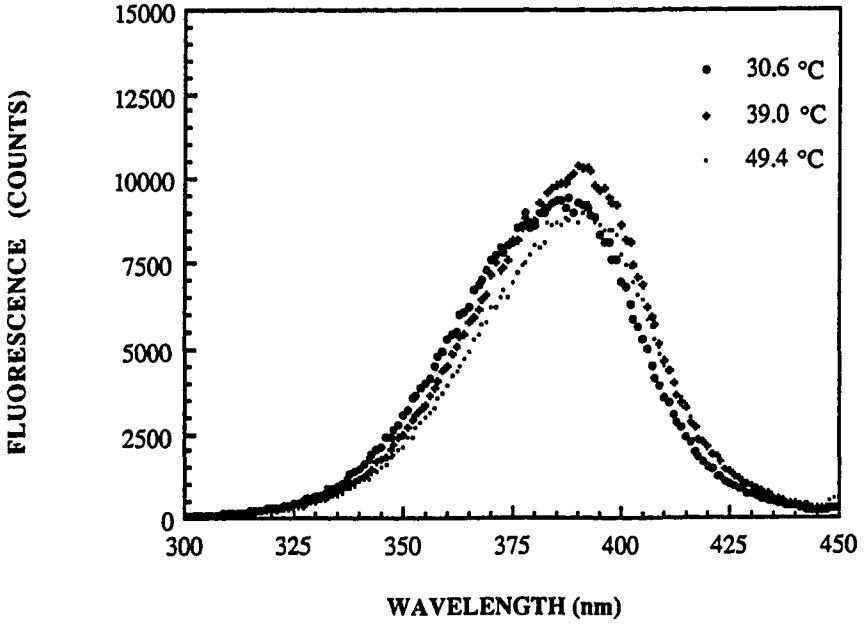

Figure 3.19. Temperature dependence of the excitation spectra of a 0.001 mM solution of 1,4-DHPN in 305 mOsm phosphate buffer at pH 7.0. Emission measurements were taken at 455 nm.

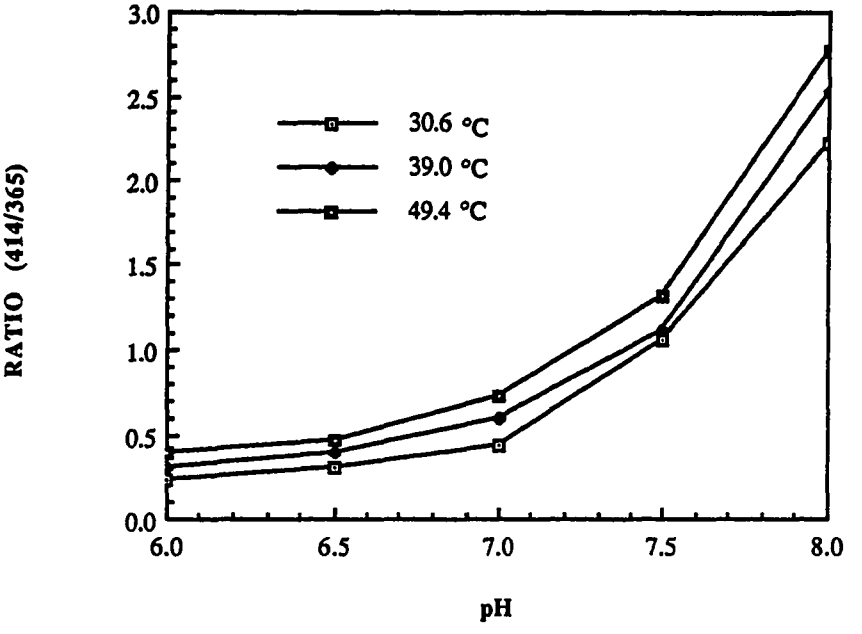

Figure 3.20. Temperature dependence of the excitation ratio (414 nm /365 nm) of a 0.001 mM solution of 1,4-DHPN in 305 mOsm phosphate buffer as a function of pH. Emission measurements were taken at 455 nm.

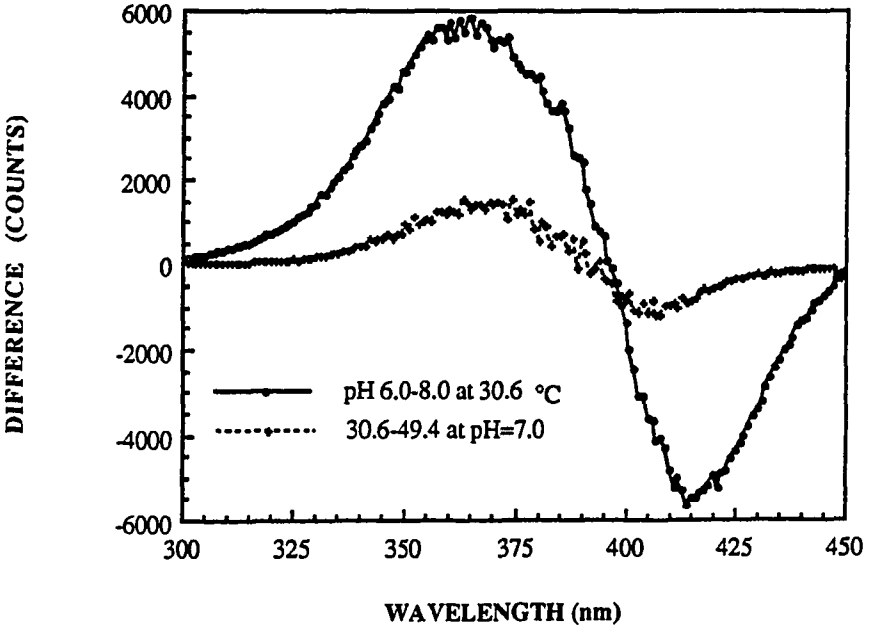

Figure 3.21. The pH and temperature excitation difference spectrums for a 0.001 mM solution of 1,4-DHPN in 305 mOsm phosphate buffer. Emission measurements were taken at 455 nm. All temperatures were measured in degrees Celsius.

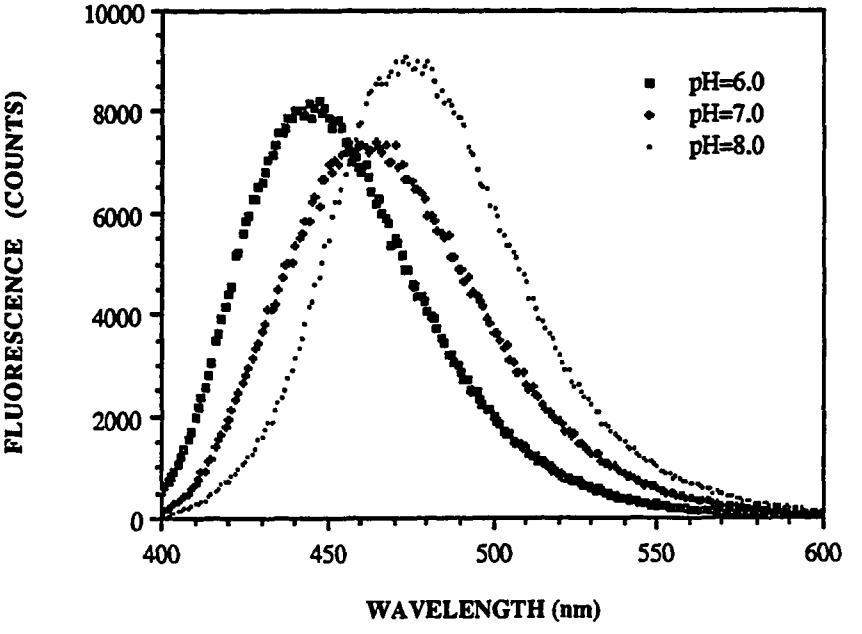

Figure 3.22. The pH dependence of the emission spectrum of a 0.001 mM solution of 1,4-DHPN in 305 mOsm phosphate buffer. Excitation was at 387 nm.

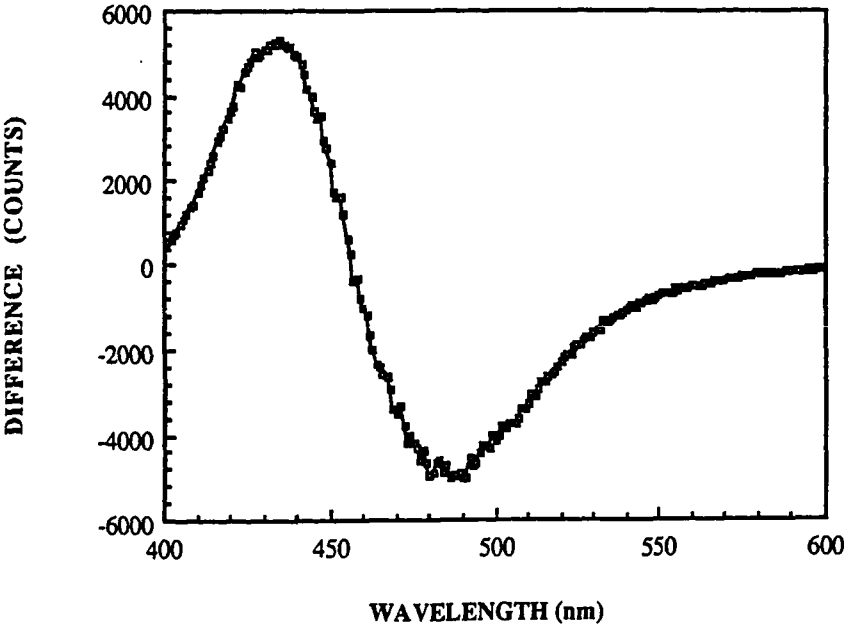

Figure 3.23. Emission pH difference spectrum (pH 6 - 8) of a 0.001 mM solution of 1,4-DHPN in 305 mOsm phosphate buffer. Excitation was at 387 nm.

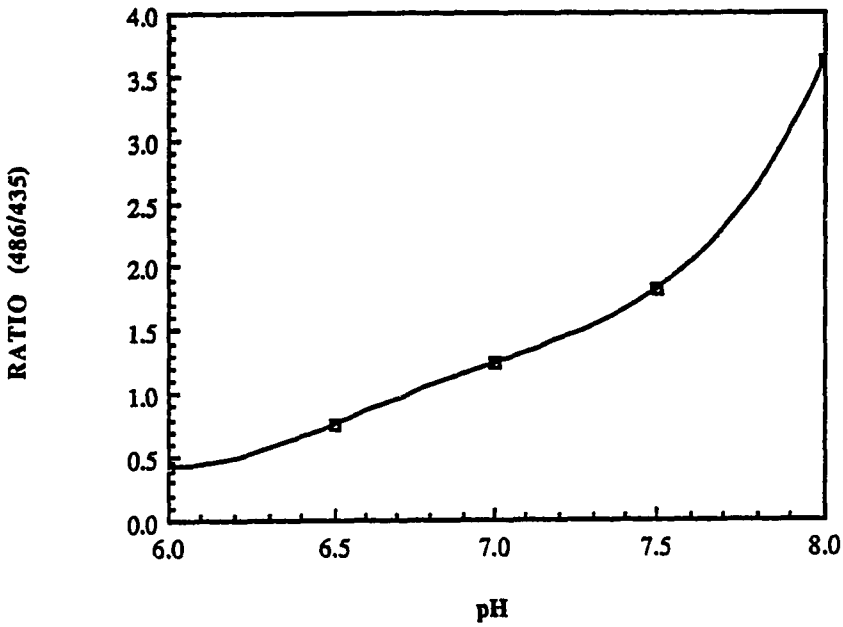

Figure 3.24. The pH dependence of the emission ratio (486 nm /435 nm) of a 0.001 mM solution of 1,4-DHPN in 305 mOsm phosphate buffer. Excitation was at 387 nm.

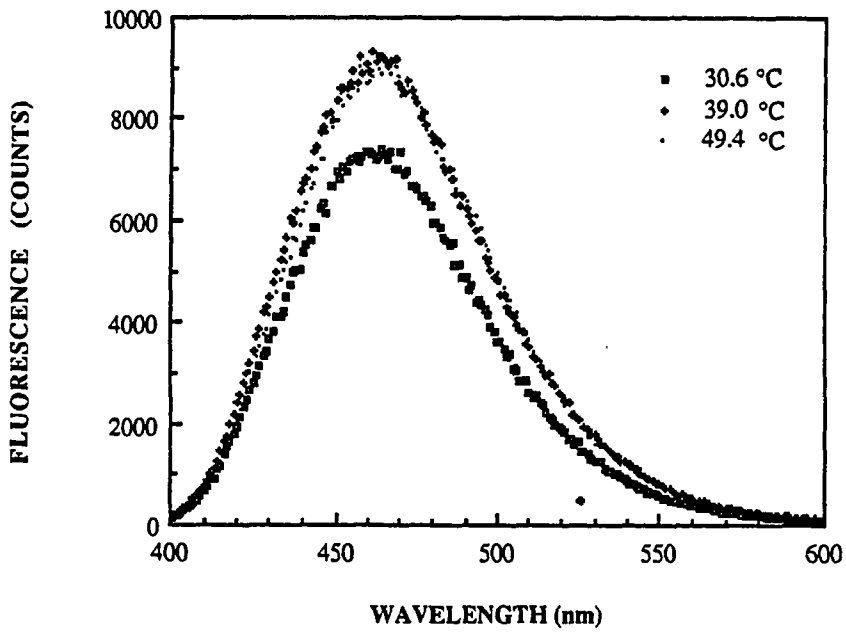

Figure 3.25. Temperature dependence of the emission spectrum of a 0.001 mM solution of 1,4-DHPN in 305 mOsm phosphate buffer at pH 7.0. Excitation was at 387 nm.

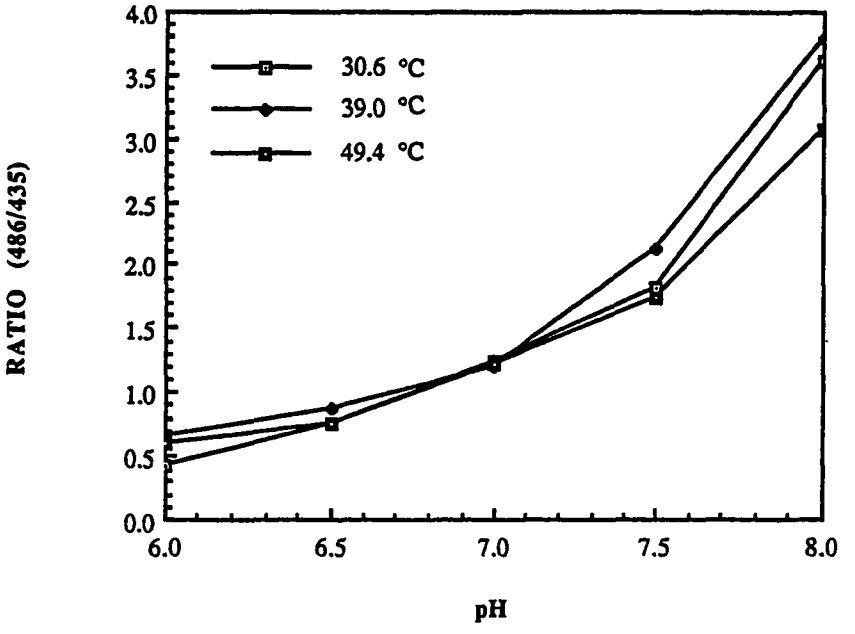

Figure 3.26. Temperature dependence of the emission ratio (486 nm /435 nm) of a 0.001 mM solution of 1,4-DHPN in 305 mOsm phosphate buffer as a function of pH. Excitation was at 387 nm.

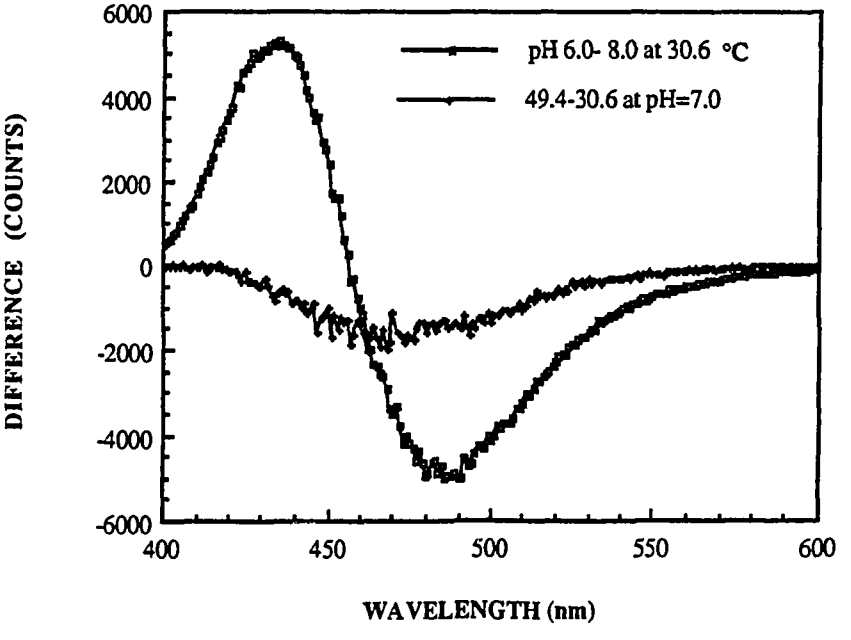

Figure 3.27. The pH and temperature emission difference spectrums for a 0.001 mM solution of 1,4-DHPN in 305 mOsm phosphate buffer. Excitation was at 387 nm. All temperatures were measured in degrees Celsius.

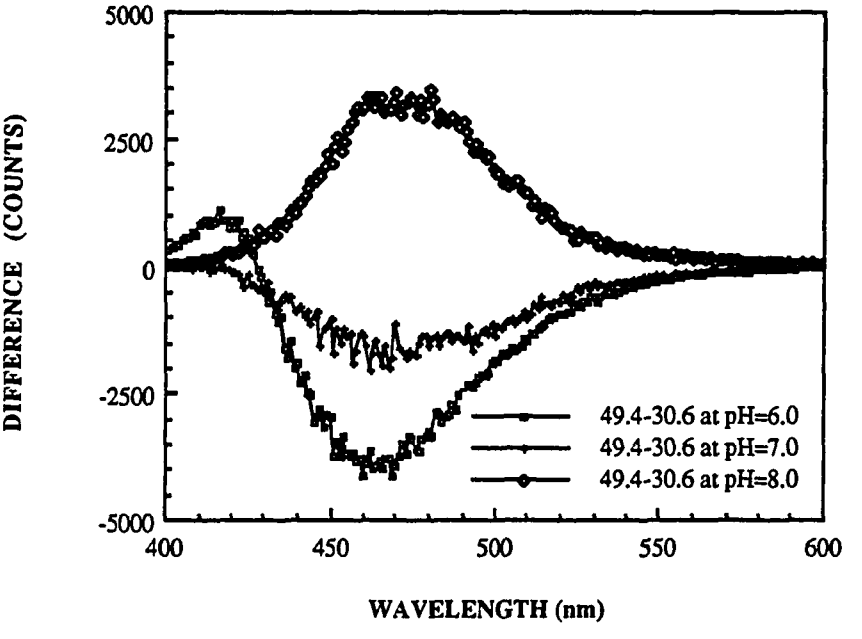

Figure 3.28. The pH dependence of the temperature emission difference spectrums of a 0.001 mM solution of 1,4-DHPN in 305 mOsm phosphate buffer. Excitation was at 387 nm. All temperatures were measured in degrees Celsius.

CHAPTER 4
INSTRUMENT DESIGN

4.1. Introduction

Instrumentation was designed to enable rapid optical measurement of pH, via the fluorophore 1,4-DHPN, using the dual emission ratio technique discussed in Chapter 3. Frequently in spectroscopic work, the short-term stability of the light-source intensity limits measurement speed and accuracy [80]. Time dependent concentration changes may also introduce errors in the measurement of the desired reaction. The dynamic ratio technique, if correctly applied, will yield increases in both measurement speed and accuracy.

A gated integrator approach, using a pulsed source and analog detection, was chosen for simultaneous signal acquisition on each channel. In general, the choice between gated integration (boxcar averaging) and phase sensitive detection (lock-in detection) is based on the time behavior of the signal [72]. If the signal is fixed frequency and has a duty cycle greater than or equal to 50%, lock-in detection is the best technique to use since the noise collected during a long gating time can easily swamp the signal. On the other hand, if the signal has a duty cycle less than 50%, such as the pulse from a flashlamp, then a gated integrator can be utilized to detect the signal only when it is present. Consequently all noise occurring outside of the gating interval is rejected.

Analog detection was chosen on the basis of the expected signal level. At very low light intensities, photon counting works well since the input discriminator tends to reduce front end noise. At high light intensities, analog detection works better because analog inputs are less prone to saturation than those of a counter. For moderate light levels such as are inherent in the present application, analog detection combined with a front end optimized for low noise operation seems to be

the best choice. A low noise front end is necessary since this input noise adds to the ever present Poisson-counting distribution noise to degrade the overall signal-to-noise ratio (SNR) of the system.

Two additional features were incorporated into the instrument design in an attempt to improve the overall SNR. The first is the addition of an optional hardware module preceding the integrator stage. This module consists of a high Q, fixed frequency bandpass filter, followed by an rms-to-dc converter. The addition of this module has several advantages. First, it is extremely effective in reducing ac and dc background due to stray light reaching the detector. Second, broadband random noise is reduced and discrete electrical frequencies, such as pickup from 60 Hz sources, are eliminated with the appropriate selection of center frequency. Third, dc offset errors such as those introduced by photodetector dark current and temperature effects are eliminated. Finally, detection of either a fundamental or harmonic of the gating pulse, allows processing to take place in a higher frequency region where 1/F noise from detectors and amplifiers is minimal. The only disadvantage in the use of this module is that sensitivity is reduced due to the loss of signal intensity caused by the reduction in overall harmonic content. Detection and processing of a single frequency is valid, since it can be demonstrated that all the photons in the light pulse contribute to the measurements at each frequency [3].

The second option for further increasing the SNR is the capability of preforming signal averaging in software. In its simplest form, signal averaging is just the summation of signals in memory. If the noise is truly random, it will have a mean value of zero and a constant rms value. After n summations, the rms signal amplitude will have increased by n , while the noise will have increased by only $n^{1/2}$. Thus, the SNR at any point is improved by a factor of $n^{1/2}$ [101].

4.2. Overall System Design

The overall design (Fig. 4.1) was kept as modular as possible, both internally and externally, for easy system access and modification. The main subsystems have been placed into four separate enclosures. These subsystems are the excitation source, optics, photodetectors, and electronics. Connections between subsystems are achieved either by means of 500 μm core optical fibers, for optical subsystems, or shielded coaxial cable terminated with BNC connectors for electrical subsystems. Control over the total system state and parameter settings is achieved using an Apple 2E microcomputer.

Step index optical fibers (Polymicro Technologies, FHP 500/600/630) were used for this study. These fibers have a synthetic silica core of 500 μm diameter encased within a doped silica cladding containing a thin polyimide outer buffer coating (Fig. 4.2). These materials give a durable low fluorescence optical fiber of approximately 630 μm in total diameter, a numerical aperture of 0.22 resulting in a full angle acceptance cone of 25.4 C°, and an attenuation of less than 50 dB/km at a wavelength of 400 nm. These fibers are placed within black Teflon sleeving (Alpha Corp.), in order to ease handling and reduce coupling of stray light into the fiber, before being terminated in LFR (Amp, Inc.) style optical connectors of the appropriate size.

The general operation of this instrument is as follows. Light energy from the flashlamp subsystem is bandpass filtered in the near uv and focused into the input of an optical fiber (Fig. 4.3) using a filter and a series of lenses contained within this module. Both the flash rate and intensity are under computer control. The distal end of this fiber connects to the direct pH input of the optical subsystem. Contained within the first of two modules inside of this subsystem is a dichroic beam splitter (LPF 1) which reflects the short excitation wavelengths (< 420 nm) toward the sensor output. These wavelengths excite the 1,4-DHPN present near the tip of the

sensor fiber and the backscattered fluorescence is returned by the same fiber to the dichroic beamsplitter. Since the fluorescence is red shifted, relative to the excitation wavelengths, transmission of fluorescence (> 430 nm) out of the first module and into the second module takes place. Within the second module, an achromatic beamsplitter (BS) and narrowband interference filters (F1 and F2) isolate the two wavelengths of interest and couple them into two separate output fibers.

The other end of these output fibers can either be connected to photomultipliers contained within the photodetector module or to PIN photodiodes contained within the electronics module. In the case of photomultipliers, the electrical output signals are coupled into the external inputs of the electronics module by means of coaxial cables. The optical amplification of each tube can be separately controlled by the computer. For PIN photodiodes, the electrical signal is directly connected to the front end electronics within the electronics module.

The electronics module (Fig. 4.4) contains two identical electronic channels which simultaneously process each optical signal. The current from each photodetector is first converted to a voltage. This voltage is then either integrated directly or patched, via coaxial cables, into and out of a second optional module for bandpass filtering and rms-to-dc conversion before integrating. The integrated pulse is then passed to a sample and hold stage, after appropriate gain equalization and polarity correction.

Output of the sample and hold circuitry of each channel is routed out of the electronics subsystem and is sequentially multiplexed onto the input of an A/D converter card contained within the Apple 2E microcomputer. The digitized signals are then further processed, displayed and stored.

A detailed description of each subsystem is given below.

4.3. Excitation Source

A bulb type Xenon flashlamp (EG&G FX-198), operating at a low repetition rate, is used as a synchronous source of excitation.The efficiency of this type of flashlamp can be as high as 15% when operated with 0.1-1.0 joules of input energy. Light output is very rich in blue and ultraviolet and is made up of a line structure superimposed on top of a strong high temperature continuum [1]. Approximately 11% of the optical energy is confined in the 300-400 nm range of interest. Flash duration, measured at one-third peak amplitude, can be calculated to be approximately 3.2 μs for the value of the discharge capacitor selected. Flash delays after triggering of less than 2.0 μs, timing jitter of less than 200 ns, and pulse output amplitude variation of less than 5% have all been reported for this type of flashlamp.

The output of this lamp (Fig. 4.5) is collimated by a parabolic reflector (Melles Griot, 02 RPM 006) with a focal length of 10.2 mm adjusted to coincide with the electrodes of the flashlamp. The near parallel beam from this source is then condensed and shaped by a pair of plano-convex lenses (Melles Griot, 01 LPX 281 and 01 LPX 108), with respective focal lengths of 200 and 50 mm, arranged in a confocal fashion with the larger lens closest to the flashlamp and plane surfaces facing each other. This gives a parallel light beam of smaller diameter which is then filtered by a shortpass filter (Dell Optics Co.) with an average transmission of 25% from 340 -380 nm and blocked to an average O.D. of 6 from 430-1000 nm. This parallel near uv component is then focused onto the launch end of the output optical fiber via an aspheric condensing lens (Melles Griot, 01 LAG 000) with a focal length of 8.5 mm. The aspheric surface minimizes spherical aberration, allowing a much shorter focal length for a given diameter than a spherical lens of equal spherical aberration. This results in low f-numbers, thus maximizing the collecting area of the lens and concentrating more energy into the fiber located at its focus. All

flashlamp optics are mounted in a brass cylinder with a diameter of 15 cm and an overall length of approximately 69 cm. Provision is made to allow slight adjustment of the long focal length lens with respect to the flashlamp in order to maximize energy coupling into the optical fiber.

The flashlamp electronics (Fig. 4.6) are housed in a 23 x 15 x 13 cm aluminum box secured to one end of the brass cylinder. This enclosure contains a 24 V at 2.5 A low voltage supply (Power One), a 300-1500 V programmable HV supply (EG&G PS-350), a flashlamp Lite-Pac trigger transformer (EG&G FYD-506), and two 1 μF energy storage capacitors, connected in parallel, and rated at 2 kV. The high voltage is programmed over its full range by means of a 2-10 VDC external reference supplied by the Apple 2E microcomputer via an 8 bit D/A card (Applied Engineering) residing in slot 3. Since the flashlamps maximum average power is rated at 10 W in free air, this puts restrictions on the flash frequency/output energy combinations, and thus indirectly on the maximum high voltage for any selected flash frequency (Figs. 4.7 and 4.8). Software allows the output energy of the flashlamp to be selected in the interval 0.1-2.25 joules. The computer then sets the high voltage to the appropriate value for the required energy and computes the highest permissible flash frequency selected to the closest 4 Hz increment, in the range 4-100 Hz. Manual override of this frequency selection is also allowed. The flashlamp trigger signal is also supplied by the computer system via a single output line of a parallel interface card (John Bell Engineering, Inc.), residing in slot 2. This drive capability of this TTL level is increased by means of a line driver residing on the interface board at the back of the electronics subsystem. Both the flashlamp reference voltage and the boosted trigger signal are available via BNC connectors mounted on the front panel of the electronics subsystem.

4.4. Optical Subsystems

The optical subsystem is composed of two separate modules: a dedicated sensor module and an optical detector module. These modules are similar in overall design and were fabricated out of black Deldrin to decrease the weight of the optical system and to prevent stray reflections from degrading performance. Each module (Fig. 4.9) currently measures approximately 5 x 5 x 10 cm with a T-shaped 2.54 cm diameter optical path machined in the plastic. Each of the three openings on a module interfaces with a standard fiber optic connector through a specially designed adaptor. On the back side of each adaptor is a holder which can accommodate a 12 mm diameter lens and up to two 12.5 mm normal incidence filters. The distance between lens and fiber can be manually adjusted. This allows alignment of the lens so that the amount of light coupled to the optical fiber can be maximized. Currently an aspheric condensing lens with a focal length of 8.5 mm (Melles Griot, 01 LAG 000) is being used.

Along the long axis of the module is a moveable mount for holding either a 19 mm diameter longpass filter or beamsplitter at a 45° incidence angle. All optics in this system, except for the lenses, were custom made by Dell Optics Company (North Bergen, N.J.) according to provided specifications. Optical coupling into and out of each module is accomplished by means of the optical fibers previously described. The modular design of such a system allows compartmentalization of the optical assembly. This makes the system extremely flexible since changes within a module can be easily made and their effect on total system performance can readily be measured. Furthermore, all modules can be made optically unique in spite of being mechanically similar.This enables complex systems to be built for performing specialized measurements.

The operation of the optical subsystem is as follows. Energy from the excitation module is focused by an aspheric condensing lens into the input of the

sensor module. This module consists of a dichroic beam splitter that is used to reflect excitation wavelengths below 420 nm toward the sensing fiber. Fluorescence from this fiber at wavelengths longer than 430 nm are transmitted by this dichroic device and coupled into the exit fiber. The broadband fluorescence output from this fiber then enters the detector module where it is again beamsplit, but this time by a 50/50 achromatic beamsplitter. This beamsplitter divides the fluorescence signal into two components. Each component is passed through a 10 nm narrowband interference filter centered at either 434 or 488 nm. Each of these filters has a peak transmission in the passband of approximately 70% and is blocked outside of this band to an O.D. of 4. The output from these filters is then coupled out of the optical subsystem and into the appropriate photodetectors using the usual optical fibers.

4.5. Photodetectors

Either PIN photodiodes or photomultiplier tubes may be selected as the photodetectors in this system. The PIN photodiodes make use of an extra high resistance (intrinsic) I layer between the P and N layers. This increases the width of the depletion region resulting in lower junction capacitance. As a result, the speed of this device is much faster than a conventional PN photodiode. Extremely low noise and low dark current are also characteristics of PIN devices.

The PIN photodiodes used in this system (Hamamatsu, S1722-01) are uv enhanced silicon photodiodes. Both diodes are housed in TO-8 style packages and are located within the electronics subsystem. They have a surface area of 13.2 mm^2, a radiant sensitivity of 0.20 A/W at 450 nm., a typical dark current of 30 nA, a junction capacitance of approximately 12 pF, and a shunt resistance of approximately 100 MΩ. The noise characteristics of this device are set by the sum of the thermal noise, caused by the shunt resistance, and the shot noise resulting from the dark current and photocurrent. The signal characteristics are determined

by the junction capacitance, effective surface area, and radiant sensitivity. Taken together, these parameters determine the SNR of the device and the theoretical lower limit of light detection by this photodetector. The minimum signal power on a detector that produces an rms SNR of 1 is defined as the noise equivalent power (NEP) for that detector. The lower the NEP, the more sensitive is the detector. For the photodiodes used in this system the NEP has been found to be approximately 100 fW/$\sqrt{Hz}$, when measured at the wavelength of peak radiant sensitivity. The actual lower limit of detectability, for such a device in an actual circuit, will be primarily determined by the characteristics of the optical signal and the performance of the front end circuitry [98]. Both photodiodes are operated in the current mode using a low noise operational amplifier that effectively holds the photodiode voltage at zero. This is an optimal configuration from the standpoints of response linearity and noise generation.

In order to detect very low intensity optical signals with acceptable SNR, the photomultiplier subsystem should be used (Fig. 4.10). This subsystem contains two 13 mm diameter head-on photomultiplier tubes (Hamamatsu, R1463-01), two regulated programmable HV supplies (Hamamatsu, C1309-04), two voltage divider socket assemblies (Hamamatsu, E849-35), and one 15 V at 1 A low voltage supply (Power One). These components are housed in an aluminum enclosure to which optical input and electrical input and output connections can be made. The gain of the photomultiplier tubes is controlled by the Apple 2E microcomputer, via the programmable HV supplies, using the 8 bit D/A card discussed in Section 4.3. The software controlled 0-10 V outputs of this D/A card are available via the front panel of the electronics subsystem. This voltage is divided down, within the photomultiplier enclosure, allowing high voltages ranging from (-190)-(-1100) V to be generated. This allows current gains ranging from 4 to over 2 x 10^6 using this subsystem.

The NEP of photomultiplier tubes is limited primarily by dark current and its associated noise. The photomultipliers used in this system have a multialkali cathode, an anode radiant sensitivity of 5.1 x 10^4 A/W at 420 nm, and a typical dark current of 10 nA. Using a typical current gain of 1.0 x 10^6, a NEP of approximately 1 fW/$\sqrt{Hz}$ can be calculated. Thus, the NEP of the photomultipliers is at least 100 times lower than that of the PIN photodiodes. This is due to the dynode chain amplification of the photomultipliers being essentially noiseless. As a consequence, the amplified shot noise of the photocathode becomes the primary noise component [22]. As in the case with PIN photodiodes, the front end circuitry plays a crucial role in determining the actual lower limit of detection.

4.6. Electronics Subsystem

The computer controlled electronic subsystem has two principle components, the main module and the optional narrowband filter module. Each of these modules is electrically shielded by being placed inside of a cast aluminum box. These two boxes are then mounted inside of a standard rack mount enclosure. All inputs and outputs are routed from the appropriate aluminum box to the front panel of the rack mount enclosure via BNC connectors and shielded cables. All digital control lines are interfaced between the electronic subsystem and the computer by means of an interface board mounted on the rear panel of the electronics subsystem (Appendix A). The final analog outputs of the electronic subsystem are multiplexed onto the 12 bit A/D converter card (Applied Engineering) residing in slot 5 of the Apple 2E microcomputer.

Two identical electrical channels are available within each module and operate as follows (Fig. 4.11). The low level signal current from either the PIN photodiodes or the photomultipliers are manually selected via a toggle switch (SW1) on the front panel of the electronics enclosure. These currents are directed

into a low noise, low drift, (Burr-Brown , OPA101BM) operational amplifier (U1) configured as a current to voltage converter. The gain of this I/V stage is software selectable in four fixed decade steps. The frequency response of this stage is set at 16 kHz, via lowpass filtering, regardless of the gain setting. This value was chosen as a compromise between minimizing noise and preserving signal characteristics so as to lessen the necessary integration time. A noise analysis of this front end [98] shows that the input voltage noise of the operational amplifier (8 nV/$\sqrt{Hz}$) undergoes a capacitive gain at higher frequencies and becomes the major component of front end output noise. The next most important noise component has been found to be the Johnson noise of the feedback resistors. Output offsets of this front end amplifier can be zeroed via a front panel potentiometer (R5) which forms part of a current injection circuit that has been optimized for low drift.

The output of the previous stage can either be coupled directly to a software controlled Miller integrator stage (U2), or fed out of this module as input to the optional narrowband filter module. The Miller integrator starts integration immediately after the flashlamp trigger, using an operator selected integration period. This stage is implemented using an operational amplifier (Burr-Brown, 3528AM) selected for its low bias current characteristic. This enables one to use long integration times without amplifier saturation. This also allows for long holding times, such as those used in multiple integrations, without objectionable voltage droop due to leakage. Use of a low leakage current polystyrene integrating capacitor also adds to the stability of this stage.

The output of the integrator stage is coupled to a variable gain stage (U3) built around a standard operational amplifier (LM741C). The configuration of this amplifier is switch selectable (SW2) between inverting and noninverting to accommodate both photodiode and photomultiplier type detectors. Four feedback positions are available, each with its own separately adjustable potentiometer. These

are selected in tandem with the switchable I/V ranges, thus allowing separate calibration of each I/V range as well as the ability to balance the electrical gain between channels. The amount of gain can be varied over approximately one decade.

The output of the variable gain stage is coupled to a digitally controlled sample/hold amplifier (U4) (Burr-Brown, SHC298AM) and routed out of the electronics subsystem via a BNC connector mounted onto the rear panel.

The dc level from the sample/hold amplifier is multiplexed onto one of 16 channels of a 12 bit A/D card (Applied Engineering). This card features a 25 μs conversion time and resides in slot 5 of the Apple 2E computer controller.

The narrowband filter module (Fig. 4.12) consists of a very low noise, high Q, Butterworth bandpass filter (U1) (A.P. Circuit Corporation, APB-6-Q12-24Hz), centered around 24 Hz with a 2 Hz bandwidth. The output of this stage is coupled through a high pass filter to a low level DC/RMS converter (U2) (Analog Devices, AD636KD). A unity gain inverting amplifier (U3) (LM741C) is used to achieve correct signal polarity for coupling back into the integrator stage of the main module. A front panel offset adjustment potentiometer (R9) can be used to zero the overall system output when this module is in operation. A frequency of 24 Hz was chosen based upon spectral measurement of noise density. This frequency is a compromise between minimum noise and optimum pulse frequency. When this module is used, signal-to-noise ratio can be improved by taking advantage of the synchronous bandlimited nature of the signal over the uncorrelated wideband background noise.

4.7. Software

The computer control, data acquisition, and output display software is written in combined Applesoft BASIC and 6502 assembly language, running under

the Apple DOS 3.3 operating system, on an Apple 2E microcomputer [26]. During system initialization the DOS 3.3 operating system is relocated to high RAM, thus freeing an additional 10.5 Kbytes of low RAM for use in storing the necessary programs and variables. Relocation is accomplished through use of Memory Management System (MMS) software (On-Line Systems, Coarsegold, CA) executed by the HELLO program during system boot (Appendix B). Upon termination, the HELLO program executes the STARTUP program. This program sets the memory range to be used by Applesoft BASIC, loads the required machine language programs, and then loads and executes the main BASIC program.

The BASIC program (Appendix C) is approximately 1000 lines, with calls to assembly language routines (Appendix D) which occupy approximately 4 Kbytes of memory. In addition, approximately 2 Kbytes of memory are set aside for data storage and communication between high and low level language routines.

Assembly language is used, due to its speed, for both overall system control and data acquisition. Assembly language however is extremely inefficient for communication involving display screen usage and for implementing complex numerical procedures. For these tasks, interpreted Applesoft BASIC was chosen since this language is readily available in the system ROM and allows interactive testing and debugging. Assembly language source code was stored in a sequential text file format and edited, assembled, and debugged using utilities available in the DOS Programmer's Tool Kit Volume II (Apple Computer, Inc.).

Overall system integration is achieved by means of a coordinated interaction between 6502 assembly routines and BASIC routines. The BASIC language supports lower level process control through the use of CALL statements which execute assembly subroutines, PEEK statements which read memory locations, and POKE statements which write memory locations. Thus, control of overall

program execution is possible in BASIC by use of shared memory locations to exchange both variables and data.

The assembly language routines are incorporated into four distinct phases which are called from the main BASIC program at the appropriate point. Phase 1 initializes system hardware and sets all system acquisition parameters with the exception of system gain. Phase 2 sets the overall system gain using either a manual or automatic calibration routine. Phase 3 is responsible for measuring initial system offsets which are subsequently used to correct raw measurement data. Phase 4 initiates the actual measurement of corrected data using a specific acquisition procedure.

The BASIC user interface is detailed in flowchart form (Fig. 4.13). It is comprised of eight distinct sections: initialization, offset adjustment, flashlamp control parameters, integrator control parameters, photomultiplier control parameters, system gain determination, measurement routines, and printer routines. The first six sections configure the system for actual operation and execute in a sequential fashion. Within the final two sections, the user can select from any of the available options.

The measurement and printer routine software supports fixed time point single sample sweep measurements, multiple sample (signal averaging) sweep measurements, variable time interval data file acquisition, fixed time point data file acquisition, statistical processing of data files, and hardcopy output of both data and statistical results.

In single sweep measurements, 10 successive data points are taken. For each data point, a voltage proportion to the integrated signal on each channel is displayed. The ratio of these voltages (CH0/CH1) is also displayed, as well as the percent change in ratio for each successive data point. In addition, the mean and standard deviation of each of these parameters, for the entire data set, is computed

and presented. The multiple sweep measurement routine works in an identical fashion, except that each data point displayed is a user selected average of from (1)-(100) separate data points.

In the data file mode, the user can choose either to acquire 200 single data points in succession at a particular point in time, or acquire up to 200 single or averaged data points separated by a fixed time interval. This interval is selectable in units of either hours, minutes, or seconds, with values ranging from (1)-(32,767). Precision of this time interval is insured by use of hardware generated timing interrupts from a Timemaster II H.O. clock card (Applied Engineering) residing in slot 4 of the Apple 2E microcomputer. Regardless of the mode selected, eight parameters are stored to disk. These include baseline levels for channel zero and channel one as well as raw measurement data for each channel, the ratio (CH0/CH1), and standard deviations for channel zero, channel one, and the ratio. In the case of fixed time point data files, baseline levels will be equal for all data points in the file and all standard deviations will be set equal to zero.

The statistical processing routine reports minimum and maximum values for each of the parameters in the data file, along with the mean, variance, and standard deviation associated with those parameters. Hardcopy printed output of this information is supported via an Epson FX-100 printer attached to the computer system by means of a Parallel Pro interface card (Applied Engineering) located in slot 1.

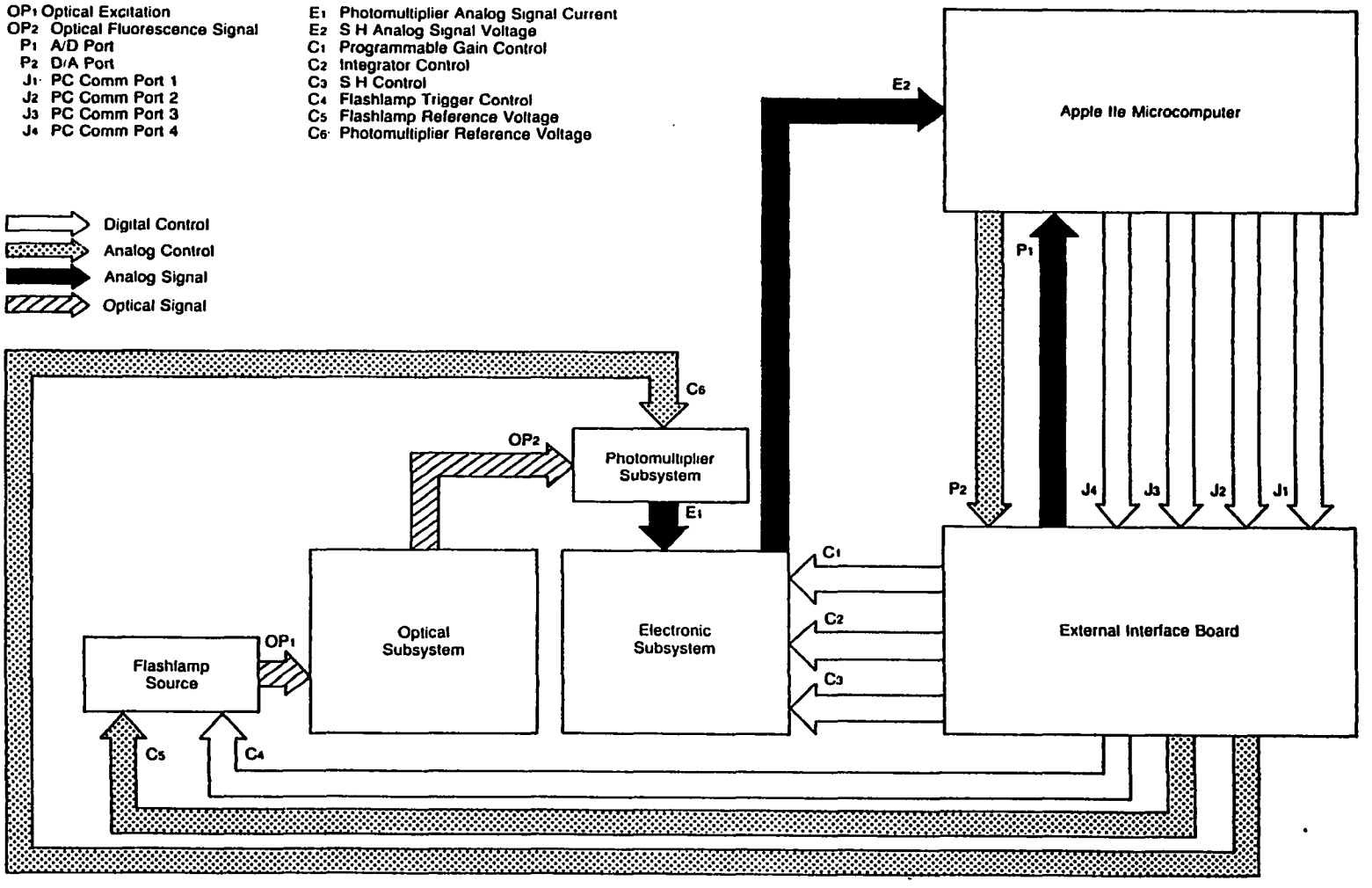

Figure 4.1. Modular overview of the entire fluorescence ratio based pH measurement system.

Silica Fiber

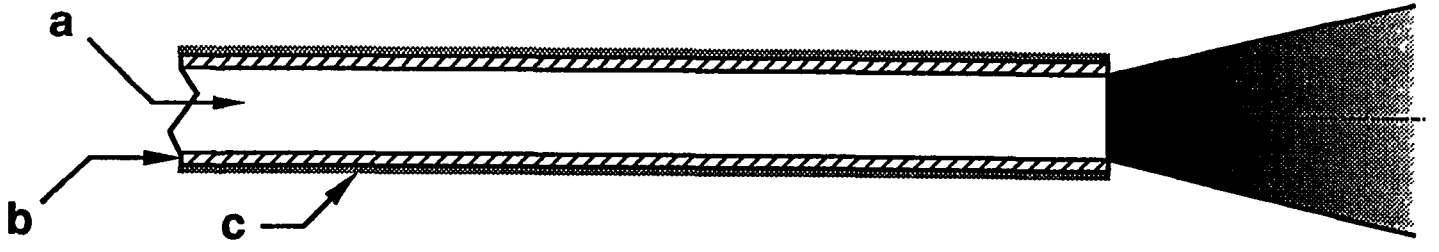

	Component	Material	Thickness
	a. Core	synthetic silica	0.500 mm
	b. Cladding	doped silica	0.100 mm
	c. Buffer	polyimide	0.030 mm

Total Diameter = 0.630 mm

Figure 4.2. Diagram of a typical step index silica core optical fiber.

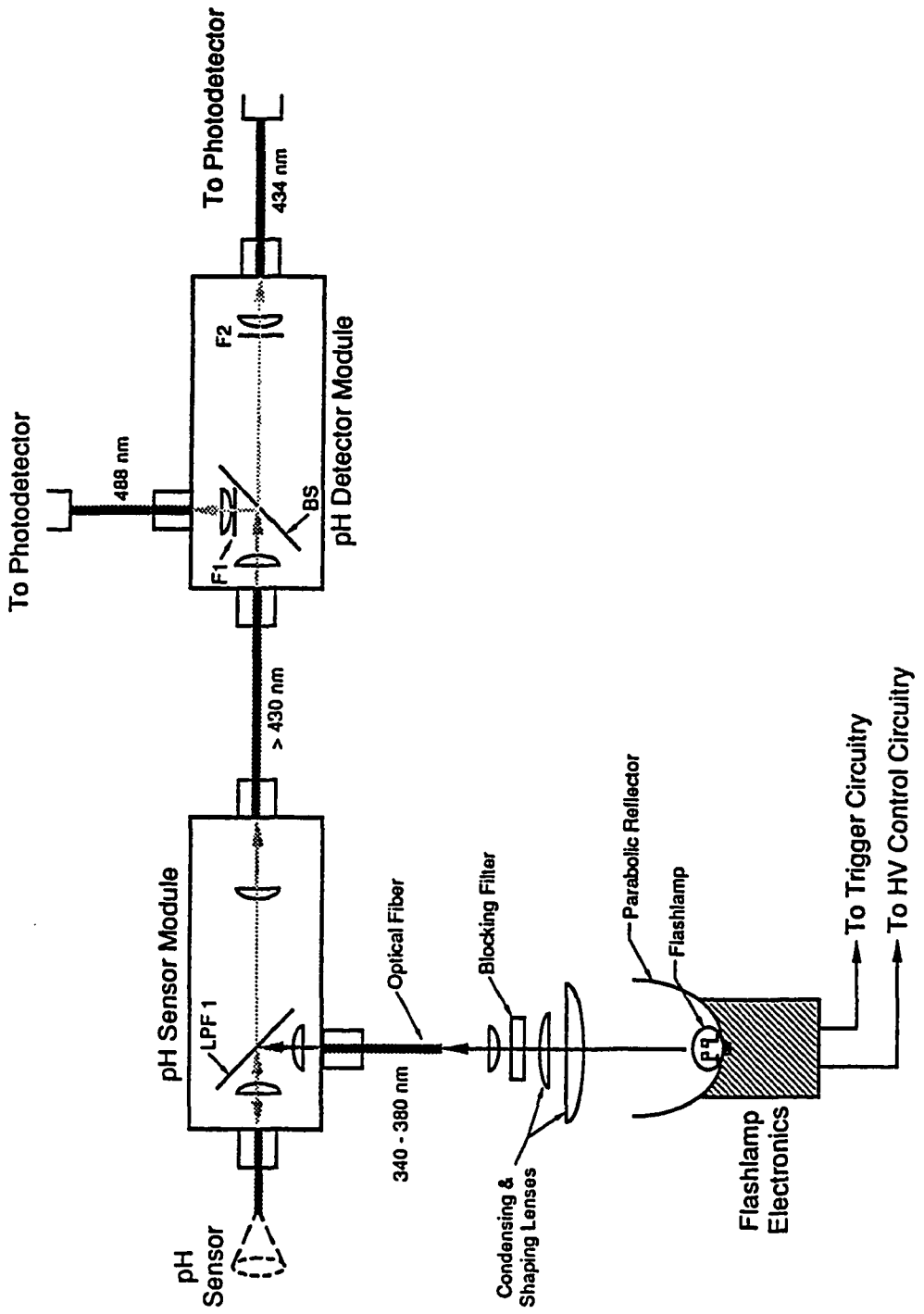

Figure 4.3. Optical diagram of the fluorescence ratio based pH measurement system.

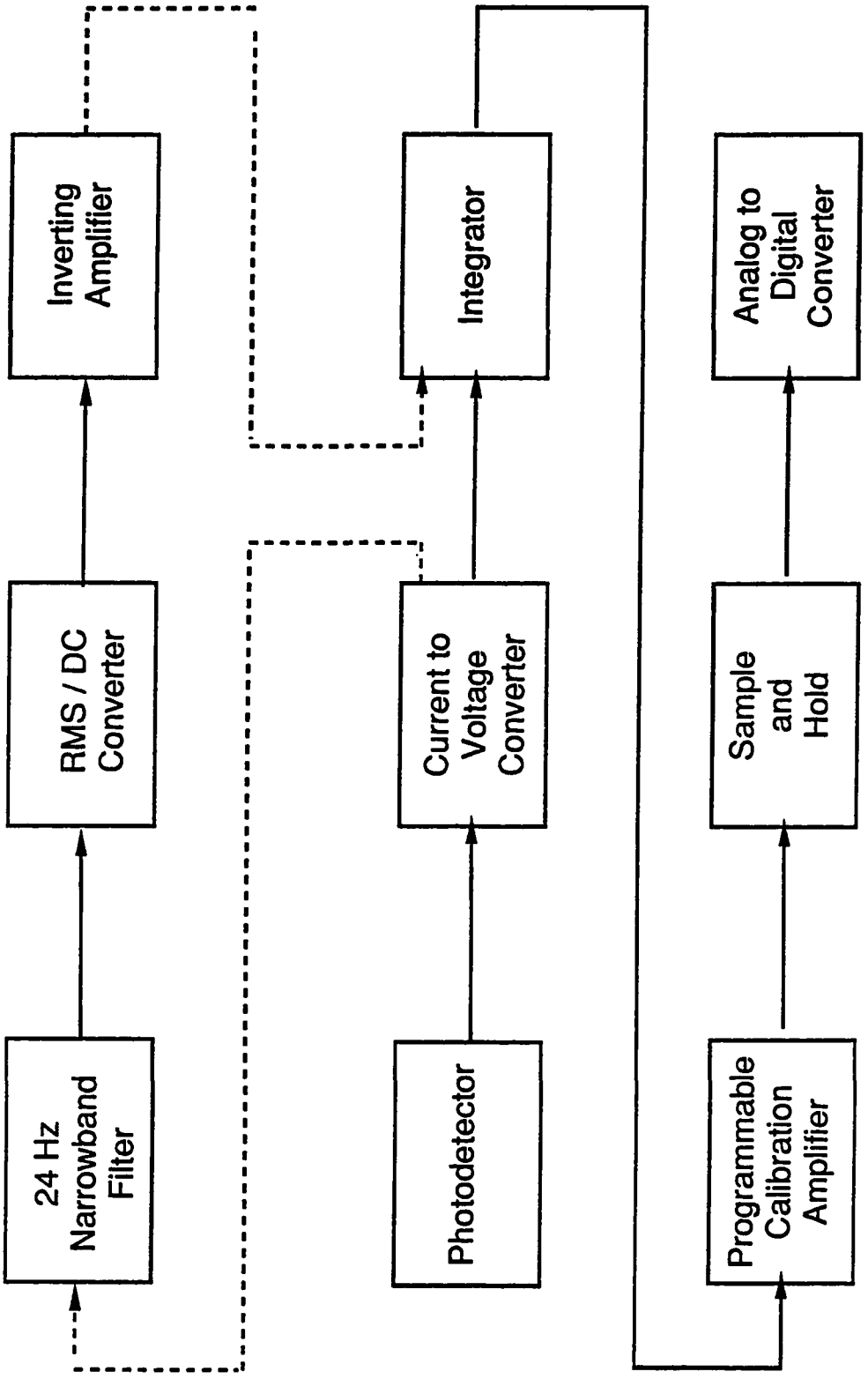

Figure 4.4. Single channel electrical block diagram of the fluorescence ratio based pH measurement system.

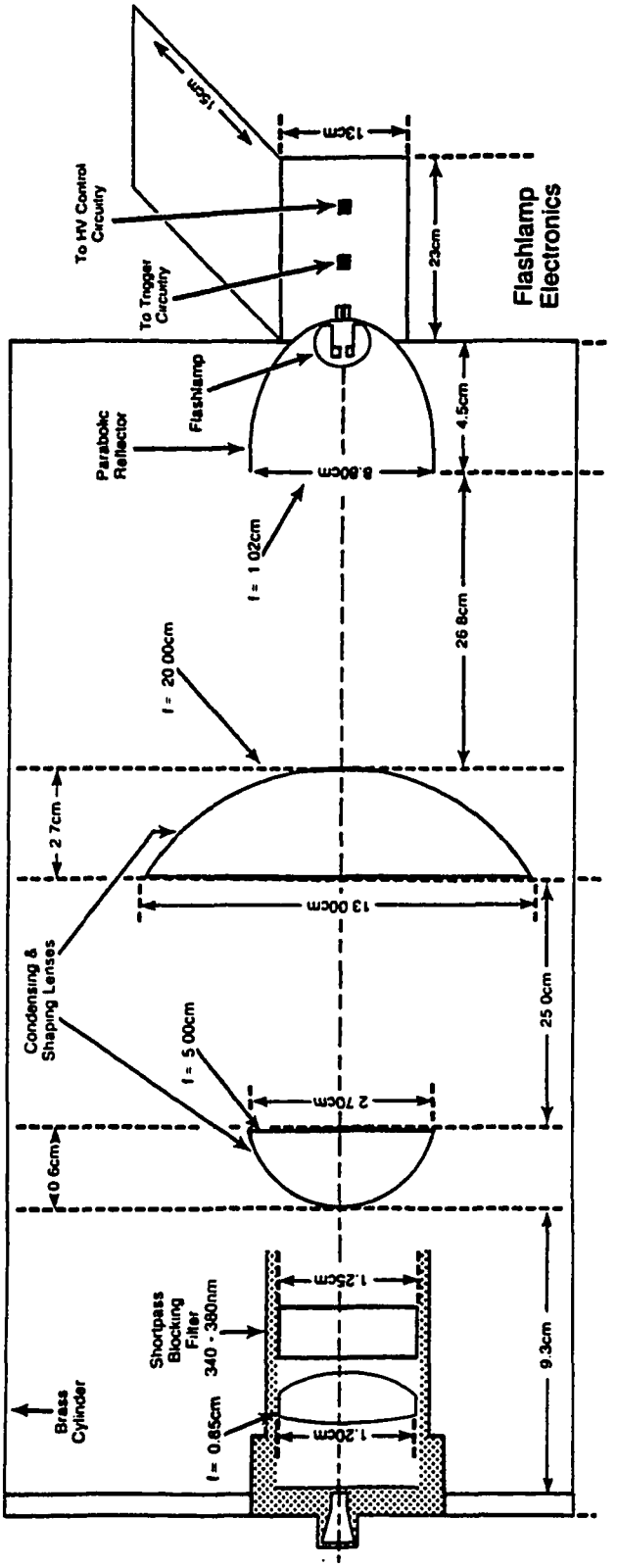

Figure 4.5. Optical diagram of the flashlamp excitation subsystem.

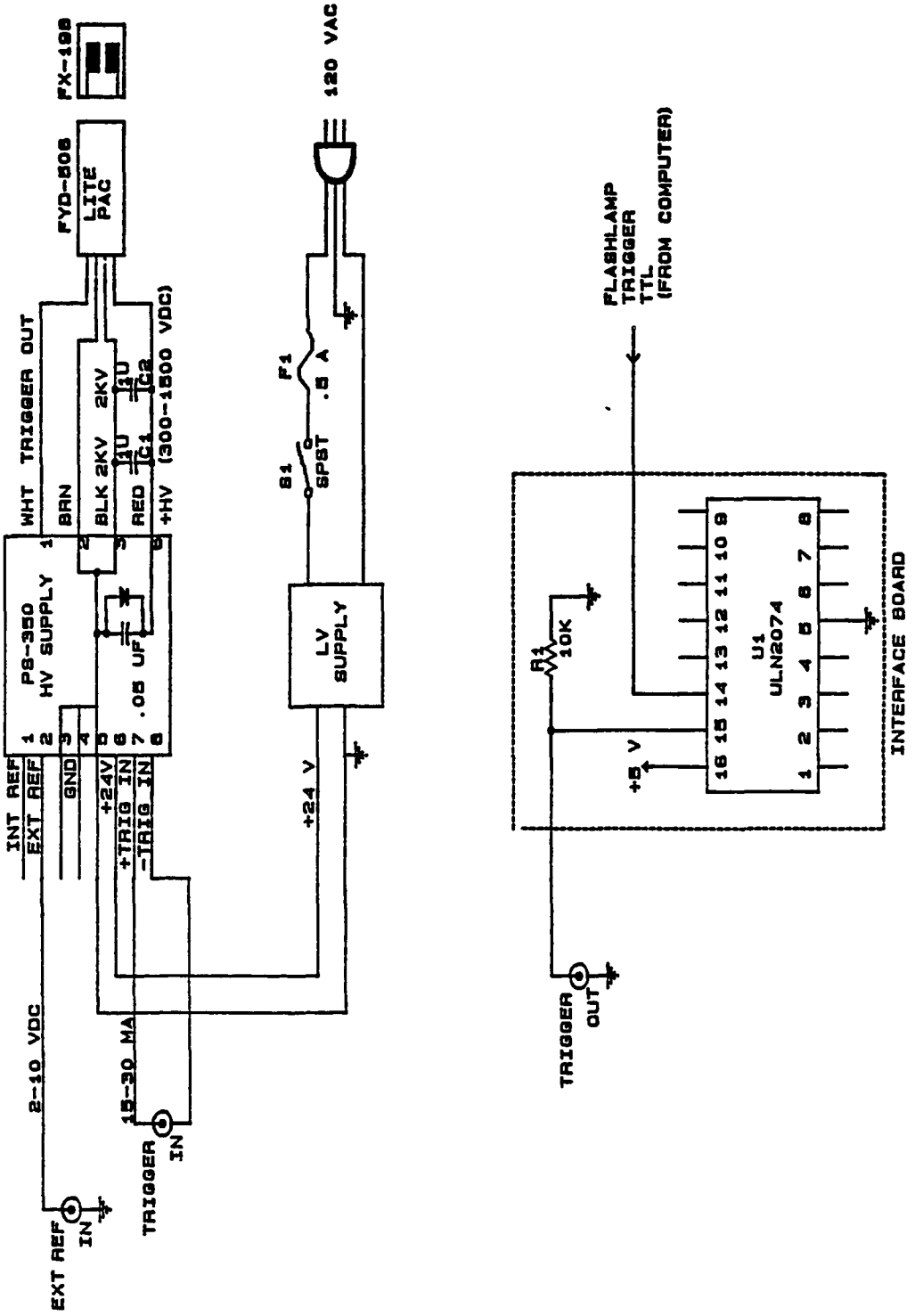

Figure 4.6. Schematic diagram of the flashlamp electronics.

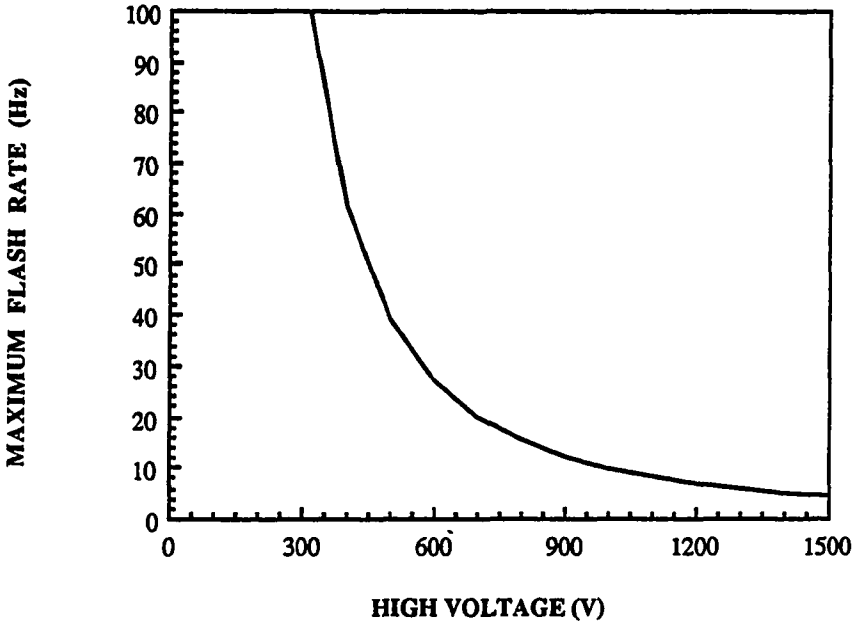

Figure 4.7. High voltage versus maximum safe flashlamp firing rate.

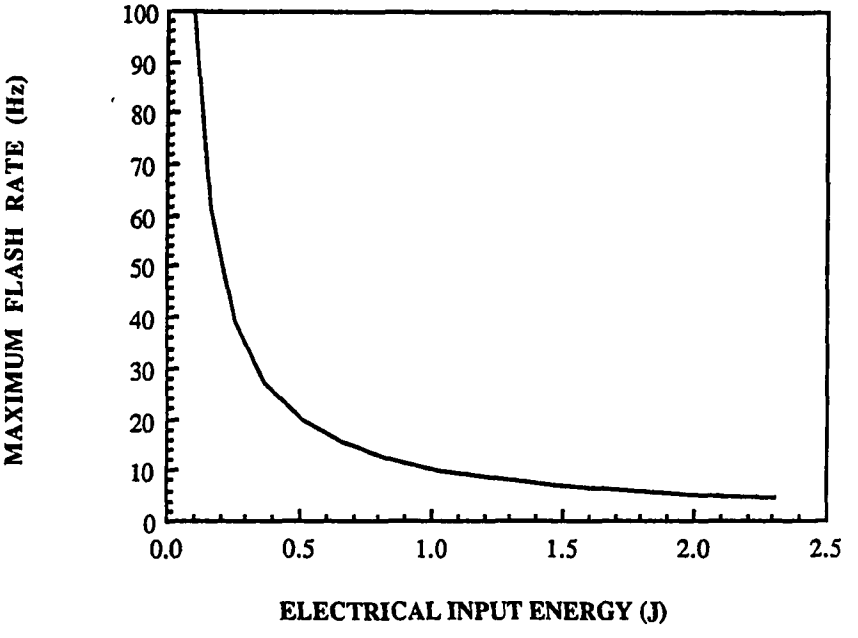

Figure 4.8. Input energy versus maximum safe flashlamp firing rate.

Part # Description

1 Aspheric Lens
Dia. = 12mm
f = 8.5mm

2 Optional
Bandpass Filter
Dia. = 12.5mm
Incidence = 90 deg.
Bandwidth = 10nm

3 50/50 Beam Splitter
Dia. = 19mm
Clr. Aperature = 17.68mm
or
Long Wavepass Filter
Dia. = 19mm
Incidence = 45 deg.
Clr. Aperature = 17.68mm

4 AMP LFR Connector
5/16 - 32, NEF- 2A THD

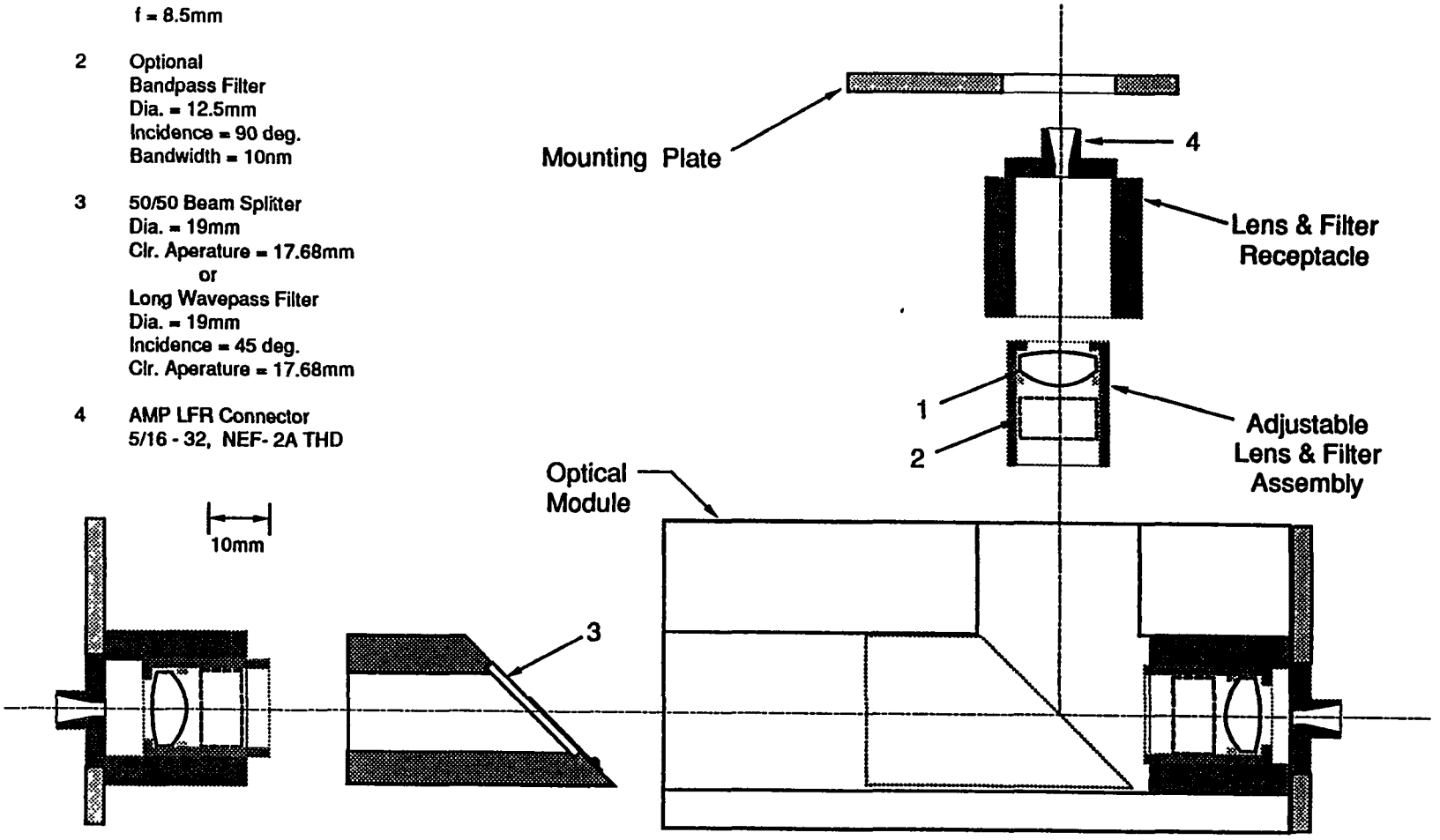

Figure 4.9. Diagram of a typical optical module.

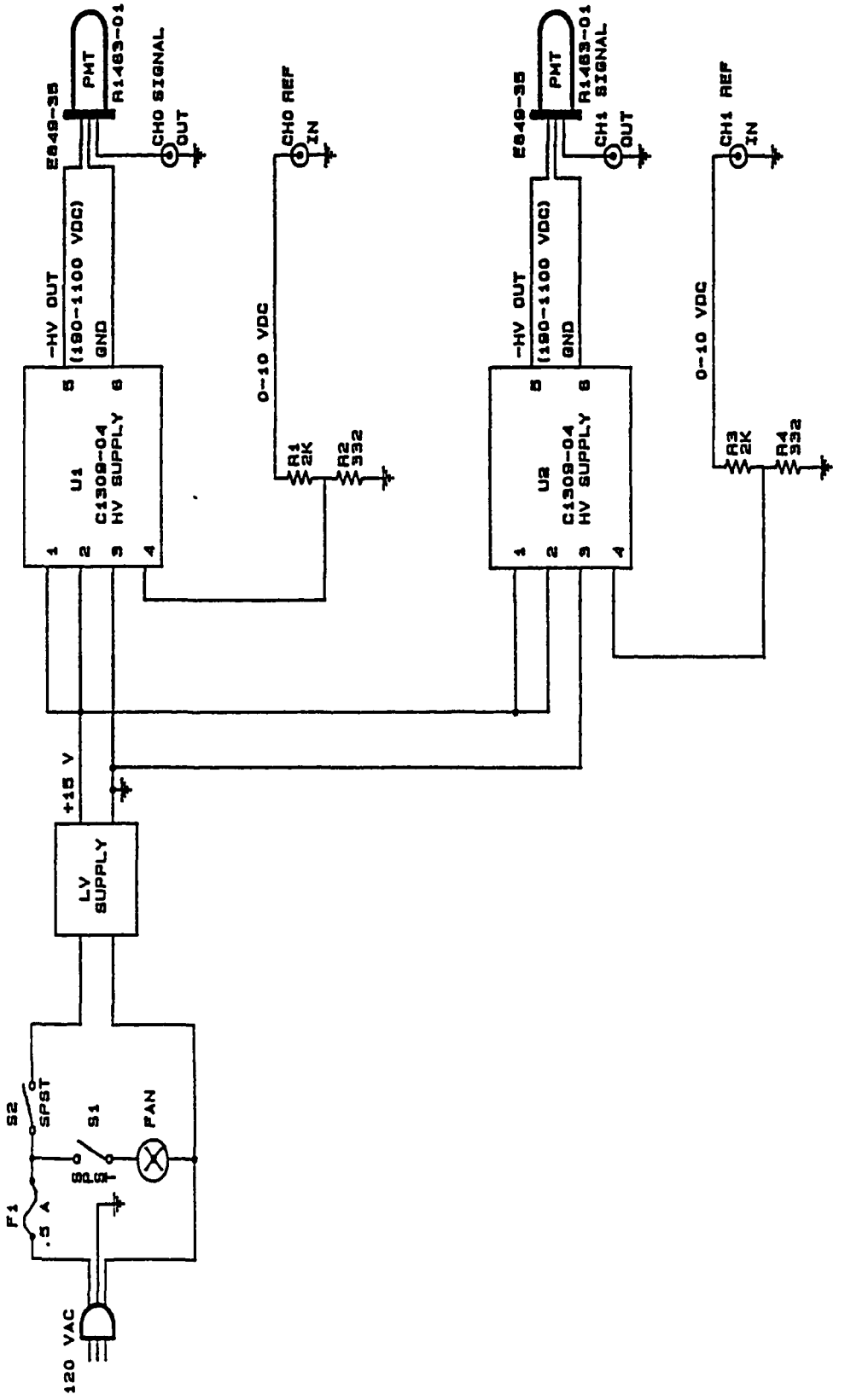

Figure 4.10. Schematic diagram of the photomultiplier electronics.

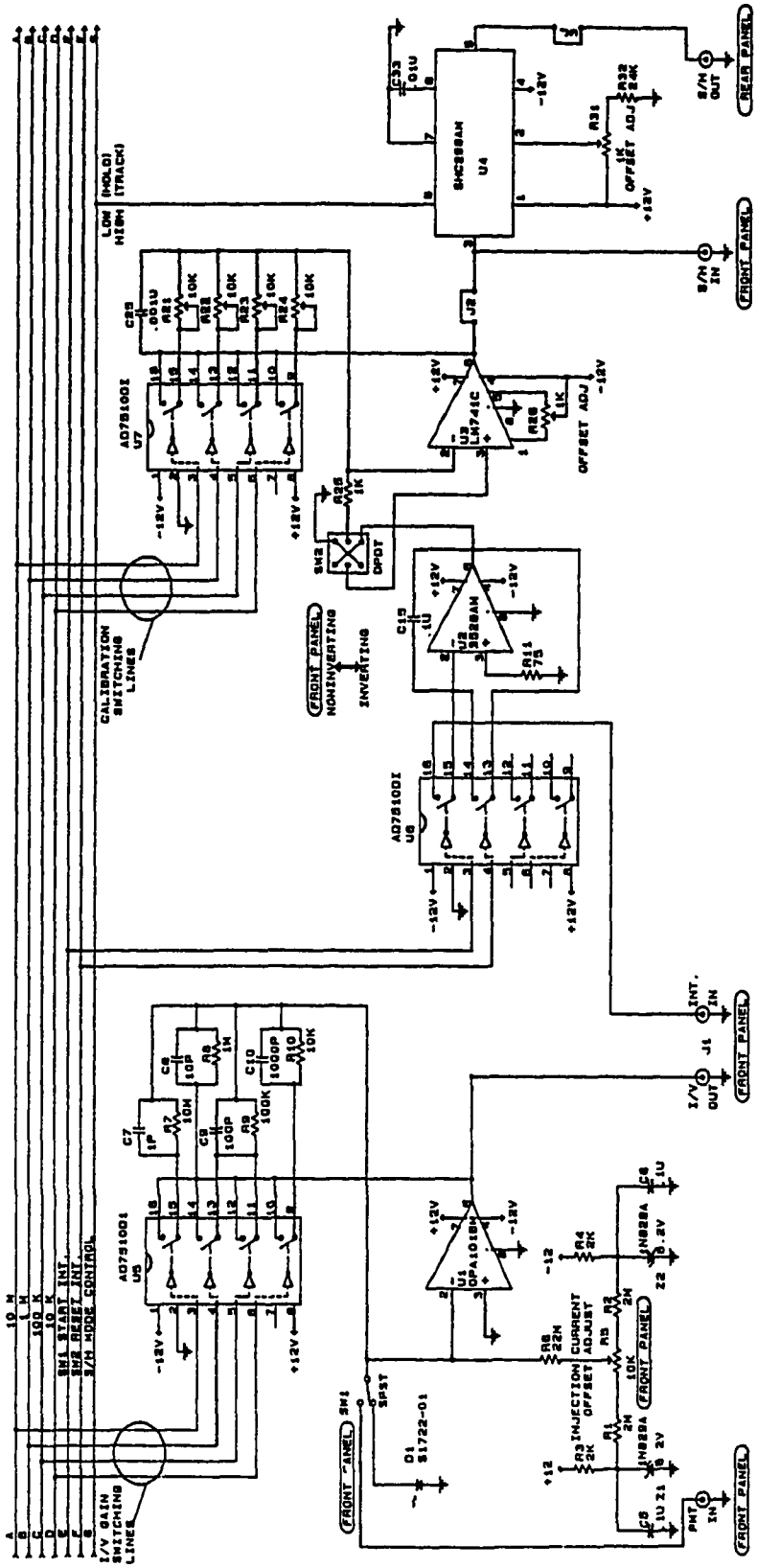

Figure 4.11. Schematic diagram of the wideband electronics module of a single electrical channel.

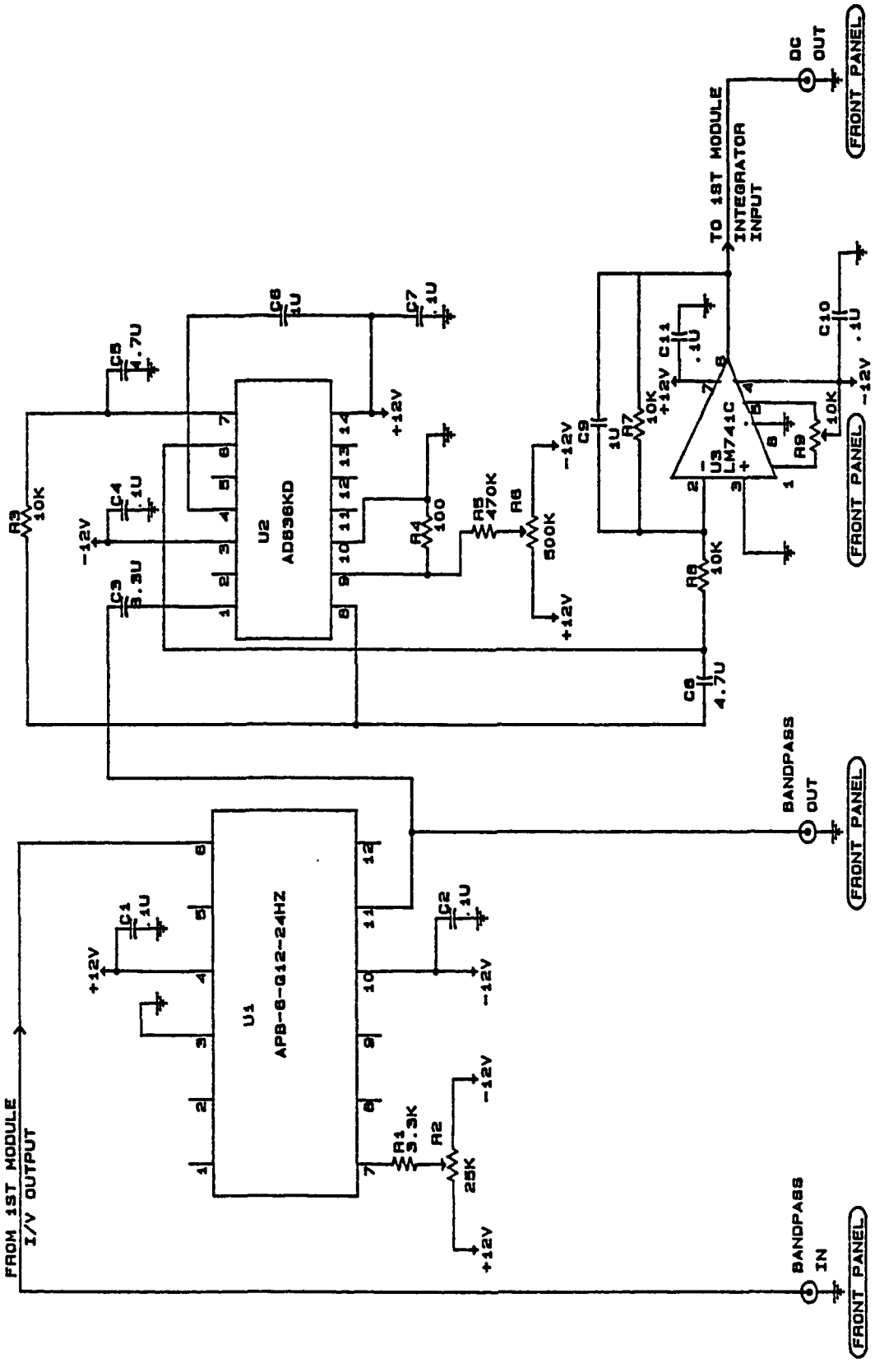

Figure 4.12. Schematic diagram of the narrowband electronics module of a single electrical channel.

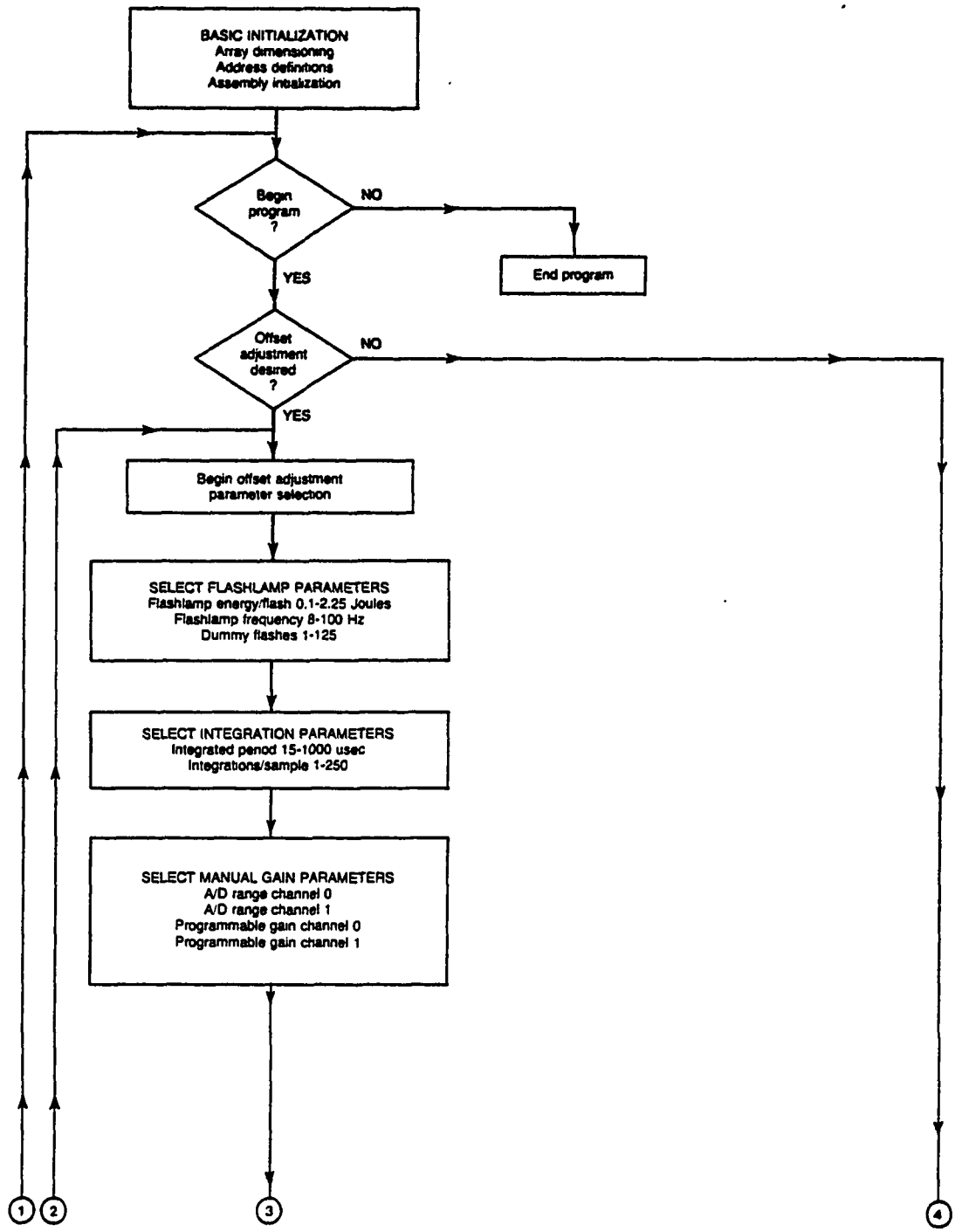

Figure 4.13. Functional flowchart of the the measurement system software (modified from Ehlert, 1988).

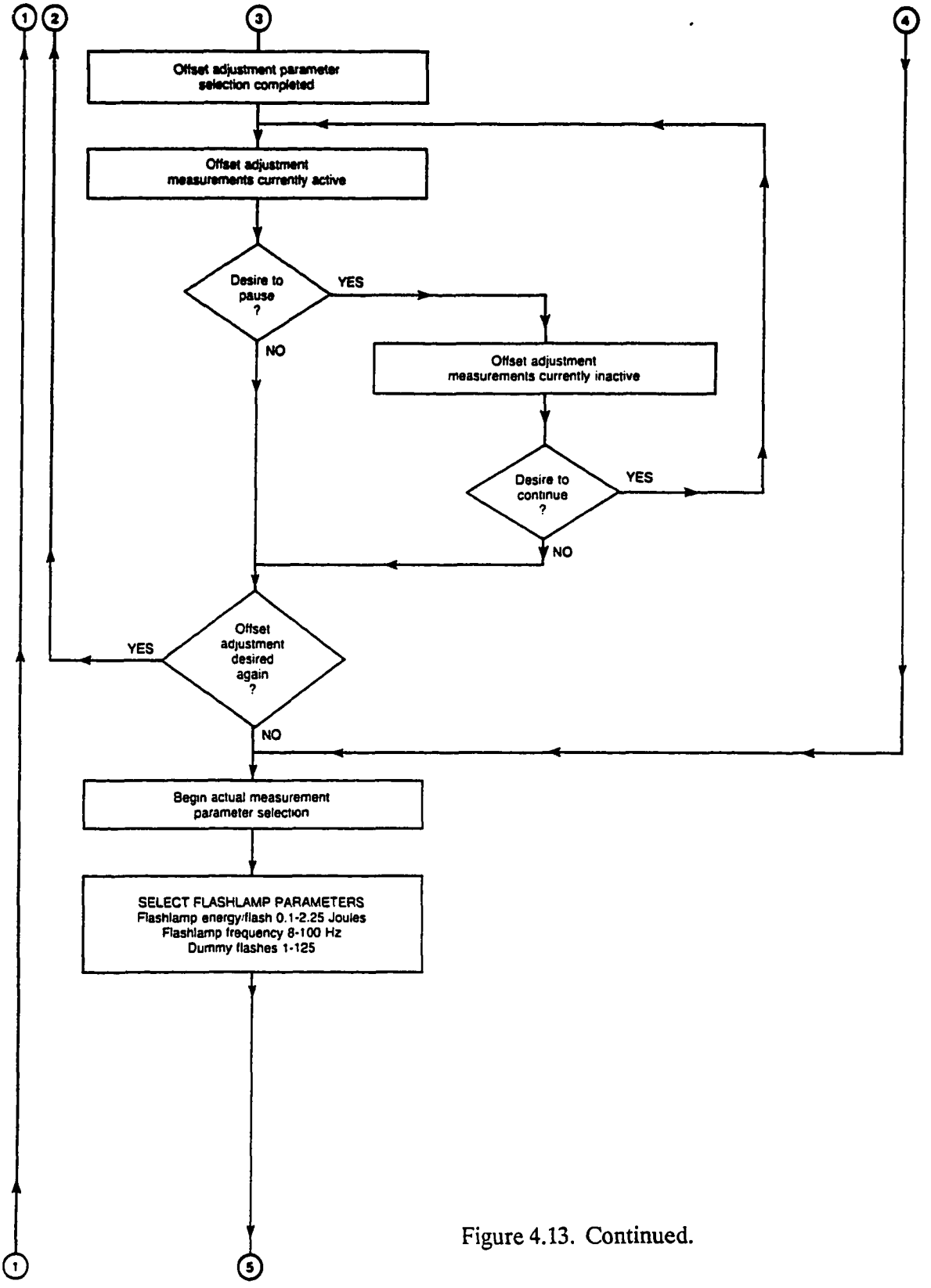

Figure 4.13. Continued.

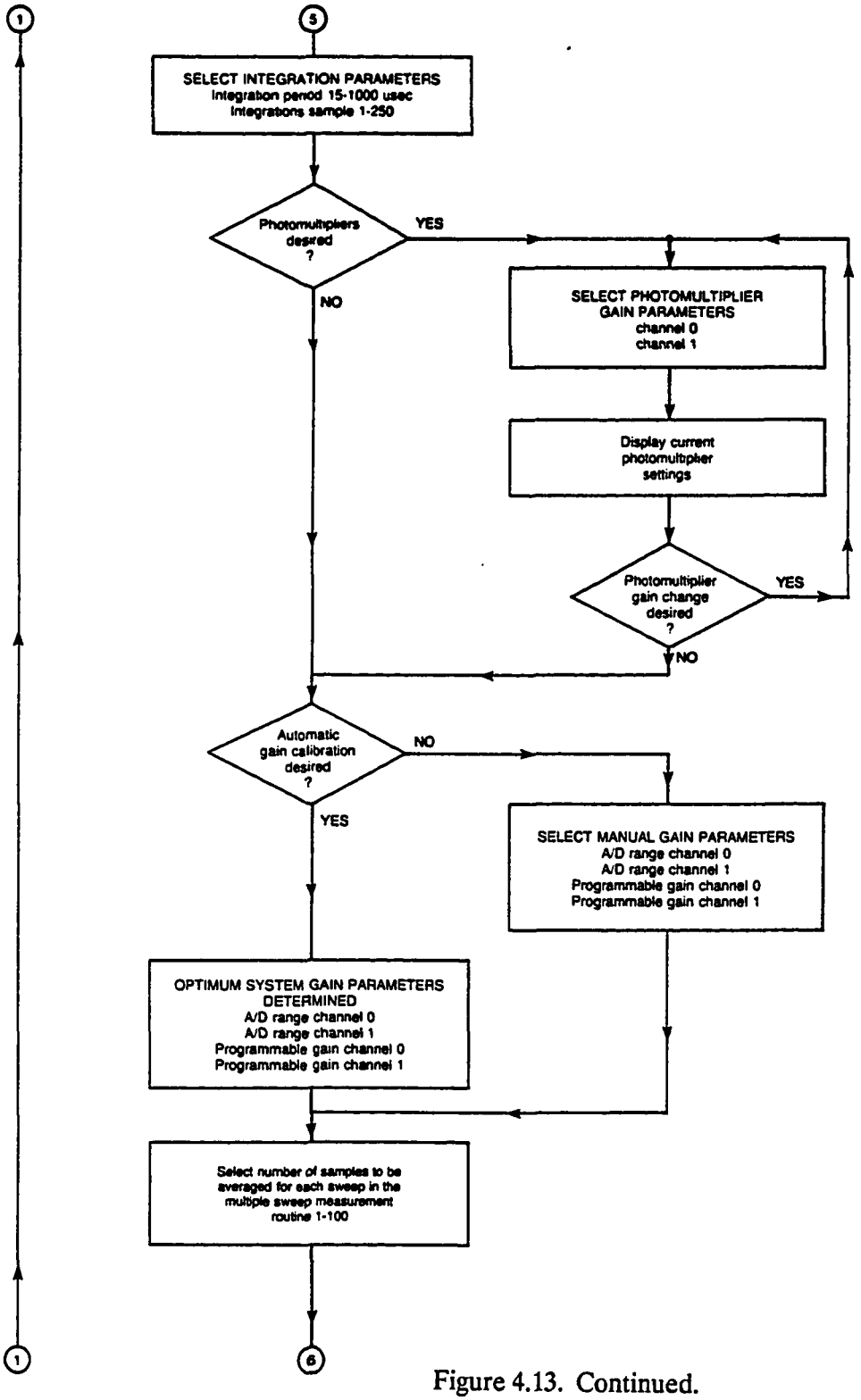

Figure 4.13. Continued.

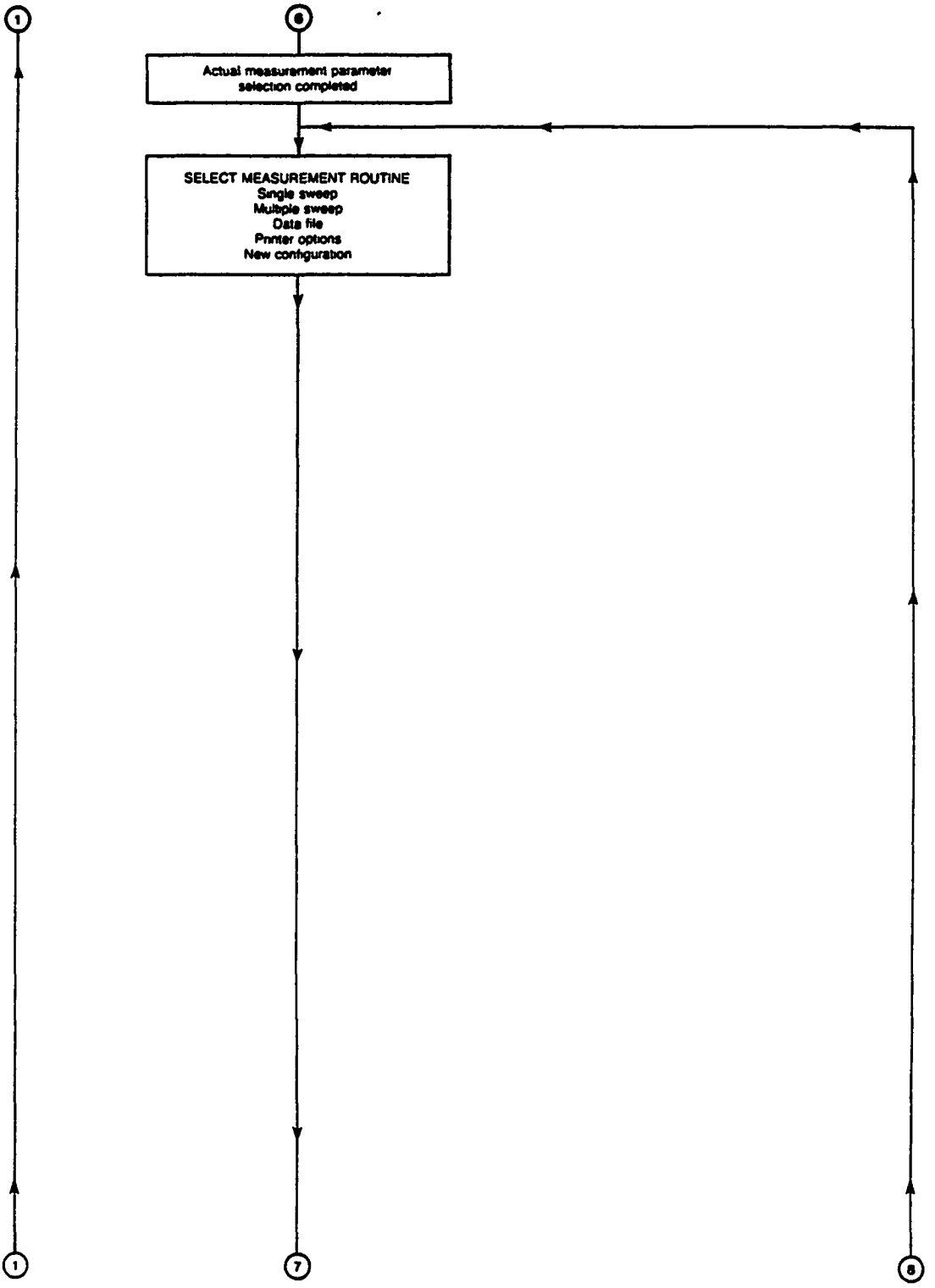

Figure 4.13. Continued.

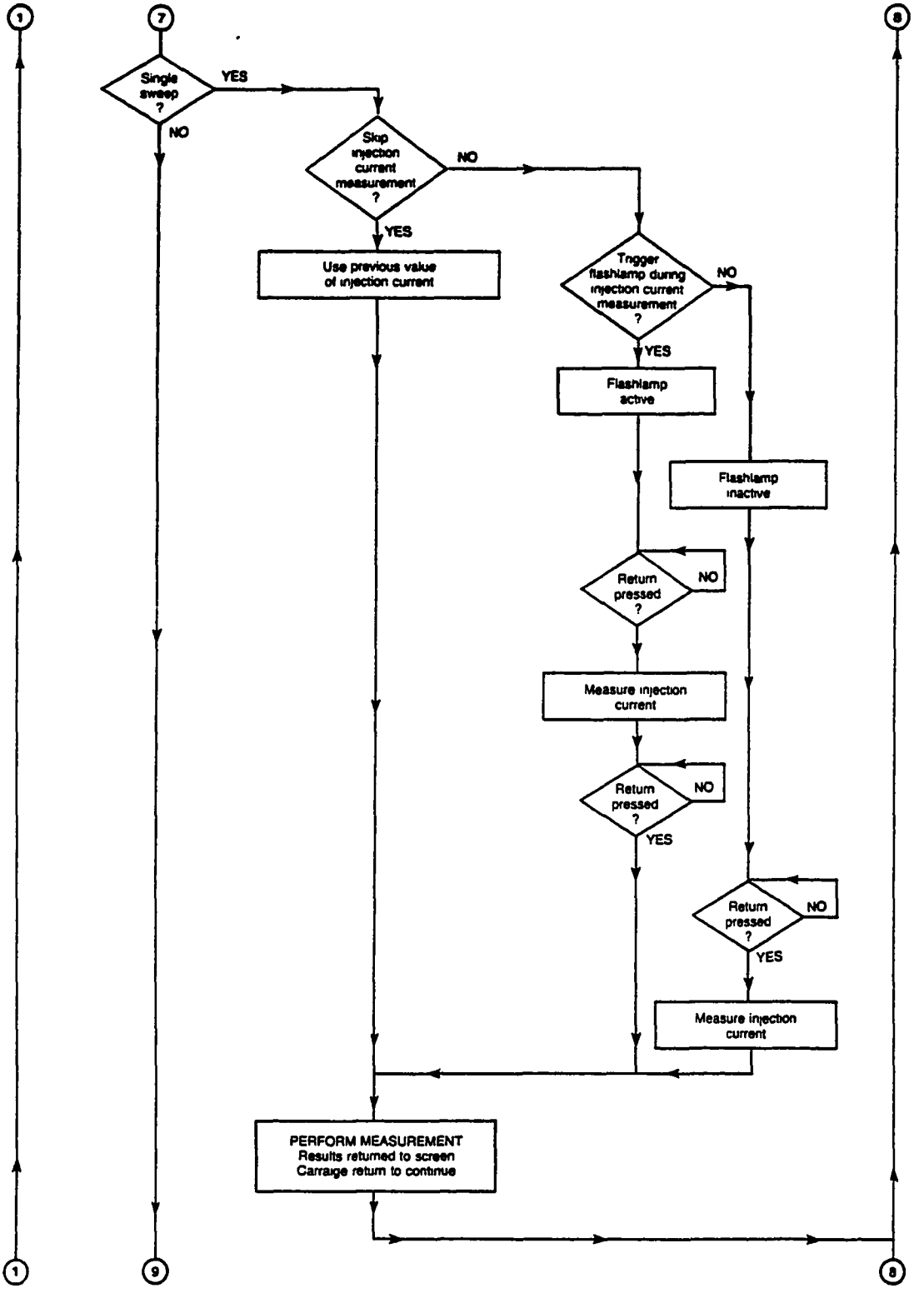

Figure 4.13. Continued.

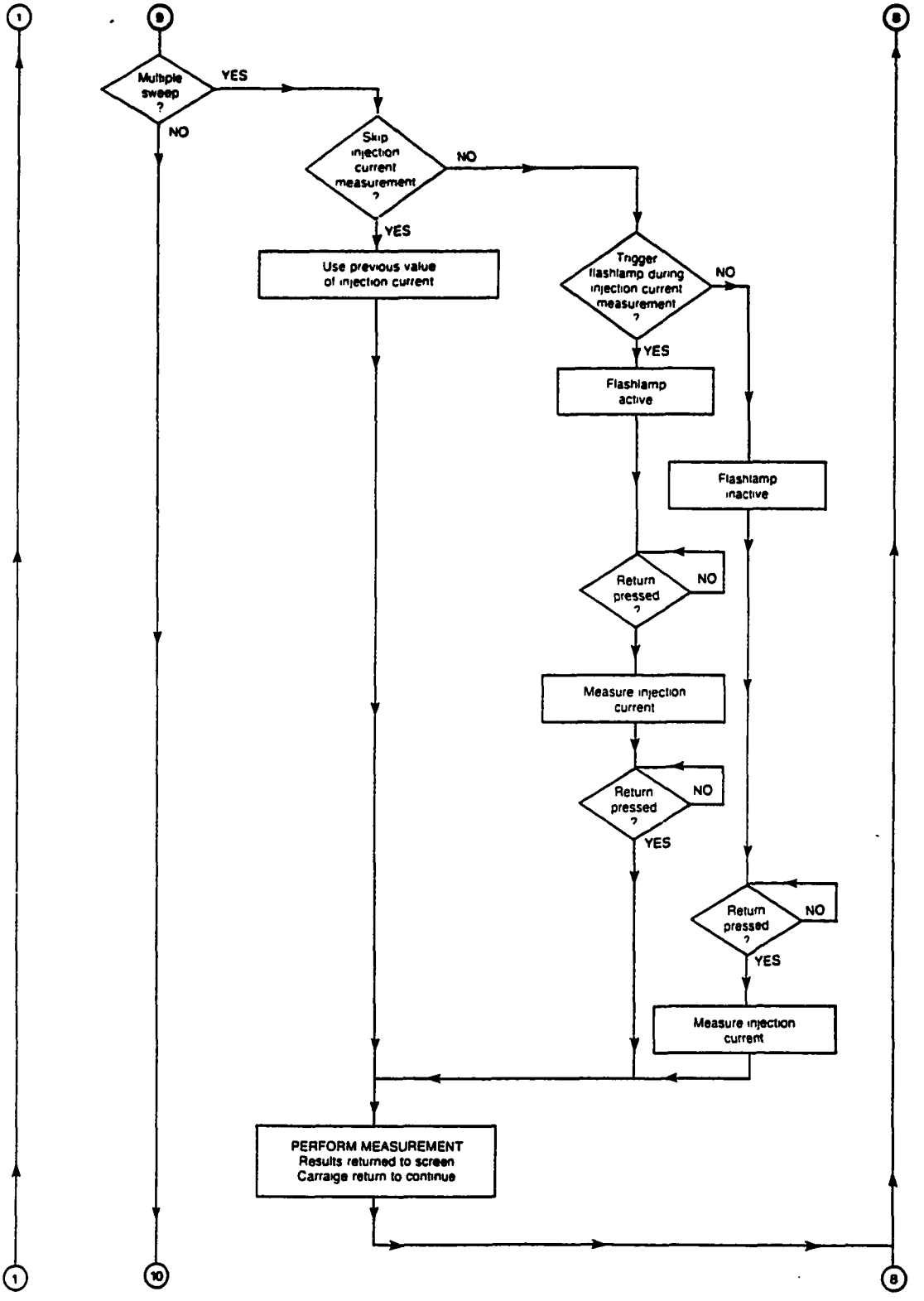

Figure 4.13. Continued.

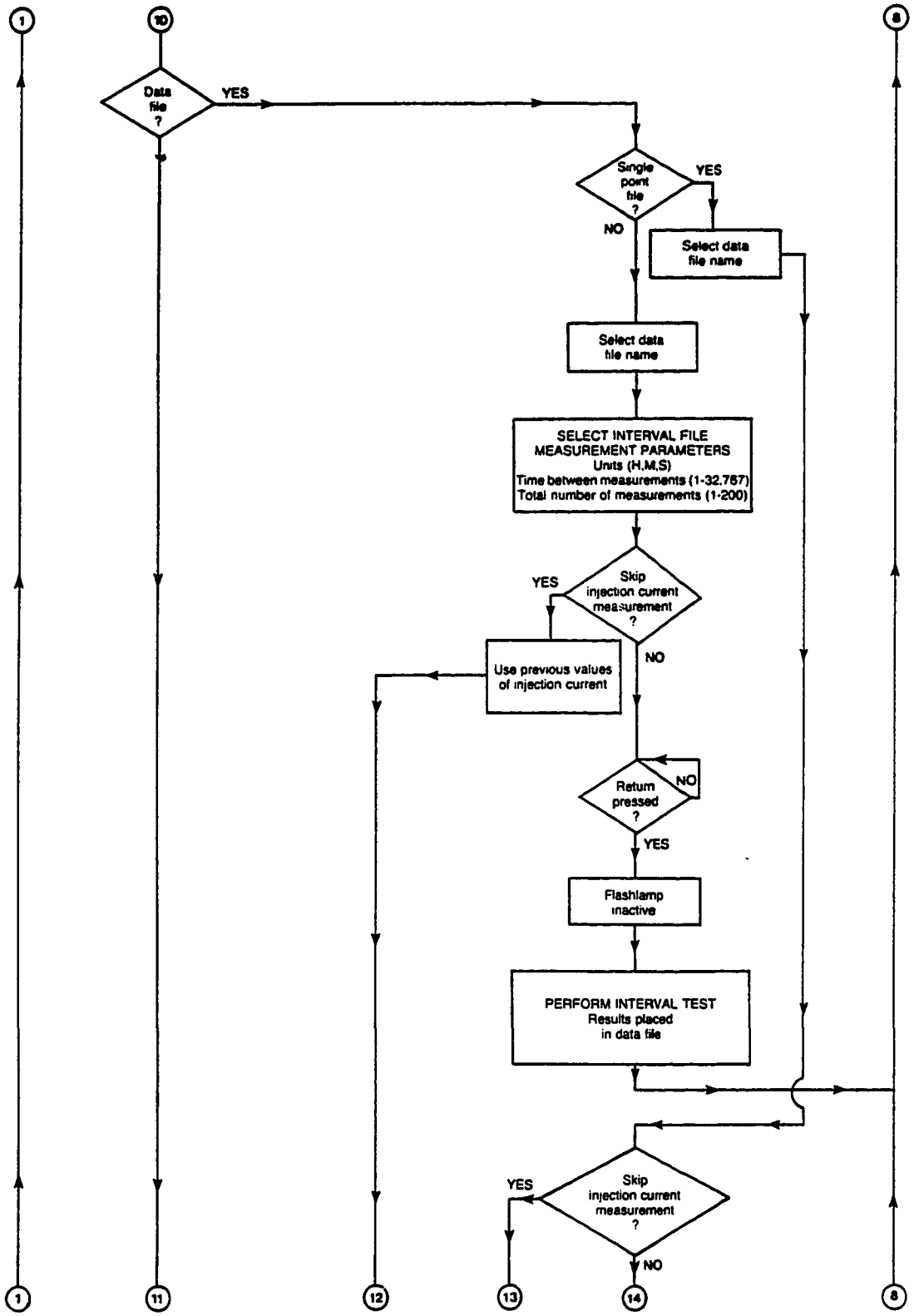

Figure 4.13. Continued.

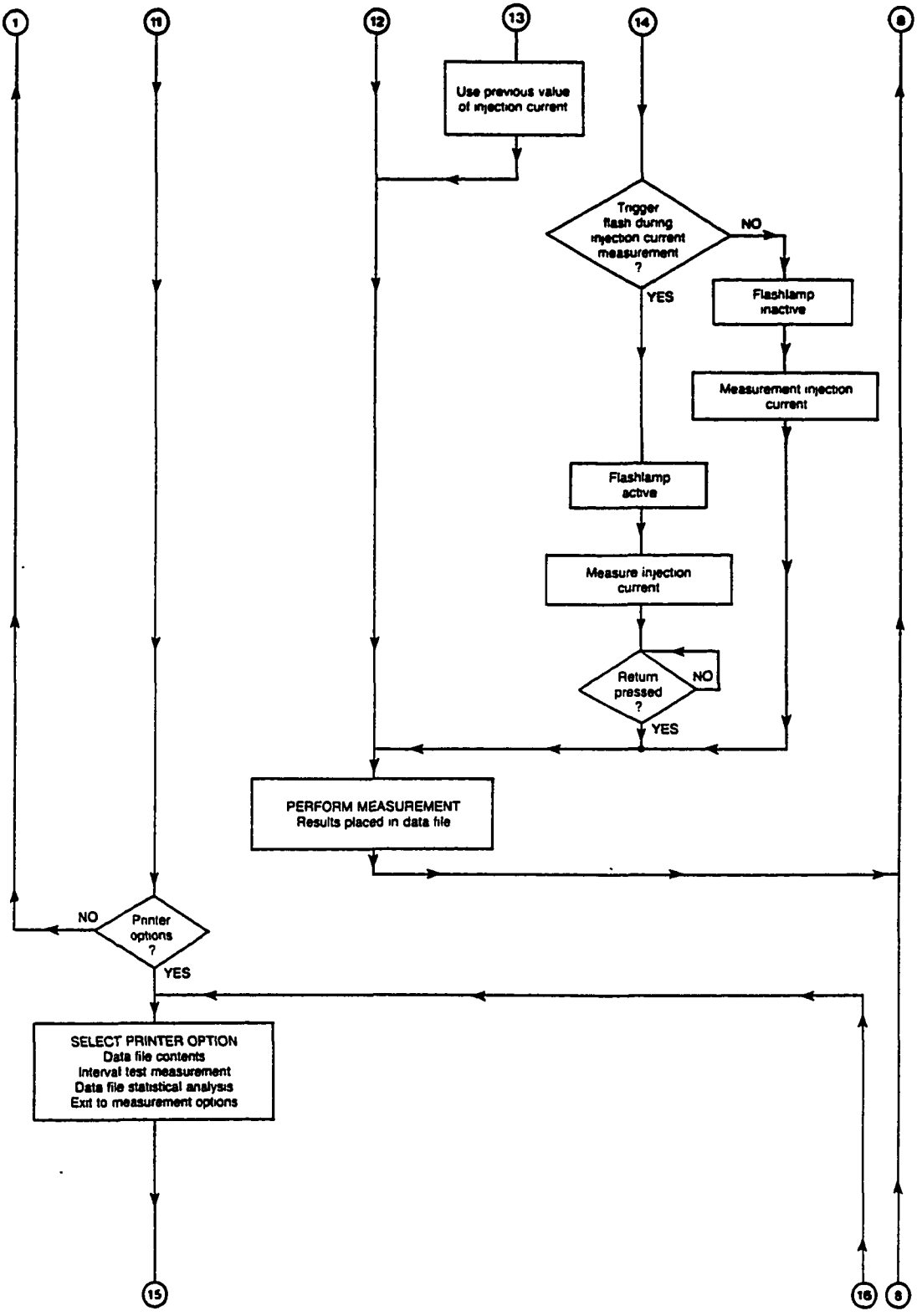

Figure 4.13. Continued.

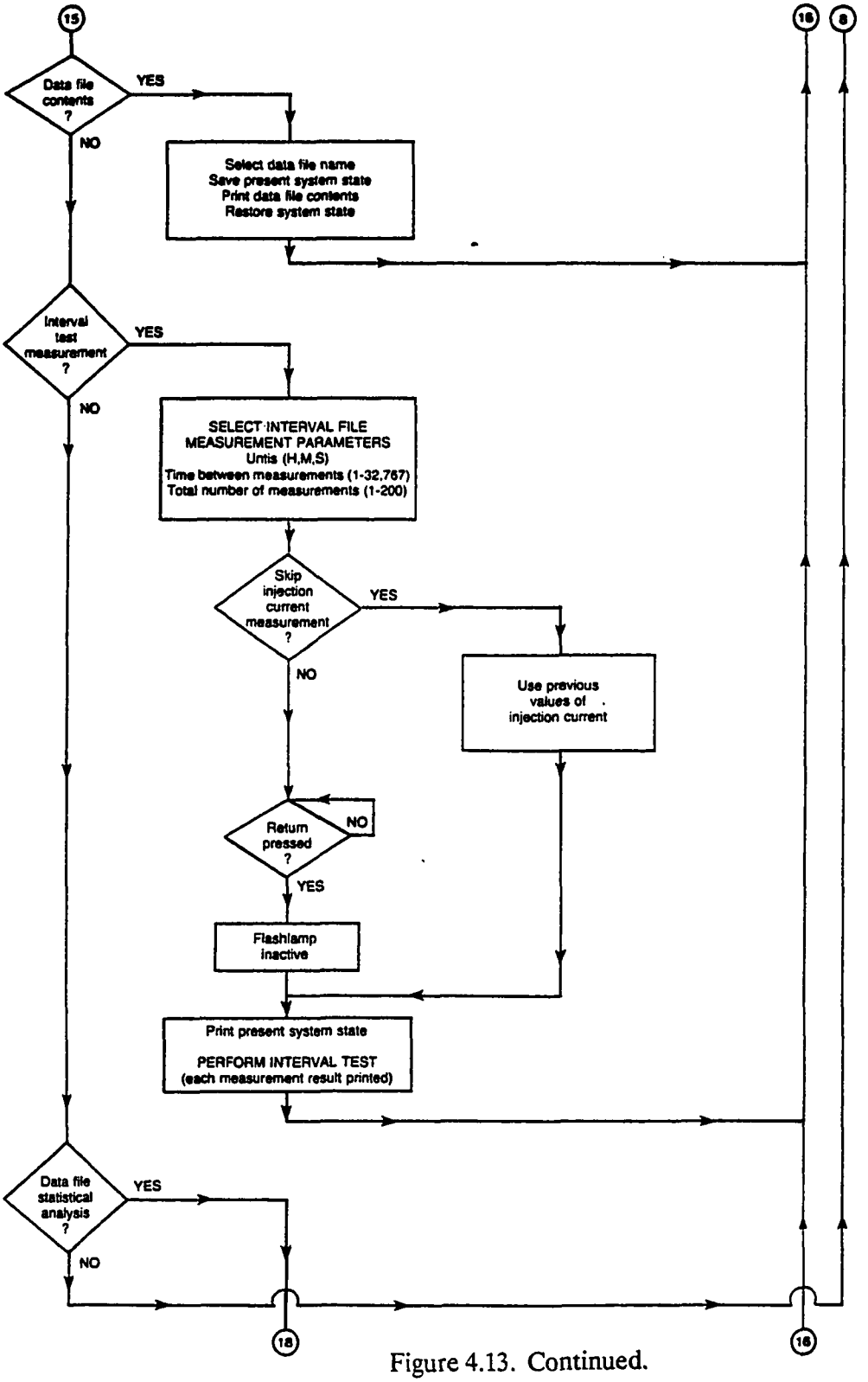

Figure 4.13. Continued.

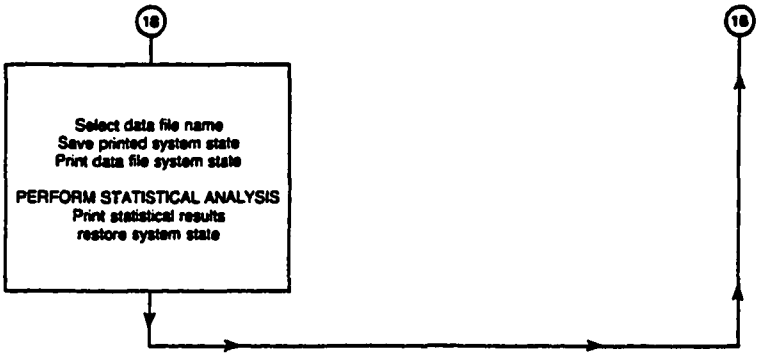

Figure 4.13. Continued.

CHAPTER 5
INSTRUMENT PERFORMANCE

5.1. Introduction

The overall performance of the optical pH measurement system and its suitability for making *in vivo* pH measurements under hyperthermic conditions were investigated.

The performance of individual subsystems were first evaluated in order to determine how well each achieved its specific design goal. The information obtained from these studies points out the strengths and weaknesses of the selected design scheme. These details should prove to be of value in optimizing subsystem performance for later improvements of this measurement system.

Next, performance evaluation of the overall measurement system using a single optical fiber immersed in solutions of free dye at various concentrations and values of pH, subjected to different temperatures was conducted. These measurements allow determination of system performance in differing sample environments. From this data, pH measurement errors introduced by temperature and pH changes, such as those occurring under hyperthermic conditions, can be determined. Knowledge of errors in pH measurement, resulting from inadequate signal intensity due to low concentrations of fluorophore, are of importance in designing a suitable pH sensing optrode. In addition, the impact of various software controlled system parameters on the pH measurement data were studied. This information will aid in selecting the optimum instrument settings needed in order to achieve a specified measurement criteria.

Design and fabrication of pH sensitive optrodes were considered from the viewpoints of size, stability, sensitivity, response time, and ease of production. An

important component of the sensor design is the choice of a semipermeable membrane. Several membranes were investigated, both in sheet and tubular form. The membranes were evaluated for their ability to easily exchange hydrogen ions, while at the same time restricting leakage of 1,4-DHPN. The size of the actual optrode was kept as small as practically possible to minimize diffusion limited response time. This allows *in vivo* use with minimal physiological perturbation.

Since none of the membranes tested had adequate differential permeability, encapsulation of 1,4-DHPN by means of liposomes was studied as a method of limiting the leakage of 1,4-DHPN from the optrode. The effect of this encapsulation technique on the kinetics of hydrogen ion transport, and thus sensor response time, was also studied.

Finally, animal studies were conducted in order to evaluate the suitability of the entire optical pH measurement system for in vivo use. Measurements of pH in the blood, leg muscle, and tumor of white rats were made under stable and varying physiological conditions. In this fashion, the steady state and dynamic characteristics of this *in vivo* measurement system could be investigated.

5.2. Subsystem Evaluation

5.2.1. Excitation Source

5.2.1.1. Procedure

The flashlamp energy storage capacitators were charged to numerous values of energy ranging from 0.0 -2.25 joules by controlling their maximum charging voltage via the Apple 2E microcomputer. Optical energy was measured at several points internal and external to the excitation subsystem using a radiometer (Photodyne Inc., Model 66XLA) in an energy mode. The sensing head of this instrument (Photodyne Inc., Model 420) is set to read actual energy or power

when used at a wavelength of 400 nm. Appropriate correction factors for other wavelengths were read from a supplied calibration table and applied to data measurements whenever appropriate. Reported data values were the average of 101 flashes taken at a frequency of 8 Hz.

5.2.1.2. Results and Discussion

A plot of electrical energy input versus optical energy output (Fig. 5.1) shows a nonlinear relationship. Both efficiency and output sensitivity are highest at low input energies. The decrease in efficiency seen at higher energies is due to excessive I^2R heating losses generated by the high peak currents associated with these energies. From this graph, overall conversion efficiency is seen to be very low, on the order of 0.002% for 1 joule of electrical input energy. This is several orders of magnitude lower than the 15% figure appearing in the manufacturers literature. Several explanations for this result are possible. Electrical losses resulting from energy dissipation in the storage capacitators and associated wiring could play a minor role in this reduced efficiency. More importantly, the measurement error could be large due to limitations in the instrumentation used and the measurement technique employed. Flashlamp energy output measurements were obtained by placing the sensor head as close to the top of the glass flashlamp bulb as was physically possible. Due to the large area of the source, the sensor could only measure a fraction of the optical energy being produced. An integrating sphere would be necessary for a more accurate determination. Furthermore, the broadband nature of the source introduces uncorrected wavelength dependent measurement errors. A spectroradiometer would be needed to accurately determine its spectral energy distribution.

The optical energy present in the excitation subsystem output fiber, with and without the shortpass filter, was subsequently measured (Fig. 5.2) and an estimate

of the peak available power was derived based on a $t_{1/3}$=3.2 μs pulse width. An input energy of 1 joule at a frequency of 8 Hz was used in these determinations. Broadband optical energy was coupled into the output fiber by the flashlamp optics with an efficiency of approximately 14%. This coupling drops to approximately 0.3% when the shortpass filter is used to restrict the spectral distribution of the optical output. This figure is consistent with the fact that approximately 4% of the flashlamp energy is contained within the bandpass of this filter which has a bandpass transmission of approximately 25%. The overall electrical-to-optical conversion efficiency for this resultant narrowband excitation source is calculated from these measurements to be approximately 8 x 10^{-6} %. Clearly, while this is a workable means of obtaining the desired optical excitation, it is far from being efficient.

5.2.2. Optics

5.2.2.1. Procedure

The optical attenuation properties of each optical module, in the optical subsystem, was measured using the optical energy from the flashlamp excitation source. The flashlamp was operated with 1 joule of input energy at a frequency of 8 Hz. Optical energy was measured using the Photodyne radiometer in an energy mode.

The shortpass filtered optical source was first coupled into the input of the sensor module and the energy output from the sensor fiber was measured. From this measurement, the efficiency of input coupling to the excitation fiber can be determined.

Next, the shortpass filter was removed from the excitation source and broadband optical energy was directed into the sensor fiber connector. Optical energy measurements were taken at the output of the sensor module, at the 488 nm

and 434 nm outputs of the detector module, and at the respective front panel optical connectors. From these measurements, the attenuation in the return fluorescence path can be determined.

5.2.2.2. Results and Discussion

The efficiency of excitation source coupling into the sensor fiber is calculated to be slightly greater than 4%. Thus, starting with 1 joule (312,500 W peak) of electrical energy at the flashlamp (Fig. 5.2), only 3.7 nJ (1.2 mW peak) of restricted wavelength excitation energy is available at the sensor tip.

A study of attenuation in the fluorescence return path (Fig. 5.3) indicates that approximately 25% of the return signal present in the sensor fiber is coupled out of the first module. Since only about 82% of the broadband input signal is at an appropriate wavelength for reflection out of this module, actual efficiency can be calculated to be closer to about 30%.

If both narrowband interference filters are removed from the optical detector module, the coupling efficiency from input to either module output is on the order of 6%. This efficiency declines to approximately 0.1% when the narrowband interference filters are restored. Since each filter has approximately 70% transmission within its passband, and only 2.8% of the flashlamp energy is reportedly within each of these bands, the above 0.1% efficiency measured with these filters is consistent with the design parameters. For a narrowband light source concentrated within the bandpass of either of these interference filters, the overall efficiency of the detector module was determined to be approximately 4%. If this same narrowband source is input to the sensor fiber, the overall return efficiency for the filtered wavelengths is on the order of 1%.

An additional attenuation of approximately 50% is contributed by the use of the front panel optical connectors. Each optical connector contributes

approximately 1.5 dB to overall signal attenuation. Thus, at the front panel connectors, the optical signal energy is on the order of 0.5% of that present for the same signal at the sensor tip.

5.2.3. Photodetectors

5.2.3.1. Procedure

Photodetector responsivity (V/W) was measured at the output of the front end current to voltage converter (I/V) using an optical source consisting of a blue LED (Siemens, LDB5410), with a peak wavelength of 480 nm; the intensity of this source was varied between 0.0 and 6.5 nW by application of a constant dc voltage to the LED. The transresistance gain of the I/V stage was fixed at 1×10^7 throughout the course of this study. Optical power was measured using a radiometer (Photodyne, Model 88XLC) with an optical head (Photodyne, Model 420) calibrated to display actual power when used at a wavelength of 400 nm. An appropriate wavelength dependent correction factor was applied to the displayed power readings in order to obtain the actual power at the selected wavelength. Noise measurements were obtained at the output of the I/V stage using a wideband ac rms voltmeter (Hewlett Packard, Model 7478A).

5.2.3.2. Results and Discussion

The dc output voltage of the front end I/V stage was plotted as a function of the optical power applied to the detector. Four different photomultiplier gains ranging from (1×10^3)-(1×10^6) were used (Fig. 5.4). The response of the photodiodes was also measured (Fig. 5.5). The optical responsivity in V/W was determined from the slope of a regression fit to each of these curves. Using the slope of these curves and the measured ac rms noise level at the I/V output for each gain level, the optical power needed to achieve a SNR=1 at this measurement point

was calculated (Fig. 5.6). The NEP for each gain was also calculated and plotted by dividing the previous results by the square root of the I/V bandwidth (16 kHz).

The NEP measured at the I/V output for the PIN photodiodes was 1.6×10^{-12}. This is only a factor of 6 worse than the typical NEP quoted by the manufacturer. These diodes are capable of detecting 0.2 nW of 480 nm optical power with a SNR=1 given the current front end design.

For photomultipliers, a NEP of 3.9×10^{-16} can be measured at the front end for a current amplification of 1×10^{6}. This allows detection of 50 fW with a SNR=1. Thus, it is seen that when operated near maximum gain the photomultipliers are approximately 4000 times more sensitive than the PIN photodiodes at the wavelengths of interest.

As in the case with photodiodes, the measured NEP at the I/V output is again very close to the calculated value for the detector alone. This is a good indication that the detector noise, rather than the front end noise, is the major limitation for the detection of very low light levels with this system.

5.2.4. Electronics

5.2.4.1. Procedure

The electronics subsystem was calibrated using photomultiplier tubes for an equal gain of 1×10^{11} V/W on either channel. This gain figure was obtained via the internal calibration potentiometers, with the photomultiplier current gain set at 10,000, the I/V transresistance gain set at 1×10^{7}, and the integration time set at 100 μs. Other ranges were calibrated to their appropriate gains relative to this standardized range.

Drift and stability tests were run on the system using a photomultiplier current gain of 10,000, a transresistance I/V gain of 1×10^{7}, and an integration time of 100 μs. The optical inputs to the photomultipliers were capped off to

eliminate all light and the system offsets were tracked from power-up, using the primary electronics module, with and without the optional narrowband electronic filter module.

The optical signals were obtained and measured using the same procedures outlined in Section 5.2.3.1. The total system responsivity curves were also generated and fitted in an analogous fashion. Again, a front end gain of 1×10^7 was used with the integration time set at 25 μs.

5.2.4.2. Results and Discussion

With the primary wideband electronics module in operation, substantial system drift occurs throughout the first hour of operation (Fig. 5.7). This drift is approximately -16 mV for channel 0 and +8 mV for channel 1. For strong signal levels the ratio error introduced by this drift is minor. However, under weak signal conditions, or when photodiodes are used, insufficient warm up time could introduce substantial measurement errors. If the narrowband filter module is used (Fig. 5.8), warm up drift is practically eliminated. In either case, adequate system stability is achieved once a steady state operating point has been reached.

Total system output voltage was plotted against optical input power at 480 nm for both photomultipliers (Fig. 5.9) and photodiodes (Fig. 5.10). From the slope of these curves total system responsivity (V/W) can be determined. These values will be used later in determining the actual fluorescence energy levels arriving at the detectors for a specific concentration of 1,4-DHPN located near the sensor tip.

5.2.5. Conclusion

With a flashlamp input energy of 1 joule (312,500 W), only 82.1 nJ (26 mW) of excitation at the appropriate wavelength can be obtained. Most of the energy loss appears to result from inefficient electrical-to-optical energy conversion.

However, as previously mentioned, problems with the optical measurement technique employed make this conclusion subject to question. In any event, the optical excitation source used in this measurement system , while functional, is extremely inefficient. Further research and development effort is needed in order to produce a more compact , efficient, and powerful source of optical excitation.

The optical modules used in this system appear to work properly. However, further work to develop more efficient optical coupling could substantially improve overall performance. Only about 4% of the optical energy coupled into the sensor module appears at the tip of the sensor fiber. Thus, for a 1 joule (312,500 W) electrical input to the flashlamp, only 3.7 nJ (1.2 mW) is available to excite the pH dependent fluorophore. Furthermore, only about 1% of the fluorescence signal at any wavelength is available at the output connectors of the detector module.

The photodetectors used in this system appear to be capable of achieving close to their theoretical limit of sensitivity when measured at the output of the front end I/V stage. This indicates that both the photodetector subassembly and the electronics subassembly have acceptable levels of performance. Stability of the electronics subassembly is good and use of narrowband filtering virtually eliminate the problem of baseline drift.

5.3. Measurement System Evaluation

5.3.1. Solution Studies

5.3.1.1. Procedure

A simultaneous potentiometric and optical titration was performed using a 2 mM solution of 2 mM 1,4-DHPN in a 50/50 ethanol/water solvent. This mixture was titrated against an NaOH solution, whose concentration had previously been determined to be 17.3 mM. The pH during the entire course of the titration was

monitored using a Beckman Model 71 pH meter. The fluorescence signals at 488 and 434 nm; as well as their ratio, were monitored using a single silica optical fiber. This fiber was attached to the sensor input of the optical pH measurement system. The system was configured for 8 Hz operation using 1 joule of input energy. Integration time was set for 100 μs, with an I/V transresistance gain of 1 x 10^7 and a photomultiplier current gain of 4000 on each channel. Each data point reflects the average of 100 samples, with 2 minutes of stabilization time allowed between data points.

Sensitivity studies were conducted by varying the concentration of 1,4-DHPN from 10 mM - 5 μM, at pH values of 6.0, 7.0, and 8.0, respectively. Instrument settings were essentially the same as those used during titration, except that the photomultiplier current gain was readjusted as necessary. Each data point obtained represents the average of 200 samples. In the wideband versus narrowband electronic processing studies, the frequency and energy settings of the flashlamp were changed to 24 Hz at 0.4 joules as required by the fixed frequency design of the narrowband filters. All other system parameters were unchanged.

Studies of the effect of temperature on ratio measurements were carried out at temperatures from 10-70 °C. Measurements were obtained at pH values of 5.94, 7.08, and 8.22. Instrument settings and measurement parameters were identical to those used in the sensitivity studies. The concentration of 1,4-DHPN was fixed at 100 μM throughout these measurements.

The effect of flashlamp frequency and input energy on measured ratios was investigated using a 100 μM solution of 1,4-DHPN at pH values of 5.93, 6.45, 7.15, 7.70, and 8.17. For the energy dependent studies, input energies ranging from 2.25-0.5 joules were used at a frequency of 8 Hz. For the frequency dependent studies, frequencies ranging from (64)-(8) Hz were used with 1 joule of input energy. Integration time was fixed at 100 μs and I/V transresistance gain was fixed

at 1 x 10^7 throughout these measurements. Again, 200 samples were averaged for each reported data point.

An investigation of the effect of integration time and sample averaging on the standard deviation of measured ratios was conducted. For the integration studies, a 100 μM solution of 1,4-DHPN at a pH of 7 was used. The flashlamp was provided with 1 joule of input energy at a frequency of 8 Hz. A transresistance gain of 1 x 10^7 was selected for the front end I/V stage. Integration times of 25, 100, 400, and 1000 μs were used and the usual 200 samples per data point were obtained. For the sample averaging studies, identically I/V gain settings, dye concentration, pH, and flashlamp parameters were chosen. Integration time was fixed at 100 μs and averages and standard deviations of 10, 100, and 1000 samples were obtained.

Finally, the effect of optical fiber characteristics on instrument sensitivity, as measured by the standard deviation of measured ratios, was studied. The instrument settings and measurement parameters were similar to those used in the integration time study, with the integration time fixed at 100 μs. A 50 μM solution of 1,4-DHPN, at pH 7, was used in testing all optical fibers. The optical fibers tested included the standard FHP 500/600/630 silica fiber with a flat polished termination, as well as terminations with integral spherical lenses having apparent focal lengths of 0.8 and 2.0 mm. In addition, a smaller FHP 320/385/415 fiber, with a flat polished termination, was evaluated.

5.3.1.2. Results and Discussion

An acid base titration of 1,4-DHPN was performed and a simultaneous plot of both potentiometrically determined pH and optical fluorescence ratio (488/434), versus volume of titrant added, was constructed (Fig. 5.11). The shape of the potentiometrically determined titration curve is typical of that obtained when a weak diprotic acid is titrated with a strong base. Details of this titration curve have

already been discussed in Section 3.2.2. The optical fluorescence ratio curve has a very different shape. It is a continuous smooth curve with no apparent inflection points. A plot of this ratio versus pH can be nicely fit by a fourth order polynomial over the pH 5 to 9 range (Fig. 5.12). Mathematically simpler fits, such as those obtained with a single exponential, give acceptable accuracy, especially when a narrower pH range is under investigation. Since this is the case in the physiological studies to be conducted, a single exponential fit will be used for system calibration in the sensor evaluation and animal testing that follow.

Plotting the measured fluorescence intensity at both 488 and 434 nm against the volume of added titrant (Fig. 5.13), as well as against pH (Fig. 5.14), shows the fluorescence intensity at 434 nm decreases rapidly as the pH is made more alkaline. Since this wavelength is primarily associated with the monoanionic form of the fluorophore, such a result is not unexpected. However, since a wavelength of 488 nm is primarily associated with the dianionic form of the fluorophore, the fluorescence intensity measured at this wavelength should be expected to increase. The slight decrease actually observed is probably due to the fact that the expected increase in fluorescence intensity at this wavelength, due to the increased concentration of the dianionic species, is offset by the volume dilution effects of the added titrant. Thus, the apparent decrease in intensity is most likely an artifact introduced by the experimental procedure. The impact of volume dilution effects on the fluorescence ratio measured in this experiment should also be considered if an accurate calibration curve is desired.

Studies of the relationship between fluorescence intensity and concentration at a pH of 7, indicate that fluorescence intensity at either 488 or 434 nm is an approximately linear function, for concentrations of 1,4-DHPN at less than about 1 mM (Fig. 5.15). For concentrations of fluorophore below 1 mM, the fluorescence ratio (488/434) appears to be independent of concentration (Fig. 5.16). However,

the standard deviation of the measured ratio is found to decrease approximately proportional to the cubed root of the concentration (Fig. 5.17). This result is somewhat puzzling since it would normally be expected that the standard deviation would decrease as the square root of the number of particles present in solution and thus, as the square root of the concentration. This discrepancy can either be an artifact introduced by attempting to fit a theoretical curve to a limited number of data points, or it could be real and related to apparent changes in solution volume being sensed at the probe tip. Further theoretical and experimental work is required in order to resolve this incongruity.

For any concentration the pH error will always be greater the more alkaline the solution. This is a direct consequence of the small amount of 434 nm fluorescence present in these solutions. For the present measurement system operated with an input energy of 1 joule, a flash rate of 8 Hz, an integration time of 100 μs, and an I/V transresistance gain of 1×10^7, a 1 mM solution of 1,4-DHPN is required to obtain a pH measurement with a standard deviation of less than 0.1 pH unit. This result was obtained at neutral pH, when 200 samples were taken. Given the above set of operating parameters, this is close to the minimum pH error that can be obtained with this system regardless of concentration. A plot of pH errors for other concentrations and pH values can easily be constructed (Fig. 5.18).

From the total system output voltage for the 488 or 434 nm channel, using a 10 mM concentration of 1,4-DHPN, the system sensitivity curves (Figs. 5.9 and 5.10) can be used to calculate the narrowband optical energy incident upon the photodetectors. Energies of 7.6 fJ (2.4 nW) at 488 nm and 5.54 fJ (1.7 nW) at 434 nm can be calculated in this fashion. These intensities are high enough to be resolved by the system photodiodes, but an SNR of approximately 10 is all that can

be expected. If lower concentrations of fluorophore are to be used or a better SNR is desired, photomultipliers must be employed.

If the efficiency of the fluorescence return path is assumed to be on the order of 0.5% at each measured wavelength, then approximately 1 pJ (300 nW) of narrowband optical energy is returned through the sensor fiber within each detected emission band. Assuming a sensor tip excitation energy of 3.7 nJ (1.2 mW), approximately 0.03% of this energy is recovered as fluorescence emission within each filtered bandpass. The spectral and spatial distribution of the fluorescence emission accounts for the majority of the observed energy reduction.

Studies were conducted to determine the effect of narrowband filtering on measurement accuracy and precision. For the same concentration of fluorophore, system output levels with the narrowband filter module in place were reduced to approximately 5% of those obtained using the wideband module. This results in a factor of 20 reduction in available sensitivity with equivalent accuracy (Fig. 5.19). However, even though the measured system output was substantially reduced, the standard deviation of the ratio was virtually identical for a given concentration of dye (Fig. 5.20). These results suggest that the use of narrowband filtering may result in increased measurement precision when adequate signal strengths are obtainable. The ability of such filtering to eliminate dc offsets, such as those caused by stray light and component drift, may offer additional measurement advantages in some cases.

A detailed study of the effect of temperature on optically measured pH values was conducted using this measurement system. The intensity of fluorescence at both 488 nm (Fig. 5.21) and 434 nm (Fig. 5.22) decreased with increasing temperature. However, the rate of change of fluorescence with temperature is seen to increase, with increasing alkalinity, for 488 nm fluorescence and decrease for 434 nm fluorescence. This effect, as previously noted, tends to minimizes the the

temperature dependent pH measurement error near neutral pH (Fig. 5.23). Over the 6.5 to 7.5 pH range, a maximum standard deviation of 0.007 pH units / °C was calculated. By calibrating this system at 40 °C, hyperthermia studies over a ± 10 °C temperature range can be conducted with a maximum standard pH error of only ± 0.07 units. The ratio error introduced by temperature dependent effects, over the above temperature and pH ranges, is smaller than the intrinsic system measurement error for the measurement conditions utilized in this experiment (Fig. 5.24). A ratio standard deviation of less than 0.1 would be needed, at all of the above pH values, before temperature dependent effects would be of equivalent significance. A plot of the fluorescence ratio and its standard deviation, as a function of both pH and temperature (Fig. 5.25), clearly demonstrates an increase in temperature dependent measurement errors at alkaline pH, as well as a decrease in measurement precision with increasing temperature.

Several system parameters were evaluated for their impact on measurement precision as determined by the standard deviations of the measured fluorescence ratios. If the flashlamp firing frequency is increased, with input energy held constant, it can be seen that while the mean ratio remains essentially unaltered (Fig. 5.26), its standard deviation increases with increasing frequency and pH (Fig. 5.27). Furthermore, the standard deviation of the ratio is found to increase in proportion to the square root of the frequency (Fig. 5.28). A similar behavior of mean ratio (Fig. 5.29) and its standard deviation (Fig. 5.30) is noted if the input energy per flash is decreased at a constant flash frequency. The decrease in the standard deviation of the measured ratio again appears to be proportional to the square root of the input energy (Fig. 5.31). Thus, the best measurement precision is obtained with the lowest flashlamp frequency and highest input energy. These values however, must be consistent with both the maximum flashlamp dissipation requirement and the maximum time allotted for acquisition of the required number

of samples. Since the number of emitted photons is proportional to the flashlamp energy, and the standard deviation has been shown to decrease as the square root of the number samples (photons), it seems reasonable to expect that the standard deviation of the fluorescence ratio would decrease as the square root of the available flashlamp energy. The frequency dependence of the standard deviation is best explained by a linear relationship existing between flashlamp frequency and energy. As the flashlamp frequency is increased beyond that recommended for a given input energy, its output energy will drop due to the limited time available for recharging the discharge capacitators. Thus, in reality the frequency dependence of the standard deviation of the fluorescence ratio is really an energy dependence.

A study of the effect of sample averaging and integration time on the measured ratio yielded expected results. The standard deviation of the measured ratio decreased as the square root of the number of samples being averaged (Fig. 5.32). An integration time of 100 μs appears to be near optimum for use with this measurement system. For values much less than this number, the standard deviation increases due to the small percentage of the overall signal being integrated (Fig. 5.33). For integration times much greater than 100 μs, the standard deviation of the measurement ratio increases due to a predominate contribution from the system noise.

Finally, the impact of sensor fiber variation on measurement precision was studied. While an increase in the standard deviation of the ratio was observed for a 36% reduction in fiber core diameter (Fig. 5.34), smaller differences were observed when flat ended fibers were compared with similar fibers incorporating spherical lenses at their tip. Both lensed fibers gave slightly better standard deviations than the flat ended fiber. The shorter focal length of 0.8 mm gave the best overall measurement precision. Since this focal length is closest to the radius of curvature the lens, near optimum beam collimation would be expected. The

significance of these differences can not be tested since only a single averaged data point was acquired with each fiber tested. These results do tend to suggest however, that by using a large diameter sensor fiber, with a collimated output, small but noticeable improvements in measurement precision can be achieved.

5.3.2. Optrode Studies

5.3.2.1. Procedure

For free fluorophore studies, a 100 μM solution of 1,4-DHPN was prepared in a normal saline solution (0.9%). The pH of this solution was adjusted to be in the 5.5 to 6.0 pH range by addition of small volumes of either NaOH or HCl. The tubing or membrane to be tested was then filled with this dye solution. The end of the tubing was tied off with thread and the entire length was immersed in a vial containing 10 ml of either normal saline, or 305 mOsm phosphate buffer, at a pH of either 7.0 or 8.0. Both the fluorescence ratio (488 nm /434 nm), and the optical intensity at each wavelength was monitored as a function of time. The flashlamp was set at a frequency of 8 Hz with an input energy of 1 joule. A 100 μs integration time was used with an I/V gain of 1×10^7. A 100 sample average was reported for each data point, requiring an acquisition time of 12.5 seconds.

For the liposome encapsulation studies, large unilamellar vesicles (LUV) were prepared from a 125 mg of a 4:1, by weight, mixture of dipalmitoylphosphatidylcholine (DPPC) and dipalmitoylphosphatidylglycerol (DPPG) (Avanti Polar Lipids), using the reverse evaporative phase process [58]. Varying amounts of Gramicidin A (Sigma Chemicals) were added to the lipid phase prior to preparation. This amount ranged from 0 to 2 mole percent of the total lipid present. The aqueous phase consists of a 10 mM 1,4-DHPN dye solution. Sucrose was added to this solution (1.04 g /10 ml) in order to achieve an approximately isosmotic concentration, and the final pH was adjusted to

approximately 7 by the addition of a small volume of NaOH. The prepared LUV were dialyzed overnight in the cold, against normal saline, in order to remove unencapsulated dye. Prior to using these LUV in sensor studies, they were diluted 1:1 with normal saline. Testing was then carried out in a manner identical to that used in the free fluorophore studies.

5.3.2.2. Results and Discussion

Several small diameter tubes of various materials were studied in order to measure their differential permeability properties. In order to be of value in pH sensor fabrication, such tubing should possess a large permeability to hydrogen ions while at the same time offering a low permeability to the small, 160 molecular weight, pH sensitive fluorophore. Small size is desirable in order to both maintain acceptable response time and minimize tissue injury while performing *in vivo* measurements. In addition, mechanical rigidity and a simple construction allow easy handling and fabrication.

The materials investigated using free dye were TFE Sub-Lite-Wall Teflon (AWG 18) (Zeus, Inc.), Nafion Perfluorinated Tubing (815X) (Perma Pure Products, Inc.), polysulfone tubing (P10-43) (Amicon Corp.), cellulose (Spectra/Por 2, MWCO 12-14K) (Spectrum Medical Industries, Inc.), and Cuprophan (150 PM) (Enka-Glanzstoff, AG). All materials except cellulose and Cuprophan were commercially available in tubular form. Cellulose and Cuprophan tubes were made using a polyurethane based epoxy (Master Bond EP30DP-1), by a modification of a published procedure [74]. All tubes had an inner diameter of approximately 1 mm with walls of varying thickness. The thickness of the walls were as follows: Teflon (40 μm), Nafion (150 μm), polysulfone (1000 μm), cellulose (30 μm), and Cuprophan (15 μm). The diffusive permeability of both polysulfone and Cuprophan, to a variety of different solutes, have been measured

[52]. Although no permeability data for hydrogen ions could be found, respective permeabilities to sucrose (343 Daltons) of 3.21 x 10^{-4} cm/s and 1.76 x 10^{-4} cm/s were measured. For smaller solutes, the permeability of both membranes increase slightly. Cuprophan appears to have a slightly higher permeability than polysulfone for solutes of less than 60 in molecular weight.

A plot of fluorescence ratio (488/434) versus time (Fig. 5.35), for free dye loaded tubes of the above material, indicates that the Teflon and Nafion tubes have very low hydrogen ion permeability as measured by a step change in external solution pH. Polysulfone has a slightly higher permeability, while both the cellulose and Cuprophan tubes show the highest permeability. Unfortunately, as indicated by the higher standard deviation of the fluorescence ratios with time, the tubes with higher hydrogen ion permeability also show substantial permeability to the selected fluorescent indicator dye. This result is clearly seen when the fluorescence intensities are plotted against time (Figs. 5.36 and 5.37). From these figures it can be concluded that dye leakage increases proportional to hydrogen ion permeability. Since Cuprophan appears to leak dye at a slightly faster rate than cellulose, its hydrogen ion permeability can also be inferred to be slightly higher. From this data, Cuprophan would appear to be the membrane of choice from a hydrogen ion permeability standpoint, however, its near total leakage of free dye with a 10 minute time period severely limits the utility of this simple sensor. Furthermore, its flaccid structure makes handling and use difficult.

The mechanical rigidity of the polysulfone tubes is a desirable feature for development of a practical sensor. The slow leakage of free dye from this tubing allowed stable pH reading for up to approximately 1 hour. However, the fairly slow response time of this tubing (τ=6.1 minutes), prohibits its use in making dynamic pH measurements. A further complication in sensing pH with this tubing is apparent when the fluorescence ratio (488 nm /434 nm) is plotted to its steady state value

(Fig. 5.38). The final value of the ratio is lower in the tubing than in free solution. This could either be indicative of a more acidic internal environment or a perturbation of the pK values of the sensing fluorophore. The highly acidic sulfonic acid group of this membrane is the most probable cause of this deviation.

In order to determine whether cellulosic type membranes would similarly perturb the steady state fluorescence ratio, 2.5 mm diameter semi-micro dialysis tubing (Spectrum Medical Industries, Part # 132600) was used. This tubing was selected since it had both a small volume, so as to not exceed the capacity of the external phosphate buffer, while at the same time possessing a volume large enough to diffusion limit the leakage of 1,4-DHPN. This restricted leakage provides acceptable signal strength when the steady state ratio is achieved. Plots of both fluorescence ratio (488 nm /434 nm) versus time (Fig. 5.39) and pH versus time (Fig. 5.40), obtained using a micro pH electrode (Lazar Research Labs, Model PAR-146), indicate that the expected final value of both pH and fluorescence ratio are reached, as steady state is approached. Thus, it can be concluded that no detectable membrane related perturbations, of either pH or fluorophore pK values, result from cellulosic tubing.

In order to test the feasibility of a rigid Cuprophan based sensor, three different sizes of pipettes were cut so as to present a uniform cross sectional area along their entire length. At one end of the resulting cylinder, a flat Cuprophan membrane was stretched and securely attached around the circumference using a small amount of epoxy (Master Bond, EP30DP-1). These cylinders were then filled to approximately the same height with free dye solution. The optical sensor fiber was next inserted into the open end of the cylinder and secured, with epoxy, at a selected distance from the membrane. Disposable pipettes with volumes of 10 ml, 1 ml, and 50 µl, and respective cylinder internal diameters of 7.9 mm, 3.2 mm, and 1.1 mm, were employed (Fig. 5.41).

Measurements of the fluorescence ratio (488 nm /434 nm) as a function of time were made using the previously described system settings, upon immersion of these sensors into a pH 8 phosphate buffer. The results indicate that the smaller the sensor, the more rapid the response time (Fig. 5.42), with the 1.1 mm sensor appearing to reach its correct steady state value in about 10 minutes. These results are consistent with those that would be expected in a diffusion limited sensor response. Further confirmation of this hypothesis is obtained when the distance between the membrane and the sensor fiber is varied, at a constant solution volume, using the 1.1 mm sensor (Fig. 5.43). Response varies from several minutes at a distance of 1 mm from the membrane to virtually undetectable in 30 minutes at a distance of 8 mm. The effect of varying the volume of the filling solution, at a constant probe to membrane distance, was next investigated using these same 1.1 mm sensors (Fig. 5.44). No measurable difference in response time could be determined, given the large measurement error margin introduced by rapid dye leakage from this sensor. This result again argues for diffusion limited response, as opposed to mass transfer limited response, within this sensor. Large membrane surface area is desirable, in order to insure that a sufficiently large number of hydrogen ions cross the membrane, per unit time. By keeping the solution volume low, rapid internal concentrations changes can occur with passage of only relatively few hydrogen ions through the membrane. Unfortunately however, since measurement sensitivity and SNR increase in proportion to the number of dye molecules being interrogated, a physical limit is imposed on the minimum acceptable sensor volume.

In order to gain an understanding of the importance of the Cuprophan membrane permeability on sensor response, the Nusselt number for mass transfer was computed. Specifically, this number compares the intensity of mass flux at the

membrane with the specific flux by pure molecular diffusion in a fluid layer of thickness L [96]. In this case it is given by the equation

$$Nu = P L / D \qquad (6.1)$$

where

P= membrane permeability (cm / s)

D= molecular diffusion coefficient (cm^2 / s)

L= thickness of fluid layer (cm)

Nusselt numbers much greater than one imply that mass transfer is primarily diffusion limited. For Nusselt numbers much less than one, membrane permeability becomes the limiting factor. Since Cuprophan permeability data was not available for hydrogen ions, a calculation was done using sucrose as a representative small molecular weight molecule. The diffusion coefficient for sucrose, in aqueous solution, has been reported to be 4.586×10^{-6} cm^2/s [5]. Using this number for a diffusion coefficient and the value previously reported for Cuprophan sucrose permeability, a solution thickness of 0.26 mm gives a Nusselt number equal to unity. Thus, it can be concluded that for optical fibers placed much closer to the membrane than 0.26 mm, membrane permeability properties would dominate the response time observed. Since the fiber tip is usually placed several millimeters from the membrane in order to provide reasonable signal levels, it again becomes clear that the observed response is primarily limited by the diffusion time for hydrogen ions in solution. A value of 9.34×10^{-5} cm^2 / s has been reported for the diffusion coefficient of hydrogen ions in solution at 25 °C [53]. Using the simple result from the solution of the diffusion equation, that the average distance that a molecule travels varies as the square root of the elapsed time [5], it can be calculated that approximately 54 seconds are required for a hydrogen ion to diffuse to a position approximately 1 mm away from the sensor membrane. Thus, for practical

membrane to fiber distances, response times of several minutes should be expected for this type of sensor.

In order to be able to minimize the degree of tissue damage associated with in the *in vivo* application of this type of sensor, several smaller diameter sensors were fabricated.These were made from both 20 and 15 µl capillary tubes, with respective inner diameters of 0.64 and 0.58 mm. The outer diameter of these tubes were 0.89 and 0.86 mm, respectively. Free dye response studies with these sensors (Fig. 5.45) suggest that they have slightly shorter response times, as would be expected based upon diffusional principles. However, the very rapid dye leakage from all of these capillary sensors makes a quantitative comparison difficult.

In order to slow the rapid leakage of 1,4-DHPN from these sensors, prior encapsulation in DPPC/DPPG liposomes was tried. Even though the intrinsic permeability of liposomal membranes to hydrogen ions is several orders of magnitude higher than for other small monovalent ions (approximately 1×10^{-4} cm/s), proton flux has been found be limited by the development of a diffusion potential resulting from the restricted flow of counterion currents [21]. For this reason, the small peptide antibiotic ionophore Gramicidin A was added to the lipid phase during liposome preparation. This ionophore is specific for monovalent cations and translocates them across the lipid membrane by means of a dimeric formed hydrophilic channel. Discrimination among various monovalent cations is not high, but an anomalously high permeability of the channel to hydrogen ions has been reported [43]. The kinetics of Gramicidin induced hydrogen ion permeability has been found to be an increasing function of the Gramicidin level, up to the point where approximately 8-10 Gramicidin molecules are incorporate in each vesicle [17]. At these levels, transmembrane hydrogen ion equilibration times of less than 1 ms have been reported [12].

Studies were conducted with suspensions of liposomes in order to determine both the Gramicidin levels necessary to achieve an acceptable response time, and the liposome concentration necessary to produce adequate signal intensity for proper fluorescence ratio determination. Liposomes containing Gramicidin levels of 0.0, 0.2, and 2.0 mole percent (of total quantity) were prepared as previously described. The initial internal pH of these liposomes was approximately 6.7 as measured by the fluorescence ratio at t=0. A 1/2 dilution was made at this time using phosphate buffer at a pH of 7.5. The fluorescence ratio as a function of time was recorded using the previously described measurement system. The results (Fig. 5.46) indicate first that a quantity of fluorophore, sufficient for optical detection, was encapsulated within the aqueous compartment of the LUV. Secondly, at a Gramicidin level of 2.0 mole percent, hydrogen ion equilibration time was well below the time resolution of the measurement system. In addition (Fig. 5.47) a maximum liposome dilution of approximately 1/2 was necessary for accurate fluorescence ratio determination.

A study was next made using standard 2.5 mm cellulosic dialysis tubing, as described previously, in order to mimic a large scale sensor. Results (Figs. 5.48 and Fig. 5.49) indicate that even at the 0.2 mole percent Gramicidin level hydrogen ion diffusion time, and not liposomal hydrogen ion permeability, is the dominant factor limiting sensor response.

The more practical polysulfone and Cuprophan capillary sensors were next investigated by replacing the free fluorophore in the previous studies with liposome (using 2.0 mole percent Gramicidin) encapsulate fluorophore.

When a sensor was fabricated using fluorophore containing liposomes within the 1.1 mm polysulfone tubing (Fig. 5.50), it can again be noted that, in addition to a slow response time, the expected steady state ratio is never attained (Fig. 5.51). From the measured fluorescence ratio, it appears that the fluorophore

is experiencing a local environment which is slightly more acidic than the external solution. Since the fluorophore is now encapsulated and shielded from direct interaction with the polysulfone, alterations in fluorophore pK values seem an unlikely explanation. It now seems more plausible that the sulfonic acid groups of the polysulfone tubing are becoming ionized, resulting in a more acidic localized environment on the inside of this tubing.

Another explanation for the discrepancy in measured fluorescence ratios is that either the local internal liposomal environment is more acidic than its external environment, or that the negatively charged liposome is again perturbing the pK values of the fluorophore. Phase fluorometry studies of free 1,4-DHPN and Gramicidin free liposome encapsulated fluorophore at pH 7 (Figs. 5.52 and 5.53), show that even at a liposome dilution of 1/10,000 in phosphate buffer, the the apparent fluorescently determined pH of the liposomal encapsulated dye can be as much as 0.5 pH units lower than that for free dye in solution. A similar result is obtained when fluorescence ratios are used to compare free fluorophore with liposome encapsulated fluorophore (Fig. 5.54). A lower fluorescence ratio and thus, an apparently lower pH is measured for the liposomal encapsulated dye. However, pH errors resulting from the low liposomal dilutions (1/2) used in this experiment, coupled with the large standard deviation of the measured ratios preclude a quantitative analysis of the results. Since environmental variables may exert a quantitatively different effect on fluorescence emission than they exert on lifetime, the quantitative pH difference measure by the ratio technique may differ from that measured using phase or modulation variables. In any event, for accurate pH determinations such effects must be taken into account during system calibration.

In order to investigate the effect of temperatures in the normal to hyperthermic range on liposome dye retention, polysulfone based liposomal

sensors were placed in pH 7 phosphate buffer at temperatures of 25, 37, and 45 °C, respectively. The fluorescence intensities at 434 and 488 nm were then measured as a function of time and plotted (Figs. 5.55 and 5.56). These studies indicate that even though increased loss of dye occurs at higher temperatures, sufficient dye is retained to enable measurement times well in excess of 1 hour, at a temperature of 45 °C.

Finally, studies were conducted using Cuprophan capillary sensors containing liposome (with 2.0 mole percent Gramicidin) encapsulated fluorophore. Both 50 and 20 µl capillary tubes were filled with a 1/2 dilution of liposomes and normal saline and placed in a pH 8 phosphate buffer at t=0. The 50 µl (1.1 mm inner diameter) capillary sensor (Fig. 5.57) achieved the expected steady state value for the fluorescence ratio with an exponential time constant of 3.2 minutes (Fig. 5.58). A plot of the corresponding pH response of this sensor is also shown (Fig. 5.59). The 20 µl (0.635 mm inner diameter) capillary sensor also reached the expected steady state ratio, and had a time constant of 3.3 minutes (Fig. 5.60). Performance of these sensors appears similar both in terms of response time and measurement error. In either case a steady state fluorescence ratio is attained within approximately 15 minutes.

5.3.3. Conclusion

A practical pH sensitive optical sensor was built and tested. This sensor consists of a capillary small tube containing the pH sensitive fluorophore 1,4-DHPN, which was encapsulated in DPPC/DPPG liposomes containing 2.0 mole percent Gramicidin. The pH sensing end of the tube contains a thin Cuprophan membrane. This membrane allows hydrogen ions to pass into the tube, while at the same time preventing external leakage of the dye encapsulated liposomes. Response time and measurement accuracy, as well as precision, of these sensors were tested

and appear acceptable for steady state or slowly changing systems.The thermal stability of liposomal based sensors was evaluated and determined to be suitable for use during hyperthermia studies lasting in excess of 1 hour. Finally, the small size of these sensors should permit *in vivo* pH measurements to be made, with minimal resultant tissue injury.

5.4. Animal Testing

5.4.1. Procedure

Whole blood was obtained from male Fisher 344 rats by laceration of the brachial artery. This blood was collected in a heparinized syringe and placed at room temperature in a glass vial containing 1000 units/ml of heparin. Liposomal based pH sensors were prepared as previously described using both 1.1 mm inner diameter polysulfone tubing and a 15 µl (0.58 mm inner diameter, 0.86 mm outer diameter) capillary tube. Blood pH was determined to be 7.24 at room temperature, using a Beckman Model 71 pH meter with a standard combination electrode. A measurement system calibration curve was determined from five data points using a 1 mM solution of 1,4-DHPN dissolved in 305 mOsm phosphate buffers ranging between pH 6.0 and 8.0 in 0.5 pH unit increments.The usual standard system measurement parameters were used.

5.4.2. Results and Discussion

The polysulfone sensor appeared to achieve a steady state with an exponential response time of 19.8 minutes (Fig. 5.61) compared to 6.1 minutes obtained during the free dye studies. Also as expected, the predicated value of the fluorescence ratio was not attained. The standard deviation and thus, the precision of these measurements was very good. This is a direct result of the large tubular volume of the sensor. At 60 minutes the pH value calculated from the fluorescence ratio was

7.06 ±.004. In contrast, the 15 µl Cuprophan capillary sensor reached a steady state response with an exponential time constant of 10.0 minutes (Fig. 5.62), compared to 3.2 minutes for the 20 µl liposome based sensors previously discussed. The expected steady state ratio was achieved with this sensor even though the measurement precision, due to volume restrictions, was not as good. At 60 minutes a pH of 7.24 ±.06 could be computed from the calibration curve using the measured ratio and its standard deviation.

The most interesting result obtained from this study is that the exponential response time increased by a factor of approximately 3, for both sensors, when going form 305 mOsm phosphate buffer to a more physiological fluid (blood). Even though the 15 µl sensor was not tested directly in phosphate buffer, it is difficult to believe that it should possess a response substantially different from the 20 µl sensor that was tested. In any case, a faster not slower response would be expected. One explanation for the response time differences is the development of a diffusion potential across either the sensor membrane or across the liposomal membrane. Such a potential would limit net proton flux across these membranes, and thus prevent hydrogen ion equilibrium from being reached. Since both sensor membranes are fairly permeable to small molecules and ions, a Donnan equilibrium, set up by the large charged protein molecule present in blood, may contribute to the development of this membrane potential. In fact, the negatively charged liposomes contained within the sensor, may also play a significant role in establishing this potential.

The liposomal membrane by itself is reported to be 6 to 10 orders of magnitude less permeable to other ions than it is to hydrogen [12]. This restriction is eased for most monovalent cations due to the presence of Gramicidin in the liposomal membrane. However, this membrane still remains relatively impermeable to anions and divalent cations. Here as before, the selective

permeability properties of the this membrane may provide the source of a hydrogen ion flux limiting diffusion potential.

Another explanation for the observed increase in response time may be due to the blocking effect of divalent cations on the alkali ion permeability of the Gramicidin channel. Ca^{++}, and to a lesser extent Mg^{++}, have been shown to reduce the conductance of the Gramicidin channel when present in concentrations of 0.1-1.0 M [6]. Rat blood plasma contains 2.6 mM Ca^{++} and 1.1 mM Mg^{++} [75]. Even though these levels are substantially less than those used in the channel blocking study reported above, they may be sufficient to account for the increase in optrode response time seen in whole blood.

5.4.3. Conclusion

A limited biological study of this optical pH measurement system indicates that with small liposomal based Cuprophan sensors, accurate and precise steady state pH measurements can be obtained. While *in vitro* testing of these sensors demonstrates an adequate response time for measuring slow pH changes, this response time rapidly degenerates for measurements in physiological fluids, such as whole blood. Further research is needed if an understanding of this phenomenon is to be obtained, and a practical solution realized.

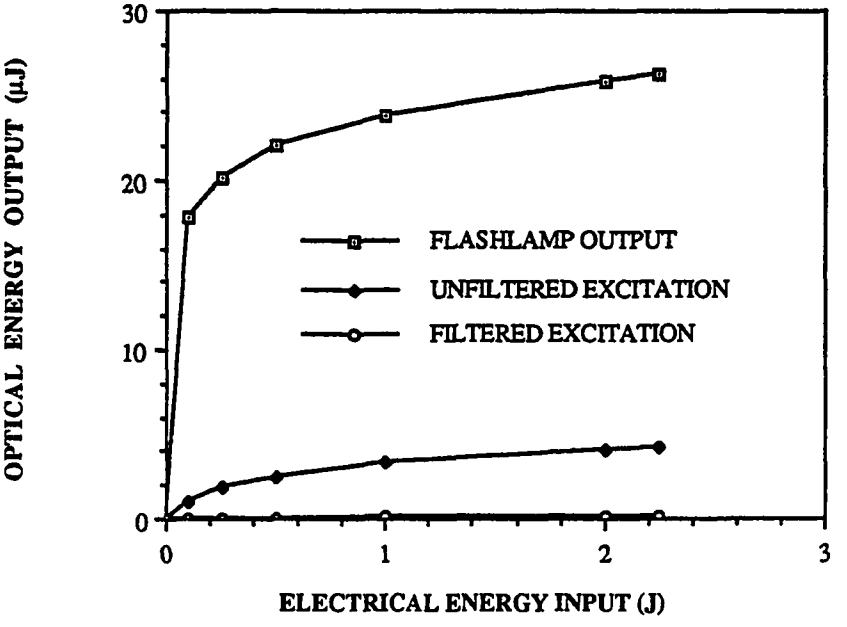

Figure 5.1. Optical energy as a function of electrical input energy. Measurements were taken at several points in the flashlamp excitation subsystem.

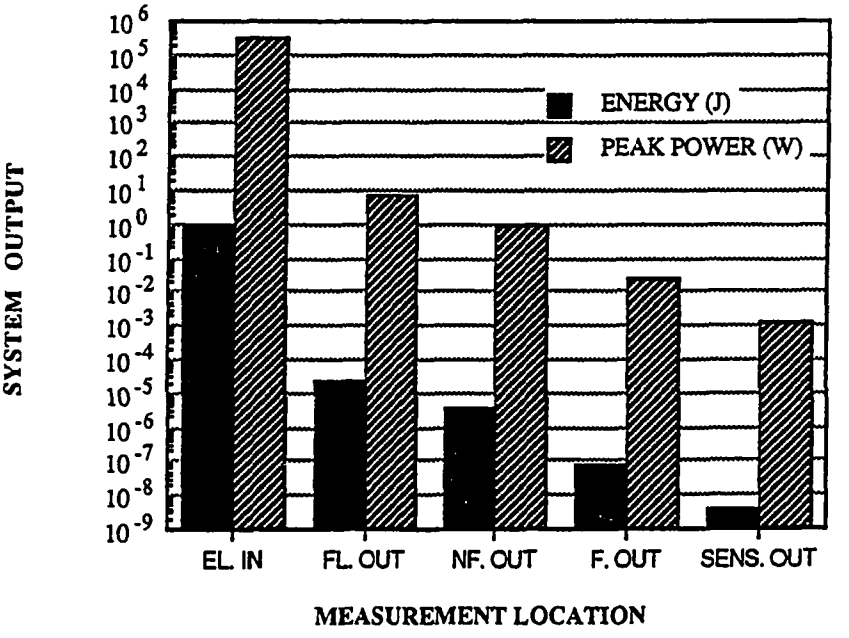

Figure 5.2. Optical energy and peak optical power measured at several locations along the excitation path. EL.IN = electrical input, FL.OUT = directly in front of flashbulb, NF.OUT = at subsystem output without shortpass filter, F.OUT = at subsystem output with shortpass filter, SENS.OUT = at the sensor output. Peak optical power was calculated using a duration of 3.2 μs.

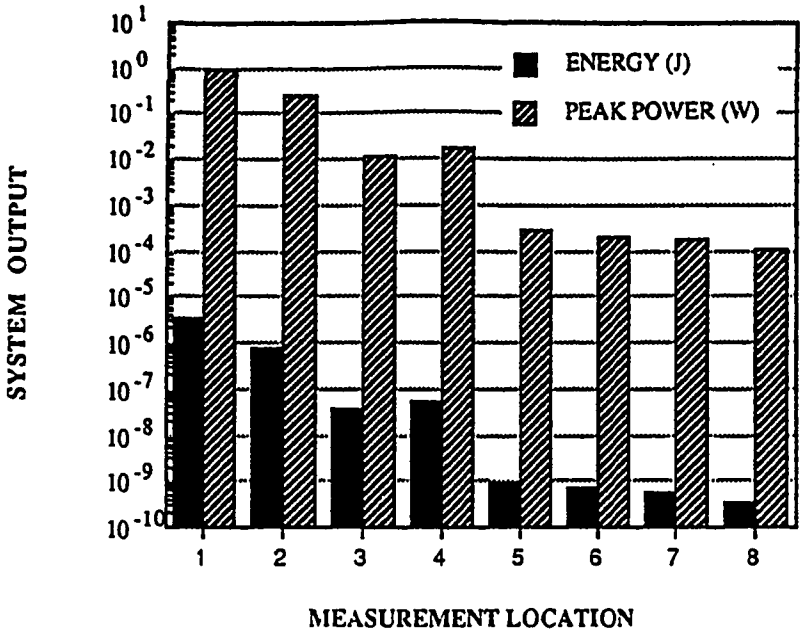

Figure 5.3. Optical energy and peak optical power measured at several locations along the emission path. The unfiltered flashlamp was input to the sensor port with 1 J of electrical input energy. 1 = output of unfiltered excitation module, 2 = output of sensor module, 3 = unfiltered 90° output of detector module, 4 = unfiltered 0° output of detector module, 5 = 488 nm (90°) output of detector module, 6 = 434 (0°) output of detector module, 7 = front panel 488 nm connector, 8 = front panel 434 nm connector.

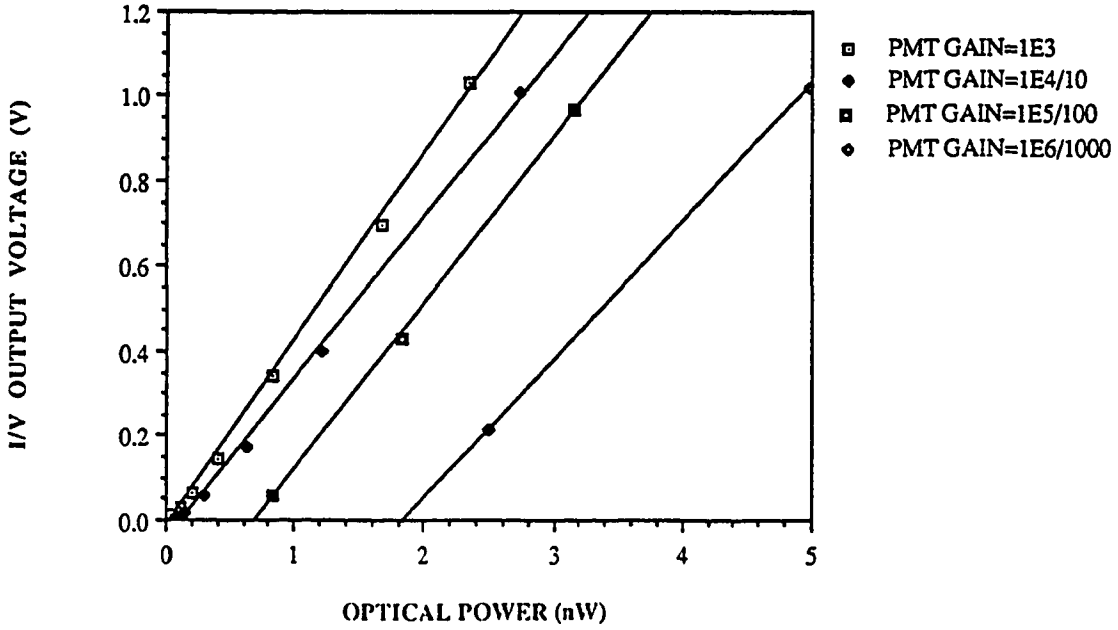

Figure 5.4. The I/V output versus optical input power as a function of photomultiplier current gain. Excitation source was a blue LED (480 nm) operated in a dc mode. An I/V transresistance gain of 10 M was used.

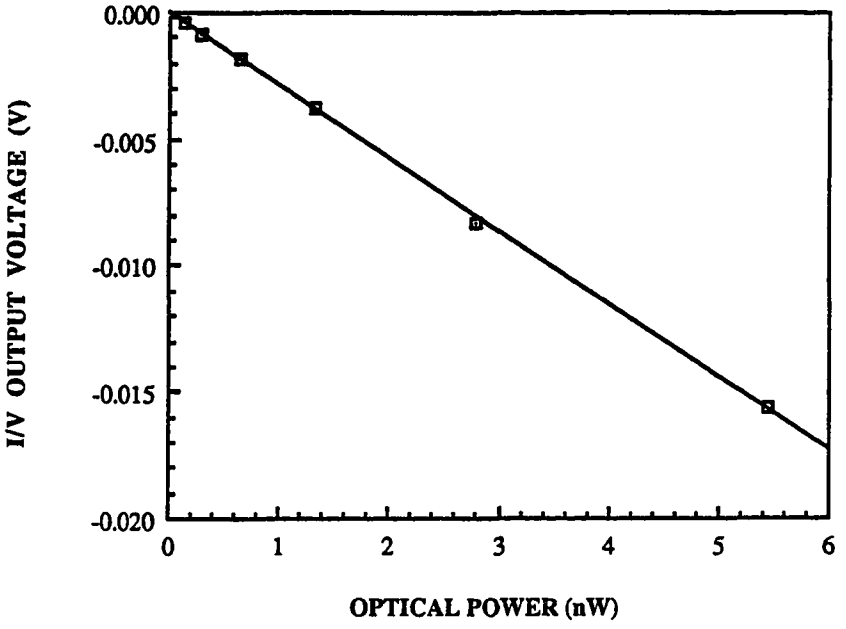

Figure 5.5. The I/V output versus optical input power for PIN photodiodes. Excitation source was a blue LED (480 nm) operated in a dc mode. An I/V transresistance gain of 10 M was used.

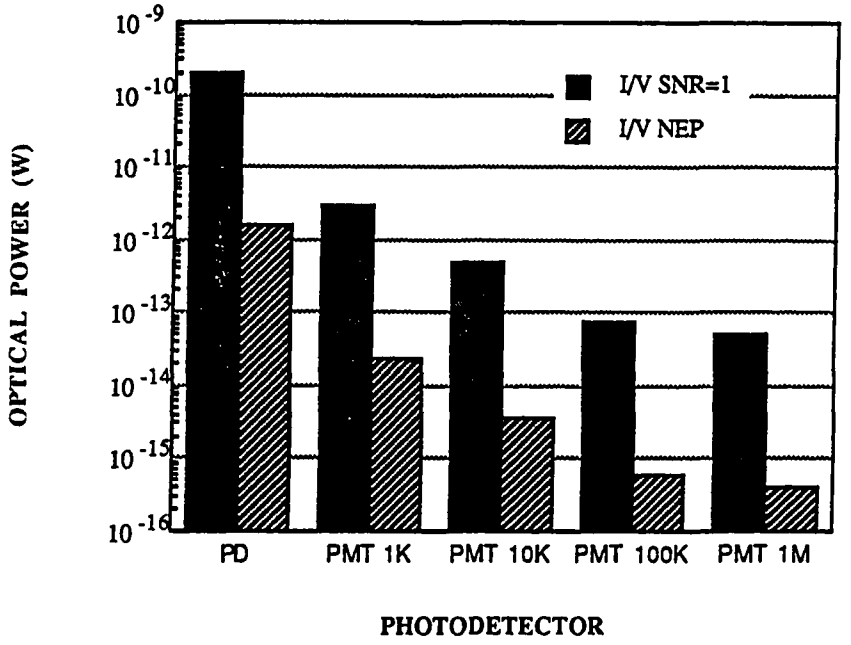

Figure 5.6. Minimum detectable optical power levels at the I/V output using PIN photodiodes and photomultipliers at various current gains settings. Excitation source was a blue LED (480 nm) operated in a dc mode. An I/V transresistance gain of 10 M was used.

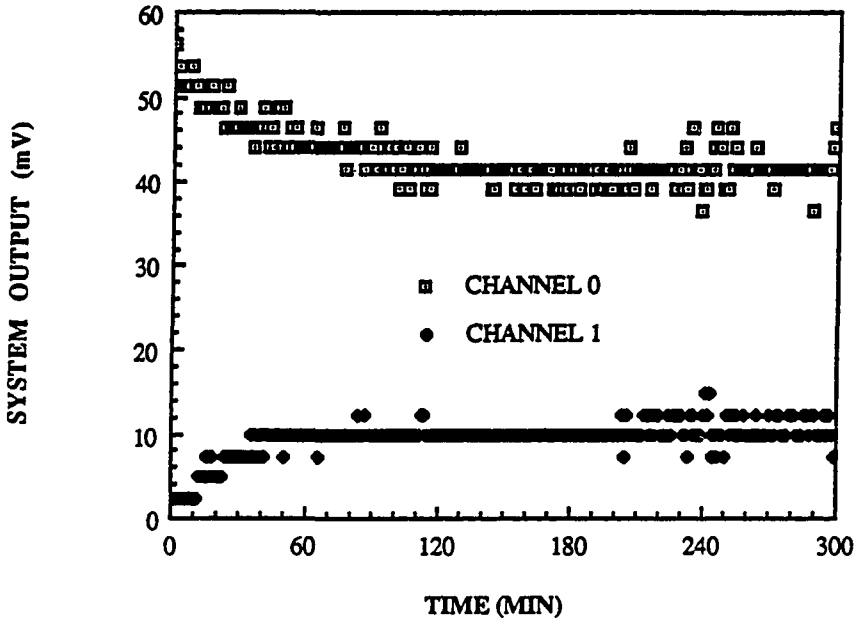

Figure 5.7. Drift and stability of the wideband electronics module using photomultiplier tubes operated at a current gain of 10,000. A system integration time of 100 μs and an I/V transresistance gain of 10 M were used. No optical signal was applied.

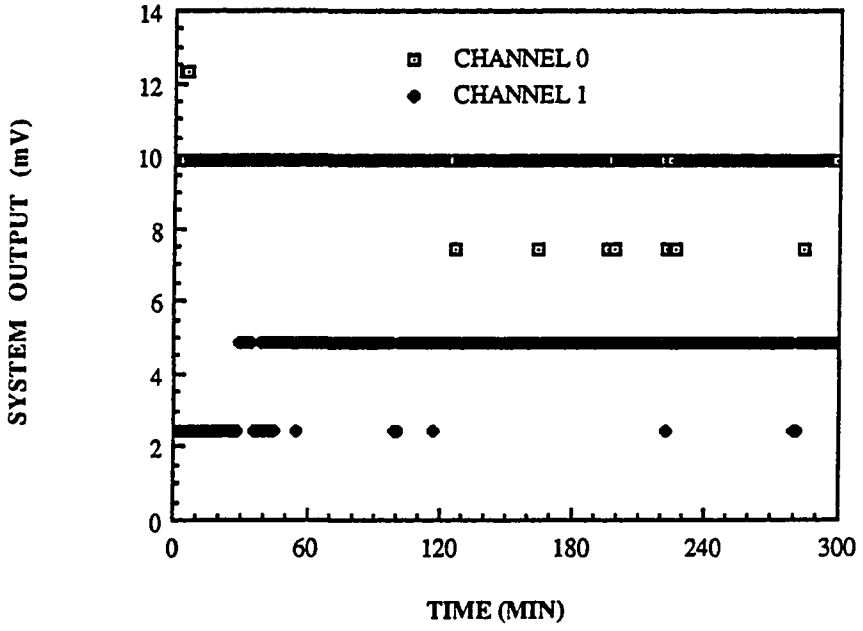

Figure 5.8. Drift and stability of the narrowband electronics module using photomultiplier tubes operated at a current gain of 10,000. A system integration time of 100 μs and an I/V transresistance gain of 10 M were used. No optical signal was applied.

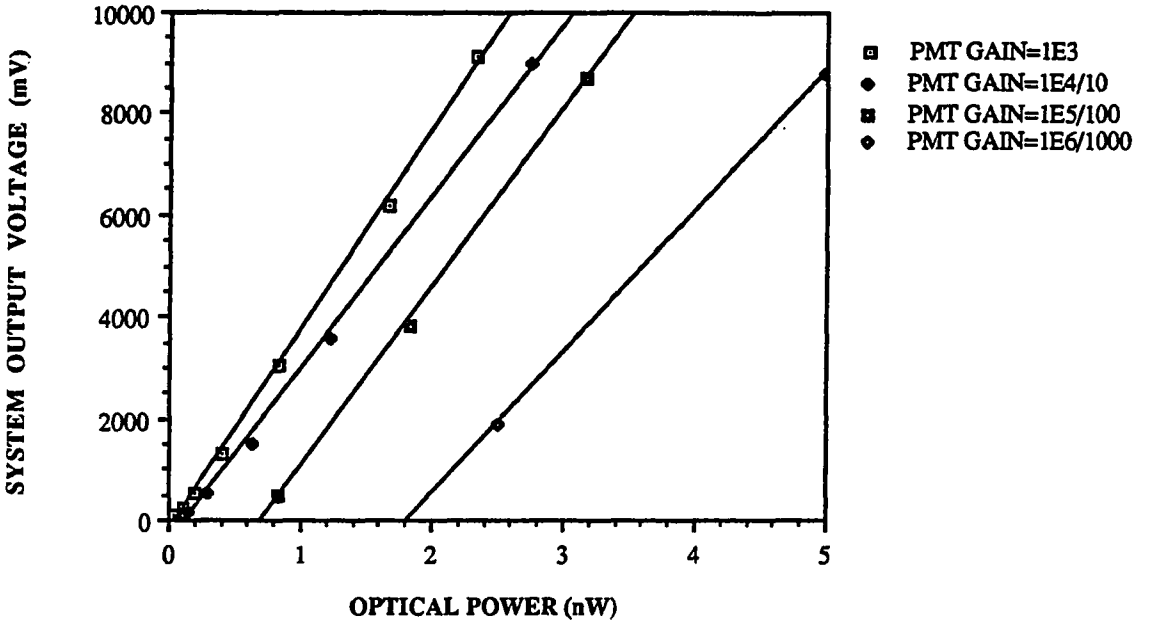

Figure 5.9. System output voltage versus optical input power as a function of photomultiplier current gain. Excitation source was a blue LED (480 nm) operated in a dc mode. An I/V transresistance gain of 10 M and an integration time of 25 μs were used.

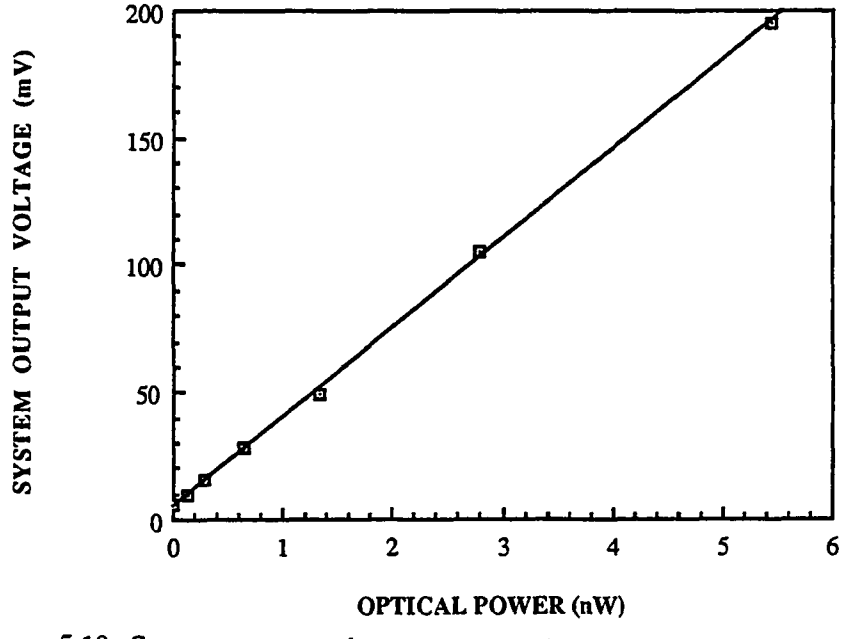

Figure 5.10. System output voltage versus optical input power for PIN photodiodes. Excitation source was a blue LED (480 nm) operated in a dc mode. An I/V transresistance gain of 10 M and an integration time of 25 μs were used.

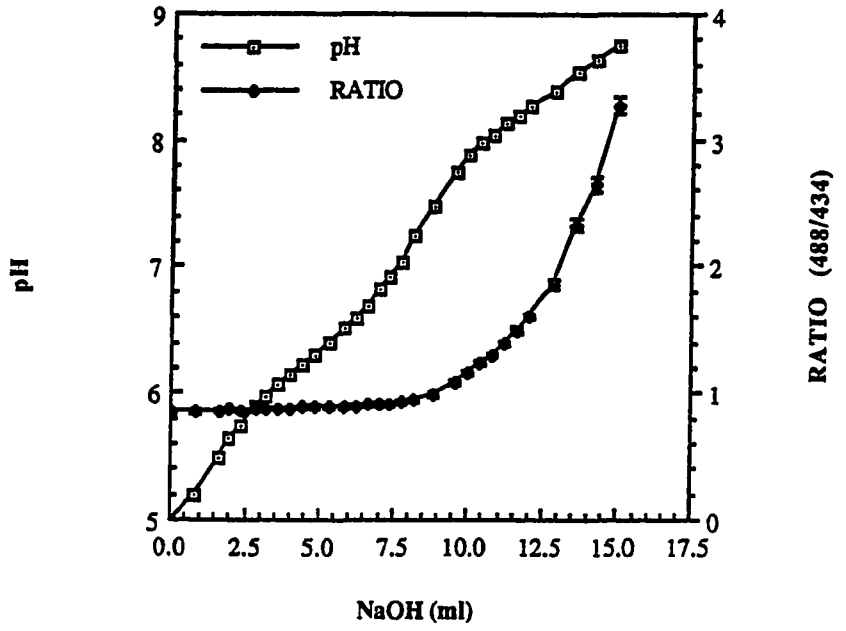

Figure 5.11. Potentiometric pH and optical fluorescence ratio for a titration of a 2 mM solution of 1,4-DHPN in a 50/50 ethanol/water solvent. Optical system parameters were set to 1 J at 8 Hz with a 100 μs integration time. The titrant was 17 mM NaOH.

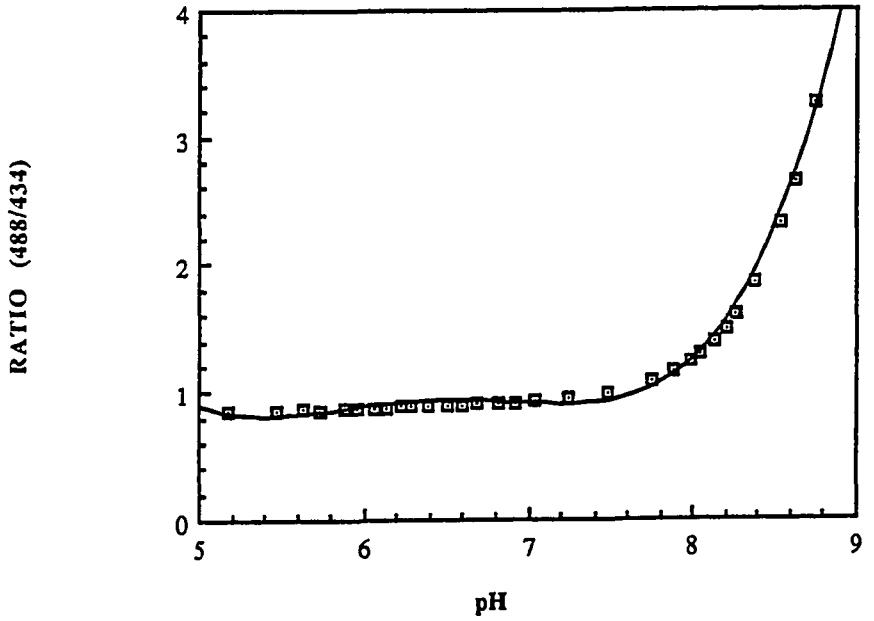

Figure 5.12. Fluorescence ratio versus pH for titration of a 2 mM solution of 1,4-DHPN in a 50/50 ethanol/water solvent. A fourth order polynomial was used to fit the data.

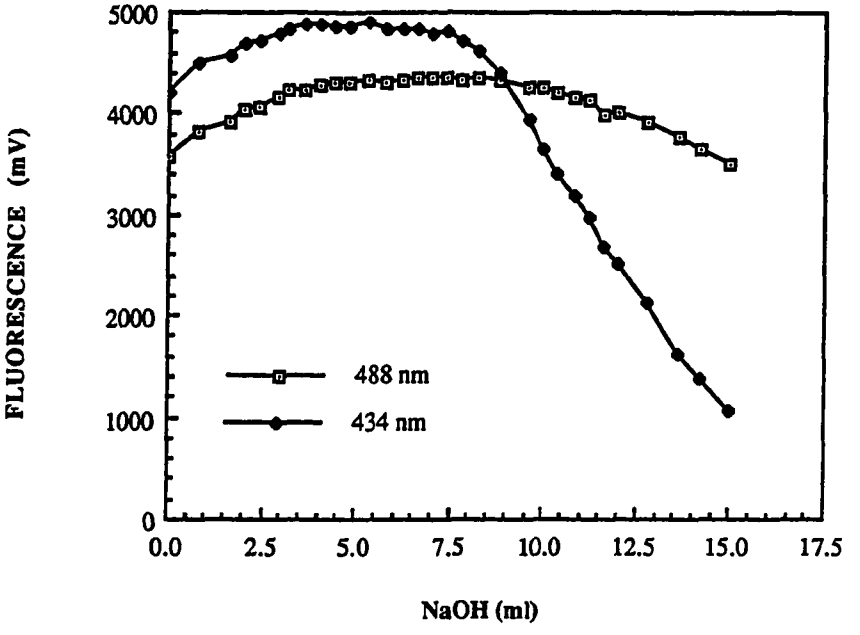

Figure 5.13. System output at 488 nm and 434 nm, as a function of the volume of titrant added, during the titration of a 2 mM solution of 1,4-DHPN in a 50/50 ethanol/water solvent.

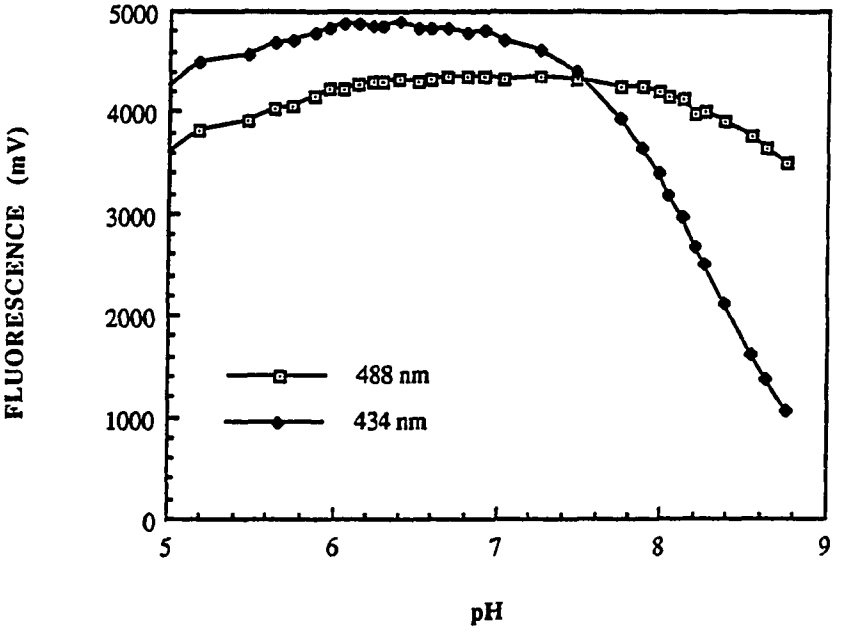

Figure 5.14. System output at 488 and 434 nm, as a function of pH, during the titration of a 2 mM solution of 1,4-DHPN in a 50/50 ethanol/water solvent.

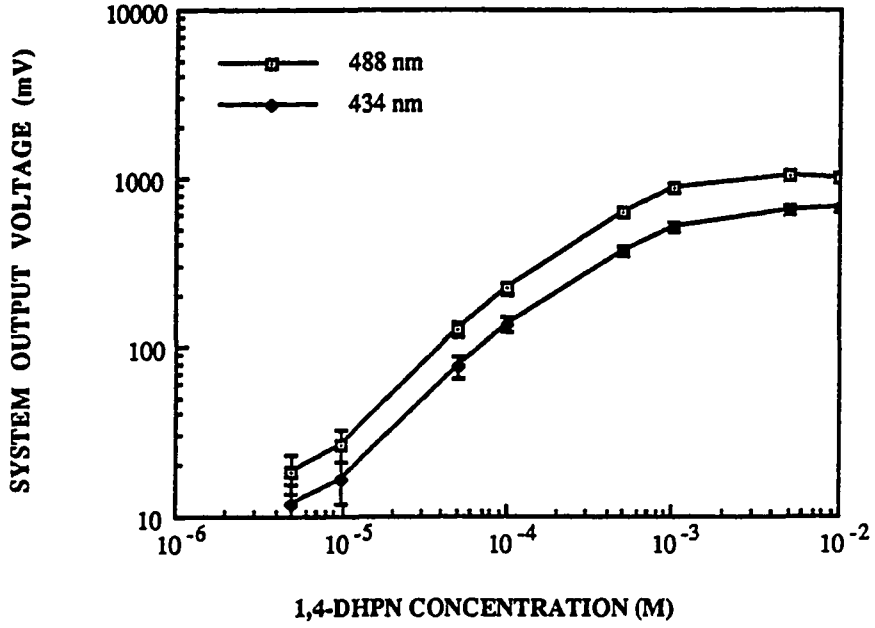

Figure 5.15. System output at 488 and 434 nm as a function of 1,4-DHPN concentration, in 305 mOsm phosphate buffer at pH 7.0.

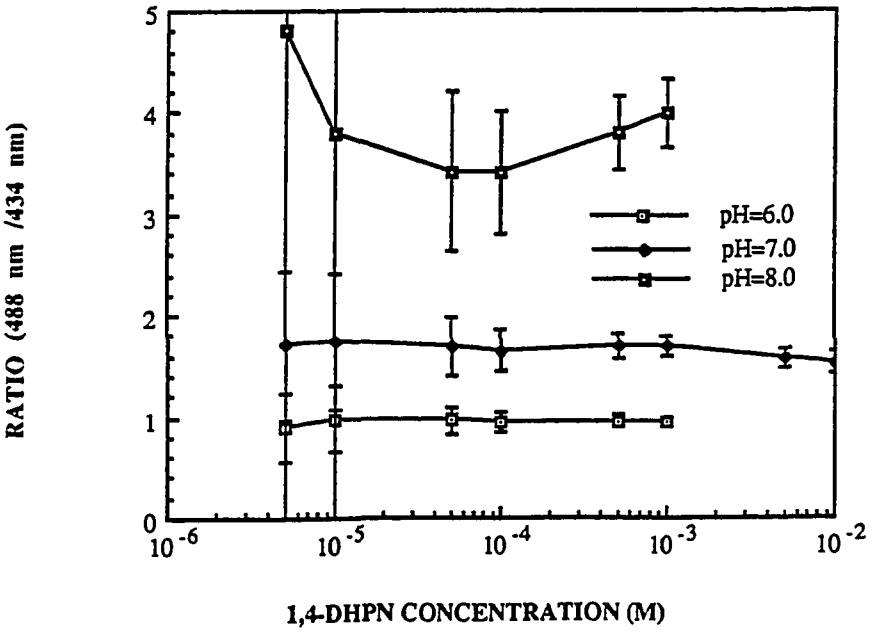

Figure 5.16. Fluorescence ratio versus concentration of 1,4-DHPN in 305 mOsm phosphate buffer at various values of pH.

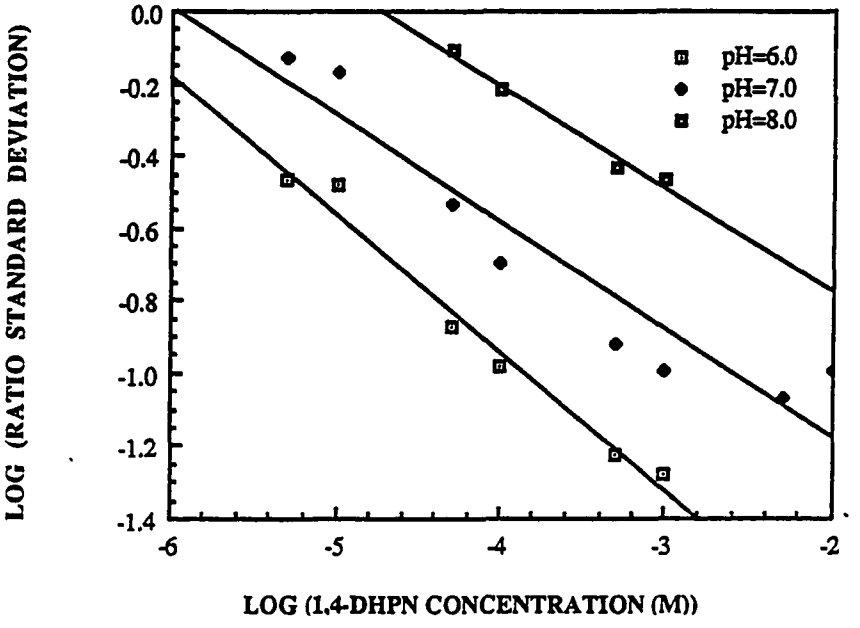

Figure 5.17. A log-log plot of the standard deviation of the fluorescence ratio as a function of concentration of 1,4-DHPN in 305 mOsm phosphate buffer at various values of pH. The slope of these curves was determined, by regression fit, to average to 0.32.

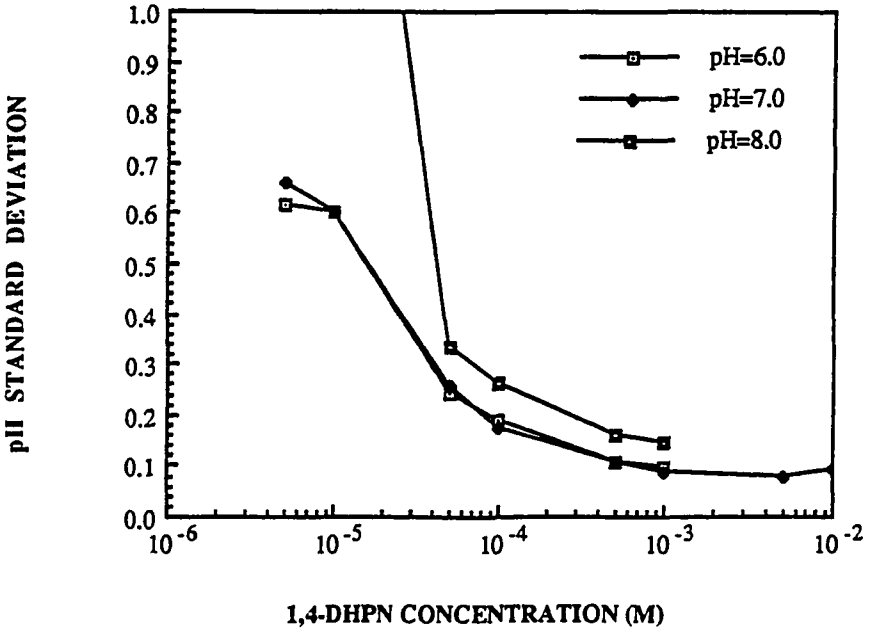

Figure 5.18. The standard deviation of pH as a function of the concentration of 1,4-DHPN, in 305 mOsm phosphate buffer at various values of pH, as calculated from ratio data.

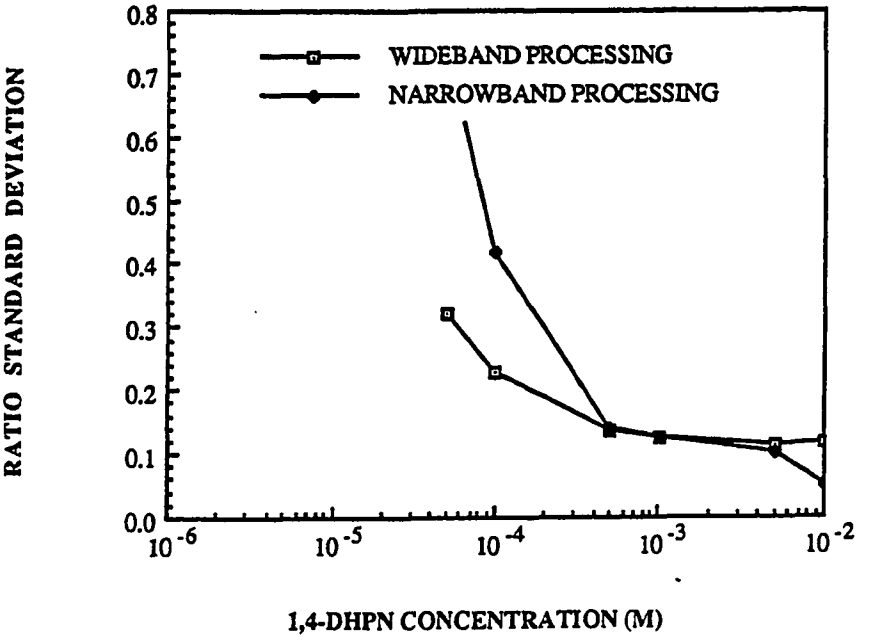

Figure 5.19. The effect of wideband and narrowband processing on the fluorescence ratio versus concentration curves. All concentrations of 1,4-DHPN were prepared in 305 mOsm phosphate buffer at pH 7.0.

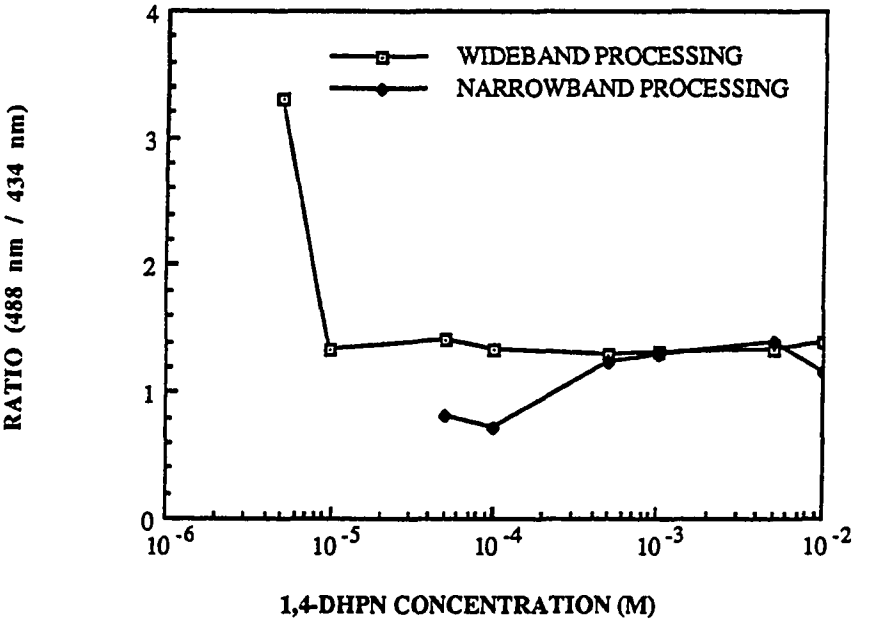

Figure 5.20. The effect of wideband versus narrowband processing on the standard deviation of the fluorescence ratio as a function of the concentration of 1,4-DHPN in solution. All solutions were prepared in 305 mOsm phosphate buffer at pH 7.0.

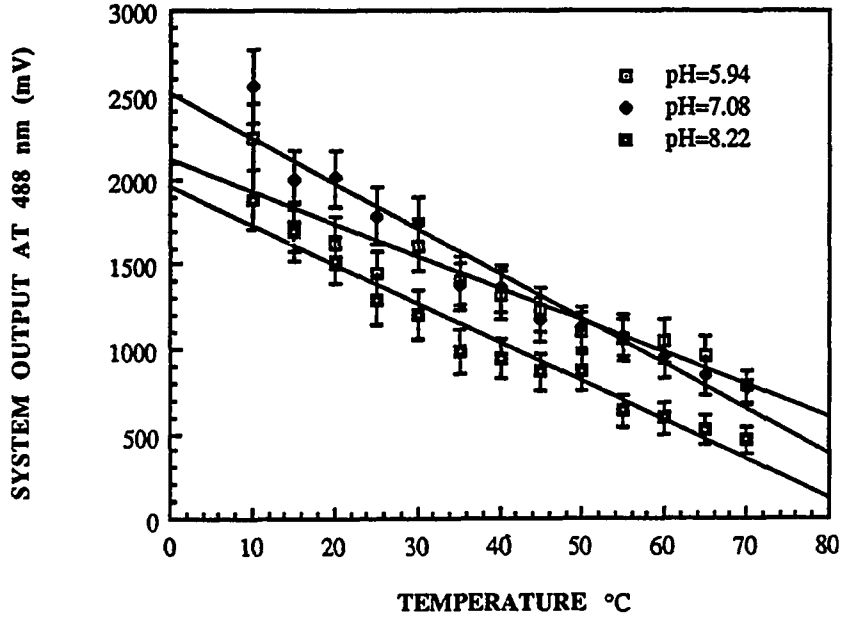

Figure 5.21. Effect of temperature on the system output at 488 nm as a function of pH. All solution were prepared in 305 mOsm phosphate buffer at a 1,4-DHPN concentration of 0.1 mM. Slopes tend to increase as the pH is made more alkaline.

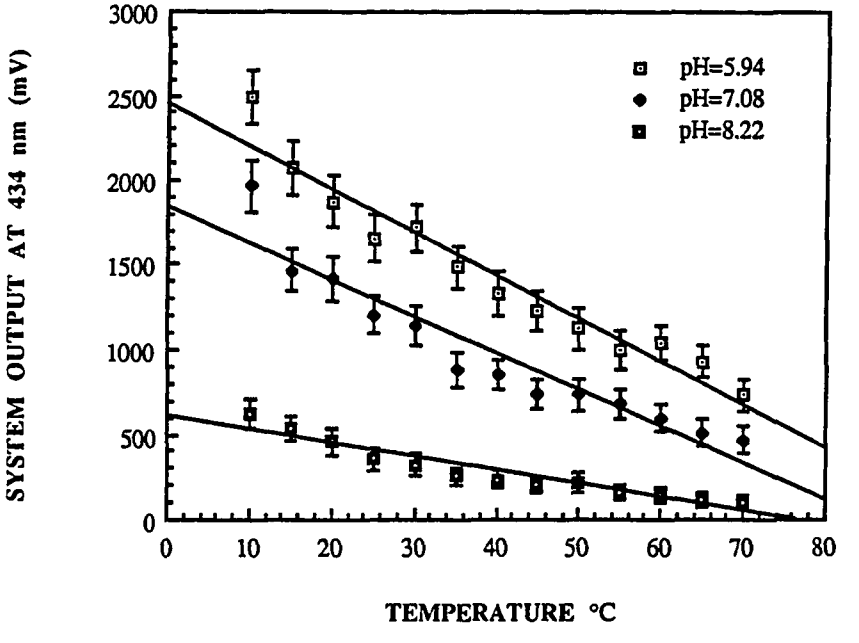

Figure 5.22. Effect of temperature on the system output at 434 nm as a function of pH. All solution were prepared in 305 mOsm phosphate buffer at a 1,4-DHPN concentration of 0.1 mM. Slopes tend to decrease as the pH is made more alkaline.

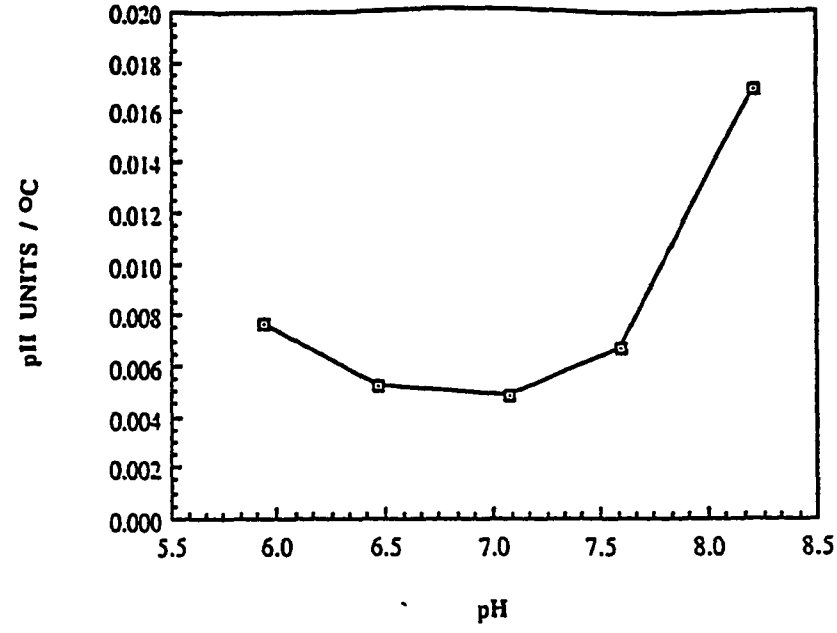

Figure 5.23. Calculated standard deviation of pH measurements/°C as a function of pH. Note minimum near pH 7.0. All measurements were taken using a 0.1 mM concentration of 1,4-DHPN dissolved in 305 mOsm phosphate buffer. System parameter of 1 J at 8 Hz and an integration time of 100 μs were used.

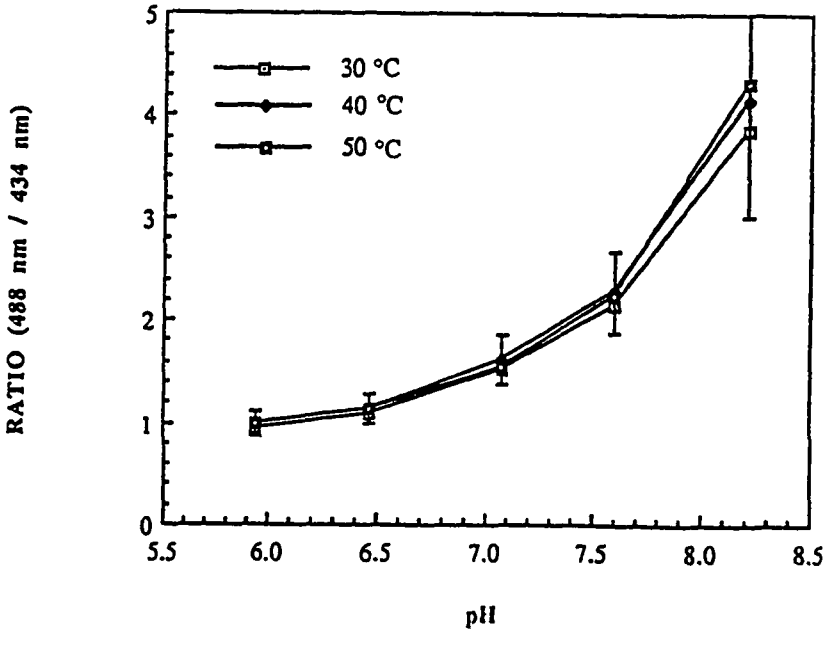

Figure 5.24. Fluorescence ratio as a function of pH at various temperatures. All measurements were taken using a 0.1 mM concentration of 1,4-DHPN dissolved in 305 mOsm phosphate buffer. System parameters of 1 J at 8 Hz and an integration time of 100 μs were used. Note that the temperature induced measurement error is less than the intrinsic measurement error at all values of pH.

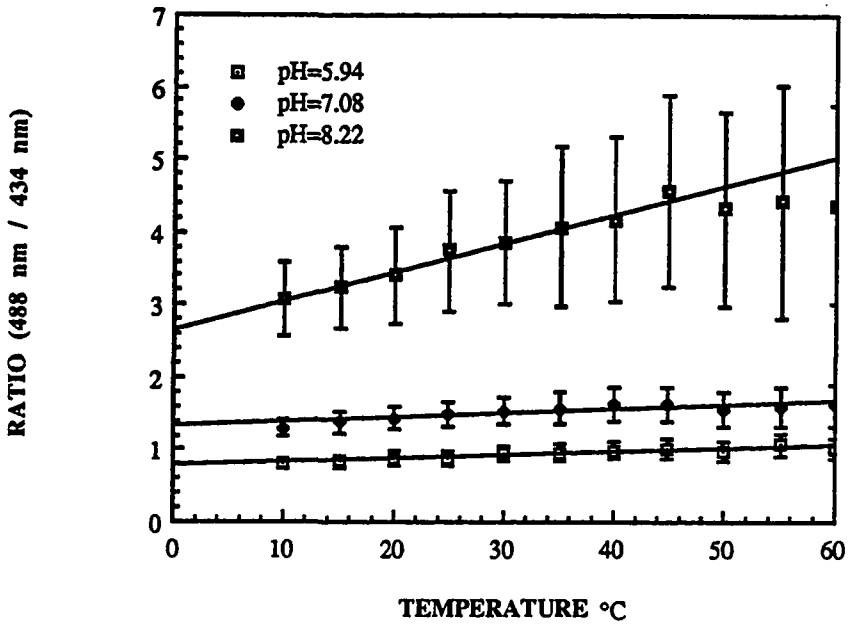

Figure 5.25. Fluorescence ratio as a function of temperature at various values of pH. All measurements were taken using a 0.1 mM concentration of 1,4-DHPN dissolved in 305 mOsm phosphate buffer. System parameters of 1 J at 8 Hz and an integration time of 100 μs were used. All temperatures were measured in degrees Celcuis. Note the larger error at higher values of both temperature and pH.

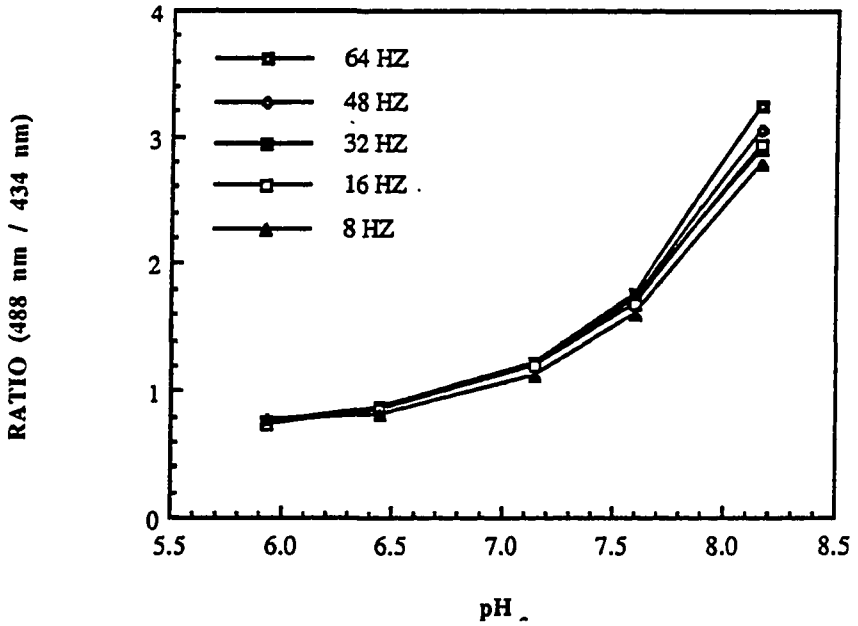

Figure 5.26. Fluoresence ratio versus pH as a function of flashlamp frequency. All measurements were taken using a 0.1 mM solution of 1,4-DHPN dissolved in 305 mOsm phosphate buffer at pH 7.0. An input energy of 1 J and an integration time of 100 μs were used.

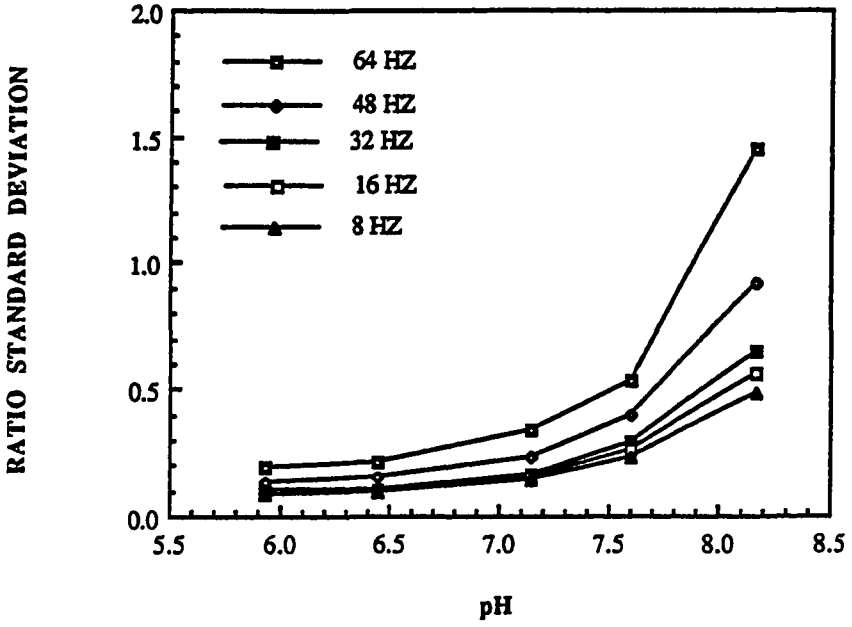

Figure 5.27. Standard deviation of the fluorescence ratio versus pH as a function of flash-lamp frequency. All measurements were taken using a 0.1 mM solution of 1,4-DHPN dissolved in 305 mOsm phosphate buffer at pH 7.0. An input energy of 1 J and an integration time of 100 μs were used.

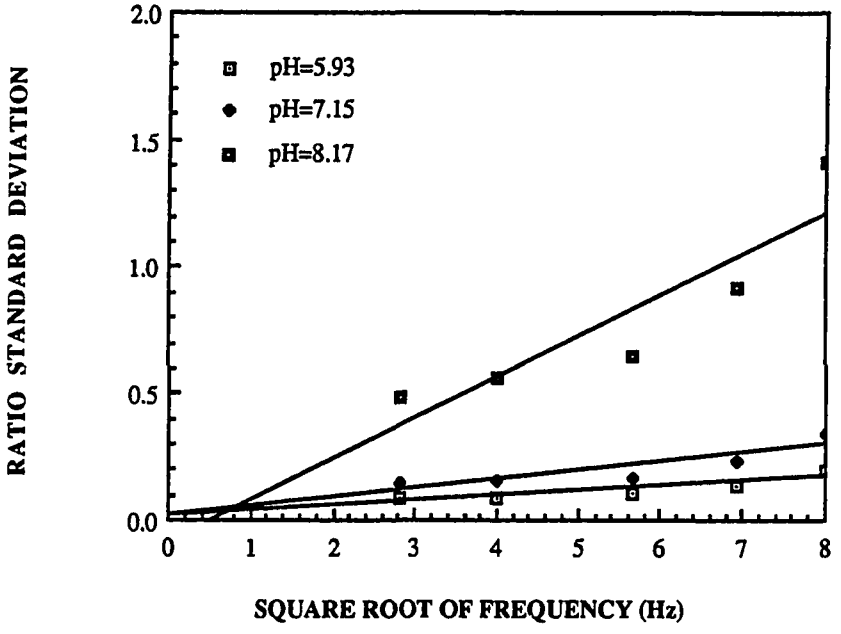

Figure 5.28. A plot of the standard deviation of the ratio versus the square root of flash-lamp frequency. All measurements were taken using a 0.1 mM solution of 1,4-DHPN dissolved in 305 mOsm phosphate buffer at pH 7.0. An input energy of 1 J and an integration time of 100 μs were used.

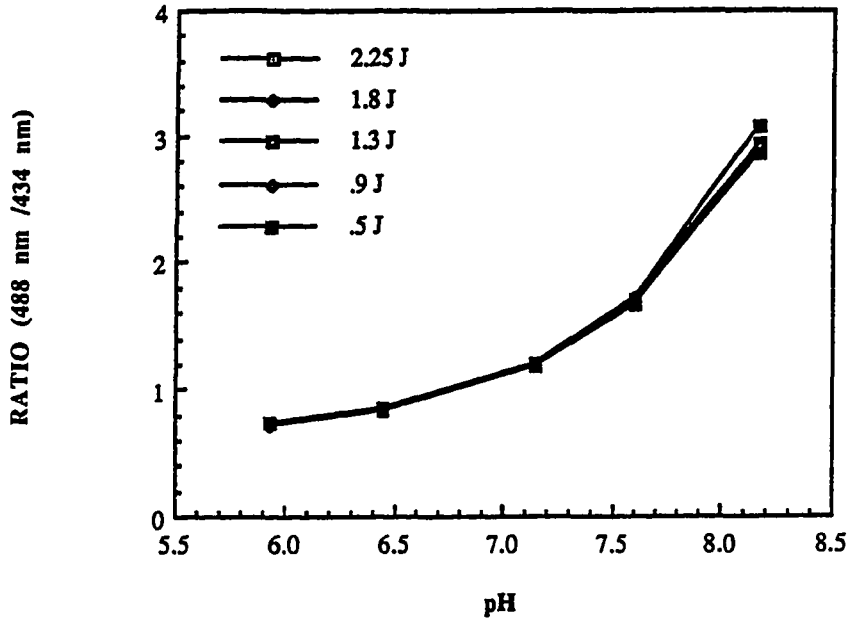

Figure 5.29. Fluorescence ratio versus pH as a function of input energy. All measurements were taken using a 0.1 mM solution of 1,4-DHPN dissolved in 305 mOsm phosphate buffer at pH 7.0. A flashlamp frequency of 8 Hz and an integration time of 100 μs were used.

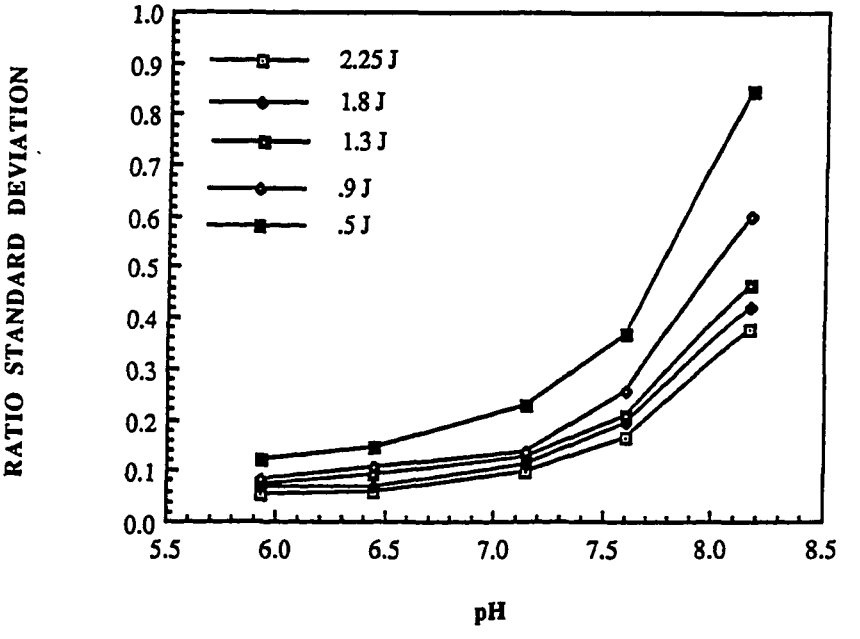

Figure 5.30. Standard deviation of the fluorescence ratio versus pH as a function of input energy. All measurements were taken using a 0.1 mM solution of 1,4-DHPN dissolved in 305 mOsm phosphate buffer at pH 7.0. A flashlamp frequency of 8 Hz and an integration time of 100 μs were used.

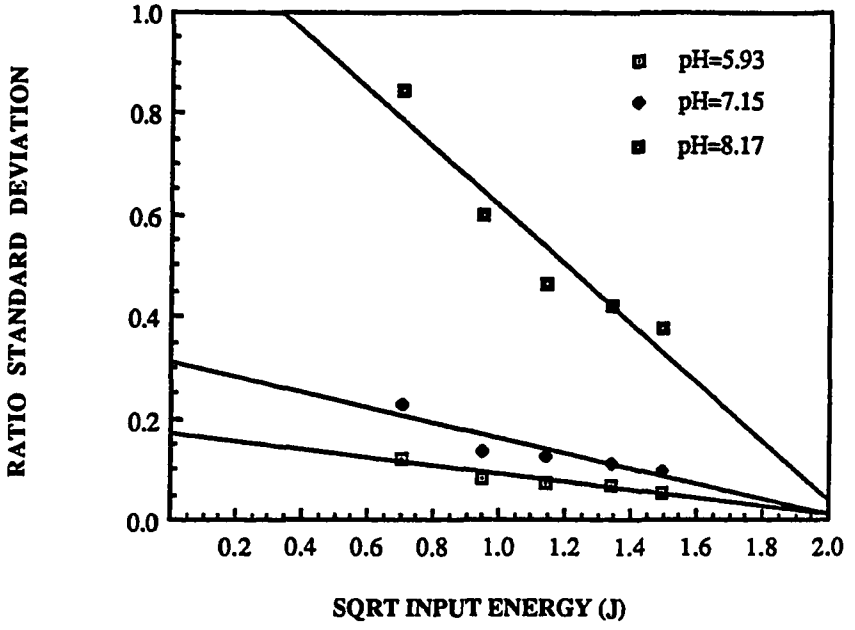

Figure 5.31. A plot of the standard deviation of the ratio versus the square root input energy. All measurements were taken using a 0.1 mM solution of 1,4-DHPN dissolved in 305 mOsm phosphate buffer at pH 7.0. An input energy of 1 J and an integration time of 100 μs were used.

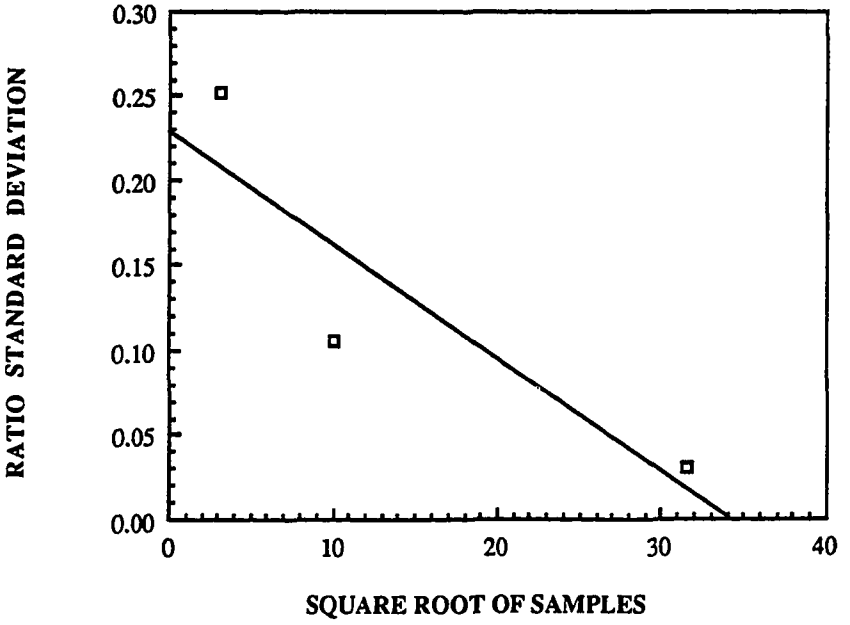

Figure 5.32. A plot of the standard deviation of the ratio versus the square root of the number of samples. All measurements were taken using a 0.1 mM solution of 1,4-DHPN dissolved in 305 mOsm phosphate buffer at pH 7.0. System parameters of 1 J at 8 Hz and an integration time of 100 μs were used.

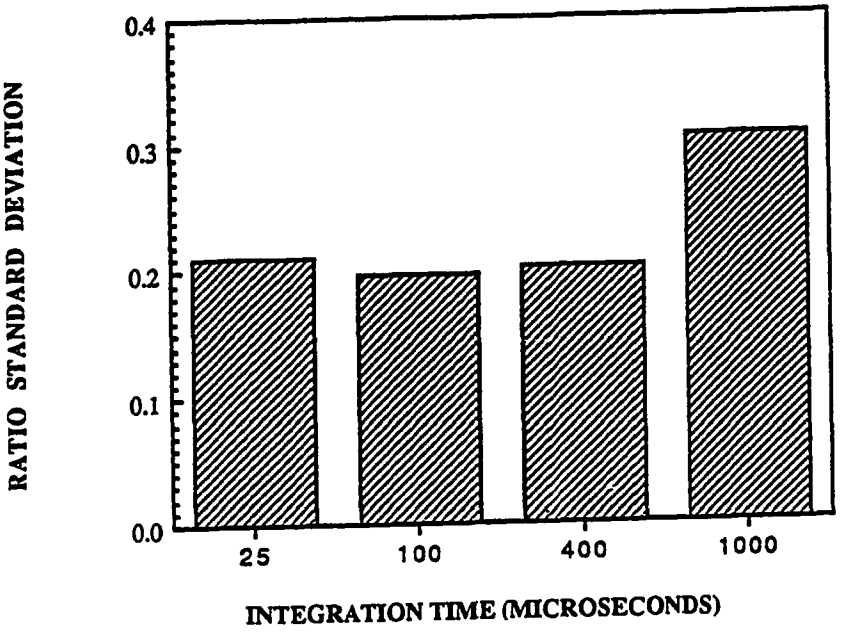

Figure 5.33. A graph of the standard deviation of the ratio versus system integration time. All measurements were taken using a 0.1 mM solution of 1,4-DHPN dissolved in 305 mOsm phosphate buffer at pH 7.0. System parameters of 1 J at 8 Hz were used.

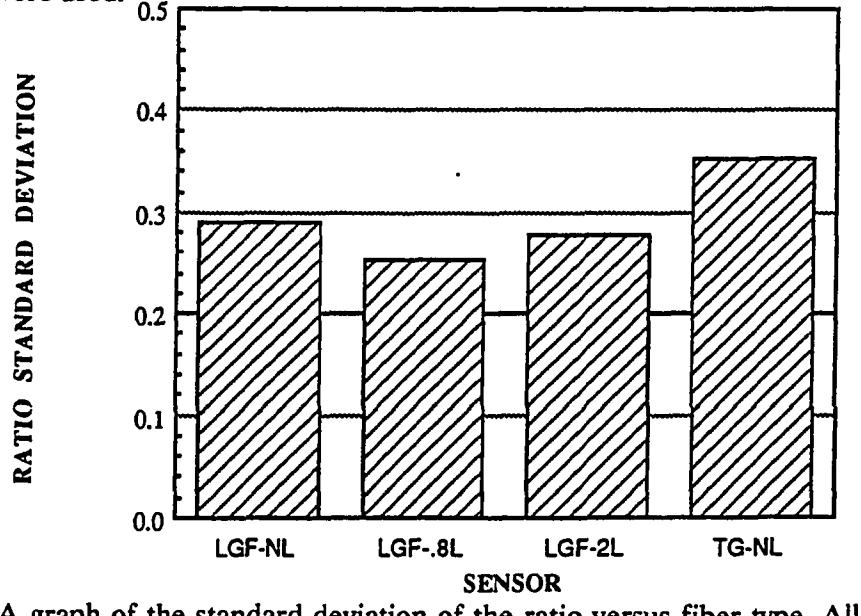

Figure 5.34. A graph of the standard deviation of the ratio versus fiber type. All measurements were taken using a 0.1 mM solution of 1,4-DHPN dissolved in 305 mOsm phosphate buffer at pH 7.0. System parameters of 1 J at 8 Hz and an integration time of 100 μs were used. LGF-NL=500 micron core with no lens, LGF-.8L=500 micron core with spherical lens of f=0.8 mm, LGF-2L=500 micron core with spherical lens of f=2.0 mm, and TG-NL=320 micron core with no lens.

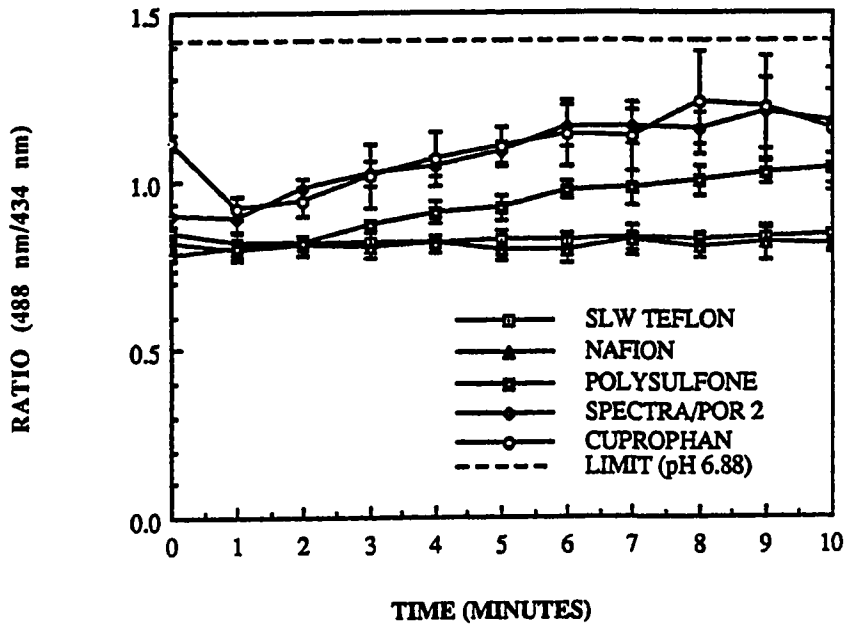

Figure 5.35. Fluorescence ratio response time curves for 1 mm inner diameter tubes of various materials when placed in a 305 mOsm phosphate buffer at pH = 6.88. The interior of the tubes was filled with a 0.1 mM solution of 1,4-DHPN dissolved in normal saline.

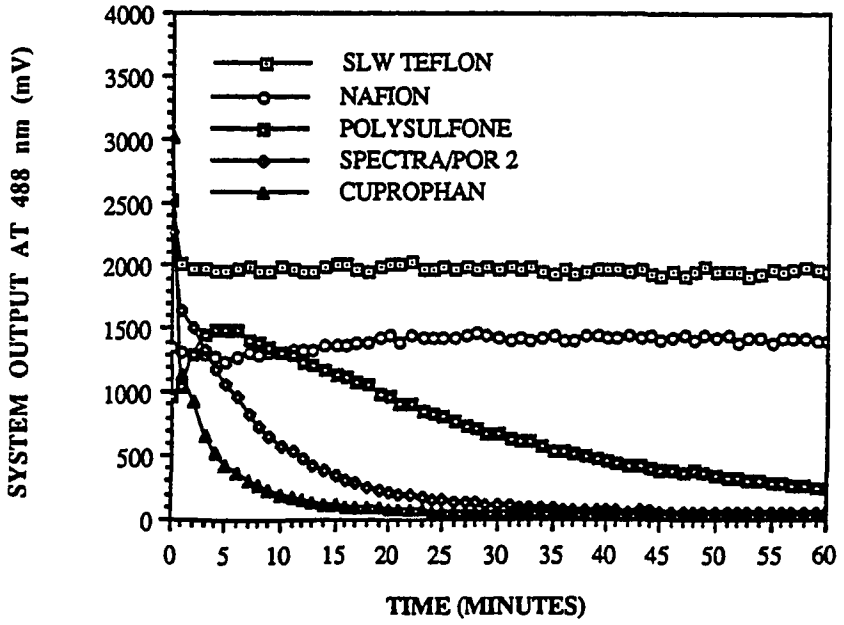

Figure 5.36. Response time curves, at 488 nm, for 1 mm inner diameter tubes of various materials when placed in a 305 mOsm phosphate buffer at pH = 6.88. The interior of the tubes was filled with a 0.1 mM solution of 1,4-DHPN dissolved in normal saline.

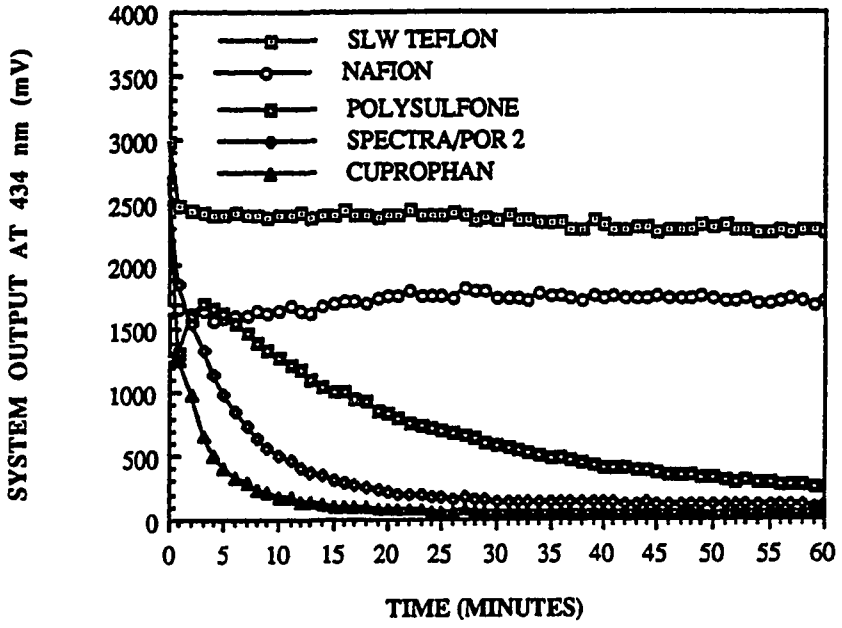

Figure 5.37. Response time curves, at 434 nm, for 1 mm inner diameter tubes of various materials when placed in a 305 mOsm phosphate buffer at pH = 6.88. The interior of the tubes was filled with a 0.1 mM solution of 1,4-DHPN dissolved in normal saline.

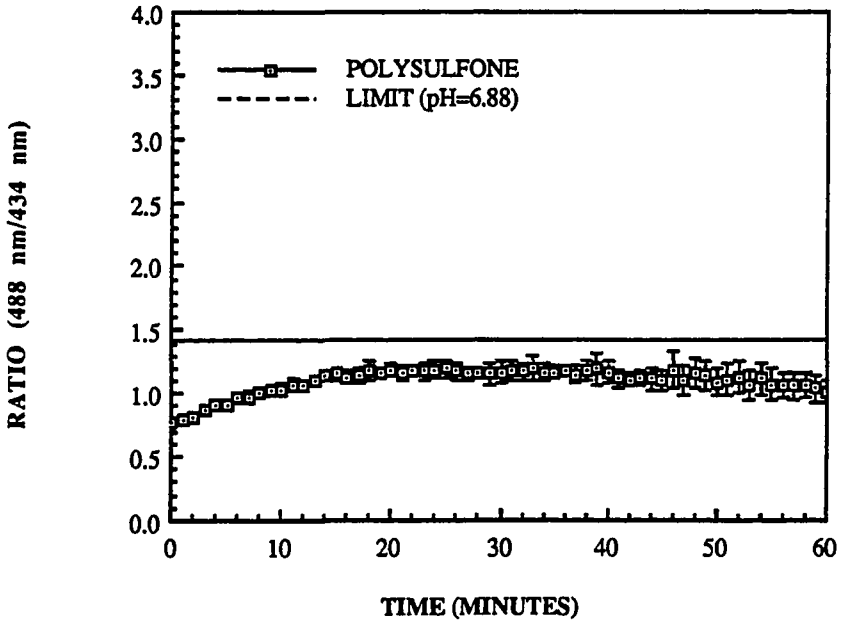

Figure 5.38. Fluorescence ratio response time curve for a 1 mm inner diameter polysulfone tube when placed in a 305 mOsm phosphate buffer at pH = 6.88. The interior of the tubes was filled with a 0.1 mM solution of 1,4-DHPN dissolved in normal saline. Sensor time constant was 6.1 minutes.

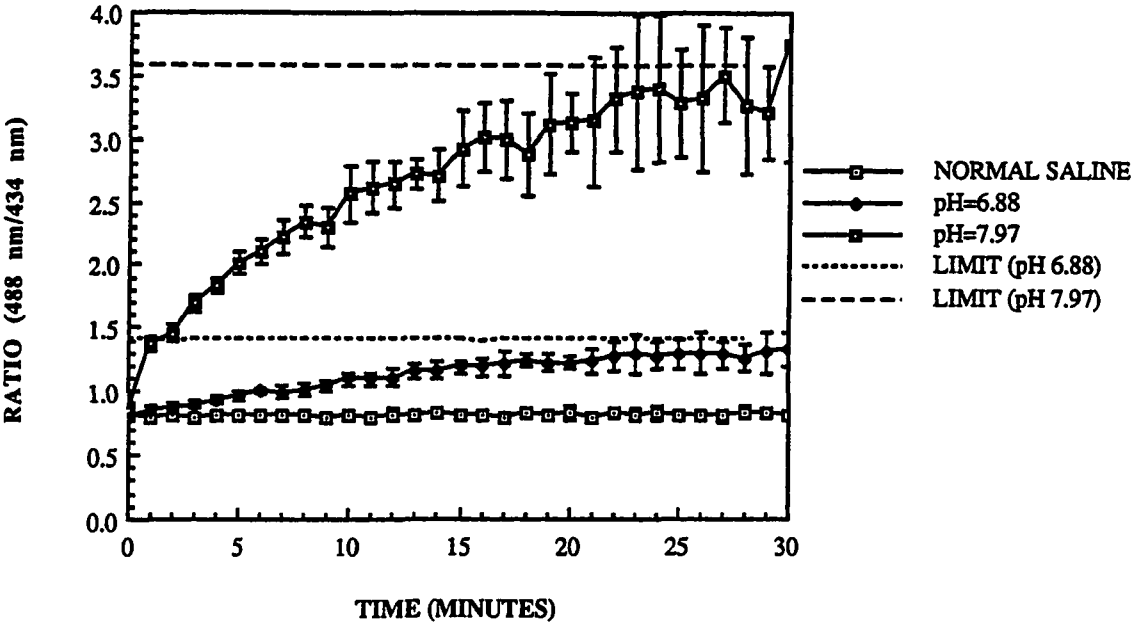

Figure 5.39. Fluorescence ratio response time curves for 2.5 mm diameter semi-micro dialysis tubing when placed in 305 mOsm phosphate buffers at various values of pH. The interior of the tubes was filled with a 0.1 mM solution of 1,4-DHPN dissolved in normal saline.

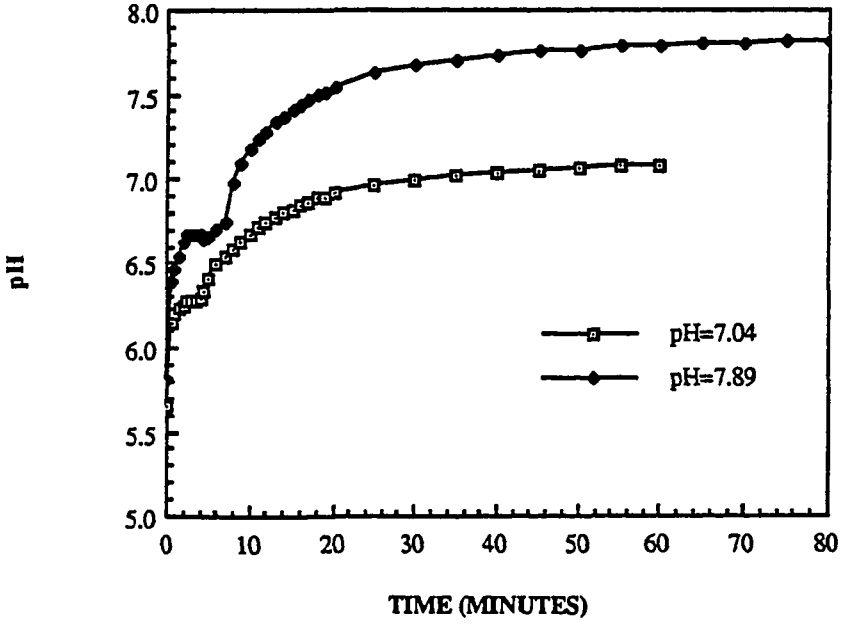

Figure 5.40. The pH response time curves for 2.5 mm diameter semi-micro dialysis tubing when placed in 305 mOsm phosphate buffers at various values of pH. The interior of the tubes was filled with normal saline and the internal pH was monitored using a micro pH electrode.

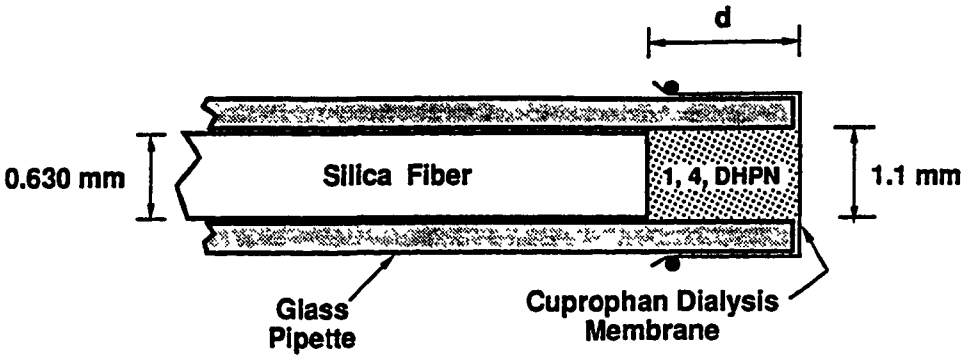

Figure 5.41. Construction of a capillary-based Cuprophan sensor using free fluorophore dissolved in normal saline.

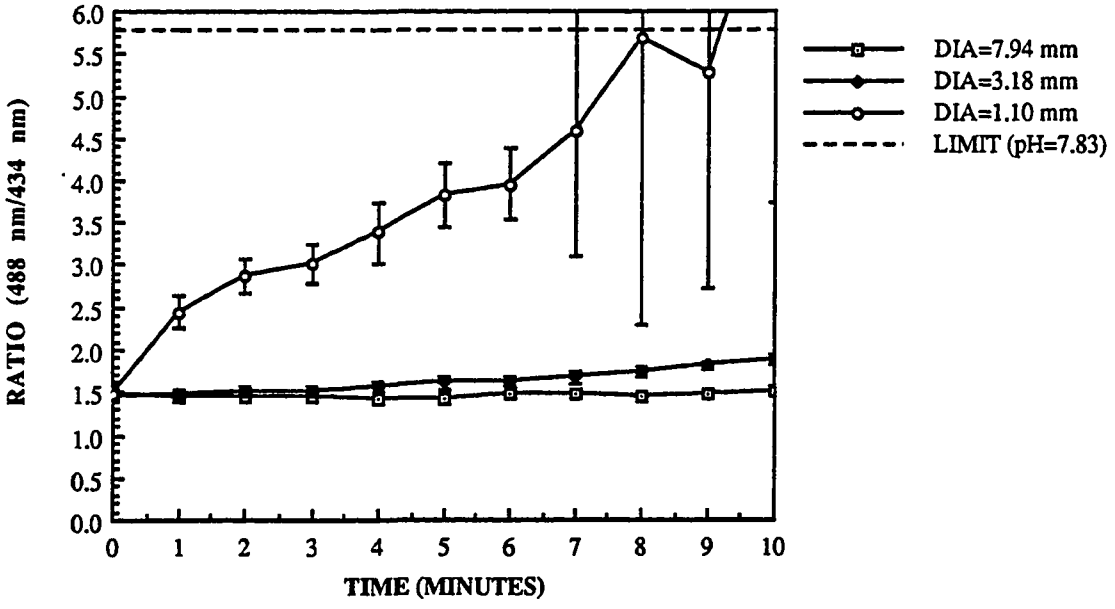

Figure 5.42. Fluorescence ratio response time curves of Cuprophan sealed tubes of various diameters. The interior of the tubes was filled with a 0.1 mM solution of 1,4-DHPN dissolved in normal saline.

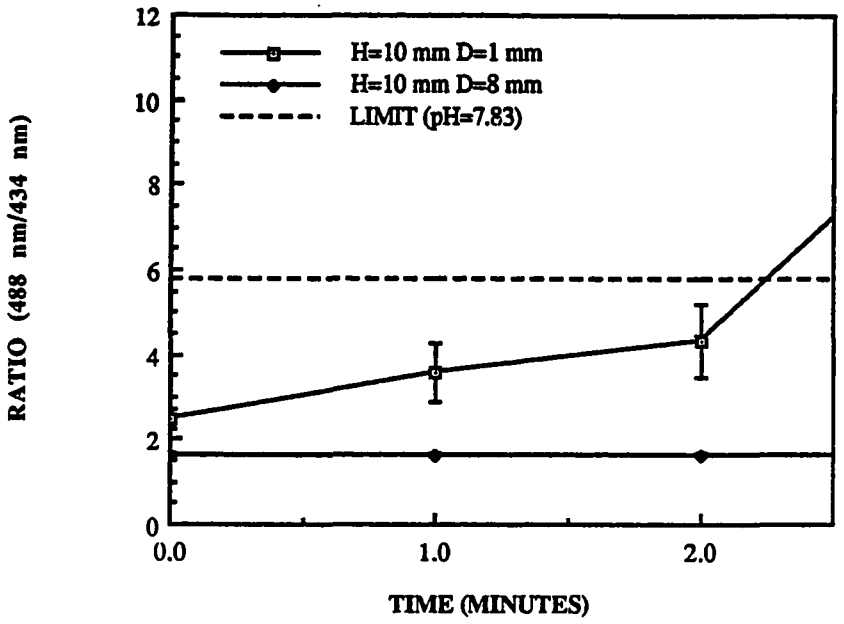

Figure 5.43. Fluorescence ratio response time curves of a 1.1 mm inner diameter capillary based Cuprophan sensor, with a constant solution volume, using a fiber positioned at different distances from the membrane. The interior of the tubes was filled with a 0.1 mM solution of 1,4-DHPN, dissolved in normal saline.

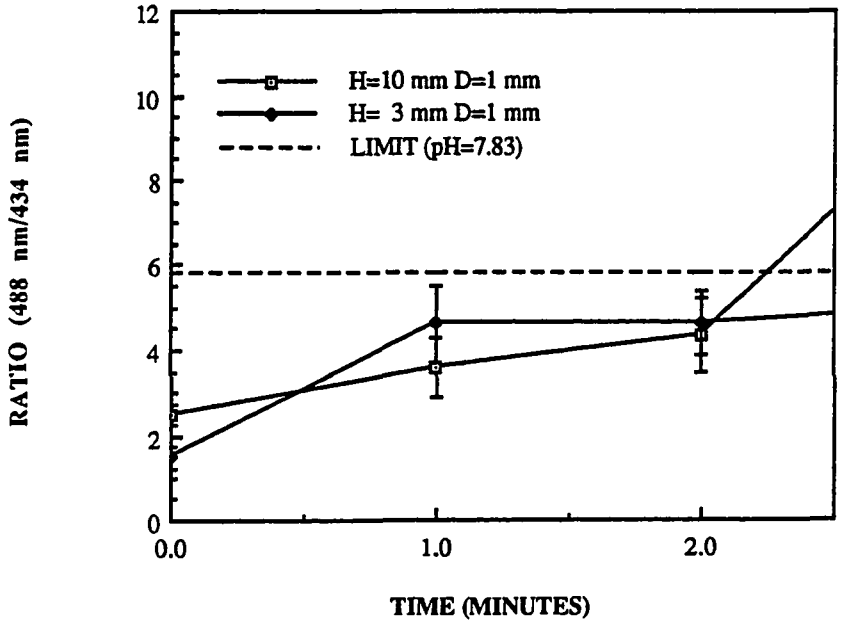

Figure 5.44. Fluorescence ratio response time curves of a 1.1 mm inner diameter capillary based Cuprophan sensor, with different solution volumes, using a fiber positioned at a constant distance from the membrane. The interior of the tubes was filled with a 0.1 mM solution of 1,4-DHPN dissolved in normal saline.

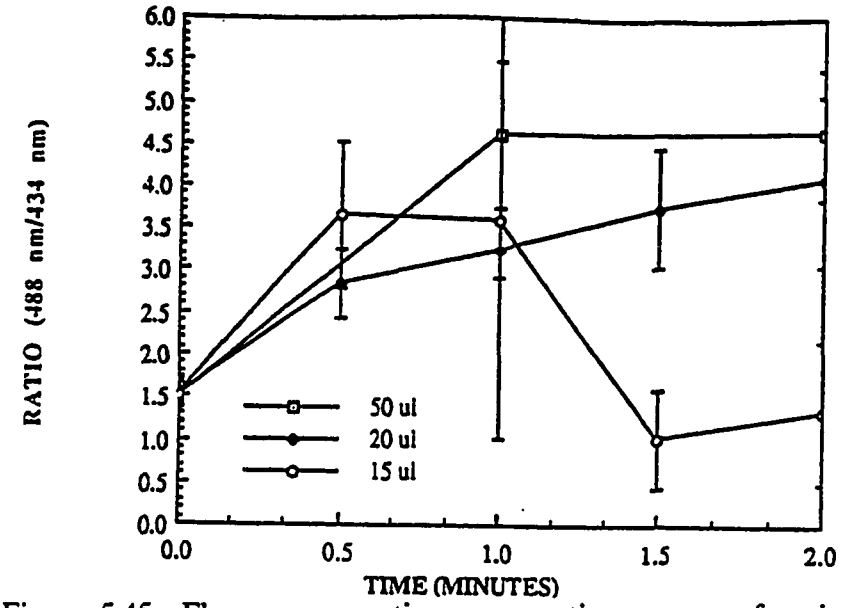

Figure 5.45. Fluorescence ratio response time curves of various size capillary based Cuprophan sensors using a fiber positioned 1 mm from the membrane. The interior of the tubes was filled with a 0.1 mM solution of 1,4-DHPN dissolved in normal saline. A 305 mOsm test solution at pH 8.0 was used.

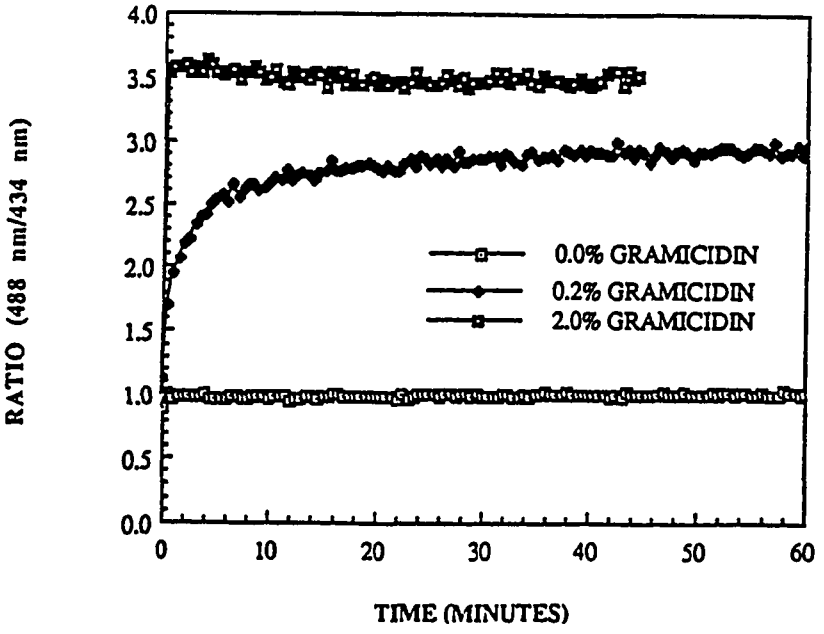

Figure 5.46. Gramacidin A dependent fluorescence ratio response time curves. Measurements were taken using a 1:1 dilution of 4:1 DPPC/DPPG LUV in 305 mOsm phosphate buffer. The LUV contained 303 mM sucrose and 10 mM 1,4-DHPN within their aqueous compartments. Various quantities of Gramicidin A (based upon mole % of total lipid) were added to the lipid phase. Note, the 2.0 % Gramicidin curve should reach the same endpoint as the 0.2% curve. The observed shift is due to differences in measurement system calibration. A pH 7.5 buffer was used.

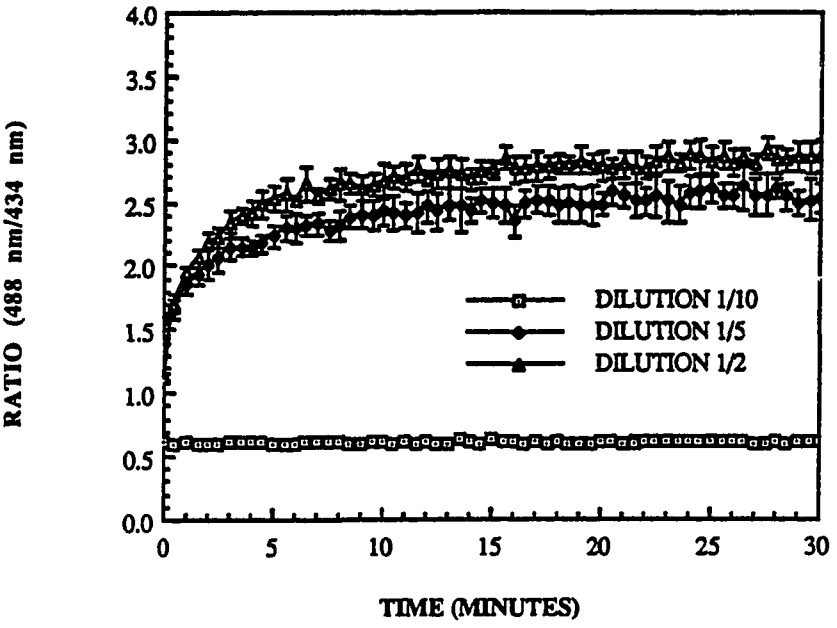

Figure 5.47. Detectibility of DPPC/DPPG LUV containing 10 mM 1,4-DHPN and 303 mM sucrose. A 0.2 mole % quantity of Gramicidin A was added to the lipid phase during preparation. Dilutions were made using 305 mOsm phosphate buffer at pH 7.5.

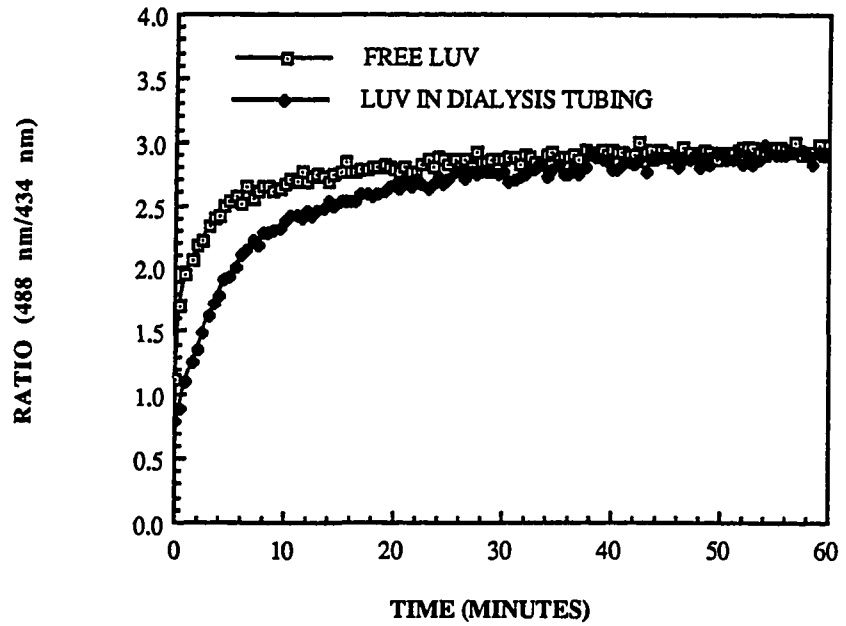

Figure 5.48. Fluorescence ratio response time curves of free and 2.5 mm diameter micro-dialysis tubing bound DPPC/DPPG LUV containing 10 mM 1,4-DHPN and 303 mM sucrose. A 0.2 mole % quantity of Gramicidin A was added to the lipid phase during preparation. The test solution was 305 mOsm phosphate buffer at pH 7.5.

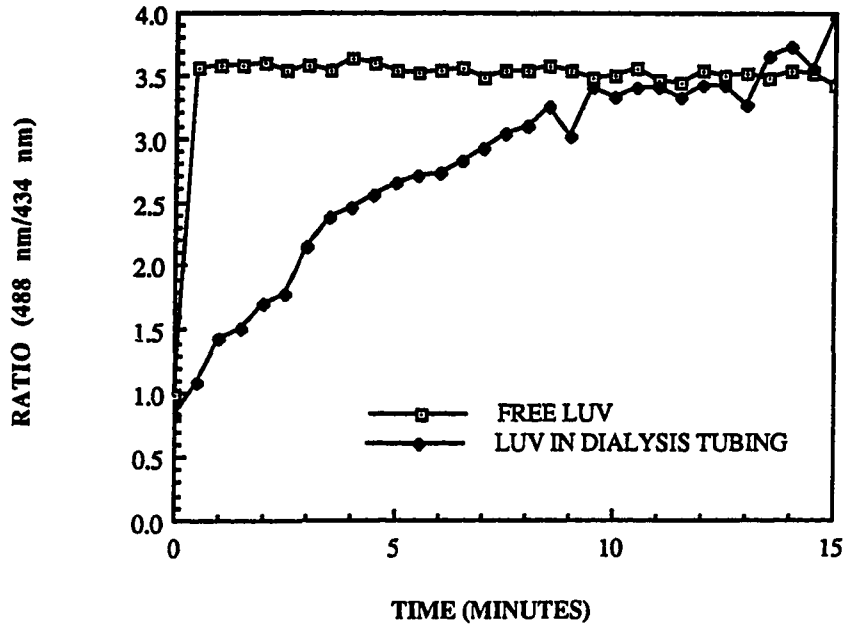

Figure 5.49. Fluorescence ratio response time curves of free and 2.5 mm diameter micro-dialysis tubing bound DPPC/DPPG LUV containing 10 mM 1,4-DHPN and 303 mM sucrose. A 2.0 mole % quantity of Gramicidin A was added to the lipid phase during preparation. The test solution was 305 mOsm phosphate buffer at pH 7.5. The high steady state ratio is due to differences in system calibration.

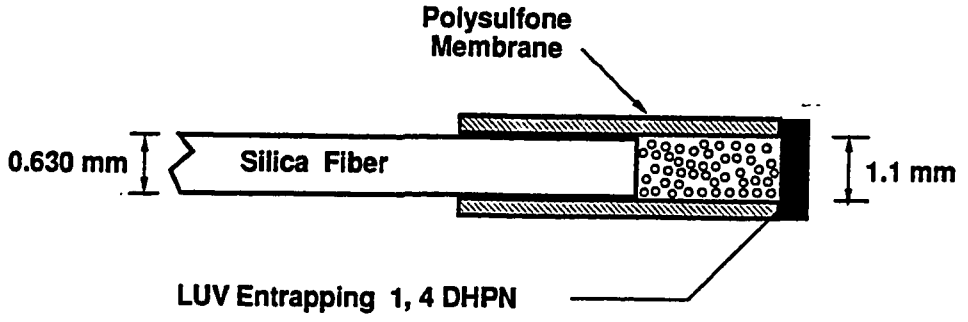

Figure 5.50. Construction of an LUV based polysulfone sensor.

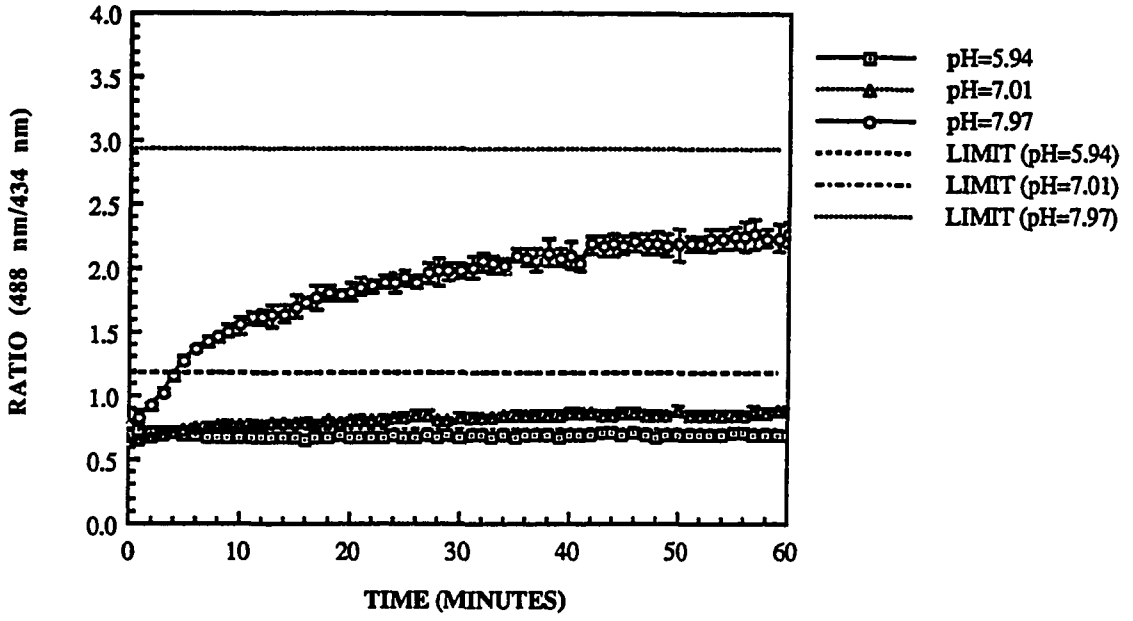

Figure 5.51. Fluorescence ratio response of a 1 mm inner diameter LUV based polysulfone sensor. The LUV contained a 2 mole % quantity of Gramicidin A added to the lipid phase. The aqueous phase consisted of 10 mM 1,4-DHPN and 303 mM sucrose. The test solutions were 305 mOsm phosphate buffers at several different values of pH.

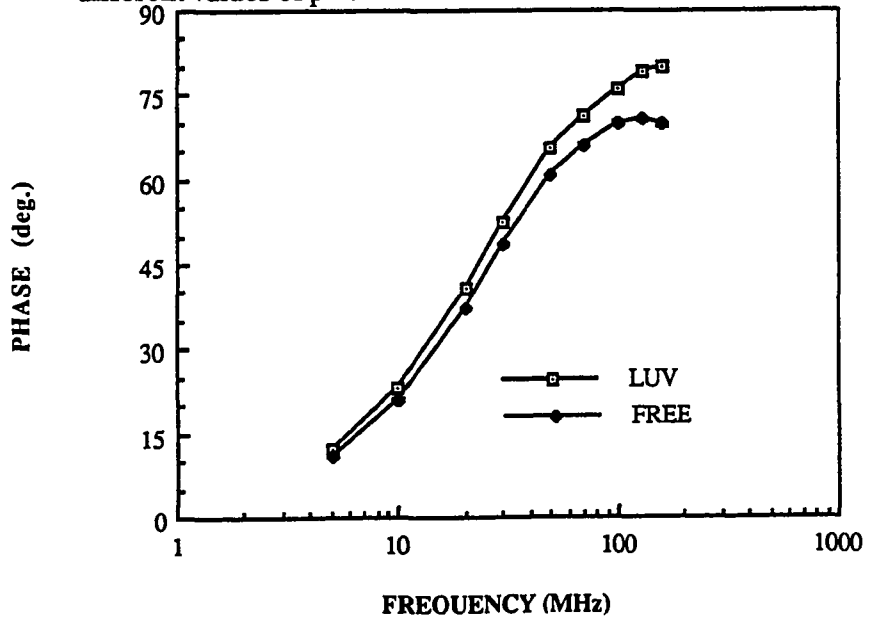

Figure 5.52. Fluorescence phase versus frequency of DPPC/DPPG LUV and free 1,4-DHPN in solution. The free dye was dissolved in 305 mOsm phosphate buffer at pH 7.0, to a concentration of 0.002 mM. LUV contained 10 mM 1,4-DHPN dissolved in normal saline. These LUV were diluted 1/10,000 in 305 mOsm phosphate buffer at pH 7.0 before use. No Gramicidin was added.

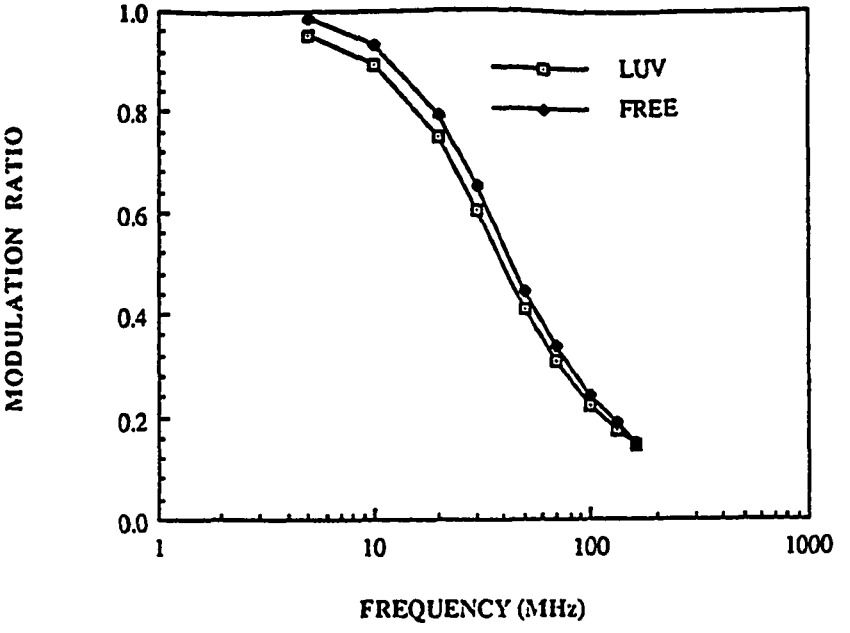

Figure 5.53. Fluorescence modulation ratio versus frequency of DPPC/DPPG LUV and free 1,4-DHPN in solution. The free dye was dissolved in 305 mOsm phosphate buffer, at pH 7.0, to a concentration of 0.002 mM. LUV contained 10 mM 1,4-DHPN dissolved in normal saline. These LUV were diluted 1/10,000 in 305 mOsm phosphate buffer at pH 7.0 before use. No Gramicidin was added.

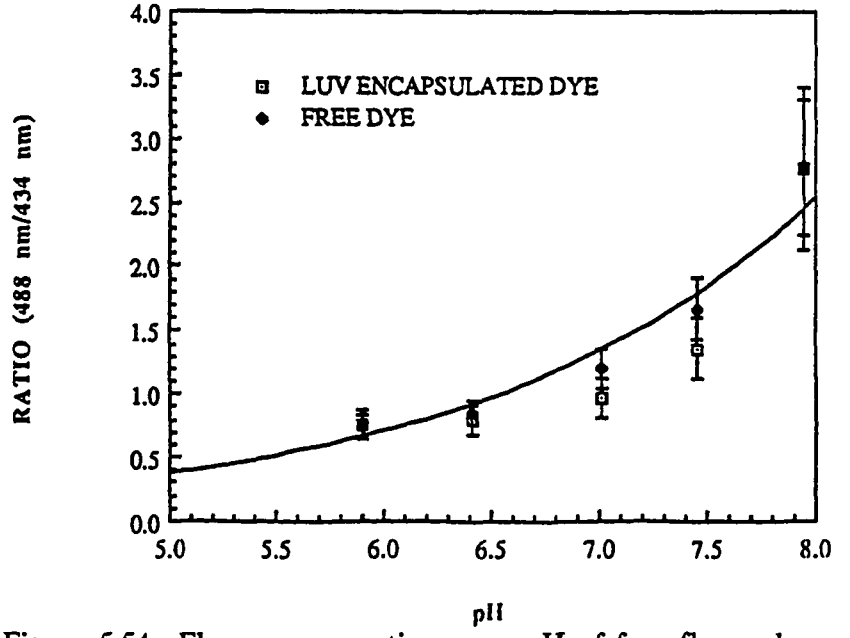

Figure 5.54. Fluorescence ratio versus pH of free fluorophore and LUV encapsulated fluorophore. Free dye was diluted to a concentration of 0.1 mM in 305 mOsm phosphate buffer at various values of pH. LUV contained a 2 mole % quantity of Gramicidin A in their lipid phase and 10 mM of 1,4-DHPN, dissolved in 303 mM sucrose, within their aqueous compartment. Liposomes were diluted 1:1 with phosphate buffer before measurement.

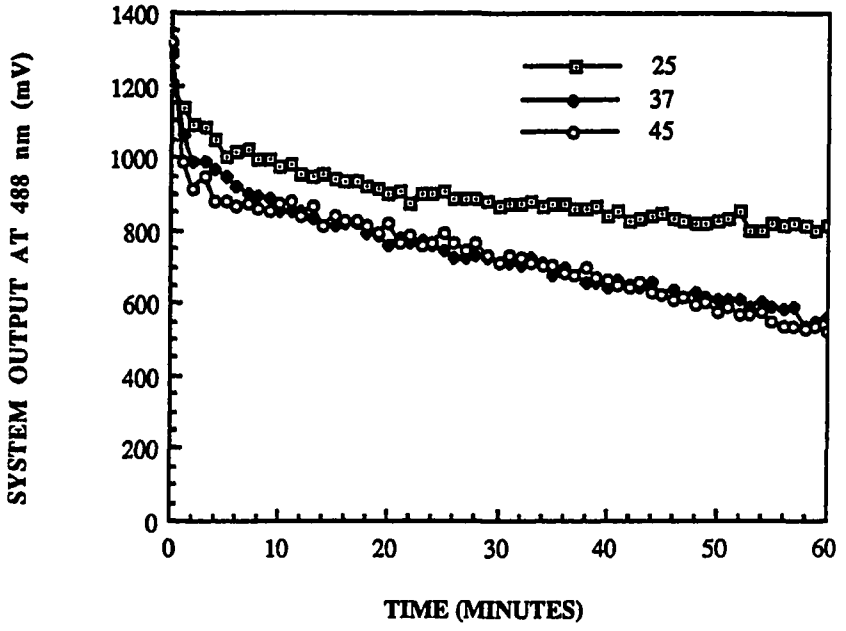

Figure 5.55. System response at 488 nm as a function of temperature for LUV based 1 mm inner diameter polysulfone sensors. LUV contained a 2.0 mole % quantity of Gramicidin A in their lipid phase and 10 mM 1,4-DHPN, dissolved in 303 mM sucrose, within their aqueous compartment. The test solution was 305 mOsm phosphate buffer at pH 7.0.

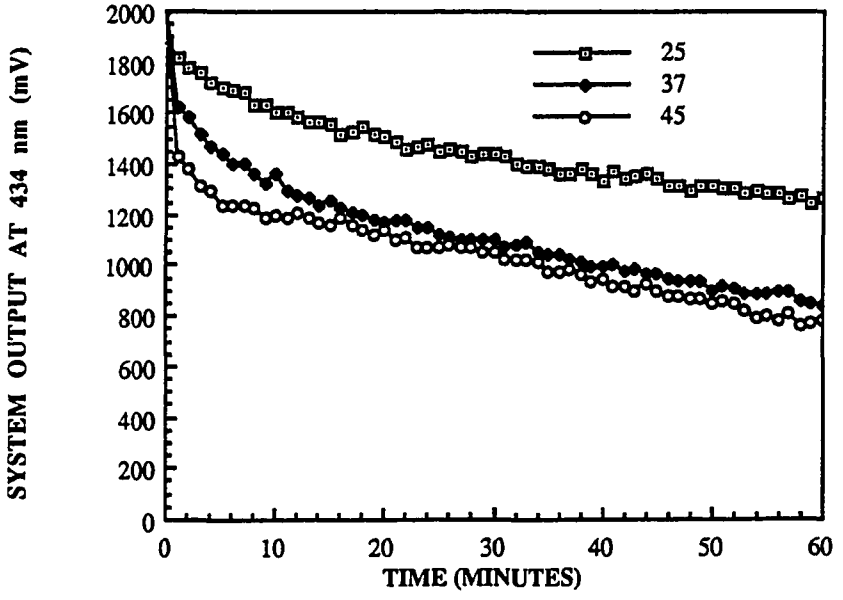

Figure 5.56. System response at 434 nm as a function of temperature for LUV based 1 mm inner diameter polysulfone sensors. LUV contained a 2.0 mole % quantity of Gramicidin A in their lipid phase and 10 mM 1,4-DHPN, dissolved in 303 mM sucrose, within their aqueous compartment. The test solution was 305 mOsm phosphate buffer at pH 7.0.

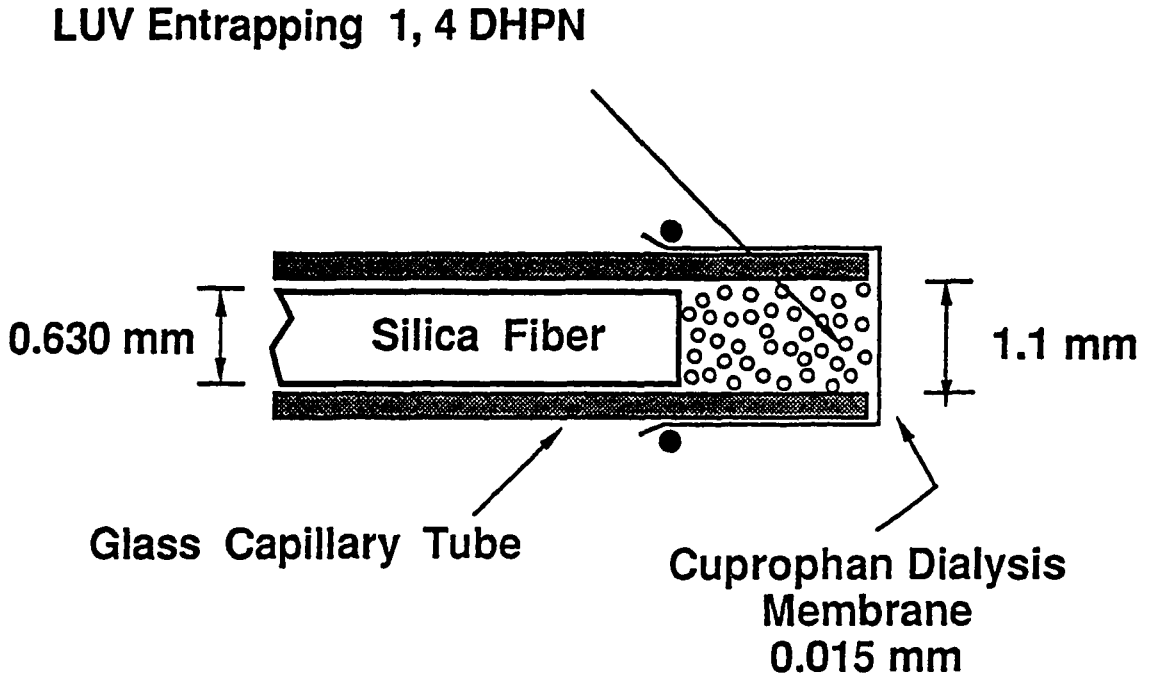

Figure 5.57. Construction of a LUV based Cuprophan capillary sensor.

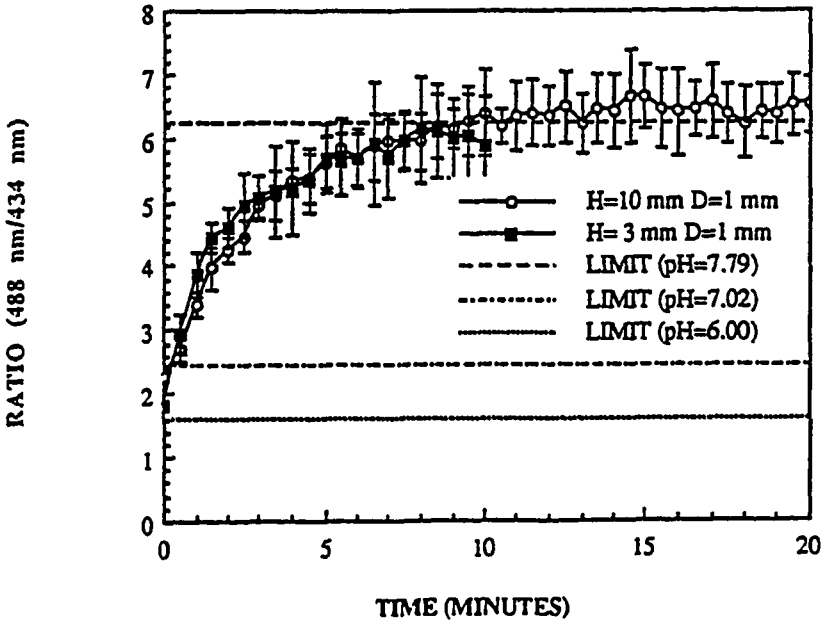

Figure 5.58. Fluorescence ratio response curve for a LUV based 1.1 mm inner diameter Cuprophan capillary sensor. LUV contained a 2.0 mole % quantity of Gramicidin A in their lipid phase and 10 mM 1,4-DHPN, dissolved in 303 mM sucrose, within their aqueous compartment. The test solution was a 305 mOsm phosphate buffer at pH 7.8. The sensor time constant was 3.2 minutes.

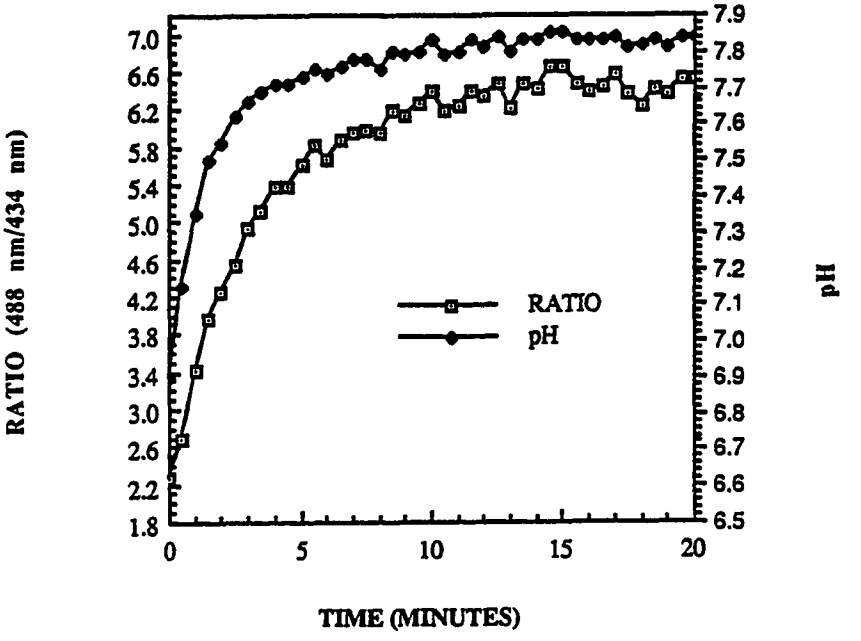

Figure 5.59. The pH response curve for the sensor of Figure 5.58 calculated by means of a standard ratio curve.

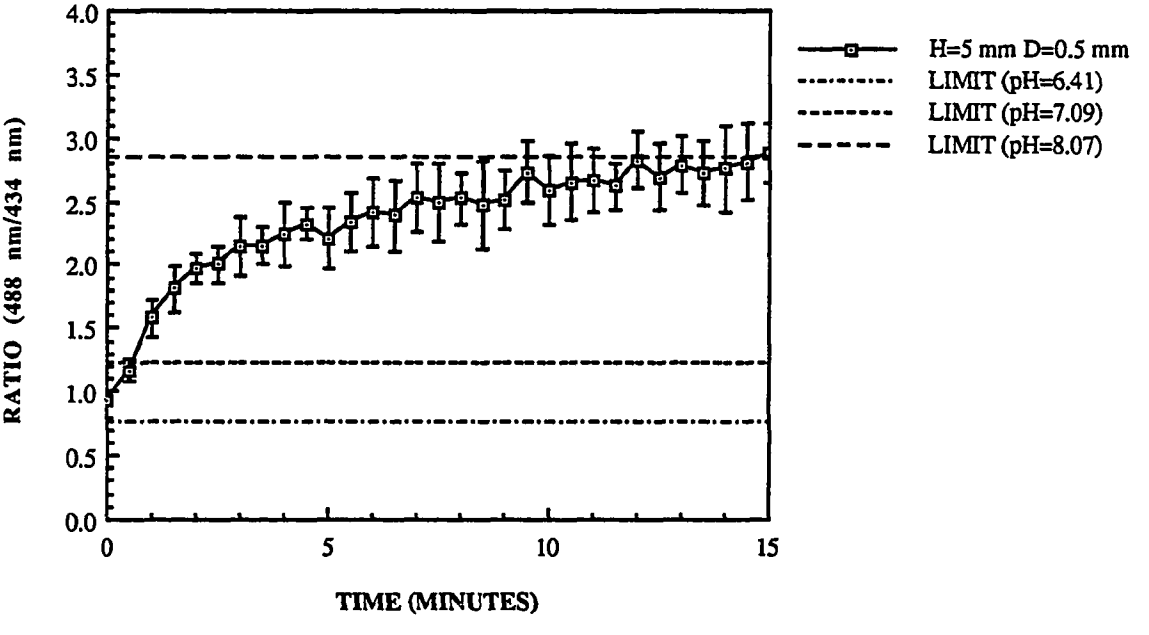

Figure 5.60. Fluorescence ratio response curve for a LUV based 0.64 mm inner diameter Cuprophan capillary sensor. LUV contained a 2.0 mole % quantity of Gramicidin A in their lipid phase and 10 mM 1,4-DHPN dissolved in 303 mM sucrose, within their aqueous compartment. The test solution was a 305 mOsm phosphate buffer at pH 8.1. The sensor time constant was 3.3 minutes.

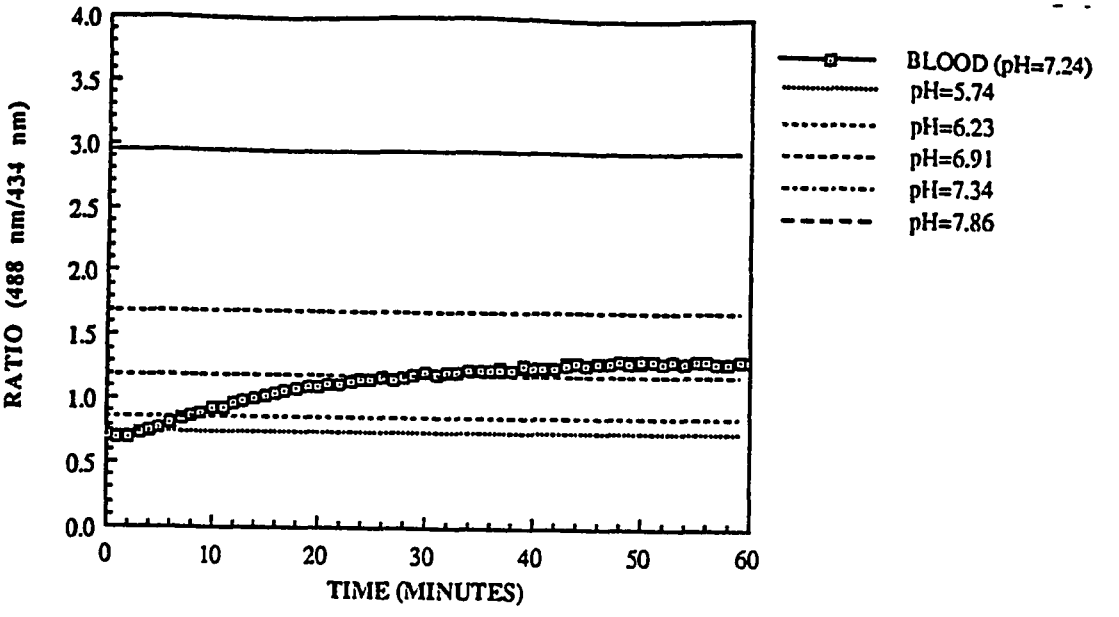

Figure 5.61. Fluorescence ratio measurement of an LUV based 1 mm inner diameter polysulfone sensor in whole blood at 25° C. LUV contained a 2.0 mole % quantity of Gramicidin A in their lipid phase and 10 mM 1,4-DHPN, dissolved in 303 mM sucrose, within their aqueous compartment. The time constant of this sensor was 19.8 minutes and it achieved a calculated pH of 7.06 at the end of 60 minutes. The measured pH of the whole blood was 7.24.

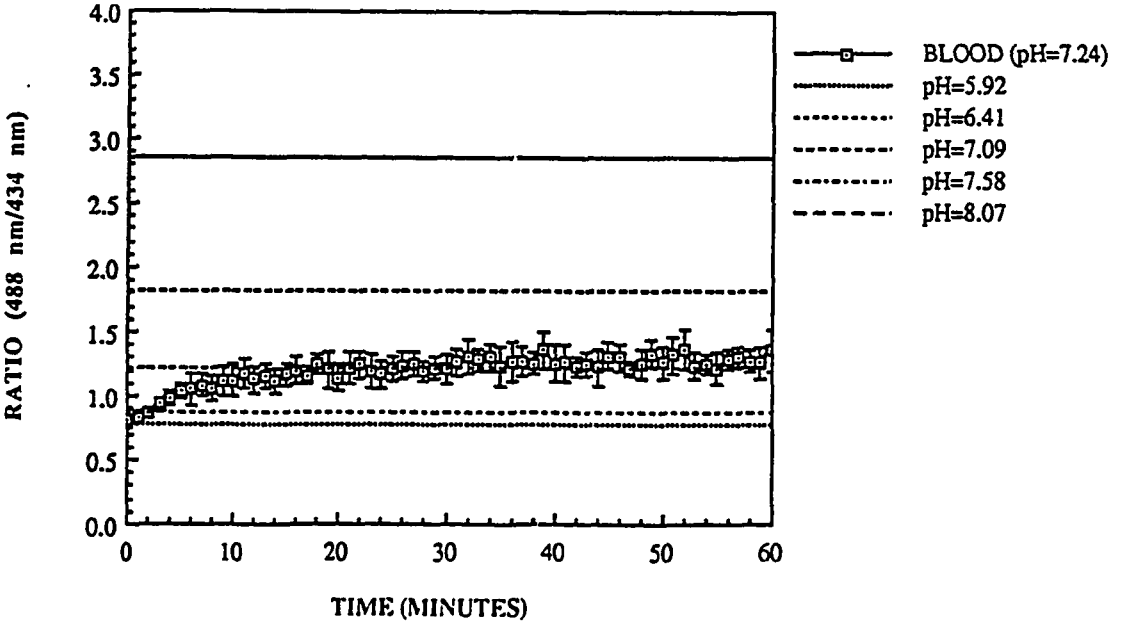

Figure 5.62. Fluorescence ratio measurement of an LUV based 0.58 mm inner diameter Cuprophan capillary sensor in whole blood at 25°C. LUV contained a 2.0 mole % quantity of Gramicidin A in their lipid phase and 10 mM 1,4-DHPN, dissolved in 303 mM sucrose, within their aqueous compartment. The time constant of this sensor was 10.0 minutes and it achieved a calculated pH of 7.24 at the end of 60 minutes. The measured pH of the whole blood was 7.24.

CHAPTER 6
SUMMARY AND RECOMMENDATIONS FOR FURTHER STUDY

A fluorescence emission ratio based fiber optic pH measurement system was developed and evaluated for potential use during clinical hyperthermia of tumors. The behavior of the pH sensitive fluorophore 1,4-DHPN was studied in solution as a function of both temperature and pH. The pH dependence of the absorption spectrum, excitation spectrum, emission spectrum, and lifetime, as given by frequency domain modulation and phase measurements, were investigated for use as a basis in developing an optical pH measurement system. The temperature and pH dependent behavior of either the fluorescence emission spectrum or the fluorescence lifetime were determined to be well suited for the intended application. The temperature dependence of both lifetime and fluorescence emission appear to be near a minimum around pH 7. When pH was determined from lifetime, using either modulation or phase measurement techniques, an average temperature induced pH error of +0.05 pH units / °C was introduced. Maximum sensitivity of this technique was obtained in the 6-7 pH range, with a calculated measurement precision of ±0.04 pH units over the 6-8 pH range. On the other hand, measurement of pH using emission wavelengths ratios shows a maximum sensitivity in the 7-8 pH range. The average temperature induced pH error was calculated to be ±0.02 pH units / °C. While both of these measurement techniques permit a simple single fiber sensor with adequate sensitivity and precision for use during induced hyperthermia, the simpler electronics and signal processing required in the emission ratio technique was attractive from an instrumentation viewpoint. As a result instrumentation was designed and built based on this measurement technique.

The resultant fluorescence emission ratio based pH measurement system consists of a flashlamp excitation source whose filtered narrowband energy is coupled by means of an optical fiber into an optical sensor module. This module contains a dichroic beamsplitter which reflects the excitation wavelengths into the sensor fiber. The pH dependent red shifted fluorescence signal travels back up the same fiber and is transmitted by the dichroic beamsplitter out of the sensor module and into a detector module. Here, the signal is split, and the two wavelengths of maximum pH sensitivity are selected by means of interference filters. These two optical signals are then transmitted to the photodetectors by means of optical fibers. The resultant electronic signals are processed separately in the electronic subsystem, digitized, and read into the memory of an Apple 2E microcomputer for subsequent digital processing and storage. All system and acquisition parameters are controlled by the Apple 2E microcomputer, using a program written in combined Applesoft BASIC and 6502 assembly language.

The weakest link in this measurement system appears to be in the conversion of input energy to optical excitation at the appropriate wavelength. Only about one part in 10,000,000 of the energy input to the flashlamp appears as output in the desired wavelength range. Since the standard deviation of the measured emission ratio has been shown to decrease as the square root of the excitation energy, a more efficient signal source would improve both sensitivity and precision of the measurement system. More efficient methods of coupling energy both into and out of optical fibers should also be found. Presently only about 4% of the available flashlamp energy gets coupled into the sensor fiber. In addition, less than 1% of the total fluorescence energy, at any desired detection wavelength, finds its way to an appropriate photodetector.

The photodetector and electronics modules work well. Overall sensitivity of these system approach their theoretical limit. At 480 nm the photodiodes are

capable of detecting optical intensities of better than 1 nW. The photomultiplier tubes can detect intensities approaching 0.1 pW.

Using a fluorophore concentration of 10 mM, about 2 nW of fluorescence signal appear at each photodetector, when 1 joule of input excitation energy is supplied by the flashlamp. This is just slightly above the minimum detectable signal level using PIN photodiodes. For adequate SNR, photomultipliers must be used with the present optical configuration. Improvements in the excitation source and optical subsystem could make photodiode detection possible.

The present measurement system was found to be capable of measuring the pH of neutral solutions of 1 mM fluorophore, with a standard deviation of better than ±0.1 pH unit, using a flashlamp input energy of 1 joule. This standard deviation is based upon a 200 sample measurement.

The pH measurement standard deviation, as a function of temperature, was found to be approximately 0.01 pH units / °C. When calibrated at 40 °C, the temperature induced measurement error is less than the the intrinsic system error over the temperature range usually employed in clinical hyperthermia.

Several materials were evaluated for use in fabricating pH sensitive optrodes. Materials having good hydrogen ion permeability coupled with good fluorophore retention were sought. A material with these properties was not found.

Cuprophan was selected for optrode fabrication based solely on its demonstrated permeability properties for hydrogen ions. Optrodes measuring less than 1 mm in diameter were fabricated by sealing the ends of small capillary tubes with a thin sheet of Cuprophan. These tubes were then filled with a 0.1 mM solution of fluorophore dissolved in normal saline. The time constants of such sensors, upon immersion in 305 mOsm phosphate buffers at various values of pH, were determined to be limited by hydrogen ion diffusion time and not membrane permeability, for reasonable membrane to optical fiber distances. The

measurement lifetime of these optrodes was limited to several minutes due to rapid leakage of the fluorophore across the membrane.

In order to extend the measurement lifetime of these optrodes, LUV made from a 4:1 mixture of DPPC/DPPG were used to encapsulate the pH sensitive fluorophore. The aqueous compartment of these LUV consisted of a 10 mM solution of 1,4-DHPN in 303 mM sucrose to achieve a near isosmotic internal environment. The kinetics of hydrogen ion transport in these LUV was found to be extremely slow. Gramicidin A was added to the lipid phase during preparation in order speed hydrogen ion transport across the membrane of these liposomes. At a Gramicidin A concentration equivalent to 2.0 mole percent of the total lipid present, the kinetics of hydrogen ion transport, across these liposomal membranes, was no longer found to be limiting.

Cuprophan capillary optrodes were again fabricated and filled with a 1:1 suspension of the previously discussed liposomes in normal saline. The response time of these membranes was again determined by immersion in 305 mOsm phosphate buffer at pH 8. The expected steady state ratio for these optrodes was reached with an exponential time constant of approximately 3 minutes. Steady state ratio stability in excess of 1 hour was achieved, even at hyperthermic temperatures.

In order to test the physiological applicability of this optical pH measurement system, the previously discussed optrode was immersed into heparinized whole blood at 25 °C. The pH of this sample was measured with a standard pH meter and determined to be 7.24 ±0.02. The calculated pH from the optical measurement system, at the end of 60 minutes , was found to be 7.24 ±0.06. An exponential time constant of approximately 10 minutes was measured.

This research has demonstrated the feasibility of a fluorescence emission ratio based pH measurement system, with physiological applicability under hyperthermic conditions. Stability, accuracy, and precision of this measurement

system appear good. Response time in phosphate buffer is marginally acceptable for studies of pH dynamics during hyperthermia. However, further degradation by an approximate factor of 3 in whole blood cannot be tolerated. The mechanisms responsible for this anomaly bears further investigation. Preliminary indications are that the hydrogen ion flux across the liposomal membranes is again becoming a limiting factor. One explanation for this effect is that a flux limiting diffusion potential is being established across the liposomal membrane by charged impermeant molecules and ions that are present in the blood, but not in the buffers used in preliminary testing. Another explanation is that the Gramicidin channels are being blocked by divalent cations, most probably Ca^{++}, which are present in the blood plasma. In either case, further modification of either the lipid membrane or the aqueous compartment may become necessary if reasonable *in vivo* time constants are to be achieved.

Finally, in order to achieve response times substantially under 1 minute, permeability limited optrodes need to be designed. This would presumably involve copolymerization of the fluorophore with a polymer on a thin film or covalent attachment of the fluorophore to a suitable support. While copolymerization of 1,4-DHPN may be possible, lack of linkable side chains on this fluorophore prevent direct covalent linkages to a supporting structure. However, a newly synthesized SNARF series of pH sensitive emission fluorophores (Molecular Probes) may be the solution. The existing optical pH measurement system can be easily adapted to utilize this new fluorophore by a change in optical filters.

APPENDIX A
PHYSICAL CONTROL LINE CONNECTIONS

External PC Interface Board Connections	Control Line Description
J1, Pin 1	10 M Feedback Resistor-CH0
J1, Pin 2	1 M Feedback Resistor-CH0
J1, Pin 3	100 K Feedback Resistor-CH0
J1, Pin 4	10 K Feedback Resistor-CH0
J1, Pin 5	10 M Feedback Resistor-CH1
J1, Pin 6	1 M Feedback Resistor-CH1
J1, Pin 7	100 K Feedback Resistor-CH1
J1, Pin 8	10 K Feedback Resistor-CH1
J1, Pin 11	Shielded Cable GND
J2, Pin 11	Shielded Cable GND
J3, Pin 1	Integrator SW2-CH0
J3, Pin 2	Integrator SW1-CH1
J3, Pin 5	S/H Mode-CH0 & CH1
J3, Pin 7	Spare 1
J3, Pin 8	Spare 2
J4, Pin 8	Flashlamp Trigger
J4, Pin 11	Shielded Cable GND
P1, Pin 1	A/D Input-CH0
P1, Pin 2	A/D Input-CH1
P2, Pin 1	Flashlamp Reference
P2, Pin 2	PMT Reference-CH0
P2, Pin 3	PMT Reference-CH1
P2, Pin 10	Shielded Cable GND

APPENDIX B
SYSTEM INITIALIZATION PROGRAMS

PROGRAM HELLO

```
10  D$=CHR$ (4)
20  PRINT D$;"BRUN MMS"
```

PROGRAM STARTUP

```
10  POKE 116,164
20  POKE 115,255
30 D$ =  CHR$ (4)
40  PRINT D$;"BLOAD PH2.OBJ0"
50  PRINT D$;"RUN PH2-REM"
60  END
```

APPENDIX C
APPLESOFT BASIC CONTROL PROGRAM

```
10 REM  FILENAME: PH2-BASIC
20 REM
30 DIM ST(4,200): REM  STATISTICAL ARRAY
40 DS% = - 23296: REM  ASSEMBLY ROUTINE DUMMY SECTOR ADDRESS
50 OF% = DS% + 32
60 UF% = DS% + 42
70 INFO% = - 18432: REM  ASSEMBLY ROUTINE DATA AREA
80 CD$ = CHR$ (4): REM  CTRL-D
90 PRINT CD$;"PR#3": REM  80 COLUMN MODE
100 CALL - 23040: REM  ASSEMBLY ROUTINE INITIALIZATION ADDRESS
110 REM ************************************************************
120 HOME
130 PRINT
140 VTAB 8
150 PRINT SPC( 25);"ENTER 'B' TO BEGIN PROGRAM"
160 VTAB 10
170 PRINT SPC( 20);"ENTER 'Q' TO QUIT PROGRAM PEACEFULLY"
180 VTAB 15
190 HTAB 25
200 INPUT "PLEASE ENTER A CHOICE ";A$
210 IF A$ = "Q" THEN 730
220 IF A$ < > "B" THEN 120
230 REM ************************************************************
240 HOME
250 VTAB 5
260 PRINT SPC( 10);"DOES ANY OF THE ELECTRONIC SUBSYSTEM OFFSET
CIRCUITRY"
270 PRINT SPC( 25);"REQUIRE ADJUSTMENT? ";OFFSET$
280 VTAB 10
290 HTAB 20
300 INPUT "PLEASE ENTER YOUR RESPONSE (Y/N) ";OFFSET$
310 IF OFFSET$ = "N" THEN 570
320 IF OFFSET$ = "Y" THEN 360
330 VTAB 15
340 PRINT SPC( 25);"PLEASE ENTER 'Y' OR 'N'"
350 GOTO 280
360 POKE DS% + 26,1
370 GOSUB 750: REM  ADJUSTMENT SELECTION
380 POKE DS% + 26,0
390 HOME
400 VTAB 5
410 PRINT SPC( 30);"DO YOU WISH TO: "
420 PRINT
430 PRINT SPC( 10);"(1) PERFORM FURTHER ADJUSTMENTS TO THE OFFSET
CIRCUITRY"
440 PRINT SPC( 10);"(2) CONFIGURE THE SYSTEM FOR ACTUAL MEASUREMENTS"
450 VTAB 10
460 HTAB 20
```

```
470 INPUT "ENTER YOUR CHOICE (1/2):  ";CHOICE%
480 IF CHOICE% = 1 THEN OFFSET$ = "Y": GOTO 530
490 IF CHOICE% = 2 THEN OFFSET$ = "N": GOTO 570
500 VTAB 15
510 PRINT  SPC( 25);"PLEASE ENTER '1' OR '2'"
520 GOTO 450
530 POKE DS% + 26,1
540 GOSUB 750
550 POKE DS% + 26,0
560 GOTO 390
570 POKE DS% + 26,0
580 GOSUB 1330: REM  FLASH LAMP PARAMETERS
590 GOSUB 1770: REM  INTEGRATION PARAMETERS
600 HOME
610 VTAB 5
620 PRINT  SPC( 20);"DO YOU WISH TO USE PHOTOMULTIPLIER TUBES? "
630 VTAB 10
640 HTAB 21
650 INPUT "PLEASE ENTER YOUR RESPONSE (Y/N) ";KEY$
660 IF KEY$ = "N" THEN G0 = 1:G1 = 1: GOSUB 9560: GOTO 680: REM  SET CURRENT
GAIN TO 1 AND FORMAT
670 GOSUB 8860: REM  PHOTOMULTIPLIER GAIN PARAMETERS
680 CALL  INT (256 *  PEEK (DS% + 0) +  PEEK (DS% + 1) + 0.5): REM  PHASE 1
690 GOSUB 2130: REM  GAIN CALIBRATION SELECTION
700 CALL  INT (256 *  PEEK (DS% + 2) +  PEEK (DS% + 3) + 0.5): REM  PHASE 2
710 GOSUB 3050: REM  MEASUREMENT SELECTION
720 GOTO 120
730 END
740 REM ************************************************************
750 HOME
760 VTAB 8
770 PRINT  SPC( 15);"THE FOLLOWING SCREENS CONFIGURE THE SYSTEM FOR"
780 PRINT  SPC( 15);"ADJUSTMENT ONLY.  THE SYSTEM MUST BE RECONFIGURED"
790 PRINT  SPC( 15);"FOR ACTUAL MEASUREMENTS FOLLOWING ADJUSTMENTS"
800 VTAB 13
810 HTAB 26
820 INPUT "PRESS RETURN TO CONTINUE";BOGUS$
830 GOSUB 1330: REM  FLASHLAMP PARAMETERS
840 GOSUB 1770: REM  INTEGRATION PARAMETERS
850 CALL  INT (256 *  PEEK (DS% + 0) +  PEEK (DS% + 1) + 0.5): REM  PHASE 1
860 GOSUB 2300: REM  MANUAL GAIN CALIBRATION
870 CALL  INT (256 *  PEEK (DS% + 2) +  PEEK (DS% + 3) + 0.5): REM  PHASE 2
880 GOSUB 4360: REM  FORMATTING VARIABLES
890 HOME
900 VTAB 5
910 PRINT  SPC( 10);"DIGITIZED VALUES FOR CHANNELS 0 AND 1 WILL BE
CONTINUOUSLY"
920 PRINT  SPC( 10);"DISPLAYED TO THE SCREEN.  CHANNEL 0 VALUES ARE
DISPLAYED IN"
930 PRINT  SPC( 10);"THE LEFT COLUMN, AND CHANNEL 1 VALUES ARE
DISPLAYED IN THE"
940 PRINT  SPC( 10);"RIGHT COLUMN."
950 VTAB 10
```

```
960 PRINT SPC( 10);"TO PAUSE THIS ROUTINE AT ANY TIME DURING EXECUTION,
SIMPLY"
970 PRINT SPC( 10);"PRESS THE SPACE BAR. TO RESUME, PRESS THE SPACE BAR
AGAIN."
980 PRINT SPC( 10);"TO EXIT THE ROUTINE AT ANY TIME, HIT ANY OTHER KEY."
990 VTAB 15
1000 HTAB 26
1010 INPUT "PRESS RETURN TO BEGIN";BOGUS$
1020 POKE - 16368,0: REM CLEAR KEYBOARD STROBE
1030 POKE DS% + 25,1: REM SINGLE SWEEP
1040 POKE DS% + 21,0: REM INJECTION CURRENT LOCATIONS
1050 POKE DS% + 22,0
1060 POKE DS% + 23,0
1070 POKE DS% + 24,0
1080 HOME
1090 VT% = 1
1100 IF PEEK ( - 16384) > 127 THEN 1250: REM STROBE BIT SET
1110 CALL INT (256 * PEEK (DS% + 6) + PEEK (DS% + 7) + 0.5)
1120 M0% = INT (256 * PEEK (INFO% + 80) + PEEK (INFO% + 81) + 0.5)
1130 TEMP$ = STR$ (M0% * A0 / 4095)
1140 GOSUB 8710
1150 M0$ = TEMP$
1160 M1% = INT (256 * PEEK (INFO% + 82) + PEEK (INFO% + 83) + 0.5)
1170 TEMP$ = STR$ (M1% * A1 / 4095)
1180 GOSUB 8710
1190 M1$ = TEMP$
1200 VT% = VT% + 1
1210 VTAB VT%
1220 PRINT SPC( 20);M0$; SPC( 15);M1$
1230 IF VT% > 22 THEN 1080
1240 GOTO 1100
1250 IF PEEK ( - 16384) = 160 THEN 1270
1260 IF PEEK ( - 16384) < > 160 THEN 1300
1270 BOGUS = PEEK ( - 16368): REM CLEAR STROBE BIT
1280 IF PEEK ( - 16384) < 127 THEN 1280: REM PAUSE MODE
1290 IF PEEK ( - 16384) = 160 THEN 1310
1300 BOGUS = PEEK ( - 16368): RETURN
1310 BOGUS = PEEK ( - 16368): GOTO 1100
1320 REM ************************************************************
1330 HOME
1340 VTAB 5
1350 PRINT SPC( 25);"FLASHLAMP ENERGY SELECTION"
1360 VTAB 8
1370 PRINT SPC( 10);"THE FLASHLAMP ENERGY MUST BE IN THE INTERVAL 0.1 -
2.25 JOULES"
1380 VTAB 10
1390 HTAB 26
1400 INPUT "ENTER THE FLASHLAMP ENERGY ";ENERGY
1410 IF ENERGY < 0.1 THEN 1700
1420 IF ENERGY > 2.25 THEN 1700
1430 REF% = INT ((25.5 / 150) * SQR (ENERGY * 1E + 6) + 0.5): REM FLASHLAMP
REFERENCE
1440 POKE DS% + 27,REF%
1450 FBOUND% = INT (10 / ENERGY + 0.5)
```

```
1460 T1 = INT (FBOUND% / 4)
1470 T2 = FBOUND% / 4
1480 IF T2 - T1 > 0.1 THEN FBOUND% = FBOUND% - 1: GOTO 1460
1490 FBOUND$ = STR$ (FBOUND%)
1500 HOME
1505 VTAB 8
1510 PRINT SPC( 25);"FLASH LAMP FREQUENCY SELECTION"
1515 VTAB 8
1520 PRINT SPC( 10);"WARNING: THE MAXIMUM FREQUENCY WHICH CAN BE
SAFELY USED FOR"
1525 PRINT SPC( 10);"THE ENERGY SELECTED IS ";FBOUND$;" HZ. CHOOSING A
HIGHER FREQUENCY"
1530 PRINT SPC( 10);"MAY LEAD TO A REDUCTION IN FLASHLAMP LIFETIME."
1535 VTAB 12
1540 PRINT SPC( 10);"THE FREQUENCY MUST BE IN THE INTERVAL 8HZ-100HZ
WITH A"
1545 PRINT SPC( 10);"RESOLUTION OF 4HZ (I.E. 8, 12, 16, 20, 24, ...)"
1550 VTAB 16
1555 HTAB 21
1560 INPUT "ENTER THE FLASH LAMP FREQUENCY ";LAMP%
1565 IF LAMP% < 8 THEN 1730
1570 IF LAMP% > 100 THEN 1730
1575 T1 = INT (LAMP% / 4)
1580 T2 = LAMP% / 4
1585 IF T2 - T1 > 0.1 THEN 1730
1590 POKE DS% + 8,LAMP%: REM FLASH LAMP FREQUENCY
1600 HOME
1610 VTAB 5
1620 PRINT SPC( 25);"MEASUREMENT DELAY PARAMETER SELECTION"
1630 VTAB 8
1640 PRINT SPC( 08);"THE FLASHLAMP WILL BE TRIGGERED SEVERAL TIMES
PRIOR TO BEGINNING DATA"
1650 PRINT SPC( 08);"ACQUISITION. THE RANGE OF ACCEPTABLE VALUES
EXTENDS FROM 1 TO 125."
1660 VTAB 15
1670 HTAB 21
1680 INPUT "   ENTER DESIRED NUMBER OF DUMMY FLASHES ";DUMMY%
1681 IF DUMMY% < 1 THEN 1730
1682 IF DUMMY% > 125 THEN 1730
1683 POKE DS% + 109,2 * DUMMY%: REM DUMMY FLASHES
1690 RETURN
1700 VTAB 23
1710 PRINT SPC( 25);"PLEASE ENTER ANOTHER VALUE"
1720 GOTO 1380
1730 VTAB 23
1740 PRINT SPC( 25);"PLEASE ENTER ANOTHER VALUE"
1750 GOTO 1550
1751 VTAB 23
1752 PRINT SPC( 25);"PLEASE ENTER ANOTHER VALUE"
1753 GOTO 1660
1760 REM ************************************************************
1770 HOME
1780 VTAB 4
1790 PRINT SPC( 20);"INTEGRATION PARAMETER SELECTION"
```

```
1800 VTAB 7
1810 PRINT SPC( 05);"AN INTEGRATION PERIOD EXTENDS FROM 15 USEC TO 1000
USEC IN"
1820 PRINT SPC( 25);"5 USEC INCREMENTS"
1830 VTAB 11
1840 HTAB 21
1850 INPUT "ENTER THE INTEGRATION PERIOD ";PERIOD%
1860 IF PERIOD% < 15 THEN 2060
1870 IF PERIOD% > 1000 THEN 2060
1880 T1 = INT (PERIOD% / 5)
1890 T2 = PERIOD% / 5
1900 IF T2 - T1 > 0.1 THEN 2060
1910 POKE DS% + 9, INT (PERIOD% * 1.02273 / 5 + 0.5): REM INTEGRATION PERIOD
1920 VTAB 23
1930 PRINT SPC( 80)
1940 VTAB 10
1950 PRINT SPC( 05);"FOR EACH FLASH, THE INTEGRATOR WILL INTEGRATE FOR
A PERIOD OF TIME"
1960 PRINT SPC( 05);"AS CHOSEN ABOVE. ADDITIONALLY, THE INTEGRATOR WILL
INGEGRATE OVER"
1970 PRINT SPC( 05);"MULTIPLE FLASHES TO OBTAIN A SINGLE SAMPLE VALUE.
THE NUMBER"
1980 PRINT SPC( 05);"OF FLASHES TO BE INTEGRATED MUST BE IN THE INTERVAL
1 TO 250."
1990 VTAB 16
2000 HTAB 15
2010 INPUT "ENTER THE NUMBER OF FLASHES TO BE INTEGRATED ";FLSH%
2020 IF FLSH% < 1 THEN 2090
2030 IF FLSH% > 250 THEN 2090
2040 POKE DS% + 10,FLSH%: REM NUMBER OF INTEGRATIONS
2050 RETURN
2060 VTAB 23
2070 PRINT SPC( 20);"PLEASE ENTER ANOTHER VALUE"
2080 GOTO 1830
2090 VTAB 23
2100 PRINT SPC( 25);"PLEASE ENTER ANOTHER VALUE"
2110 GOTO 1990
2120 REM ************************************************************
2130 HOME
2140 VTAB 5
2150 PRINT SPC( 05);"THE SYSTEM ALLOWS FOR BOTH MANUAL AND AUTOMATIC
GAIN CALIBRATIONS"
2160 PRINT SPC( 05);"BOTH CHANNELS CAN BE INDIVIDUALLY CALIBRATED AND
REQUIRE TWO"
2170 PRINT SPC( 05);"GAIN VALUES: A/D CHANNEL & PROGRAMMABLE GAIN I/V
AMPLIFIER"
2180 VTAB 10
2190 HTAB 20
2200 INPUT "DO YOU PREFER MANUAL CALIBRATION (Y/N) ";MAN$
2210 IF MAN$ = "N" THEN 2260
2220 IF MAN$ = "Y" THEN 2300
2230 VTAB 20
2240 PRINT SPC( 20);"PLEASE ENTER 'Y' OR 'N'"
2250 GOTO 2180
```

```
2260 POKE DS% + 14,0: REM  MANUAL CALIBRATION FLAG
2270 VTAB 15
2280 PRINT  SPC( 20);"SYSTEM IS PERFORMING CALIBRATION"
2290 RETURN
2300 POKE DS% + 14,1: REM  MANUAL CALIBRATION FLAG
2310 HOME
2320 VTAB 2
2330 PRINT  SPC( 25);"A/D MANUAL CALIBRATION MENU"
2340 VTAB 5
2350 PRINT  SPC( 15);"THE A/D IS CONFIGURED FOR UNIPOLAR OPERATION"
2360 VTAB 7
2370 PRINT  SPC( 25);"VOLTAGE RANGE"; SPC( 10);"GAIN"
2380 VTAB 9
2390 PRINT  SPC( 27);"0/ +10 V"; SPC( 14);"0"
2400 PRINT  SPC( 27);"0/ + 5 V"; SPC( 14);"1"
2410 PRINT  SPC( 27);"0/ + 2 V"; SPC( 14);"2"
2420 PRINT  SPC( 27);"0/ + 1 V"; SPC( 14);"3"
2430 PRINT  SPC( 27);"0/ +500 MV"; SPC( 12);"4"
2440 PRINT  SPC( 27);"0/ +200 MV"; SPC( 12);"5"
2450 PRINT  SPC( 27);"0/ +100 MV"; SPC( 12);"6"
2460 PRINT  SPC( 27);"0/ + 50 MV"; SPC( 12);"7"
2470 VTAB 19
2480 HTAB 25
2490 INPUT "ENTER CHANNEL 0 A/D GAIN (0-7)  ";A0%
2500 IF A0% < 0 THEN 2920
2510 IF A0% > 7 THEN 2920
2520 POKE DS% + 16,A0%: REM  CHANNEL 0 A/D RANGE
2530 VTAB 21
2540 HTAB 25
2550 INPUT "ENTER CHANNEL 1 A/D GAIN (0-7)  ";A1%
2560 IF A1% < 0 THEN 2950
2570 IF A1% > 7 THEN 2950
2580 POKE DS% + 18,A1%: REM  CHANNEL 1 A/D RANGE
2590 HOME
2600 VTAB 4
2610 PRINT  SPC( 10);"PROGRAMMABLE GAIN AMPLIFIER MANUAL CALIBRATION
SELECTION MENU"
2620 VTAB 7
2630 PRINT  SPC( 10);"THE PROGRAMMABLE GAIN I/V AMPLIFIER PRECEDES THE
INTEGRATOR CIRCUITRY."
2640 PRINT  SPC( 10);"IDEALLY, THE INTEGRATED SIGNAL OF INTEREST SHOULD
BE 'CLOSE' TO"
2650 PRINT  SPC( 10);"THE A/D RANGE, BUT KEPT JUST BELOW ITS MAXIMUM
VALUE"
2660 VTAB 12
2670 PRINT  SPC( 25);"AMPLIFICATION LEVEL"; SPC( 10);"GAIN"
2680 VTAB 14
2690 PRINT  SPC( 32);"     10,000"; SPC( 13);"0"
2700 PRINT  SPC( 32);"    100,000"; SPC( 13);"1"
2710 PRINT  SPC( 32);"  1,000,000"; SPC( 13);"2"
2720 PRINT  SPC( 32);" 10,000,000"; SPC( 13);"3"
2730 VTAB 20
2740 HTAB 25
2750 INPUT "ENTER CHANNEL 0 PROGRAMMABLE GAIN (0-3)  ";V0%
```

```
2760 IF V0% < 0 THEN 2980
2770 IF V0% > 3 THEN 2980
2780 IF V0% = 0 THEN  POKE DS% + 15,8: REM  CH0 PROGRAMMABLE GAIN
2790 IF V0% = 1 THEN  POKE DS% + 15,4
2800 IF V0% = 2 THEN  POKE DS% + 15,2
2810 IF V0% = 3 THEN  POKE DS% + 15,1
2820 VTAB 22
2830 HTAB 25
2840 INPUT "ENTER CHANNEL 1 PROGRAMMABLE GAIN (0-3)  ";V1%
2850 IF V1% < 0 THEN 3010
2860 IF V1% > 3 THEN 3010
2870 IF V1% = 0 THEN  POKE DS% + 17,128: REM  CH1 PROGRAMMABLE GAIN
2880 IF V1% = 1 THEN  POKE DS% + 17,64
2890 IF V1% = 2 THEN  POKE DS% + 17,32
2900 IF V1% = 3 THEN  POKE DS% + 17,16
2910 RETURN
2920 VTAB 21
2930 PRINT  SPC( 25);"PLEASE ENTER ANOTHER VALUE"
2940 GOTO 2470
2950 VTAB 23
2960 PRINT  SPC( 25);"PLEASE ENTER ANOTHER VALUE"
2970 GOTO 2530
2980 VTAB 22
2990 PRINT  SPC( 30);"PLEASE ENTER ANOTHER VALUE"
3000 GOTO 2730
3010 VTAB 24
3020 PRINT  SPC( 30);"PLEASE ENTER ANOTHER VALUE"
3030 GOTO 2820
3040 REM ************************************************************
3050 HOME
3060 VTAB 10
3070 PRINT  SPC( 10);"THE MULTIPLE SWEEP MEASUREMENT ROUTINE WILL
RETURN AVERAGED  "
3080 PRINT  SPC( 10);"VALUES FOR EACH SET OF SAMPLES TAKEN.  THE NUMBER
OF SAMPLES  "
3090 PRINT  SPC( 10);"COMPRISING EACH SET MUST BE IN THE INTERVAL 1 TO
100."
3100 VTAB 16
3110 HTAB 20
3120 INPUT "ENTER THE NUMBER OF SAMPLES DESIRED  ";SAMPLES%
3130 IF SAMPLES% < 1 THEN 3170
3140 IF SAMPLES% > 100 THEN 3170
3150 POKE DS% + 12,SAMPLES%: REM  NUMBER OF SAMPLES
3160 GOTO 3200
3170 VTAB 23
3180 PRINT  SPC( 25);"PLEASE ENTER ANOTHER VALUE"
3190 GOTO 3100
3200 HOME
3210 VTAB 1
3220 PRINT  SPC( 30);"MEASUREMENT ROUTINE SELECTION"
3230 VTAB 3
3240 PRINT  SPC( 10);"CHOICE"; SPC( 25);"DESCRIPTION"
3250 VTAB 5
```

```
3260 PRINT SPC( 05);"1-SINGLE SWEEP"; SPC( 08);"10 SAMPLES PER CHANNEL WILL
BE MEASURED."
3270 PRINT SPC( 27);"THE CORRECTED DATA WILL BE RETURNED."
3280 VTAB 8
3290 PRINT SPC( 05);"2-MULTIPLE SWEEP"; SPC( 06); STR$ (SAMPLES%);" SAMPLES
PER CHANNEL WILL BE MEASURED"
3300 PRINT SPC( 27);"THESE SAMPLES WILL BE AVERAGED TO FORM ONE"
3310 PRINT SPC( 27);"COMPUTATIONAL RESULT. 10 COMPUTATIONAL"
3320 PRINT SPC( 27);"RESULTS WILL BE RETURNED."
3330 VTAB 13
3340 PRINT SPC( 05);"3-DATA FILE"; SPC( 11);"A SPECIFIED NUMBER OF SAMPLES
PER CHANNEL WILL BE "
3350 PRINT SPC( 27);"MEASURED. THE COMPENSATED DATA WILL BE SAVED TO A
"
3360 PRINT SPC( 27);"DATA FILE ON DISK."
3370 VTAB 17
3380 PRINT SPC( 05);"4-PRINTER"; SPC( 13);"PRINTER OPTION MENU"
3390 VTAB 19
3400 PRINT SPC( 05);"5-NEW CONFIGURATION"; SPC( 03);"RETURNS TO
BEGINNING OF PROGRAM."
3410 VTAB 22
3420 HTAB 17
3430 INPUT "ENTER THE NUMBER ASSOCIATED WITH YOUR CHOICE (1-5)  ";MODE%
3440 IF MODE% < 1 THEN 3520
3450 IF MODE% > 5 THEN 3520
3460 POKE DS% + 25,MODE%: REM  MEASUREMENT ROUTINE CHOICE
3470 IF MODE% = 1 THEN 3550
3480 IF MODE% = 2 THEN 3550
3490 IF MODE% = 3 THEN 4860
3500 IF MODE% = 4 THEN 5480
3510 IF MODE% = 5 THEN  RETURN : REM  TO MAIN SEGMENT
3520 VTAB 23
3530 PRINT SPC( 25);"PLEASE ENTER ANOTHER VALUE"
3540 GOTO 3410
3550 HOME
3552 VTAB 4
3554 HTAB 15
3556 INPUT "DO YOU WISH TO SKIP INJECTION CURRENT MEASUREMENTS (Y/N)
";SKIP$
3558 IF SKIP$ = "Y" THEN  POKE DS% + 54,0: GOTO 3570
3560 VTAB 8
3562 PRINT SPC( 15);"DO YOU DESIRE FLASHLAMP TRIGGERING DURING THE
INJECTION"
3564 HTAB 16
3566 INPUT "CURRENT MEASUREMENT (1=NO, 2=YES)  ";IJ%
3568 POKE DS% + 54,IJ%: REM   INJ.ACTIVE FLAG
3570 VTAB 12
3572 HTAB 21
3580 INPUT "PRESS RETURN WHEN READY TO EXECUTE";BOGUS$
3582 IF SKIP$ = "N" THEN 3590
3584 VTAB 16
3586 PRINT SPC( 15);"PREVIOUS INJECTION CURRENT VALUES WILL BE USED"
3588 GOTO 3620
3590 VTAB 16
```

```
3600 PRINT SPC( 20);"MEASURING INJECTION CURRENT VALUES"
3610 CALL INT (256 * PEEK (DS% + 4) + PEEK (DS% + 5) + 0.5): REM PHASE 3
3615 IF IJ% = 2 THEN VTAB 18: HTAB 21: INPUT "PRESS RETURN WHEN READY TO
CONTINUE ";BOGUS$
3620 VTAB 20
3630 PRINT SPC( 25);"PERFORMING MEASUREMENT "
3640 CALL INT (256 * PEEK (DS% + 6) + PEEK (DS% + 7) + 0.5): REM PHASE 4
3650 HOME
3660 IF MODE% = 1 THEN PRINT SPC( 25);"SINGLE SWEEP RESULTS"
3670 IF MODE% = 2 THEN PRINT SPC( 25);"MULTIPLE SWEEP RESULTS"
3680 GOSUB 4360
3690 VTAB 3
3700 PRINT SPC( 02);"CH0 CURRENT GAIN: ";G0$; SPC( 07);"CH1 CURRENT GAIN:
";G1$
3710 PRINT SPC( 02);"CH0 PROGRAMMABLE GAIN: ";P0$; SPC( 05);"CH1
PROGRAMMABLE GAIN: ";P1$
3720 PRINT SPC( 02);"CH0 A/D RANGE: ";A0$; SPC( 10);"CH1 A/D RANGE: ";A1$
3730 J0% = 256 * PEEK (DS% + 21) + PEEK (DS% + 22): REM CH0 INJECTION
CURRENT
3740 J1% = 256 * PEEK (DS% + 23) + PEEK (DS% + 24): REM CH1 INJECTION
CURRENT
3750 GOSUB 4620: REM FORMAT
3760 PRINT SPC( 02);"CH0 INJECTION CURRENT: ";J0$; SPC( 02);"CH1 INJECTION
CURRENT: ";J1$
3770 VTAB 8
3780 PRINT SPC( 03);"CHANNEL 0"; SPC( 08);"CHANNEL 1"; SPC( 07);"RATIO
(CH0/CH1)"; SPC( 08);"%^RATIO"
3790 VT% = 10
3800 BASE% = INFO%
3810 C0% = INT (256 * PEEK (BASE% + 0) + PEEK (BASE% + 1) + 0.5): REM CH0
DATA
3820 C1% = INT (256 * PEEK (BASE% + 2) + PEEK (BASE% + 3) + 0.5): REM CH1
DATA
3821 ST(0,0) = C0%
3822 ST(1,0) = C1%
3830 GOSUB 4700: REM FORMAT
3840 RTEMP = (256 * PEEK (BASE% + 4) + PEEK (BASE% + 5) + PEEK (BASE% + 6) /
256 + PEEK (BASE% + 7) / 65.536E + 3)
3845 RA = RTEMP * (A0 / A1)
3846 ST(2,0) = RTEMP
3850 BASE% = BASE% + 8
3860 CHANGE = 0
3870 GOSUB 4780: REM FORMAT
3880 VTAB VT%
3890 IF PEEK (UF% + 0) = 0 THEN VTAB VT%: HTAB 38: PRINT RA$
3900 IF PEEK (UF% + 0) = 1 THEN INVERSE : VTAB VT%: HTAB 38: PRINT RA$
3910 NORMAL
3920 IF PEEK (OF% + 0) = 0 THEN VTAB VT%: HTAB 3: PRINT C0$; SPC( 04);C1$
3930 IF PEEK (OF% + 0) = 1 THEN INVERSE : VTAB VT%: HTAB 3: PRINT C0$; SPC(
04);C1$
3940 NORMAL
3950 VT% = VT% + 1
3960 FOR LOOP = 1 TO 9
3970 C0% = INT (256 * PEEK (BASE% + 0) + PEEK (BASE% + 1) + 0.5)
```

```
3980 C1% = INT (256 * PEEK (BASE% + 2) + PEEK (BASE% + 3) + 0.5)
3981 ST(0,LOOP) = C0%
3982 ST(1,LOOP) = C1%
3990 GOSUB 4700
4000 RP = RTEMP: REM PREVIOUS RATIO
4010 RTEMP = (256 * PEEK (BASE% + 4) + PEEK (BASE% + 5) + PEEK (BASE% + 6) /
256 + PEEK (BASE% + 7) / 65.536E + 3)
4015 RA = RTEMP * (A0 / A1)
4016 ST(2,LOOP) = RTEMP
4020 BASE% = BASE% + 8
4030 CHANGE = ((RTEMP - RP) / RP) * 100
4040 GOSUB 4780
4050 VTAB VT%
4060 IF CHANGE < 0 THEN PRINT SPC( 57);CHANGE$
4070 IF CHANGE > = 0 THEN PRINT SPC( 58);CHANGE$
4080 IF PEEK (UF% + LOOP) = 0 THEN VTAB VT%: HTAB 38: PRINT RA$
4090 IF PEEK (UF% + LOOP) = 1 THEN INVERSE : VTAB VT%: HTAB 38: PRINT RA$
4100 NORMAL
4110 IF PEEK (OF% + LOOP) = 0 THEN VTAB VT%: HTAB 3: PRINT C0$; SPC( 04);C1$
4120 IF PEEK (OF% + LOOP) = 1 THEN INVERSE : VTAB VT%: HTAB 3: PRINT C0$;
SPC( 04);C1$
4130 NORMAL
4140 VT% = VT% + 1
4150 NEXT LOOP
4160 M0% = INT (256 * PEEK (BASE% + 0) + PEEK (BASE% + 1) + 0.5)
4170 TEMP$ = STR$ (M0% * A0 / 4095)
4180 GOSUB 8710
4190 M0$ = TEMP$: REM CHANNEL 0 MEAN
4200 M1% = INT (256 * PEEK (BASE% + 2) + PEEK (BASE% + 3) + 0.5)
4210 TEMP$ = STR$ (M1% * A1 / 4095)
4220 GOSUB 8710
4230 M1$ = TEMP$: REM CHANNEL 1 MEAN
4240 MR = (256 * PEEK (BASE% + 4) + PEEK (BASE% + 5) + PEEK (BASE% + 6) / 256 +
PEEK (BASE% + 7) / 65.536E + 3)
4250 TEMP$ = STR$ (MR * A0 / A1)
4260 GOSUB 8710
4270 MR$ = TEMP$
4271 VTAB 21
4272 PRINT SPC( 02);M0$; SPC( 04);M1$; SPC( 03);MR$; SPC( 06);" AVG. VALUES"
4273 V0 = 0.0
4274 V1 = 0.0
4275 V2 = 0.0
4276 FOR LOOP = 0 TO 9
4277 V0 = V0 + (ST(0,LOOP) - M0%) * (ST(0,LOOP) - M0%)
4278 V1 = V1 + (ST(1,LOOP) - M1%) * (ST(1,LOOP) - M1%)
4279 V2 = V2 + (ST(2,LOOP) - MR) * (ST(2,LOOP) - MR)
4280 NEXT LOOP
4281 V0 = V0 / 9
4282 V1 = V1 / 9
4283 V2 = V2 / 9
4284 TEMP$ = STR$ ((A0 / 4095) * SQR (V0))
4285 GOSUB 8710
4286 S0$ = TEMP$
4287 TEMP$ = STR$ ((A1 / 4095) * SQR (V1))
```

```
4288 GOSUB 8710
4289 S1$ = TEMP$
4290 TEMP$ = STR$ ((A0 / A1) * SQR (V2))
4291 GOSUB 8710
4292 S2$ = TEMP$
4293 PRINT SPC( 02);S0$; SPC( 04);S1$; SPC( 03);S2$; SPC( 07);"STD. DEV."
4300 VTAB 24
4310 HTAB 20
4320 INPUT "PRESS RETURN WHEN FINISHED VIEWING SCREEN ";BOGUS$
4330 GOTO 3200
4340 REM ************************************************************
4350 REM FILENAME: PH2-BASIC
4360 IF PEEK (DS% + 15) = 8 THEN P0$ = "  10,000": REM  CH0 PROGRAMMABLE
GAIN
4370 IF PEEK (DS% + 15) = 4 THEN P0$ = "  100,000"
4380 IF PEEK (DS% + 15) = 2 THEN P0$ = "  1,000,000"
4390 IF PEEK (DS% + 15) = 1 THEN P0$ = " 10,000,000"
4400 IF PEEK (DS% + 16) = 0 THEN A0$ = " +10 V  ":A0 = 10000.0: REM  CH0 A/D
RANGE
4410 IF PEEK (DS% + 16) = 1 THEN A0$ = " +5 V  ":A0 = 5000.0
4420 IF PEEK (DS% + 16) = 2 THEN A0$ = " +2 V  ":A0 = 2000.0
4430 IF PEEK (DS% + 16) = 3 THEN A0$ = " +1 V  ":A0 = 1000.0
4440 IF PEEK (DS% + 16) = 4 THEN A0$ = " +500 mV":A0 = 500.0
4450 IF PEEK (DS% + 16) = 5 THEN A0$ = " +200 mV":A0 = 200.0
4460 IF PEEK (DS% + 16) = 6 THEN A0$ = " +100 mV":A0 = 100.0
4470 IF PEEK (DS% + 16) = 7 THEN A0$ = " +50 mV ":A0 = 50.0
4480 IF PEEK (DS% + 17) = 128 THEN P1$ = "  10,000": REM  CH1 PROGRAMMABLE
GAIN
4490 IF PEEK (DS% + 17) = 64 THEN P1$ = "  100,000"
4500 IF PEEK (DS% + 17) = 32 THEN P1$ = "  1,000,000"
4510 IF PEEK (DS% + 17) = 16 THEN P1$ = " 10,000,000"
4520 IF PEEK (DS% + 18) = 0 THEN A1$ = " +10 V  ":A1 = 10000.0: REM  CH1 A/D
RANGE
4530 IF PEEK (DS% + 18) = 1 THEN A1$ = " +5 V  ":A1 = 5000.0
4540 IF PEEK (DS% + 18) = 2 THEN A1$ = " +2 V  ":A1 = 2000.0
4550 IF PEEK (DS% + 18) = 3 THEN A1$ = " +1 V  ":A1 = 1000.0
4560 IF PEEK (DS% + 18) = 4 THEN A1$ = " +500 mV":A1 = 500.0
4570 IF PEEK (DS% + 18) = 5 THEN A1$ = " +200 mV":A1 = 200.0
4580 IF PEEK (DS% + 18) = 6 THEN A1$ = " +100 mV":A1 = 100.0
4590 IF PEEK (DS% + 18) = 7 THEN A1$ = " +50 mV ":A1 = 50.0
4600 RETURN
4610 REM ************************************************************
4620 TEMP$ = STR$ (J0% * A0 / 4095)
4630 GOSUB 8710
4640 J0$ = TEMP$
4650 TEMP$ = STR$ (J1% * A1 / 4095)
4660 GOSUB 8710
4670 J1$ = TEMP$
4680 RETURN
4690 REM ************************************************************
4700 TEMP$ = STR$ (C0% * A0 / 4095)
4710 GOSUB 8710
4720 C0$ = TEMP$
4730 TEMP$ = STR$ (C1% * A1 / 4095)
```

```
4740 GOSUB 8710
4750 C1$ = TEMP$
4760 RETURN
4770 REM ************************************************************
4780 TEMP$ = STR$ (RA)
4790 GOSUB 8710
4800 RA$ = TEMP$
4810 TEMP$ = STR$ (CHANGE)
4820 GOSUB 8710
4830 CHANGE$ = TEMP$
4840 RETURN
4850 REM ************************************************************
4860 HOME
4870 VTAB 4
4880 PRINT SPC( 10);"A DATA FILE WILL BE CREATED CONTAINING ALL SYSTEM
PARAMETERS,"
4890 PRINT SPC( 10);"CORRECTED DATA, AND INJECTION CURRENT FOR A
SPECIFIED "
4900 PRINT SPC( 10);"NUMBER OF SAMPLES IN EITHER A SINGLE POINT OR
INTERVAL MODE."
4901 VTAB 8: HTAB 20
4902 INPUT "WHICH MODE DO YOU PREFER (S=SINGLE,I=INTERVAL) ";KEY$
4904 IF KEY$ = "S" THEN 4910
4906 IF KEY$ = "I" THEN 4910
4908 GOTO 4860
4910 VTAB 10
4920 PRINT SPC( 10);"WARNING: IF YOU DESIGNATE THIS DATA FILE WITH AN
ALREADY"
4930 PRINT SPC( 10);"EXISTING FILE NAME, THE PREVIOUS DATA FILE CONTENTS
WILL BE"
4940 PRINT SPC( 10);"LOST."
4950 VTAB 14
4960 PRINT SPC( 10);"IF YOU DESIRE TO SEE THE DISK CONTENTS BEFORE
NAMING THE"
4970 PRINT SPC( 10);"FILE, SIMPLY ENTER '?' FOR THE FILENAME."
4980 VTAB 17
4990 HTAB 20
5000 INPUT "ENTER THE DESIRED DATA FILE NAME  ";FILE$
5010 IF FILE$ < > "?" THEN 5080
5020 HOME
5030 PRINT CD$;"CATALOG,S6,D2": REM  DISPLAY DISKETTE CONTENTS
5040 PRINT
5050 HTAB 20
5060 INPUT "PRESS RETURN WHEN READY TO CONTINUE ";BOGUS$
5070 GOTO 4860
5080 IF KEY$ = "I" THEN 6980
5081 PRINT
5082 VTAB 19
5083 HTAB 15
5084 INPUT "DO YOU WISH TO SKIP INJECTION CURRENT MEASUREMENTS (Y/N)
";SKIP$
5085 IF SKIP$ = "Y" THEN  POKE DS% + 54,0: GOTO 5091
5086 VTAB 21
```

```
5087 PRINT SPC( 15);"DO YOU DESIRE FLASHLAMP TRIGGERING DURING THE
INJECTION"
5088 HTAB 16
5089 INPUT "CURRENT MEASUREMENT (1=NO, 2=YES) ";IJ%
5090 POKE DS% + 54,IJ%: REM  INJ.ACTIVE FLAG
5091 IF SKIP$ = "N" THEN 5100
5092 VTAB 22
5093 PRINT SPC( 15);"PREVIOUS INJECTION CURRENT VALUES WILL BE USED"
5094 GOTO 5110
5100 PRINT
5101 PRINT SPC( 20);"MEASURING INJECTION CURRENT VALUES"
5102 PRINT
5105 CALL INT (256 * PEEK (DS% + 4) + PEEK (DS% + 5) + 0.5): REM  PHASE 3
5108 IF IJ% = 2 THEN HTAB 20: INPUT "PRESS RETURN WHEN READY TO
CONTINUE ";BOGUS$
5110 PRINT
5120 PRINT SPC( 25);"PERFORMING MEASUREMENT"
5130 CALL INT (256 * PEEK (DS% + 6) + PEEK (DS% + 7) + 0.5): REM PHASE 4
5140 PRINT
5150 PRINT SPC( 20);"DATA FILE BEING WRITTEN TO DISKETTE"
5152 TYPE$ = "SINGLE POINT"
5154 MEAS% = 200
5156 TIME% = 0
5158 UN$ = "SECONDS"
5160 PRINT CD$;"OPEN ";FILE$;",S6,D2"
5170 PRINT CD$;"DELETE ";FILE$;",S6,D2"
5180 PRINT CD$;"OPEN ";FILE$;",S6,D2"
5190 PRINT CD$;"WRITE ";FILE$
5192 PRINT TYPE$
5194 PRINT MEAS%
5196 PRINT TIME%
5198 PRINT UN$
5200 PRINT STR$ (ENERGY): REM ENERGY PER FLASH
5210 PRINT STR$ (LAMP%): REM FLASHLAMP FREQUENCY
5220 PRINT STR$ (PERIOD%): REM INTEGRATION PERIOD
5230 PRINT STR$ (FLSH%): REM MULTIPLE INTEGRATION COUNT
5240 PRINT G0$: REM CHANNEL 0 CURRENT GAIN
5250 PRINT G1$: REM CHANNEL 1 CURRENT GAIN
5260 I1% = PEEK (DS% + 15): REM  CHANNEL 0 PROGRAMMABLE GAIN
5270 I2% = PEEK (DS% + 16): REM  CHANNEL 0 A/D RANGE
5280 I3% = PEEK (DS% + 17): REM  CHANNEL 1 PROGRAMMABLE GAIN
5290 I4% = PEEK (DS% + 18): REM  CHANNEL 1 A/D RANGE
5291 GOSUB 6620
5292 PRINT P0
5293 PRINT A0
5294 PRINT P1
5295 PRINT A1
5300 IF KEY$ = "I" THEN 7430
5302 J0% = 256 * PEEK (DS% + 21) + PEEK (DS% + 22)
5304 J1% = 256 * PEEK (DS% + 23) + PEEK (DS% + 24)
5306 J0 = J0% * A0 / 4095
5308 J1 = J1% * A1 / 4095
5340 REM ************************************************************
5350 D1% = - 18176
```

```
5360 D2% = - 17920
5370 D3% = - 17664
5380 D4% = -17408
5390  FOR SAMPLE = 1 TO 200
5400 C0% = 256 *  PEEK (D1% + SAMPLE - 1) +  PEEK (D2% + SAMPLE - 1) - J0%
5402 C1% = 256 *  PEEK (D3% + SAMPLE - 1) +  PEEK (D4% + SAMPLE - 1) - J1%
5404 C0 = C0% * A0 / 4095
5406 C1 = C1% * A1 / 4095
5408  IF C1% = 0 THEN RA = 1.0E15
5410  IF C1% < > 0 THEN RA = (C0% / C1%) * (A0 / A1)
5412  PRINT J0","J1","C0","C1","RA","0","0","0
5440  NEXT SAMPLE
5450  PRINT CD$;"CLOSE ";FILE$
5460  GOTO 3200
5470  REM ************************************************************
5480  HOME
5490  VTAB 1
5500  PRINT  SPC( 30);"PRINTER OPTION SELECTION"
5510  VTAB 3
5520  PRINT  SPC( 07);"CHOICE"; SPC( 23);"DESCRIPTION"
5530  VTAB 5
5540  PRINT  SPC( 04);"1-DATA FILE"; SPC( 05);"THE RESULTS OF AN EXISTING DATA
FILE CREATED FROM"
5550  PRINT  SPC( 20);"THE PREVIOUS MENU WILL BE DUMPED TO THE PRINTER"
5560  VTAB 08
5570  PRINT  SPC( 04);"2-INTERVAL"; SPC( 06);"THE SYSTEM WILL TAKE A USER
SPECIFIED NUMBER OF"
5580  PRINT  SPC( 20);"MEASUREMENTS.  ADDITIONALLY, THE USER SPECIFIES
THE"
5590  PRINT  SPC( 20);"INTERVAL OF TIME BETWEEN MEASUREMENTS IN
SECONDS."
5600  PRINT  SPC( 20);"THE COMPUTATIONAL RESULTS WILL BE DUMPED TO THE"
5610  PRINT  SPC( 20);"PRINTER ALONG WITH SYSTEM PARAMTERTERS."
5620  VTAB 14
5630  PRINT  SPC( 04);"3-STATISTICS"; SPC( 04);"AN EXISTING DATA FILE WILL BE
POST PROCESSED FOR"
5640  PRINT  SPC( 20);"STATISTICAL PARAMETERS."
5650  VTAB 17
5660  PRINT  SPC( 04);"4-EXIT"; SPC( 10);"RETURN TO PREVIOUS MENU"
5670  VTAB 20
5680  HTAB 17
5690  INPUT "ENTER THE NUMBER ASSOCIATED WITH YOUR CHOICE  ";PR%
5700  IF PR% < 1 THEN 5760
5710  IF PR% > 4 THEN 5760
5720  IF PR% = 1 THEN 5800
5730  IF PR% = 2 THEN KEY$ = "BOGUS": GOTO 6980
5740  IF PR% = 3 THEN 7770
5750  IF PR% = 4 THEN 3200
5760  VTAB 24
5770  PRINT  SPC( 25);"PLEASE ENTER ANOTHER VALUE"
5780  GOTO 5480
5790  REM ************************************************************
5800  HOME
5810  VTAB 7
```

```
5820 PRINT SPC( 20);"BE SURE THE PRINTER IS 'ON LINE'"
5830 VTAB 10
5840 PRINT SPC( 10);"IF YOU DESIRE TO SEE THE DISK CONTENTS BEFORE
NAMING"
5850 PRINT SPC( 10);"THE FILE, SIMPLY ENTER '?' FOR THE FILENAME."
5860 VTAB 15
5870 HTAB 20
5880 INPUT "ENTER THE DESIRED DATA FILE NAME ";FILE$
5890 IF FILE$ < > "?" THEN 5960
5900 HOME
5910 PRINT CD$;"CATALOG,S6,D2"
5920 PRINT
5930 HTAB 20
5940 INPUT "PRESS RETURN TO CONTINUE ";BOGUS$
5950 GOTO 5800
5960 VTAB 20
5970 PRINT SPC( 22);"PRINTING THE DATA FILE ";FILE$
5980 PRINT CD$;"PR# 1": REM ACTIVATE PRINTER
5990 PRINT CD$;"OPEN ";FILE$;",S6,D2"
6000 PRINT CD$;"READ ";FILE$
6010 GOSUB 6180: REM SYSTEM PARAMETERS
6020 PRINT "SAMPLE #"; SPC( 06);"CH0 INJECTION"; SPC( 10);"CH1 INJECTION"; SPC(
10);"CHANNEL 0 DATA"; SPC( 10);"CHANNEL 1 DATA"; SPC( 13);"RATIO"
6030 PRINT
6040 FOR LOOP = 1 TO MEAS%
6042 INPUT J0,J1,C0,C1,RA,S0,S1,S2
6044 TEMP$ = STR$ (J0)
6046 GOSUB 8710
6048 J0$ = TEMP$
6050 TEMP$ = STR$ (J1)
6052 GOSUB 8710
6054 J1$ = TEMP$
6056 TEMP$ = STR$ (C0)
6058 GOSUB 8710
6060 C0$ = TEMP$
6062 TEMP$ = STR$ (C1)
6064 GOSUB 8710
6066 C1$ = TEMP$
6068 TEMP$ = STR$ (RA)
6070 GOSUB 8710
6072 RA$ = TEMP$
6090 GOSUB 8780: REM FORMAT
6100 PRINT SPC( 04);LOOP$; SPC( 09);J0$; SPC( 09);J1$; SPC( 09);C0$; SPC( 09);C1$;
SPC( 09);RA$
6110 NEXT LOOP
6120 GOSUB 6880
6130 PRINT CHR$ (140): REM FORM FEED
6140 PRINT CD$;"PR# 3": REM REACTIVATE 80 COLUMN
6150 PRINT CD$;"CLOSE ";FILE$
6160 GOTO 5480
6170 REM ************************************************************
6180 PRINT "FILENAME: ";FILE$
6190 PRINT
6191 INPUT TYPE$
```

```
6192 PRINT "FILE TYPE: ";TYPE$
6193 INPUT MEAS%
6194 PRINT "NUMBER OF MEASUREMENTS: ";MEAS%
6195 INPUT TIME%
6196 PRINT "TIME BETWEEN MEASUREMENTS: ";TIME%
6197 INPUT UN$
6198 PRINT "MEASUREMENT UNIT: ";UN$
6200 INPUT IN$
6210 PRINT "ENERGY PER FLASH: ";IN$;" JOULES"
6220 INPUT IN$
6230 PRINT "FLASH LAMP FREQUENCY: ";IN$;" HZ"
6240 INPUT IN$
6250 PRINT "INTEGRATION PERIOD: ";IN$;" USEC"
6260 INPUT IN$
6270 PRINT "MULTIPLE INTEGRATION COUNT: ";IN$
6280 PRINT
6290 GOSUB 6460
6300 INPUT G0$
6310 INPUT G1$
6320 PRINT "CHANNEL 0 CURRENT GAIN: ";G0$; SPC( 04);"CHANNEL 1 CURRENT
GAIN: ";G1$
6330 GOSUB 6560
6340 GOSUB 6620
6350 PRINT "CHANNEL 0 PROGRAMMABLE GAIN: ";P0$; SPC( 02);"CHANNEL 1
PROGRAMMABLE GAIN: ";P1$
6360 PRINT "CHANNEL 0 A/D RANGE:   ";A0$; SPC( 12);"CHANNEL 1 A/D RANGE:
";A1$
6370 PRINT
6440 RETURN
6450 REM ************************************************************
6460 T1$ = P0$
6470 T2 = A0
6480 T2$ = A0$
6490 T3$ = P1$
6500 T4 = A1
6510 T4$ = A1$
6520 T5$ = G0$
6530 T6$ = G1$
6540 RETURN
6550 REM ************************************************************
6560 INPUT P0
6561 INPUT A0
6562 INPUT P1
6563 INPUT A1
6564 IF P0 = 10000 THEN I1% = 8
6565 IF P0 = 100000 THEN I1% = 4
6566 IF P0 = 1000000 THEN I1% = 2
6567 IF P0 = 10000000 THEN I1% = 1
6568 IF A0 = 10000.0 THEN I2% = 0
6569 IF A0 = 5000.0 THEN I2% = 1
6570 IF A0 = 2000.0 THEN I2% = 2
6571 IF A0 = 1000.0 THEN I2% = 3
6572 IF A0 = 500.0 THEN I2% = 4
6573 IF A0 = 200.0 THEN I2% = 5
```

```
6574 IF A0 = 100.0 THEN I2% = 6
6575 IF A0 = 50.0 THEN I2% = 7
6576 IF P1 = 10000 THEN I3% = 128
6577 IF P1 = 100000 THEN I3% = 64
6578 IF P1 = 1000000 THEN I3% = 32
6579 IF P1 = 10000000 THEN I3% = 16
6580 IF A1 = 10000.0 THEN I4% = 0
6581 IF A1 = 5000.0 THEN I4% = 1
6582 IF A1 = 2000.0 THEN I4% = 2
6583 IF A1 = 1000.0 THEN I4% = 3
6584 IF A1 = 500.0 THEN I4% = 4
6585 IF A1 = 200.0 THEN I4% = 5
6586 IF A1 = 100.0 THEN I4% = 6
6587 IF A1 = 50.0 THEN I4% = 7
6600 RETURN
6610 REM ************************************************************
6620 IF I1% = 8 THEN P0$ = "    10,000":P0 = 10000
6630 IF I1% = 4 THEN P0$ = "   100,000":P0 = 100000
6640 IF I1% = 2 THEN P0$ = " 1,000,000":P0 = 1000000
6650 IF I1% = 1 THEN P0$ = "10,000,000":P0 = 10000000
6660 IF I2% = 0 THEN A0$ = "+10 V  ":A0 = 10000.0
6670 IF I2% = 1 THEN A0$ = "+5 V   ":A0 = 5000.0
6680 IF I2% = 2 THEN A0$ = "+2 V   ":A0 = 2000.0
6690 IF I2% = 3 THEN A0$ = "+1 V   ":A0 = 1000.0
6700 IF I2% = 4 THEN A0$ = "+500 mV":A0 = 500.0
6710 IF I2% = 5 THEN A0$ = "+200 mV":A0 = 200.0
6720 IF I2% = 6 THEN A0$ = "+100 mV":A0 = 100.0
6730 IF I2% = 7 THEN A0$ = "+50 mV ":A0 = 50.0
6740 IF I3% = 128 THEN P1$ = "    10,000":P1 = 10000
6750 IF I3% = 64 THEN P1$ = "   100,000":P1 = 100000
6760 IF I3% = 32 THEN P1$ = " 1,000,000":P1 = 1000000
6770 IF I3% = 16 THEN P1$ = "10,000,000":P1 = 10000000
6780 IF I4% = 0 THEN A1$ = "+10 V  ":A1 = 10000.0
6790 IF I4% = 1 THEN A1$ = "+5 V   ":A1 = 5000.0
6800 IF I4% = 2 THEN A1$ = "+2 V   ":A1 = 2000.0
6810 IF I4% = 3 THEN A1$ = "+1 V   ":A1 = 1000.0
6820 IF I4% = 4 THEN A1$ = "+500 mV":A1 = 500.0
6830 IF I4% = 5 THEN A1$ = "+200 mV":A1 = 200.0
6840 IF I4% = 6 THEN A1$ = "+100 mV":A1 = 100.0
6850 IF I4% = 7 THEN A1$ = "+50 mV ":A1 = 50.0
6860 RETURN
6870 REM ************************************************************
6880 P0$ = T1$
6890 A0 = T2
6900 A0$ = T2$
6910 P1$ = T3$
6920 A1 = T4
6930 A1$ = T4$
6940 G0$ = T5$
6950 G1$ = T6$
6960 RETURN
6970 REM ************************************************************
6980 HOME
7000 PRINT SPC( 22);"INTERVAL MEASUREMENT ROUTINE"
```

```
7002 IF KEY$ < > "I" THEN 7010
7004 VTAB 3
7006 HTAB 15
7008 PRINT SPC( 04);"RESULTS WILL BE SAVED TO A DATA FILE"
7010 VTAB 5
7020 HTAB 15
7030 INPUT "ENTER THE DESIRED MEASUREMENT UNIT (H,M,S) ";UN$
7040 VTAB 7
7050 HTAB 15
7060 INPUT "ENTER THE DESIRED TIME BETWEEN MEASUREMENTS ";TIME%
7070 VTAB 9
7080 HTAB 15
7090 INPUT "ENTER THE TOTAL NUMBER OF MEASUREMENTS YOU DESIRE
";MEAS%
7092 VTAB 11
7094 HTAB 15
7096 INPUT "DO YOU WISH TO SKIP INJECTION CURRENT MEASUREMENTS (Y/N)
";SKIP$
7097 VTAB 14
7098 IF SKIP$ = "Y" THEN PRINT SPC( 14);"NO INJECTION CURRENT
MEASUREMENTS ARE PERFORMED"
7100 VTAB 17
7110 IF KEY$ < > "I" THEN PRINT SPC( 20);"BE SURE THE PRINTER IS 'ON LINE'"
7140 VTAB 19
7150 HTAB 26
7160 INPUT "PRESS RETURN TO BEGIN ";BOGUS$
7170 VTAB 22
7180 PRINT SPC( 20);"EXECUTING INTERVAL MEASUREMENT"
7190 IF UN$ = "H" THEN UN$ = "HOURS": POKE DS% + 100,4: POKE DS% + 101,12:
REM SELECT HOUR UNITS
7200 IF UN$ = "M" THEN UN$ = "MINUTES": POKE DS% + 100,4: POKE DS% + 101,5:
REM SELECT MINUTE UNITS
7210 IF UN$ = "S" THEN UN$ = "SECONDS": POKE DS% + 100,12: POKE DS% + 101,4:
REM SELECT SECOND UNITS
7220 POKE DS% + 25,2: REM MULTIPLE SWEEP
7222 IF KEY$ = "I" THEN 7422
7230 PRINT CD$;"PR# 1": REM REACTIVATE PRINTER
7240 PRINT "TOTAL NUMBER OF MEASUREMENTS: "; STR$ (MEAS%)
7250 PRINT "TIME BETWEEN MEASUREMENTS: "; STR$ (TIME%);" ";UN$
7260 PRINT
7270 PRINT "ENERGY PER FLASH: "; STR$ (ENERGY);" JOULES"
7280 PRINT "FLASH LAMP FREQUENCY: "; STR$ (LAMP%);" HZ"
7290 PRINT "INTEGRATION PERIOD: "; STR$ (PERIOD%);" USEC"
7300 PRINT "MULTIPLE INTEGRATION COUNT: "; STR$ (FLSH%)
7310 PRINT "SAMPLES AVERAGED FOR DATA VALUES: " STR$ (SAMPLES%)
7320 PRINT
7330 GOSUB 4360
7340 PRINT "CHANNEL 0 CURRENT GAIN: ";G0$
7350 PRINT "CHANNEL 0 PROGRAMMABLE GAIN: ";P0$
7360 PRINT "CHANNEL 0 A/D RANGE: ";A0$
7370 PRINT
7380 PRINT "CHANNEL 1 CURRENT GAIN: ";G1$
7390 PRINT "CHANNEL 1 PROGRAMMABLE GAIN: ";P1$
7400 PRINT "CHANNEL 1 A/D RANGE: ";A1$
```

```
7410 PRINT
7420 PRINT
7422 TYPE$ = "INTERVAL"
7424 IF KEY$ = "I" THEN 5160
7430 CHANGE = 0
7440 POKE DS% + 102,0: REM CLEAR TIME.OUT FLAG
7450 CALL INT (256 * PEEK (DS% + 103) + PEEK (DS% + 104) + 0.5): REM START
CLOCK
7460 IF PEEK (DS% + 102) = 0 THEN 7460: REM WAIT FOR START OF INTERVAL
7470 FOR LOOP = 1 TO MEAS%
7480 POKE DS% + 102,0: REM CLEAR TIME.OUT COUNTER
7485 POKE DS% + 54,0: REM RESET INJ.ACTIVE FLAG FOR PHASE 4
7490 IF SKIP$ = "N" THEN POKE DS% + 54,1: CALL INT (256 * PEEK (DS% + 4) +
PEEK (DS% + 5) + 0.5): REM PHASE 3
7500 CALL INT (256 * PEEK (DS% + 6) + PEEK (DS% + 7) + 0.5): REM PHASE 4
7510 CALL INT (256 * PEEK (DS% + 107) + PEEK (DS% + 108) + 0.5): REM REENABLE
PROCESSOR INTERRUPTS
7520 J0% = 256 * PEEK (DS% + 21) + PEEK (DS% + 22): REM CH0 INJECTION
CURRENT
7530 J1% = 256 * PEEK (DS% + 23) + PEEK (DS% + 24): REM CH1 INJECTION
CURRENT
7540 GOSUB 4620: REM FORMAT
7542 J0 = J0% * A0 / 4095
7544 J1 = J1% * A1 / 4095
7550 IF KEY$ < > "I" THEN PRINT
7551 BASE% = INFO%
7552 FOR COUNT = 0 TO 9
7553 ST(0,COUNT) = INT (256 * PEEK (BASE% + 0) + PEEK (BASE% + 1) + 0.5)
7554 ST(1,COUNT) = INT (256 * PEEK (BASE% + 2) + PEEK (BASE% + 3) + 0.5)
7555 ST(2,COUNT) = (256 * PEEK (BASE% + 4) + PEEK (BASE% + 5) + PEEK (BASE%
+ 6) / 256 + PEEK (BASE% + 7) / 65.536E03)
7556 BASE% = BASE% + 8
7557 NEXT COUNT
7560 C0% = INT (256 * PEEK (INFO% + 80) + PEEK (INFO% + 81) + 0.5)
7570 C1% = INT (256 * PEEK (INFO% + 82) + PEEK (INFO% + 83) + 0.5)
7572 C0 = C0% * A0 / 4095
7574 C1 = C1% * A1 / 4095
7580 GOSUB 4700
7590 RP = RTEMP
7600 RTEMP = (256 * PEEK (INFO% + 84) + PEEK (INFO% + 85) + PEEK (INFO% + 86) /
256 + PEEK (INFO% + 87) / 65.536E + 3)
7605 RA = RTEMP * (A0 / A1)
7610 IF LOOP > 1 THEN CHANGE = ((RTEMP - RP) / RP) * 100
7611 GOSUB 4780
7612 V0 = 0.0
7613 V1 = 0.0
7614 V2 = 0.0
7615 FOR COUNT = 0 TO 9
7616 V0 = V0 + (ST(0,COUNT) - C0%) * (ST(0,COUNT) - C0%)
7617 V1 = V1 + (ST(1,COUNT) - C1%) * (ST(1,COUNT) - C1%)
7618 V2 = V2 + (ST(2,COUNT) - RTEMP) * (ST(2,COUNT) - RTEMP)
7619 NEXT COUNT
7620 VO = V0 / 9
7621 V1 = V1 / 9
```

```
7622 V2 = V2 / 9
7623 TEMP$ = STR$ ((A0 / 4095) * SQR (V0)):S0 = (A0 / 4095) * SQR (V0)
7624 GOSUB 8710
7625 S0$ = TEMP$
7626 TEMP$ = STR$ ((A1 / 4095) * SQR (V1)):S1 = (A1 / 4095) * SQR (V1)
7627 GOSUB 8710
7628 S1$ = TEMP$
7629 TEMP$ = STR$ ((A0 / A1) * SQR (V2)):S2 = (A0 / A1) * SQR (V2)
7630 GOSUB 8710
7631 S2$ = TEMP$
7635 IF KEY$ < > "I" THEN PRINT "MEAS #"; STR$ (LOOP); SPC( 03);"CH0 INJECTION
CURRENT: ";J0$; SPC( 03);"CH0 DATA: ";C0$; SPC( 03);"CH0 STD. DEV. ";S0$
7640 IF KEY$ < > "I" THEN PRINT SPC( 06); SPC( LEN ( STR$ (LOOP))); SPC(
03);"CH1 INJECTION CURRENT: ";J1$; SPC( 03);"CH1 DATA: ";C1$; SPC( 03);"CH1 STD.
DEV. ";S1$
7650 IF KEY$ < > "I" THEN PRINT SPC( 09); SPC( LEN ( STR$ (LOOP)));"RATIO:
";RA$; SPC( 46);"RATIO STD. DEV. ";S2$
7660 IF KEY$ < > "I" THEN PRINT SPC( 09); SPC( LEN ( STR$ (LOOP)));"%^RATIO:
";CHANGE$
7670 IF KEY$ < > "I" THEN PRINT
7675 IF KEY$ = "I" THEN PRINT J0","J1","C0","C1","RA","S0","S1","S2
7680 IF PEEK (DS% + 102) > TIME% THEN PRINT "MEASUREMENT INTERVAL TOO
SHORT FOR SELECTED PARAMETERS ": GOTO 7710: REM START AGAIN
7690 IF PEEK (DS% + 102) < TIME% THEN 7690: REM WAIT FOR TIME.OUT COUNT
TO EXPIRE
7700 NEXT LOOP
7705 IF KEY$ = "I" THEN PRINT CD$;"CLOSE";FILE$
7710 POKE DS% + 102,0: REM CLEAR TIME.OUT COUNTER
7720 CALL INT (256 * PEEK (DS% + 105) + PEEK (DS% + 106) + 0.5): REM DISABLE
CLOCK AND PROCESSOR INTERRUPTS
7730 IF KEY$ < > "I" THEN PRINT CHR$ (140)
7740 IF KEY$ < > "I" THEN PRINT CD$;"PR# 3": REM REACTIVATE 80 COLUMN
7750 IF KEY$ < > "I" THEN GOTO 5480
7755 IF KEY$ = "I" THEN GOTO 3200
7760 REM ************************************************************
7770 HOME
7780 VTAB 7
7790 PRINT SPC( 20);"BE SURE THE PRINTER IS 'ON LINE'"
7800 VTAB 10
7810 PRINT SPC( 10);"IF YOU DESIRE TO SEE THE DISK CONTENTS BEFORE
NAMING"
7820 PRINT SPC( 10);"THE FILE, SIMPLY ENTER '?' FOR THE FILENAME."
7830 VTAB 15
7840 HTAB 20
7850 INPUT "ENTER THE DESIRED DATA FILE NAME ";FILE$
7860 IF FILE$ < > "?" THEN 7930
7870 HOME
7880 PRINT CD$;"CATALOG,S6,D2"
7890 PRINT
7900 HTAB 20
7910 INPUT "PRESS RETURN TO CONTINUE ";BOGUS$
7920 GOTO 7770
7930 VTAB 20
7940 PRINT SPC( 15);"PRINTING THE DATA FILE STATISTICAL RESULTS "
```

```
7950 PRINT CD$;"PR# 1": REM  ACTIVATE PRINTER
7960 PRINT CD$;"OPEN ";FILE$;",S6,D2"
7970 PRINT CD$;"READ ";FILE$
7980 GOSUB 6180: REM  PRINT SYSTEM PARAMETERS
7990 PRINT
8000 M0 = 0.0: REM  MEAN VALUE
8010 M1 = 0.0
8011 M2 = 0.0
8012 M3 = 0.0
8013 M4 = 0.0
8020 L0 = 10000: REM    LOW VALUE
8030 H0 = - 10000: REM    HIGH VALUE
8040 L1 = 10000
8050 H1 = - 10000
8051 L2 = 1.0E15
8052 H2 = - 1.0E15
8053 L3 = 10000
8054 H3 = - 10000
8055 L4 = 10000
8056 H4 = - 10000
8060 FOR LOOP = 1 TO MEAS%: REM  MEAS% SAMPLES
8070  INPUT J0,J1,C0,C1,RA,S0,S1,S2
8080 ST(0,LOOP) = C0
8090 ST(1,LOOP) = C1
8091 ST(2,LOOP) = RA
8092 ST(3,LOOP) = J0
8093 ST(4,LOOP) = J1
8100 M0 = M0 + ST(0,LOOP)
8110 M1 = M1 + ST(1,LOOP)
8111 M2 = M2 + ST(2,LOOP)
8112 M3 = M3 + ST(3,LOOP)
8113 M4 = M4 + ST(4,LOOP)
8120  IF ST(0,LOOP) < L0 THEN L0 = ST(0,LOOP)
8130  IF ST(0,LOOP) > H0 THEN H0 = ST(0,LOOP)
8140  IF ST(1,LOOP) < L1 THEN L1 = ST(1,LOOP)
8150  IF ST(1,LOOP) > H1 THEN H1 = ST(1,LOOP)
8151  IF ST(2,LOOP) < L2 THEN L2 = ST(2,LOOP)
8152  IF ST(2,LOOP) > H2 THEN H2 = ST(2,LOOP)
8153  IF ST(3,LOOP) < L3 THEN L3 = ST(3,LOOP)
8154  IF ST(3,LOOP) > H3 THEN H3 = ST(3,LOOP)
8155  IF ST(4,LOOP) < L4 THEN L4 = ST(4,LOOP)
8156  IF ST(4,LOOP) > H4 THEN H4 = ST(4,LOOP)
8160  NEXT LOOP
8170  PRINT CD$;"CLOSE ";FILE$
8180 M0 = M0 / MEAS%
8190 M1 = M1 / MEAS%
8191 M2 = M2 / MEAS%
8192 M3 = M3 / MEAS%
8193 M4 = M4 / MEAS%
8200 V0 = 0.0: REM  CHANNEL 0 VARIANCE
8210 V1 = 0.0: REM  CHANNEL 1 VARIANCE
8211 V2 = 0.0: REM  RATIO VARIANCE
8212 V3 = 0.0: REM  CHANNEL 0 INJECTION VARIANCE
8213 V4 = 0.0: REM  CHANNEL 1 INJECTION VARIANCE
```

```
8220 FOR LOOP = 1 TO MEAS%
8230 V0 = V0 + (ST(0,LOOP) - M0) * (ST(0,LOOP) - M0)
8240 V1 = V1 + (ST(1,LOOP) - M1) * (ST(1,LOOP) - M1)
8241 V2 = V2 + (ST(2,LOOP) - M2) * (ST(2,LOOP) - M2)
8242 V3 = V3 + (ST(3,LOOP) - M3) * (ST(3,LOOP) - M3)
8243 V4 = V4 + (ST(4,LOOP) - M4) * (ST(4,LOOP) - M4)
8250 NEXT LOOP
8260 V0 = V0 / (MEAS% - 1)
8270 V1 = V1 / (MEAS% - 1)
8271 V2 = V2 / (MEAS% - 1)
8272 V3 = V3 / (MEAS% - 1)
8273 V4 = V4 / (MEAS% - 1)
8280 S0 = SQR (V0): REM CHANNEL 0 STANDARD DEVIATION
8290 S1 = SQR (V1): REM CHANNEL 1 STANDARD DEVIATION
8291 S2 = SQR (V2): REM RATIO STANDARD DEVIATION
8292 S3 = SQR (V3): REM CHANNEL 0 INJECTION STANDARD DEVIATION
8293 S4 = SQR (V4): REM CHANNEL 1 INJECTION STANDARD DEVIATION
8300 TEMP$ = STR$ (L0)
8310 GOSUB 8710
8320 L0$ = TEMP$
8330 TEMP$ = STR$ (L1)
8340 GOSUB 8710
8350 L1$ = TEMP$
8351 TEMP$ = STR$ (L2)
8352 GOSUB 8710
8353 L2$ = TEMP$
8354 TEMP$ = STR$ (L3)
8355 GOSUB 8710
8356 L3$ = TEMP$
8357 TEMP$ = STR$ (L4)
8358 GOSUB 8710
8359 L4$ = TEMP$
8360 TEMP$ = STR$ (H0)
8370 GOSUB 8710
8380 H0$ = TEMP$
8390 TEMP$ = STR$ (H1)
8400 GOSUB 8710
8410 H1$ = TEMP$
8411 TEMP$ = STR$ (H2)
8412 GOSUB 8710
8413 H2$ = TEMP$
8414 TEMP$ = STR$ (H3)
8415 GOSUB 8710
8416 H3$ = TEMP$
8417 TEMP$ = STR$ (H4)
8418 GOSUB 8710
8419 H4$ = TEMP$
8420 TEMP$ = STR$ (M0)
8430 GOSUB 8710
8440 M0$ = TEMP$
8450 TEMP$ = STR$ (M1)
8460 GOSUB 8710
8470 M1$ = TEMP$
8471 TEMP$ = STR$ (M2)
```

```
8472  GOSUB 8710
8473 M2$ = TEMP$
8474 TEMP$ =  STR$ (M3)
8475  GOSUB 8710
8476 M3$ = TEMP$
8477 TEMP$ =  STR$ (M4)
8478  GOSUB 8710
8479 M4$ = TEMP$
8480 TEMP$ =  STR$ (V0)
8490  GOSUB 8710
8500 V0$ = TEMP$
8510 TEMP$ =  STR$ (V1)
8520  GOSUB 8710
8530 V1$ = TEMP$
8531 TEMP$ =  STR$ (V2)
8532  GOSUB 8710
8533 V2$ = TEMP$
8534 TEMP$ =  STR$ (V3)
8535  GOSUB 8710
8536 V3$ = TEMP$
8537 TEMP$ =  STR$ (V4)
8538  GOSUB 8710
8539 V4$ = TEMP$
8540 TEMP$ =  STR$ (S0)
8550  GOSUB 8710
8560 S0$ = TEMP$
8570 TEMP$ =  STR$ (S1)
8580  GOSUB 8710
8581 S1$ = TEMP$
8582 TEMP$ =  STR$ (S2)
8583  GOSUB 8710
8584 S2$ = TEMP$
8585 TEMP$ =  STR$ (S3)
8586  GOSUB 8710
8587 S3$ = TEMP$
8588 TEMP$ =  STR$ (S4)
8589  GOSUB 8710
8590 S4$ = TEMP$
8594  PRINT
8596  PRINT "PARAMETER"; SPC( 11);"CH0 INJECTION"; SPC( 10);"CH1 INJECTION";
SPC( 10);"CHANNEL 0 DATA"; SPC( 10);"CHANNEL 1 DATA"; SPC( 10);"RATIO"
8597  PRINT
8598  PRINT "MINIMUM"; SPC( 13);L3$; SPC( 09);L4$; SPC( 09);L0$; SPC( 10);L1$; SPC(
10);L2$
8599  PRINT "MAXIMUM"; SPC( 13);H3$; SPC( 09);H4$; SPC( 09);H0$; SPC( 10);H1$;
SPC( 10);H2$
8600  PRINT
8601  PRINT "MEAN"; SPC( 16);M3$; SPC( 09);M4$; SPC( 09);M0$; SPC( 10);M1$; SPC(
10);M2$
8602  PRINT "VARIANCE"; SPC( 12);V3$; SPC( 09);V4$; SPC( 09);V0$; SPC( 10);V1$; SPC(
10);V2$
8603  PRINT "STANDARD DEV."; SPC( 07);S3$; SPC( 09);S4$; SPC( 09);S0$; SPC( 10);S1$;
SPC( 10);S2$
8660  GOSUB 6880
```

```
8670 PRINT CHR$ (140)
8680 PRINT CD$;"PR# 3": REM REACTIVATE 80 COLUMN
8690 GOTO 5480
8700 REM ************************************************************
8710 LGTH% = LEN (TEMP$)
8720 IF LGTH% = 14 THEN RETURN
8730 FOR PAD = 1 TO 14 - LGTH%
8740 TEMP$ = TEMP$ + " "
8750 NEXT PAD
8760 RETURN
8770 REM ************************************************************
8780 LOOP$ = STR$ (LOOP)
8790 LGTH% = LEN (LOOP$)
8800 IF LGTH% = 4 THEN RETURN
8810 FOR PAD = 1 TO 4 - LGTH%
8820 LOOP$ = LOOP$ + " "
8830 NEXT PAD
8840 RETURN
8850 REM
************************************************************************
8860 HOME
8870 VTAB 3
8880 PRINT SPC( 24);"PHOTOMULTIPLIER GAIN SELECTION"
8890 VTAB 6
8900 PRINT SPC( 24);"THE GAIN OF EACH PHOTOMULTIPLIER "
8910 PRINT SPC( 24);"CAN BE ADJUSTED INDEPENDENTLY AND "
8920 PRINT SPC( 24);"MUST BE IN THE INTERVAL 4.0 - 2.0E06 "
8930 VTAB 10
8940 HTAB 25
8950 INPUT "ENTER THE GAIN FOR PHOTOMULTIPLIER CH0 ";G0
8960 IF G0 < 4.0 THEN 8930
8970 IF G0 > 2.0E06 THEN 8930
8980 VTAB 11
8990 HTAB 25
9000 INPUT "ENTER THE GAIN FOR PHOTOMULTIPLIER CH1 ";G1
9010 IF G1 < 4.0 THEN 8980
9020 IF G1 > 2.0E06 THEN 8980
9030 ZT0 = (.434294482 * LOG (G0 / 3.1622776E - 17)) / 7.5: REM HV CH0
9040 O0 = 10 ^ ZT0
9050 ZT1 = (.434294482 * LOG (G1 / 3.1622776E - 17)) / 7.5: REM HV CH1
9060 O1 = 10 ^ ZT1
9070 R0 = (1.6127616E - 18) * O0 ^ 7.5: REM CH0 ANODE RADIANT SENSITIVITY
9080 R1 = (1.6127616E - 18) * O1 ^ 7.5: REM CH1 ANODE RADIANT SENSITIVITY
9090 W0 = 1.0E - 05 / R0: REM MAXIMUM CH0 INPUT INTENSITY
9100 W1 = 1.0E - 05 / R1: REM MAXIMUM CH1 INPUT INTENSITY
9110 Z0 = ( - O0 + 1100) / 650: REM REFERENCE VOLTAGE CH0
9120 Z1 = ( - O1 + 1100) / 650: REM REFERENCE VOLTAGE CH1
9130 X0% = INT ((255 * Z0 / 1.423670669) + .5): REM CH0 GAIN CONTROL VALUE
9140 X1% = INT ((255 * Z1 / 1.423670669) + .5): REM CH1 GAIN CONTROL
9150 VTAB 14
9160 PRINT SPC( 41);"CH0"; SPC( 16);"CH1"
9170 VTAB 16
9180 GOSUB 9560: REM FORMAT
9190 TEMP$ = STR$ ( - O0)
```

```
9200  GOSUB 8710
9210 O0$ = TEMP$
9220 TEMP$ =  STR$ ( - O1)
9230  GOSUB 8710
9240 O1$ = TEMP$
9250 TEMP$ =  STR$ (R0)
9260  GOSUB 8710
9270 R0$ = TEMP$
9280 TEMP$ =  STR$ (R1)
9290  GOSUB 8710
9300 R1$ = TEMP$
9310 TEMP$ =  STR$ (W0)
9320  GOSUB 8710
9330 W0$ = TEMP$
9340 TEMP$ =  STR$ (W1)
9350  GOSUB 8710
9360 W1$ = TEMP$
9370 TEMP$ =  STR$ (Z0)
9380  GOSUB 8710
9390 Z0$ = TEMP$
9400 TEMP$ =  STR$ (Z1)
9410  GOSUB 8710
9420 Z1$ = TEMP$
9430  PRINT  SPC( 5);"CURRENT GAIN: "; SPC( 17);G0$; SPC( 5);G1$
9440  PRINT  SPC( 5);"ANODE SENSITIVITY (A/W): "; SPC( 06);R0$; SPC( 5);R1$
9450  PRINT  SPC( 5);"REFERENCE VOLTAGE (V): "; SPC( 8);Z0$; SPC( 5);Z1$
9460  PRINT  SPC( 5);"HIGH VOLTAGE (V): "; SPC( 13);O0$; SPC( 5);O1$
9470  PRINT  SPC( 5);"MAXIMUM INTENSITY (W): "; SPC( 8);W0$; SPC( 5);W1$
9480  PRINT
9490  HTAB 25
9500  INPUT "ARE THESE PARAMETERS OK (Y/N)? ";KEY$
9510  IF KEY$ = "N" THEN 8860: REM  IF NO START OVER
9520  POKE DS% + 28,X0%: REM  WRITE CHO CONTROL BYTE
9530  POKE DS% + 29,X1%: REM  WRITE CH1 CONTROL BYTE
9540  RETURN
9550  REM
*************************************************************************
9560 TEMP$ =  STR$ (G0)
9570  GOSUB 8710
9580 G0$ = TEMP$
9590 TEMP$ =  STR$ (G1)
9600  GOSUB 8710
9610 G1$ = TEMP$
9620  RETURN
9630  REM
*************************************************************************
```

APPENDIX D
ASSEMBLY (6502) CONTROL PROGRAM

```
SOURCE   FILE: JMC1.0
SOURCE   FILE: JMC1.1
SOURCE   FILE: JMC1.2
0000:                1 ;TAB SETTINGS: 18,23,35
0000:                2 ;
0000:                3 ;***************     SYSTEM EQUATES     ****************
0000:                4 ;
0000:                5 ;**    JOHN BELL PARALLEL INTERFACE CARD - SLOT 2    **
0000:                6 ;************     U2 WIRED FOR IRQ'S      ***************
0000:                7 ;
0000:        C200    8 U1.DRB      EQU  $C200        ;DATA REGISTER B
0000:        C201    9 U1.DRA      EQU  $C201        ;DATA REGISTER A
0000:        C202   10 U1.DDRB     EQU  $C202        ;DATA DIRECTION REGISTER
B
0000:        C203   11 U1.DDRA     EQU  $C203        ;DATA DIRECTION REGISTER
A
0000:        C204   12 U1.T1C.L    EQU  $C204        ;T1 LOW ORDER COUNTER
0000:        C205   13 U1.T1C.H    EQU  $C205        ;T1 HIGH ORDER COUNTER
0000:        C206   14 U1.T1L.L    EQU  $C206        ;T1 LOW ORDER LATCH
0000:        C207   15 U1.T1L.H    EQU  $C207        ;T1 HIGH ORDER LATCH
0000:        C208   16 U1.T2C.L    EQU  $C208        ;T2 LOW ORDER COUNTER
0000:        C209   17 U1.T2C.H    EQU  $C209        ;T2 HIGH ORDER COUNTER
0000:        C20B   18 U1.ACR      EQU  $C20B        ;AUXILLARY CONTROL REG
0000:        C20C   19 U1.PCR      EQU  $C20C        ;PERIPHERAL CONTROL REG
0000:        C20D   20 U1.IFR      EQU  $C20D        ;INTERRUPT FLAG REG
0000:        C20E   21 U1.IER      EQU  $C20E        ;INTERRUPT ENABLE REG
0000:               22 ;
0000:        C280   23 U2.DRB      EQU  $C280        ;DATA REGISTER B
0000:        C281   24 U2.DRA      EQU  $C281        ;DATA REGISTER A
0000:        C282   25 U2.DDRB     EQU  $C282        ;DATA DIRECTION REGISTER
B
0000:        C283   26 U2.DDRA     EQU  $C283        ;DATA DIRECTION REGISTER
A
0000:        C284   27 U2.T1C.L    EQU  $C284        ;T1 LOW ORDER COUNTER
0000:        C285   28 U2.T1C.H    EQU  $C285        ;T1 HIGH ORDER COUNTER
0000:        C286   29 U2.T1L.L    EQU  $C286        ;T1 LOW ORDER LATCH
0000:        C287   30 U2.T1L.H    EQU  $C287        ;T1 HIGH ORDER LATCH
0000:        C288   31 U2.T2C.L    EQU  $C288        ;T2 LOW ORDER COUNTER
0000:        C289   32 U2.T2C.H    EQU  $C289        ;T2 HIGH ORDER COUNTER
0000:        C28B   33 U2.ACR      EQU  $C28B        ;AUXILLARY CONTROL REG
0000:        C28C   34 U2.PCR      EQU  $C28C        ;PERIPHERAL CONTROL REG
0000:        C28D   35 U2.IFR      EQU  $C28D        ;INTERRUPT FLAG REG
0000:        C28E   36 U2.IER      EQU  $C28E        ;INTERRUPT ENABLE REG
0000:               37 ;
0000:               38 ;****    APPLIED ENGINEERING D/A CARD - SLOT 3    *****
0000:               39 ;
0000:        C0B8   40 DA.CTRL1    EQU  $C0B8        ;D/A CONTROL BYTE (CH1/8)
0000:        C0B9   41 DA.CTRL2    EQU  $C0B9        ;D/A CONTROL BYTE (CH2/8)
0000:        C0BA   42 DA.CTRL3    EQU  $C0BA        ;D/A CONTROL BYTE (CH3/8)
0000:        C0BB   43 DA.CTRL4    EQU  $C0BB        ;D/A CONTROL BYTE (CH4/8)
0000:        C0BC   44 DA.CTRL5    EQU  $C0BC        ;D/A CONTROL BYTE (CH5/8)
0000:               45 ;
0000:               46 ;**   APPLIED ENGINEERING 12 BIT A/D CARD - SLOT 5   **
```

```
0000:                47 ;
0000:          C0D0  48 AD.LOW       EQU  $C0D0        ;LOW BYTE A/D DATA
0000:          C0D1  49 AD.HIGH      EQU  $C0D1        ;HIGH BYTE A/D DATA
0000:          C0D2  50 START.CONV   EQU  $C0D2        ;START CONVERSION ADDRESS
0000:          C0D3  51 AD.CTRL      EQU  $C0D3        ;A/D CONTROL BYTE
0000:                52 ;
0000:                53 ;***   APPLIED ENGINEERING TIMEMASTER II - SLOT 4   ***
0000:                54 ;
0000:          C0C0  55 DRA.CLK      EQU  $C0C0        ;DATA/DIRECTION REGISTER
A
0000:          C0C1  56 CRA.CLK      EQU  $C0C1        ;CONTROL REGISTER A
0000:          C0C2  57 DRB.CLK      EQU  $C0C2        ;DATA/DIRECTION REGISTER
B
0000:          C0C3  58 CRB.CLK      EQU  $C0C3        ;CONTROL REGISTER B
0000:                59 ;
0000:          B800  60 SCRATCH      EQU  $B800        ;GENERAL SCRATCH PAD AREA
0000:          B900  61 SCRATCH0     EQU  $B900        ;SCRATCH PAD AREA CH0
0000:          BA00  62 SCRATCH0.A   EQU  $BA00        ;CH0 AUXILLARY AREA
0000:          BB00  63 SCRATCH1     EQU  $BB00        ;SCRATCH PAD AREA CH1
0000:          BC00  64 SCRATCH1.A   EQU  $BC00        ;CH1 AUXILLARY AREA
0000:          BD00  65 RAT.INT      EQU  $BD00        ;RATIO INTEGER PART
0000:          BE00  66 RAT.FRAC     EQU  $BE00        ;RATIO FRACTIONAL PART
0000:                67 ;
0000:          FDED  68 COUT         EQU  $FDED        ;FIRMWARE ROUTINE "COUT"
0000:                69 ;
0000:                70 ;**************     DUMMY SECTOR     ******************
0000:                71 ;
0000:                72               DSECT
A500:          A500  73               ORG  $A500
A500:          0001  74 PHASE1.H     DS   1            ;PHASE 1 STARTING ADDRESS
A501:          0001  75 PHASE1.L     DS   1
A502:          0001  76 PHASE2.H     DS   1            ;PHASE 2 STARTING ADDRESS
A503:          0001  77 PHASE2.L     DS   1
A504:          0001  78 PHASE3.H     DS   1            ;PHASE 3 STARTING ADDRESS
A505:          0001  79 PHASE3.L     DS   1
A506:          0001  80 PHASE4.H     DS   1            ;PHASE 4 STARTING ADDRESS
A507:          0001  81 PHASE4.L     DS   1
A508:          0001  82 FLASH.F      DS   1            ;FLASH LAMP FREQUENCY
A509:          0001  83 INT.PERIOD   DS   1            ;INTEGRATION PERIOD
LENGTH
A50A:          0001  84 INT.NUM      DS   1            ;NO. MULTIPLE
INTEGRATIONS
A50B:          0001  85 INT.CNT      DS   1            ;INTEGRATION COUNT
A50C:          0001  86 SAMPLE.NUM   DS   1            ;NO. SAMPLES DESIRED
A50D:          0001  87 SAMPLE.CNT   DS   1            ;SAMPLE COUNT
A50E:          0001  88 MANUAL       DS   1            ;MANUAL CALIBRATION FLAG
A50F:          0001  89 CH0.PGAIN    DS   1            ;CH0 PROGRAMMABLE GAIN
A510:          0001  90 CH0.AD.GAIN  DS   1            ;CHANNEL 0 A/D GAIN
A511:          0001  91 CH1.PGAIN    DS   1            ;CH1 PROGRAMMABLE GAIN
A512:          0001  92 CH1.AD.GAIN  DS   1            ;CHANNEL 1 A/D GAIN
A513:          0001  93 AD.CH0.CTRL  DS   1            ;A/D CHANNEL 0 CONTROL
A514:          0001  94 AD.CH1.CTRL  DS   1            ;A/D CHANNEL 1 CONTROL
A515:          0001  95 CH0.INJ.H    DS   1            ;H BYTE INJECTION CURRENT
A516:          0001  96 CH0.INJ.L    DS   1            ;L BYTE INJECTION CURRENT
A517:          0001  97 CH1.INJ.H    DS   1            ;H BYTE INJECTION CURRENT
A518:          0001  98 CH1.INJ.L    DS   1            ;L BYTE INJECTION CURRENT
A519:          0001  99 MEAS.MODE    DS   1            ;MEASUREMENT ROUTINE
CHOICE
```

```
A51A:           0001  100 OFFSET.ADJ   DS   1          ;OFFSET ADJUSTMENT FLAG
A51B:           0001  101 DA.COPY1      DS   1          ;D/A CH1 CONTROL COPY
A51C:           0001  102 DA.COPY2      DS   1          ;D/A CH2 CONTROL COPY
A51D:           0001  103 DA.COPY3      DS   1          ;D/A CH3 CONTROL COPY
A51E:           0001  104 DA.COPY4      DS   1          ;D/A CH4 CONTROL COPY
A51F:           0001  105 DA.COPY5      DS   1          ;D/A CH5 CONTROL COPY
A520:           0001  106 OF.SW1        DS   1          ;OVERFLOW ERROR FLAGS
A521:           0001  107 OF.SW2        DS   1
A522:           0001  108 OF.SW3        DS   1          ;FLAG IS SET IF AN
A523:           0001  109 OF.SW4        DS   1          ;OVERFLOW WAS DETECTED
A524:           0001  110 OF.SW5        DS   1          ;DURING MEASUREMENT
A525:           0001  111 OF.SW6        DS   1          ;SWEEP
A526:           0001  112 OF.SW7        DS   1
A527:           0001  113 OF.SW8        DS   1
A528:           0001  114 OF.SW9        DS   1
A529:           0001  115 OF.SW10       DS   1
A52A:           0001  116 UF.SW1        DS   1          ;UNDERFLOW ERROR FLAGS
A52B:           0001  117 UF.SW2        DS   1
A52C:           0001  118 UF.SW3        DS   1          ;FLAG IS SET IF AN
A52D:           0001  119 UF.SW4        DS   1          ;UNDERFLOW WAS DETECTED
A52E:           0001  120 UF.SW5        DS   1          ;DURING MEASUREMENT
A52F:           0001  121 UF.SW6        DS   1          ;SWEEP
A530:           0001  122 UF.SW7        DS   1
A531:           0001  123 UF.SW8        DS   1
A532:           0001  124 UF.SW9        DS   1
A533:           0001  125 UF.SW10       DS   1
A534:           0001  126 SWEEP.CNT     DS   1          ;SWEEP COUNT
A535:           0001  127 SMPL.AVAIL    DS   1          ;SAMPLE AVAILABLE FLAG
A536:           0001  128 INJ.ACTIVE    DS   1          ;INJECTION CURRENT FLAG
A537:           0001  129 INJ.STATUS    DS   1          ;LEVEL STATUS INDICATOR
A538:           0001  130 MEAS.ACTIVE   DS   1          ;GENERAL MEASUREMENT FLAG
A539:           0001  131 DATA.ACTIVE   DS   1          ;DATA MEASUREMENT FLAG
A53A:           0001  132 SYNC.OK       DS   1          ;SYNCHRONIZATION FLAG
A53B:           0001  133 DATA.SETTLE   DS   1          ;DATA SETTLING COUNT
A53C:           0001  134 FLASH.H       DS   1          ;FLASHLAMP TIMER VALUES
A53D:           0001  135 FLASH.L       DS   1
A53E:           0001  136 INT.LOOP      DS   1          ;INTEGRATION LOOP
VARIABLE
A53F:           0001  137 MEAS.TEMP.H   DS   1          ;TEMPORARY MEAS.
VARIABLES
A540:           0001  138 MEAS.TEMP.L   DS   1
A541:           0001  139 REMAIN.H      DS   1          ;HIGH BYTE REMAINDER
A542:           0001  140 REMAIN.MH     DS   1
A543:           0001  141 REMAIN.M      DS   1
A544:           0001  142 REMAIN.ML     DS   1
A545:           0001  143 REMAIN.L      DS   1          ;LOW BYTE REMAINDER
A546:           0001  144 DIV.QUOT.H    DS   1          ;H BYTE DIVIDEND/QUOTIENT
A547:           0001  145 DIV.QUOT.MH   DS   1
A548:           0001  146 DIV.QUOT.M    DS   1
A549:           0001  147 DIV.QUOT.ML   DS   1
A54A:           0001  148 DIV.QUOT.L    DS   1          ;L BYTE DIVIDEND/QUOTIENT
A54B:           0001  149 DIVISOR.H     DS   1          ;HIGH BYTE DIVISOR
A54C:           0001  150 DIVISOR.MH    DS   1
A54D:           0001  151 DIVISOR.M     DS   1
A54E:           0001  152 DIVISOR.ML    DS   1
A54F:           0001  153 DIVISOR.L     DS   1          ;LOW BYTE DIVISOR
A550:           0001  154 DIV.TEMPX     DS   1          ;COPY OF X REGISTER
A551:           0001  155 DIV.TEMP.MH   DS   1          ;TEMPORARY VARIABLES
```

```
A552:        0001  156 DIV.TEMP.M  DS   1
A553:        0001  157 DIV.TEMP.ML DS   1
A554:        0001  158 DIV.TEMP.L  DS   1
A555:        0001  159 CH0.SUM.H   DS   1          ;CHANNEL 0
A556:        0001  160 CH0.SUM.M   DS   1          ;SUM LOCATIONS
A557:        0001  161 CH0.SUM.L   DS   1
A558:        0001  162 CH1.SUM.H   DS   1          ;CHANNEL 1
A559:        0001  163 CH1.SUM.M   DS   1          ;SUM LOCATIONS
A55A:        0001  164 CH1.SUM.L   DS   1
A55B:        0001  165 RAT.SUM.H   DS   1          ;RATIO SUM LOCATIONS
A55C:        0001  166 RAT.SUM.MH  DS   1
A55D:        0001  167 RAT.SUM.M   DS   1
A55E:        0001  168 RAT.SUM.ML  DS   1
A55F:        0001  169 RAT.SUM.L   DS   1
A560:        0001  170 INVALID     DS   1          ;SYSTEM ERROR FLAG
A561:        0001  171 DLY.TEMPX   DS   1          ;COPY OF X REGISTER
A562:        0001  172 DLY.TEMPY   DS   1          ;COPY OF Y REGISTER
A563:        0001  173 DELAY       DS   1          ;DELAY PARAMETER
A564:        0001  174 CLK.CNTRL.A DS   1          ;CLOCK CONTROL REGISTER A
COPY
A565:        0001  175 CLK.CNTRL.B DS   1          ;CLOCK CONTROL REGISTER B
COPY
A566:        0001  176 TIME.OUT    DS   1          ;CLOCK INTERVAL TIME UP
COUNT
A567:        0001  177 CLKSTART.H  DS   1          ;CLKSTART STARTING ADDRESS
A568:        0001  178 CLKSTART.L  DS   1
A569:        0001  179 CLKSTOP.H   DS   1          ;CLKSTOP STARTING ADDRESS
A56A:        0001  180 CLKSTOP.L   DS   1
A56B:        0001  181 ENABLE.H    DS   1          ;INTERRUPT ENABLE STARTING
ADDRESS
A56C:        0001  182 ENABLE.L    DS   1
A56D:        0001  183 DUMMY.FLASH DS   1          ;DUMMY FLASHES TO ACHIEVE
S.S.
0000:              184              DEND
0000:              185 ;
0000:              186 ;**********     INITIALIZATION ROUTINE     ************
----- NEXT OBJECT FILE NAME IS JMC1.0.OBJ0
A600:        A600  187              ORG  $A600
A600:78            188              SEI              ;DISABLE PROCESSOR IRQ'S
A601:A9 B5         189              LDA  #<ISR       ;INTERRUPT VECTOR POINTER
A603:8D FF 03      190              STA  $03FF       ;MSB
A606:A9 18         191              LDA  #>ISR
A608:8D FE 03      192              STA  $03FE       ;LSB
A60B:A9 A6         193              LDA  #<PHASE1    ;PHASE1 STARTING ADDRESS
A60D:8D 00 A5      194              STA  PHASE1.H
A610:A9 B4         195              LDA  #>PHASE1
A612:8D 01 A5      196              STA  PHASE1.L
A615:A9 A8         197              LDA  #<PHASE2    ;PHASE2 STARTING ADDRESS
A617:8D 02 A5      198              STA  PHASE2.H
A61A:A9 2D         199              LDA  #>PHASE2
A61C:8D 03 A5      200              STA  PHASE2.L
A61F:A9 AA         201              LDA  #<PHASE3    ;PHASE3 STARTING ADDRESS
A621:8D 04 A5      202              STA  PHASE3.H
A624:A9 00         203              LDA  #>PHASE3
A626:8D 05 A5      204              STA  PHASE3.L
A629:A9 AB         205              LDA  #<PHASE4    ;PHASE4 STARTING ADDRESS
A62B:8D 06 A5      206              STA  PHASE4.H
A62E:A9 61         207              LDA  #>PHASE4
```

```
A630:8D 07 A5      208             STA  PHASE4.L
A633:A9 B4         209             LDA  #<CLKSTART  ;CLKSTART STARTING ADDRESS
A635:8D 67 A5      210             STA  CLKSTART.H
A638:A9 E1         211             LDA  #>CLKSTART
A63A:8D 68 A5      212             STA  CLKSTART.L
A63D:A9 B4         213             LDA  #<CLKSTOP   ;CLKSTOP STARTING ADDRESS
A63F:8D 69 A5      214             STA  CLKSTOP.H
A642:A9 FA         215             LDA  #>CLKSTOP
A644:8D 6A A5      216             STA  CLKSTOP.L
A647:A9 B5         217             LDA  #<ENABLE    ;ENABLE STARTING ADDRESS
A649:8D 6B A5      218             STA  ENABLE.H
A64C:A9 16         219             LDA  #>ENABLE
A64E:8D 6C A5      220             STA  ENABLE.L
A651:20 58 A6      221             JSR  CONFIG       ;CONFIGURE JOHN BELL CARD
A654:20 89 A6      222             JSR  TMASTER     ;CONFIGURE TIMEMASTER II
A657:60            223             RTS               ;RETURN FROM BASIC CALL
A658:              224 ;
A658:              225 ;*****     JOHN BELL CARD MODE CONFIGURATIONS     *****
A658:              226 ;
A658:A9 FF         227 CONFIG      LDA  #%11111111   ;ALL PORTS OUTPUTS
A65A:8D 03 C2      228             STA  U1.DDRA      ;PROGRAMMABLE GAIN
A65D:8D 02 C2      229             STA  U1.DDRB      ;S/H MODE CONTROL
A660:8D 83 C2      230             STA  U2.DDRA      ;INTEGRATOR CONTROL
A663:8D 82 C2      231             STA  U2.DDRB      ;FLASHLAMP TRIGGER PULSES
A666:A9 40         232             LDA  #%01000000   ;T1 FOR SQUARE WAVES
A668:8D 8B C2      233             STA  U2.ACR       ;T2 FOR ONE SHOT
A66B:A9 00         234             LDA  #%00000000   ;U1 TIMERS NOT USED
A66D:8D 0B C2      235             STA  U1.ACR
A670:A9 00         236             LDA  #%00000000   ;CA1,CA2,CB1,CB2 CONTROL
A672:8D 0C C2      237             STA  U1.PCR       ;NOT USED - DON'T CARE
A675:8D 8C C2      238             STA  U2.PCR
A678:A9 7F         239             LDA  #%01111111   ;DISABLE ALL INTERRUPTS
A67A:8D 0E C2      240             STA  U1.IER
A67D:8D 8E C2      241             STA  U2.IER
A680:A9 7F         242             LDA  #%01111111   ;CLEAR THE IFR'S
A682:8D 0D C2      243             STA  U1.IFR
A685:8D 8D C2      244             STA  U2.IFR
A688:60            245             RTS
A689:              246 ;
A689:              247 ;************** TIMEMASTER II MODE CONFIGURATION
**********
A689:              248 ;
A689:A9 00         249 TMASTER     LDA  #$0          ;POINT AT DIRECTION
REGISTERS
A68B:8D C1 C0      250             STA  CRA.CLK
A68E:8D C3 C0      251             STA  CRB.CLK
A691:8D C0 C0      252             STA  DRA.CLK      ;PORT A ALL INPUT
A694:A9 FF         253             LDA  #$FF
A696:8D C2 C0      254             STA  DRB.CLK      ;PORT B ALL OUTPUT
A699:A9 04         255             LDA  #$04         ;DISABLE CLOCK INTERRUPTS
A69B:8D 64 A5      256             STA  CLK.CNTRL.A
A69E:8D 65 A5      257             STA  CLK.CNTRL.B
A6A1:AD 64 A5      258             LDA  CLK.CNTRL.A
A6A4:8D C1 C0      259             STA  CRA.CLK
A6A7:AD 65 A5      260             LDA  CLK.CNTRL.B
A6AA:8D C3 C0      261             STA  CRB.CLK
A6AD:AD C0 C0      262             LDA  DRA.CLK      ;CLEAR INTERRUPT FLAGS
A6B0:AD C2 C0      263             LDA  DRB.CLK
```

```
A6B3:60          264            RTS
A6B4:            265 ;
A6B4:            266 ;*************     PHASE 1 ROUTINE     ****************
A6B4:            267 ;
A6B4:20 C4 A6    268 PHASE1     JSR  TABLE        ;INITIALIZE TIMER TABLE
A6B7:20 B5 A7    269            JSR  TIMER        ;FLASHLAMP TIMER VALUE
A6BA:20 CB A7    270            JSR  SYS.INIT     ;SYSTEM INITIALIZATION
A6BD:20 02 A8    271            JSR  DA.CTRL      ;D/A CONTROL
A6C0:20 21 A8    272            JSR  INT.CAL      ;INTEGRATOR CONTROL
A6C3:60          273            RTS               ;RETURN FROM BASIC CALL
A6C4:            274 ;
A6C4:            275 ;**********     JUMP TABLE FOR TIMERS     *************
A6C4:            276 ;
A6C4:A9 F9       277 TABLE      LDA  #$F9         ;FLASH.H VALUE FOR 8 HZ
A6C6:8D 00 B8    278            STA  SCRATCH+$00
A6C9:A9 AE       279            LDA  #$AE         ;FLASH.L VALUE FOR 8 HZ
A6CB:8D 01 B8    280            STA  SCRATCH+$01
A6CE:A9 A6       281            LDA  #$A6         ;12 HZ
A6D0:8D 02 B8    282            STA  SCRATCH+$02
A6D3:A9 74       283            LDA  #$74
A6D5:8D 03 B8    284            STA  SCRATCH+$03
A6D8:A9 7C       285            LDA  #$7C         ;16 HZ
A6DA:8D 04 B8    286            STA  SCRATCH+$04
A6DD:A9 D6       287            LDA  #$D6
A6DF:8D 05 B8    288            STA  SCRATCH+$05
A6E2:A9 63       289            LDA  #$63         ;20 HZ
A6E4:8D 06 B8    290            STA  SCRATCH+$06
A6E7:A9 DE       291            LDA  #$DE
A6E9:8D 07 B8    292            STA  SCRATCH+$07
A6EC:A9 53       293            LDA  #$53         ;24HZ
A6EE:8D 08 B8    294            STA  SCRATCH+$08
A6F1:A9 39       295            LDA  #$39
A6F3:8D 09 B8    296            STA  SCRATCH+$09
A6F6:A9 47       297            LDA  #$47         ;28HZ
A6F8:8D 0A B8    298            STA  SCRATCH+$0A
A6FB:A9 55       299            LDA  #$55
A6FD:8D 0B B8    300            STA  SCRATCH+$0B
A700:A9 3E       301            LDA  #$3E         ;32 HZ
A702:8D 0C B8    302            STA  SCRATCH+$0C
A705:A9 6A       303            LDA  #$6A
A707:8D 0D B8    304            STA  SCRATCH+$0D
A70A:A9 37       305            LDA  #$37         ;36 HZ
A70C:8D 0E B8    306            STA  SCRATCH+$0E
A70F:A9 7B       307            LDA  #$7B
A711:8D 0F B8    308            STA  SCRATCH+$0F
A714:A9 31       309            LDA  #$31         ;40 HZ
A716:8D 10 B8    310            STA  SCRATCH+$10
A719:A9 EE       311            LDA  #$EE
A71B:8D 11 B8    312            STA  SCRATCH+$11
A71E:A9 2D       313            LDA  #$2D         ;44 HZ
A720:8D 12 B8    314            STA  SCRATCH+$12
A723:A9 64       315            LDA  #$64
A725:8D 13 B8    316            STA  SCRATCH+$13
A728:A9 29       317            LDA  #$29         ;48 HZ
A72A:8D 14 B8    318            STA  SCRATCH+$14
A72D:A9 9C       319            LDA  #$9C
A72F:8D 15 B8    320            STA  SCRATCH+$15
A732:A9 26       321            LDA  #$26         ;52 HZ
```

```
A734:8D 16 B8      322            STA  SCRATCH+$16
A737:A9 68         323            LDA  #$68
A739:8D 17 B8      324            STA  SCRATCH+$17
A73C:A9 23         325            LDA  #$23          ;56 HZ
A73E:8D 18 B8      326            STA  SCRATCH+$18
A741:A9 AA         327            LDA  #$AA
A743:8D 19 B8      328            STA  SCRATCH+$19
A746:A9 21         329            LDA  #$21          ;60 HZ
A748:8D 1A B8      330            STA  SCRATCH+$1A
A74B:A9 48         331            LDA  #$48
A74D:8D 1B B8      332            STA  SCRATCH+$1B
A750:A9 1F         333            LDA  #$1F          ;64 HZ
A752:8D 1C B8      334            STA  SCRATCH+$1C
A755:A9 35         335            LDA  #$35
A757:8D 1D B8      336            STA  SCRATCH+$1D
A75A:A9 1D         337            LDA  #$1D          ;68 HZ
A75C:8D 1E B8      338            STA  SCRATCH+$1E
A75F:A9 5E         339            LDA  #$5E
A761:8D 1F B8      340            STA  SCRATCH+$1F
A764:A9 16         341            LDA  #$16          ;72 HZ
A766:8D 20 B8      342            STA  SCRATCH+$20
A769:A9 6C         343            LDA  #$6C
A76B:8D 21 B8      344            STA  SCRATCH+$21
A76E:A9 1A         345            LDA  #$1A          ;76 HZ
A770:8D 22 B8      346            STA  SCRATCH+$22
A773:A9 47         347            LDA  #$47
A775:8D 23 B8      348            STA  SCRATCH+$23
A778:A9 18         349            LDA  #$18          ;80 HZ
A77A:8D 24 B8      350            STA  SCRATCH+$24
A77D:A9 F6         351            LDA  #$F6
A77F:8D 25 B8      352            STA  SCRATCH+$25
A782:A9 17         353            LDA  #$17          ;84 HZ
A784:8D 26 B8      354            STA  SCRATCH+$26
A787:A9 C5         355            LDA  #$C5
A789:8D 27 B8      356            STA  SCRATCH+$27
A78C:A9 16         357            LDA  #$16          ;88 HZ
A78E:8D 28 B8      358            STA  SCRATCH+$28
A791:A9 B1         359            LDA  #$B1
A793:8D 29 B8      360            STA  SCRATCH+$29
A796:A9 15         361            LDA  #$15          ;92 HZ
A798:8D 2A B8      362            STA  SCRATCH+$2A
A79B:A9 B5         363            LDA  #$B5
A79D:8D 2B B8      364            STA  SCRATCH+$2B
A7A0:A9 14         365            LDA  #$14          ;96 HZ
A7A2:8D 2C B8      366            STA  SCRATCH+$2C
A7A5:A9 CC         367            LDA  #$CC
A7A7:8D 2D B8      368            STA  SCRATCH+$2D
A7AA:A9 13         369            LDA  #$13          ;100 HZ
A7AC:8D 2E B8      370            STA  SCRATCH+$2E
A7AF:A9 F8         371            LDA  #$F8
A7B1:8D 2F B8      372            STA  SCRATCH+$2F
A7B4:60            373            RTS
A7B5:              374 ;
A7B5:              375 ;****    DETERMINATION OF FLASHLAMP TIMER VALUE    ****
A7B5:              376 ;
A7B5:AD 08 A5      377 TIMER      LDA  FLASH.F
A7B8:38            378            SEC                ;SUBTRACT 8 AND DIVIDE
A7B9:E9 08         379            SBC  #08           ;BY 2 TO PROPERLY
```

```
A7BB:4A          380             LSR             ;INDEX JUMP TABLE
A7BC:AA          381             TAX             ;TRANSFER FOR ADDRESSING
A7BD:BD 00 B8    382             LDA  SCRATCH,X
A7C0:8D 3C A5    383             STA  FLASH.H    ;HIGH BYTE
A7C3:E8          384             INX
A7C4:BD 00 B8    385             LDA  SCRATCH,X
A7C7:8D 3D A5    386             STA  FLASH.L    ;LOW BYTE
A7CA:60          387             RTS
A7CB:            388 ;
A7CB:            389 ;*******     SYSTEM INITIALIZATION ROUTINE     ********
A7CB:            390 ;
A7CB:A9 00       391 SYS.INIT    LDA  #$00       ;INITIALIZE D/A CHANNELS
A7CD:8D B8 C0    392             STA  DA.CTRL1
A7D0:A9 FF       393             LDA  #$FF
A7D2:8D B9 C0    394             STA  DA.CTRL2
A7D5:8D BA C0    395             STA  DA.CTRL3
A7D8:8D BB C0    396             STA  DA.CTRL4
A7DB:8D BC C0    397             STA  DA.CTRL5
A7DE:AD 3D A5    398             LDA  FLASH.L    ;LOAD TIMERS FOR
A7E1:8D 84 C2    399             STA  U2.T1C.L   ;FLASHLAMP TRIGGER
A7E4:AD 3C A5    400             LDA  FLASH.H
A7E7:8D 85 C2    401             STA  U2.T1C.H   ;INITIATES COUNTDOWN
A7EA:A9 88       402             LDA  #%10001000 ;PROGRAMMABLE GAINS = 2
A7EC:8D 01 C2    403             STA  U1.DRA
A7EF:A9 31       404             LDA  #%00110001 ;DISCHARGE INTEGRATORS
A7F1:8D 81 C2    405             STA  U2.DRA     ;PLACE S/H IN "TRACK"
MODE
A7F4:A9 00       406             LDA  #%00000000 ;TRIGGER LEVEL HIGH
A7F6:8D 80 C2    407             STA  U2.DRB
A7F9:A9 00       408             LDA  #00        ;INITIALIZE INJECTION
A7FB:8D 36 A5    409             STA  INJ.ACTIVE ;CURRENT AND MEASUREMENT
A7FE:8D 39 A5    410             STA  DATA.ACTIVE;FLAGS
A801:60          411             RTS
A802:            412 ;
A802:            413 ;************     D/A CONTROL ROUTINE     *************
A802:            414 ;
A802:AD 1B A5    415 DA.CTRL     LDA  DA.COPY1   ;FLASHLAMP REFERENCE
A805:8D B8 C0    416             STA  DA.CTRL1   ;VOLTAGE
A808:AD 1C A5    417             LDA  DA.COPY2   ;HV PHOTOMULTIPLIER CH0
A80B:8D B9 C0    418             STA  DA.CTRL2
A80E:AD 1D A5    419             LDA  DA.COPY3   ;HV PHOTOMULTIPLIER CH1
A811:8D BA C0    420             STA  DA.CTRL3
A814:AD 1E A5    421             LDA  DA.COPY4   ;HV PHOTOMULTIPLIER CH2
A817:8D BB C0    422             STA  DA.CTRL4
A81A:AD 1F A5    423             LDA  DA.COPY5   ;HV PHOTOMULTIPLIER CH3
A81D:8D BC C0    424             STA  DA.CTRL5
A820:60          425             RTS
A821:            426 ;
A821:            427 ;****     DETERMINATION OF INTEGRATION PERIOD     *****
A821:            428 ;
A821:A9 00       429 INT.CAL     LDA  #00
A823:AD 09 A5    430             LDA  INT.PERIOD ;SUBTRACT TWO FOR PROPER
A826:38          431             SEC             ;INDEXING
A827:E9 02       432             SBC  #02
A829:8D 3E A5    433             STA  INT.LOOP   ;INTEGRATOR TIMING BYTE
A82C:60          434             RTS
A82D:            435 ;
A82D:            436 ;*************     PHASE 2 ROUTINE     ****************
```

```
A82D:                437 ;
A82D:AD 0E A5        438 PHASE2      LDA  MANUAL       ;CHECK FOR MANUAL CALIB.
A830:F0 11   A843    439             BEQ  AUTO         ;NO
A832:C9 01           440             CMP  #01
A834:F0 09   A83F    441             BEQ  MAN          ;YES
A836:A9 80           442             LDA  #%10000000   ;ERRONEOUS CALL TO PHASE
2
A838:8D 60 A5        443             STA  INVALID      ;SYSTEM ERROR BYTE
A83B:20 7A B4        444             JSR  ERROR        ;SYSTEM ERROR ROUTINE
A83E:60              445             RTS               ;RETURN FROM BASIC CALL
A83F:20 58 A8        446 MAN         JSR  MAN.CAL      ;SET UP CONTROL BYTES
A842:60              447             RTS               ;RETURN FROM BASIC CALL
A843:20 7C A8        448 AUTO        JSR  AUTO.CAL0    ;CALIBRATE CHANNEL 0
A846:20 3E A9        449             JSR  AUTO.CAL1    ;CALIBRATE CHANNEL 1
A849:AD 0F A5        450             LDA  CH0.PGAIN    ;SET UP PROGRAMMABLE GAIN
A84C:0D 11 A5        451             ORA  CH1.PGAIN
A84F:8D 01 C2        452             STA  U1.DRA
A852:A9 00           453             LDA  #%00000000   ;TRIGGER LEVEL LOW
A854:8D 80 C2        454             STA  U2.DRB
A857:60              455             RTS               ;RETURN FROM BASIC CALL
A858:                456 ;
A858:                457 ;*****     MANUAL SYSTEM CALIBRATION ROUTINE     ******
A858:                458 ;
A858:AD 0F A5        459 MAN.CAL     LDA  CH0.PGAIN    ;SET UP PROGRAMMABLE GAIN
A85B:0D 11 A5        460             ORA  CH1.PGAIN
A85E:8D 01 C2        461             STA  U1.DRA
A861:AD 10 A5        462             LDA  CH0.AD.GAIN  ;SET UP CH0 A/D CONTROL
A864:2A              463             ROL               ;INFORMATION CONTAINED IN
A865:2A              464             ROL               ;LOW ORDER NIBBLE
A866:2A              465             ROL
A867:18              466             CLC               ;SET MULTIPLEXER CHANNEL
A868:2A              467             ROL
A869:29 71           468             AND  #%01110001
A86B:8D 13 A5        469             STA  AD.CH0.CTRL  ;A/D CH0 CONTROL BYTE
A86E:AD 12 A5        470             LDA  CH1.AD.GAIN  ;SET UP CH1 A/D CONTROL
A871:2A              471             ROL               ;INFORMATION CONTAINED IN
A872:2A              472             ROL               ;LOW ORDER NIBBLE
A873:2A              473             ROL
A874:38              474             SEC               ;SET MULTIPLEXER CHANNEL
A875:2A              475             ROL
A876:29 71           476             AND  #%01110001
A878:8D 14 A5        477             STA  AD.CH1.CTRL  ;A/D CH1 CONTROL BYTE
A87B:60              478             RTS
A87C:                479 ;
A87C:                480 ;****    AUTOMATIC GAIN CALIBRATION CH0 ROUTINE    ****
A87C:                481 ;
A87C:AD 0A A5        482 AUTO.CAL0   LDA  INT.NUM      ;MULT. INTEGRATION COUNT
A87F:8D 0B A5        483             STA  INT.CNT
A882:A9 00           484             LDA  #00          ;S/H DATA AVAILABLE
A884:8D 35 A5        485             STA  SMPL.AVAIL   ;FLAG INITIALLY ZERO
A887:A9 88           486             LDA  #%10001000   ;CH0 INITIAL GAIN = 2
A889:8D 01 C2        487             STA  U1.DRA
A88C:20 58 B4        488             JSR  OUT.SETTLE   ;OUTPUT MUST SETTLE
A88F:20 2D AE        489             JSR  PRE.MEAS     ;PRE-MEASUREMENT
A892:A9 10           490 RANGE.CAL0  LDA  #%00010000   ;CH0 INIT A/D RANGE = 5V
A894:8D 13 A5        491             STA  AD.CH0.CTRL
A897:8D D3 C0        492             STA  AD.CTRL      ;A/D CONTROL LOCATION
```

```
A89A:A9 31          493              LDA  #%00110001   ;PLACE S/H IN "TRACK"
MODE
A89C:8D 81 C2       494              STA  U2.DRA
A89F:AD 35 A5       495 WAIT1.CAL0   LDA  SMPL.AVAIL   ;WAIT FOR SAMPLE
AVAILABLE
A8A2:F0 FB   A89F   496              BEQ  WAIT1.CAL0
A8A4:20 6F B4       497              JSR  CONVERT      ;PERFORM A/D CONVERSION
A8A7:AD D1 C0       498              LDA  AD.HIGH
A8AA:29 0F          499              AND  #%00001111   ;KEEP ONLY DATA BITS
A8AC:C9 0F          500              CMP  #%00001111   ;CHECK FOR A/D "OVERFLOW"
A8AE:90 07   A8B7   501              BCC  CONT.CAL0    ;NO
A8B0:AD D0 C0       502              LDA  AD.LOW
A8B3:C9 E0          503              CMP  #%11100000
A8B5:B0 23   A8DA   504              BCS  PGAIN.FIX0   ;YES
A8B7:AD 13 A5       505 CONT.CAL0    LDA  AD.CH0.CTRL
A8BA:C9 70          506              CMP  #%01110000   ;CHECK IF AT MIN. RANGE
A8BC:F0 27   A8E5   507              BEQ  PGAIN.CAL0   ;YES
A8BE:18             508              CLC               ;NO, DECREASE A/D RANGE
A8BF:69 10          509              ADC  #%00010000
A8C1:8D 13 A5       510              STA  AD.CH0.CTRL
A8C4:8D D3 C0       511              STA  AD.CTRL
A8C7:A9 31          512              LDA  #%00110001   ;PLACE S/H IN "TRACK"
MODE
A8C9:8D 81 C2       513              STA  U2.DRA
A8CC:AD 0A A5       514              LDA  INT.NUM      ;RESET MULTIPLE
A8CF:8D 0B A5       515              STA  INT.CNT      ;INTEGRATION COUNT
A8D2:A9 00          516              LDA  #00          ;RESET SAMPLE AVAILABLE
A8D4:8D 35 A5       517              STA  SMPL.AVAIL   ;FLAG
A8D7:4C 9F A8       518              JMP  WAIT1.CAL0
A8DA:AD 01 C2       519 PGAIN.FIX0   LDA  U1.DRA       ;SAVE CH0 PROGRAMMABLE
A8DD:29 0F          520              AND  #%00001111   ;GAIN SETTING
A8DF:8D 0F A5       521              STA  CH0.PGAIN
A8E2:4C 2A A9       522              JMP  FINAL.CAL0   ;FINAL A/D CALIBRATION
A8E5:AD 01 C2       523 PGAIN.CAL0   LDA  U1.DRA
A8E8:C9 81          524              CMP  #%10000001   ;CHECK IF AT MAX. GAIN
A8EA:F0 28   A914   525              BEQ  EXIT.CAL0    ;YES
A8EC:A9 31          526              LDA  #%00110001   ;PLACE S/H IN "TRACK"
MODE
A8EE:8D 81 C2       527              STA  U2.DRA
A8F1:AD 01 C2       528              LDA  U1.DRA       ;INCREASE PROGRAMMABLE
GAIN
A8F4:29 0F          529              AND  #%00001111   ;SINCE OVERFLOW NOT YET
A8F6:4A             530              LSR               ;DETECTED
A8F7:18             531              CLC
A8F8:69 80          532              ADC  #%10000000   ;RESTORE CH1 MINIMUM GAIN
A8FA:8D 01 C2       533              STA  U1.DRA
A8FD:20 60 AE       534              JSR  POST.MEAS    ;POST-MEASUREMENT
A900:20 58 B4       535              JSR  OUT.SETTLE   ;OUTPUTS MUST SETTLE
A903:20 2D AE       536              JSR  PRE.MEAS     ;PRE-MEASUREMENT
A906:AD 0A A5       537              LDA  INT.NUM      ;RESET MULTIPLE
A909:8D 0B A5       538              STA  INT.CNT      ;INTEGRATION COUNT
A90C:A9 00          539              LDA  #00          ;RESET SAMPLE AVAILABLE
A90E:8D 35 A5       540              STA  SMPL.AVAIL   ;FLAG
A911:4C 92 A8       541              JMP  RANGE.CAL0
A914:AD 01 C2       542 EXIT.CAL0    LDA  U1.DRA       ;SAVE PROGRAMMABLE GAIN
A917:29 0F          543              AND  #%00001111   ;FOR INSPECTION WITHIN
A919:8D 0F A5       544              STA  CH0.PGAIN    ;BASIC ROUTINE
A91C:AD 13 A5       545              LDA  AD.CH0.CTRL
```

```
A91F:4A             546              LSR               ;SAVE A/D RANGE
A920:4A             547              LSR               ;FOR INSPECTION WITHIN
A921:4A             548              LSR               ;BASIC ROUTINE
A922:4A             549              LSR
A923:8D 10 A5       550              STA  CH0.AD.GAIN  ;SAVE A/D RANGE
A926:20 60 AE       551              JSR  POST.MEAS    ;POST-MEASUREMENT
A929:60             552              RTS
A92A:AD 13 A5       553 FINAL.CAL0   LDA  AD.CH0.CTRL  ;INCREASE A/D RANGE TO
A92D:38             554              SEC               ;NEXT HIGHEST RANGE
A92E:E9 10          555              SBC  #%00010000   ;SINCE OVERFLOW DETECTED
A930:8D 13 A5       556              STA  AD.CH0.CTRL
A933:4A             557              LSR               ;SAVE A/D RANGE
A934:4A             558              LSR               ;FOR INSPECTION WITHIN
A935:4A             559              LSR               ;BASIC ROUTINE
A936:4A             560              LSR
A937:8D 10 A5       561              STA  CH0.AD.GAIN
A93A:20 60 AE       562              JSR  POST.MEAS    ;POST-MEASUREMENT
A93D:60             563              RTS
A93E:               564 ;
A93E:               565 ;****    AUTOMATIC GAIN CALIBRATION CH1 ROUTINE    ****
A93E:               566 ;
A93E:AD 0A A5       567 AUTO.CAL1    LDA  INT.NUM      ;MULT. INTEGRATION COUNT
A941:8D 0B A5       568              STA  INT.CNT
A944:A9 00          569              LDA  #00          ;S/H DATA AVAILABLE
A946:8D 35 A5       570              STA  SMPL.AVAIL   ;FLAG INITIALLY ZERO
A949:A9 88          571              LDA  #%10001000   ;CH1 INITIAL GAIN = 2
A94B:8D 01 C2       572              STA  U1.DRA
A94E:20 58 B4       573              JSR  OUT.SETTLE   ;OUTPUT MUST SETTLE
A951:20 2D AE       574              JSR  PRE.MEAS     ;PRE-MEASUREMENT
A954:A9 11          575 RANGE.CAL1   LDA  #%00010001   ;CH1 INIT A/D RANGE = 5V
A956:8D 14 A5       576              STA  AD.CH1.CTRL
A959:8D D3 C0       577              STA  AD.CTRL      ;A/D CONTROL LOCATION
A95C:A9 31          578              LDA  #%00110001   ;PLACE S/H IN "TRACK"
MODE
A95E:8D 81 C2       579              STA  U2.DRA
A961:AD 35 A5       580 WAIT1.CAL1   LDA  SMPL.AVAIL   ;WAIT FOR SAMPLE
AVAILABLE
A964:F0 FB   A961   581              BEQ  WAIT1.CAL1
A966:20 6F B4       582              JSR  CONVERT      ;PERFORM A/D CONVERSION
A969:AD D1 C0       583              LDA  AD.HIGH
A96C:29 0F          584              AND  #%00001111   ;KEEP ONLY DATA BITS
A96E:C9 0F          585              CMP  #%00001111   ;CHECK FOR A/D "OVERFLOW"
A970:90 07   A979   586              BCC  CONT.CAL1    ;NO
A972:AD D0 C0       587              LDA  AD.LOW
A975:C9 E0          588              CMP  #%11100000
A977:B0 23   A99C   589              BCS  PGAIN.FIX1   ;YES
A979:AD 14 A5       590 CONT.CAL1    LDA  AD.CH1.CTRL
A97C:C9 71          591              CMP  #%01110001   ;CHECK IF AT MIN. RANGE
A97E:F0 27   A9A7   592              BEQ  PGAIN.CAL1   ;YES
A980:18             593              CLC               ;NO, DECREASE A/D RANGE
A981:69 10          594              ADC  #%00010000
A983:8D 14 A5       595              STA  AD.CH1.CTRL
A986:8D D3 C0       596              STA  AD.CTRL
A989:A9 31          597              LDA  #%00110001   ;PLACE S/H IN "TRACK"
MODE
A98B:8D 81 C2       598              STA  U2.DRA
A98E:AD 0A A5       599              LDA  INT.NUM      ;RESET MULTIPLE
A991:8D 0B A5       600              STA  INT.CNT      ;INTEGRATION COUNT
```

```
A994:A9 00        601             LDA  #00          ;RESET SAMPLE AVAILABLE
A996:8D 35 A5     602             STA  SMPL.AVAIL   ;FLAG
A999:4C 61 A9     603             JMP  WAIT1.CAL1
A99C:AD 01 C2     604 PGAIN.FIX1  LDA  U1.DRA       ;SAVE CH1 PROGRAMMABLE
A99F:29 F0        605             AND  #%11110000   ;GAIN SETTING
A9A1:8D 11 A5     606             STA  CH1.PGAIN
A9A4:4C EC A9     607             JMP  FINAL.CAL1   ;FINAL A/D CALIBRATION
A9A7:AD 01 C2     608 PGAIN.CAL1  LDA  U1.DRA
A9AA:C9 18        609             CMP  #%00011000   ;CHECK IF AT MAX. GAIN
A9AC:F0 28   A9D6 610             BEQ  EXIT.CAL1    ;YES
A9AE:A9 31        611             LDA  #%00110001   ;PLACE S/H IN "TRACK"
MODE
A9B0:8D 81 C2     612             STA  U2.DRA
A9B3:AD 01 C2     613             LDA  U1.DRA       ;INCREASE PROGRAMMABLE
GAIN
A9B6:29 F0        614             AND  #%11110000   ;SINCE OVERFLOW NOT YET
A9B8:4A           615             LSR
A9B9:18           616             CLC
A9BA:69 08        617             ADC  #%00001000   ;RESTORE CH0 MINIMUM GAIN
A9BC:8D 01 C2     618             STA  U1.DRA
A9BF:20 60 AE     619             JSR  POST.MEAS    ;POST-MEASUREMENT
A9C2:20 58 B4     620             JSR  OUT.SETTLE   ;OUTPUTS MUST SETTLE
A9C5:20 2D AE     621             JSR  PRE.MEAS     ;PRE-MEASUREMENT
A9C8:AD 0A A5     622             LDA  INT.NUM      ;RESET MULTIPLE
A9CB:8D 0B A5     623             STA  INT.CNT      ;INTEGRATION COUNT
A9CE:A9 00        624             LDA  #00          ;RESET SAMPLE AVAILABLE
A9D0:8D 35 A5     625             STA  SMPL.AVAIL   ;FLAG
A9D3:4C 54 A9     626             JMP  RANGE.CAL1
A9D6:AD 01 C2     627 EXIT.CAL1   LDA  U1.DRA       ;SAVE PROGRAMMABLE GAIN
A9D9:29 F0        628             AND  #%11110000   ;FOR INSPECTION WITHIN
A9DB:8D 11 A5     629             STA  CH1.PGAIN    ;BASIC ROUTINE
A9DE:AD 14 A5     630             LDA  AD.CH1.CTRL
A9E1:4A           631             LSR               ;SAVE A/D RANGE
A9E2:4A           632             LSR               ;FOR INSPECTION WITHIN
A9E3:4A           633             LSR               ;BASIC ROUTINE
A9E4:4A           634             LSR
A9E5:8D 12 A5     635             STA  CH1.AD.GAIN
A9E8:20 60 AE     636             JSR  POST.MEAS    ;POST-MEASUREMENT
A9EB:60           637             RTS
A9EC:AD 14 A5     638 FINAL.CAL1  LDA  AD.CH1.CTRL  ;INCREASE A/D RANGE TO
A9EF:38           639             SEC               ;NEXT HIGHEST RANGE
A9F0:E9 10        640             SBC  #%00010000   ;SINCE OVERFLOW DETECTED
A9F2:8D 14 A5     641             STA  AD.CH1.CTRL
A9F5:4A           642             LSR               ;SAVE A/D RANGE
A9F6:4A           643             LSR               ;FOR INSPECTION WITHIN
A9F7:4A           644             LSR               ;BASIC ROUTINE
A9F8:4A           645             LSR
A9F9:8D 12 A5     646             STA  CH1.AD.GAIN
A9FC:20 60 AE     647             JSR  POST.MEAS    ;POST-MEASUREMENT
A9FF:60           648             RTS
AA00:             649 ;
AA00:             650 ;*************      PHASE 3 ROUTINE      ***************
AA00:             651 ;
AA00:20 0F B0     652 PHASE3      JSR  INIT.SUMS    ;INITIALIZE SUM LOCATIONS
AA03:AD 36 A5     653             LDA  INJ.ACTIVE   ;CHECK FOR FLASH DURING
AA06:C9 01        654             CMP  #$01         ;INJECTION CURRENT MEAS.
AA08:D0 10   AA1A 655             BNE  FLASH.INJ
AA0A:20 2A AA     656             JSR  PRE.INJ      ;PRE INJECTION CURRENT
```

```
AA0D:20 4B AA      657              JSR  MEAS.INJ      ;INJECTION CURRENT MEAS.
AA10:20 BF AA      658              JSR  POST.INJ      ;POST INJECTION CURRENT
AA13:20 03 AB      659              JSR  AVG.INJ0      ;AVG CHANNEL 0 VALUE
AA16:20 32 AB      660              JSR  AVG.INJ1      ;AVG CHANNEL 1 VALUE
AA19:60            661              RTS                ;RETURN FROM BASIC CALL
AA1A:20 2D AE      662 FLASH.INJ    JSR  PRE.MEAS      ;PRE MEASUREMENT
AA1D:20 4B AA      663              JSR  MEAS.INJ      ;INJECTION CURRENT MEAS.
AA20:20 60 AE      664              JSR  POST.MEAS     ;POST MEASUREMENT
AA23:20 03 AB      665              JSR  AVG.INJ0      ;AVG CHANNEL 0 VALUE
AA26:20 32 AB      666              JSR  AVG.INJ1      ;AVG CHANNEL 1 VALUE
AA29:60            667              RTS                ;RETURN FROM BASIC CALL
AA2A:              668 ;
AA2A:              669 ;*******     PRE INJECTION CURRENT ROUTINE     ********
AA2A:              670 ;
AA2A:A9 00         671 PRE.INJ      LDA  #00           ;RESET SYNCHRONIZATION
FLAG
AA2C:8D 3A A5      672              STA  SYNC.OK       ;AND INJECTION CURRENT
AA2F:8D 36 A5      673              STA  INJ.ACTIVE    ;MEASUREMENT FLAG
AA32:8D 37 A5      674              STA  INJ.STATUS    ;LEVEL STATUS INDICATOR
AA35:A9 7F         675              LDA  #%01111111    ;CLEAR ANY INTERRUPTS
AA37:8D 8D C2      676              STA  U2.IFR
AA3A:A9 C0         677              LDA  #%11000000    ;ENABLE U2 T1 VIA
AA3C:8D 8E C2      678              STA  U2.IER        ;INTERRUPTS
AA3F:58            679              CLI                ;ENABLE PROCESSOR IRQ'S
AA40:AD 3A A5      680 SYNC.INJ     LDA  SYNC.OK       ;WAIT FOR PROPER
AA43:F0 FB   AA40  681              BEQ  SYNC.INJ      ;SYNCHRONIZATION
AA45:A9 01         682              LDA  #01           ;SET INJECTION CURRENT
AA47:8D 36 A5      683              STA  INJ.ACTIVE    ;MEASUREMENT FLAG
AA4A:60            684              RTS
AA4B:              685 ;
AA4B:              686 ;****    INJECTION CURRENT MEASUREMENT ROUTINE    *****
AA4B:              687 ;
AA4B:A9 64         688 MEAS.INJ     LDA  #100          ;NUMBER SAMPLES DESIRED
AA4D:8D 0D A5      689              STA  SAMPLE.CNT    ;TO BE AVERAGED
AA50:A0 00         690              LDY  #$00          ;ADDRESS INDEX
AA52:A9 31         691              LDA  #%00110001    ;PLACE S/H IN "TRACK"
MODE
AA54:8D 81 C2      692              STA  U2.DRA
AA57:AD 13 A5      693              LDA  AD.CH0.CTRL   ;SET UP A/D FOR CH0
AA5A:8D D3 C0      694              STA  AD.CTRL
AA5D:AD 0A A5      695              LDA  INT.NUM       ;MULT. INTEGRATION COUNT
AA60:8D 0B A5      696              STA  INT.CNT
AA63:A9 00         697              LDA  #00           ;RESET SAMPLE AVAILABLE
AA65:8D 35 A5      698              STA  SMPL.AVAIL    ;FLAG
AA68:AD 35 A5      699 WAIT.INJ     LDA  SMPL.AVAIL    ;WAIT FOR SAMPLE
AVAILABLE
AA6B:F0 FB   AA68  700              BEQ  WAIT.INJ
AA6D:20 6F B4      701              JSR  CONVERT       ;PERFORM A/D CONVERSION
AA70:AD D1 C0      702              LDA  AD.HIGH
AA73:29 0F         703              AND  #%00001111    ;KEEP ONLY DATA BITS
AA75:99 00 B9      704              STA  SCRATCH0,Y    ;HIGH BYTE CH0
AA78:AD D0 C0      705              LDA  AD.LOW
AA7B:99 01 B9      706              STA  SCRATCH0+1,Y  ;LOW BYTE CH0
AA7E:20 CB AA      707              JSR  SUM.CH0
AA81:AD 14 A5      708              LDA  AD.CH1.CTRL   ;SET UP A/D FOR CH1
AA84:8D D3 C0      709              STA  AD.CTRL
AA87:20 66 B4      710              JSR  MUX.SETTLE    ;A/D MUX MUST SETTLE
AA8A:20 6F B4      711              JSR  CONVERT       ;PERFORM A/D CONVERSION
```

```
AA8D:AD D1 C0      712              LDA  AD.HIGH
AA90:29 0F         713              AND  #%00001111    ;KEEP ONLY DATA BITS
AA92:99 00 BB      714              STA  SCRATCH1,Y    ;HIGH BYTE CH1
AA95:AD D0 C0      715              LDA  AD.LOW
AA98:99 01 BB      716              STA  SCRATCH1+1,Y  ;LOW BYTE CH1
AA9B:20 E7 AA      717              JSR  SUM.CH1
AA9E:C8            718              INY                ;UPDATE ADDRESS INDEX
AA9F:C8            719              INY
AAA0:AD 13 A5      720              LDA  AD.CH0.CTRL   ;SET UP A/D FOR CH0
AAA3:8D D3 C0      721              STA  AD.CTRL
AAA6:CE 0D A5      722              DEC  SAMPLE.CNT    ;DECREMENT SAMPLE COUNT
AAA9:F0 13   AABE  723              BEQ  FINISH.DK     ;CHECK FOR COMPLETION
AAAB:A9 31         724              LDA  #%00110001    ;PLACE S/H IN "TRACK"
MODE
AAAD:8D 81 C2      725              STA  U2.DRA
AAB0:AD 0A A5      726              LDA  INT.NUM       ;RESET MULTIPLE
AAB3:8D 0B A5      727              STA  INT.CNT       ;INTEGRATION COUNT
AAB6:A9 00         728              LDA  #00           ;RESET SAMPLE AVAILABLE
AAB8:8D 35 A5      729              STA  SMPL.AVAIL    ;FLAG
AABB:4C 68 AA      730              JMP  WAIT.INJ      ;CONTINUE MEASUREMENTS
AABE:60            731 FINISH.DK    RTS
AABF:              732 ;
AABF:              733 ;*******     POST INJECTION CURRENT ROUTINE    ********
AABF:              734 ;
AABF:78            735 POST.INJ     SEI                ;DISABLE PROCESSOR IRQ'S
AAC0:A9 00         736              LDA  #00           ;RESET INJECTION CURRENT
AAC2:8D 36 A5      737              STA  INJ.ACTIVE    ;MEASUREMENT FLAG
AAC5:A9 40         738              LDA  #%01000000    ;DISABLE U2 T1 VIA
AAC7:8D 8E C2      739              STA  U2.IER        ;INTERRUPTS
AACA:60            740              RTS
AACB:              741 ;
AACB:              742 ;*****     CHANNEL 0 DATA SUMMATION ROUTINE     *****
AACB:              743 ;
AACB:18            744 SUM.CH0      CLC                ;SUM TOGETHER WITH
AACC:AD 57 A5      745              LDA  CH0.SUM.L     ;PREVIOUS SAMPLES
AACF:79 01 B9      746              ADC  SCRATCH0+1,Y  ;LOW BYTE CH1 DATA
AAD2:8D 57 A5      747              STA  CH0.SUM.L
AAD5:AD 56 A5      748              LDA  CH0.SUM.M
AAD8:79 00 B9      749              ADC  SCRATCH0,Y    ;HIGH BYTE CH1 DATA
AADB:8D 56 A5      750              STA  CH0.SUM.M
AADE:AD 55 A5      751              LDA  CH0.SUM.H
AAE1:69 00         752              ADC  #$00          ;ALLOW FOR PROPAGATION
AAE3:8D 55 A5      753              STA  CH0.SUM.H
AAE6:60            754              RTS
AAE7:              755 ;
AAE7:              756 ;*****     CHANNEL 1 DATA SUMMATION ROUTINE     *****
AAE7:              757 ;
AAE7:18            758 SUM.CH1      CLC                ;SUM TOGETHER WITH
AAE8:AD 5A A5      759              LDA  CH1.SUM.L     ;PREVIOUS SAMPLES
AAEB:79 01 BB      760              ADC  SCRATCH1+1,Y  ;LOW BYTE CH1 DATA
AAEE:8D 5A A5      761              STA  CH1.SUM.L
AAF1:AD 59 A5      762              LDA  CH1.SUM.M
AAF4:79 00 BB      763              ADC  SCRATCH1,Y    ;HIGH BYTE CH1 DATA
AAF7:8D 59 A5      764              STA  CH1.SUM.M
AAFA:AD 58 A5      765              LDA  CH1.SUM.H
AAFD:69 00         766              ADC  #00           ;ALLOW FOR PROPAGATION
AAFF:8D 58 A5      767              STA  CH1.SUM.H
AB02:60            768              RTS
```

```
AB03:                 769 ;
AB03:                 770 ;*****    CHANNEL 0 INJECTION CURRENT AVERAGE
******
AB03:                 771 ;
AB03:AD 55 A5         772 AVG.INJ0    LDA  CH0.SUM.H     ;COMPUTE AVERAGE VALUE
AB06:8D 46 A5         773             STA  DIV.QUOT.H    ;FOR CHANNEL 0 DATA
AB09:AD 56 A5         774             LDA  CH0.SUM.M
AB0C:8D 48 A5         775             STA  DIV.QUOT.M    ;LOAD DIVIDEND LOCATIONS
AB0F:AD 57 A5         776             LDA  CH0.SUM.L     ;WITH SUM OF CH0 DATA
AB12:8D 4A A5         777             STA  DIV.QUOT.L
AB15:A9 00            778             LDA  #00           ;LOAD DIVISOR LOCATIONS
AB17:8D 4B A5         779             STA  DIVISOR.H     ;FOR TOTAL SAMPLE COUNT
AB1A:8D 4D A5         780             STA  DIVISOR.M     ;EQUAL TO 100
AB1D:A9 64            781             LDA  #100
AB1F:8D 4F A5         782             STA  DIVISOR.L
AB22:20 DA B2         783             JSR  DIVIDE.24
AB25:AD 4A A5         784             LDA  DIV.QUOT.L    ;RETRIEVE QUOTIENT AND
AB28:8D 16 A5         785             STA  CH0.INJ.L     ;SAVE AS CH0 INJECTION
AB2B:AD 48 A5         786             LDA  DIV.QUOT.M    ;CURRENT RESPONSE
AB2E:8D 15 A5         787             STA  CH0.INJ.H
AB31:60               788             RTS
AB32:                 789 ;
AB32:                 790 ;*****    CHANNEL 1 INJECTION CURRENT AVERAGE    ******
AB32:                 791 ;
AB32:AD 58 A5         792 AVG.INJ1    LDA  CH1.SUM.H     ;COMPUTE AVERAGE VALUE
AB35:8D 46 A5         793             STA  DIV.QUOT.H    ;FOR CHANNEL 1
AB38:AD 59 A5         794             LDA  CH1.SUM.M
AB3B:8D 48 A5         795             STA  DIV.QUOT.M    ;LOAD DIVIDEND LOCATIONS
AB3E:AD 5A A5         796             LDA  CH1.SUM.L     ;WITH SUM OF CH1 DATA
AB41:8D 4A A5         797             STA  DIV.QUOT.L
AB44:A9 00            798             LDA  #$00          ;LOAD DIVISOR LOCATIONS
AB46:8D 4B A5         799             STA  DIVISOR.H     ;FOR TOTAL SAMPLE COUNT
AB49:8D 4D A5         800             STA  DIVISOR.M     ;EQUAL TO 100
AB4C:A9 64            801             LDA  #100
AB4E:8D 4F A5         802             STA  DIVISOR.L
AB51:20 DA B2         803             JSR  DIVIDE.24
AB54:AD 4A A5         804             LDA  DIV.QUOT.L    ;RETRIEVE QUOTIENT AND
AB57:8D 18 A5         805             STA  CH1.INJ.L     ;SAVE AS CH1 INJECTION
AB5A:AD 48 A5         806             LDA  DIV.QUOT.M    ;CURRENT RESPONSE
AB5D:8D 17 A5         807             STA  CH1.INJ.H
AB60:60               808             RTS
AB61:                 809 ;
AB61:                 810             CHN  JMC1.1        ;CHAIN IN NEXT SOURCE
FILE
AB61:                   1 ;
AB61:                   2 ;***************     PHASE 4 ROUTINE     ***************
AB61:                   3 ;
AB61:AD 19 A5           4 PHASE4        LDA  MEAS.MODE     ;DETERMINE SELECTED MODE
AB64:C9 01              5               CMP  #01
AB66:F0 11    AB79      6               BEQ  CHOICE.1      ;SINGLE SWEEP
AB68:C9 02              7               CMP  #02
AB6A:F0 10    AB7C      8               BEQ  CHOICE.2      ;MULTIPLE SWEEP
AB6C:C9 03              9               CMP  #03
AB6E:F0 0F    AB7F     10               BEQ  CHOICE.3      ;DATA FILE
AB70:A9 40             11               LDA  #%01000000    ;ERRONEOUS CALL TO PHASE
4
AB72:8D 60 A5          12               STA  INVALID       ;SYSTEM ERROR BYTE
AB75:20 7A B4          13               JSR  ERROR         ;SYSTEM ERROR ROUTINE
```

```
AB78:60              14              RTS             ;RETURN FROM BASIC CALL
AB79:4C 82 AB        15 CHOICE.1     JMP  S.SWEEP
AB7C:4C 5B AC        16 CHOICE.2     JMP  M.SWEEP
AB7F:4C 71 AD        17 CHOICE.3     JMP  DATA.FILE
AB82:20 EE AD        18 S.SWEEP      JSR  INIT.SWEEP   ;INITIALIZE ERROR FLAGS
AB85:20 2D AE        19              JSR  PRE.MEAS     ;PRE-MEASUREMENT
AB88:A9 01           20              LDA  #01          ;FIRST SWEEP
AB8A:8D 34 A5        21              STA  SWEEP.CNT
AB8D:A0 00           22              LDY  #$00         ;ADRESS INDEX
AB8F:A9 31           23              LDA  #%00110001   ;PLACE S/H IN "TRACK"
MODE
AB91:8D 81 C2        24              STA  U2.DRA
AB94:AD 13 A5        25              LDA  AD.CH0.CTRL  ;SET UP A/D FOR CH0
AB97:8D D3 C0        26              STA  AD.CTRL
AB9A:AD 0A A5        27              LDA  INT.NUM      ;MULT. INTEGRATION COUNT
AB9D:8D 0B A5        28              STA  INT.CNT
ABA0:A9 00           29              LDA  #00          ;S/H DATA AVAILABLE
ABA2:8D 35 A5        30              STA  SMPL.AVAIL   ;FLAG INITIALLY ZERO
ABA5:AD 35 A5        31 WAIT.SS      LDA  SMPL.AVAIL   ;WAIT FOR SAMPLE
AVAILABLE
ABA8:F0 FB   ABA5    32              BEQ  WAIT.SS
ABAA:20 6F B4        33              JSR  CONVERT      ;PERFORM A/D CONVERSION
ABAD:AD D1 C0        34              LDA  AD.HIGH      ;RETRIEVE H BYTE RAW DATA
ABB0:29 0F           35              AND  #%00001111   ;KEEP ONLY DATA BITS
ABB2:8D 3F A5        36              STA  MEAS.TEMP.H
ABB5:AD D0 C0        37              LDA  AD.LOW       ;RETRIEVE L BYTE RAW DATA
ABB8:8D 40 A5        38              STA  MEAS.TEMP.L
ABBB:20 6F AE        39              JSR  OF.CHK.SS    ;CHECK FOR A/D OVERFLOW
ABBE:AD 40 A5        40              LDA  MEAS.TEMP.L
ABC1:38              41              SEC               ;SUBTRACT LOW ORDER BYTE
ABC2:ED 16 A5        42              SBC  CH0.INJ.L    ;INJECTION CURRENT
ABC5:99 01 B8        43              STA  SCRATCH+1,Y  ;L BYTE CH0 DATA
ABC8:AD 3F A5        44              LDA  MEAS.TEMP.H  ;SUBTRACT HIGH ORDER BYTE
ABCB:ED 15 A5        45              SBC  CH0.INJ.H    ;INJECTION CURRENT
ABCE:99 00 B8        46              STA  SCRATCH,Y    ;H BYTE CH0 DATA
ABD1:20 AB AE        47              JSR  UF.CHK.SS    ;CHECK FOR UNDERFLOW
ABD4:AD 1A A5        48              LDA  OFFSET.ADJ
ABD7:D0 03   ABDC    49              BNE  SKIP.Z.CH0   ;SKIP FOR OFFSET ROUTINE
ABD9:20 ED AE        50              JSR  ZERO.SS      ;CHECK FOR "ZERO" DATA
ABDC:C8              51 SKIP.Z.CH0   INY               ;UPDATE ADDRESS INDEX
ABDD:C8              52              INY
ABDE:AD 14 A5        53              LDA  AD.CH1.CTRL  ;SET UP A/D FOR CH1
ABE1:8D D3 C0        54              STA  AD.CTRL
ABE4:20 66 B4        55              JSR  MUX.SETTLE   ;A/D MUX MUST SETTLE
ABE7:20 6F B4        56              JSR  CONVERT      ;PERFORM A/D CONVERSION
ABEA:AD D1 C0        57              LDA  AD.HIGH      ;RETRIEVE H BYTE RAW DATA
ABED:29 0F           58              AND  #%00001111   ;KEEP ONLY DATA BITS
ABEF:8D 3F A5        59              STA  MEAS.TEMP.H
ABF2:AD D0 C0        60              LDA  AD.LOW       ;RETRIEVE L BYTE RAW DATA
ABF5:8D 40 A5        61              STA  MEAS.TEMP.L
ABF8:20 6F AE        62              JSR  OF.CHK.SS    ;CHECK FOR A/D OVERFLOW
ABFB:AD 40 A5        63              LDA  MEAS.TEMP.L
ABFE:38              64              SEC               ;SUBTRACT LOW ORDER BYTE
ABFF:ED 18 A5        65              SBC  CH1.INJ.L    ;INJECTION CURRENT
AC02:99 01 B8        66              STA  SCRATCH+1,Y  ;L BYTE CH1 DATA
AC05:AD 3F A5        67              LDA  MEAS.TEMP.H  ;SUBTRACT HIGH ORDER BYTE
AC08:ED 17 A5        68              SBC  CH1.INJ.H    ;INJECTION CURRENT
AC0B:99 00 B8        69              STA  SCRATCH,Y    ;H BYTE CH1 DATA
```

```
AC0E:20 AB AE       70              JSR  UF.CHK.SS     ;CHECK FOR UNDERFLOW
AC11:AD 1A A5       71              LDA  OFFSET.ADJ
AC14:D0 03   AC19   72              BNE  SKIP.Z.CH1    ;SKIP FOR OFFSET ROUTINE
AC16:20 ED AE       73              JSR  ZERO.SS       ;CHECK FOR "ZERO" DATA
AC19:C8             74 SKIP.Z.CH1   INY                ;UPDATE ADDRESS INDEX
AC1A:C8             75              INY
AC1B:AD 1A A5       76              LDA  OFFSET.ADJ
AC1E:D0 03   AC23   77              BNE  SKIP.RATIO    ;SKIP FOR OFFSET ROUTINE
AC20:20 33 B0       78              JSR  RATIO.SS      ;COMPUTE RATIO
AC23:C8             79 SKIP.RATIO   INY
AC24:C8             80              INY                ;UPDATE ADDRESS INDEX
AC25:C8             81              INY
AC26:C8             82              INY
AC27:EE 34 A5       83              INC  SWEEP.CNT     ;SWEEP COMPLETED
AC2A:AD 34 A5       84              LDA  SWEEP.CNT
AC2D:C9 0B          85              CMP  #11           ;CHECK FOR ALL 10 SWEEPS
AC2F:F0 19   AC4A   86              BEQ  FINISH.SS     ;YES
AC31:A9 31          87              LDA  #%00110001    ;PLACE S/H IN "TRACK"
MODE
AC33:8D 81 C2       88              STA  U2.DRA
AC36:AD 13 A5       89              LDA  AD.CH0.CTRL   ;SET UP A/D FOR CH0
AC39:8D D3 C0       90              STA  AD.CTRL
AC3C:AD 0A A5       91              LDA  INT.NUM       ;RESET MULTIPLE
AC3F:8D 0B A5       92              STA  INT.CNT       ;INTEGRATION COUNT
AC42:A9 00          93              LDA  #00           ;RESET SAMPLE AVAILABLE
AC44:8D 35 A5       94              STA  SMPL.AVAIL    ;FLAG
AC47:4C A5 AB       95              JMP  WAIT.SS       ;CONTINUE MEASUREMENTS
AC4A:20 60 AE       96 FINISH.SS    JSR  POST.MEAS     ;POST-MEASUREMENT
AC4D:20 97 B1       97              JSR  SWEEP.AVG     ;AVERAGE SWEEP VALUES
AC50:A9 31          98              LDA  #%00110001    ;PLACE S/H IN "TRACK"
MODE
AC52:8D 81 C2       99              STA  U2.DRA
AC55:A9 00         100              LDA  #%00000000    ;TRIGGER LEVEL LOW
AC57:8D 80 C2      101              STA  U2.DRB
AC5A:60            102              RTS                ;RETURN FROM BASIC CALL
AC5B:              103 ;
AC5B:20 EE AD      104 M.SWEEP      JSR  INIT.SWEEP    ;INITIALIZE ERROR FLAGS
AC5E:20 0F B0      105              JSR  INIT.SUMS     ;INITIALIZE SUM LOCATIONS
AC61:20 2D AE      106              JSR  PRE.MEAS      ;PRE-MEASUREMENT
AC64:A9 01         107              LDA  #01           ;FIRST SWEEP
AC66:8D 34 A5      108              STA  SWEEP.CNT
AC69:AD 0C A5      109              LDA  SAMPLE.NUM    ;SAMPLE COUNT PER SWEEP
AC6C:8D 0D A5      110              STA  SAMPLE.CNT
AC6F:A2 00         111              LDX  #$00          ;ADDRESS INDEX
AC71:A0 00         112              LDY  #$00          ;ADDRESS INDEX
AC73:A9 31         113              LDA  #%00110001    ;PLACE S/H IN "TRACK"
MODE
AC75:8D 81 C2      114              STA  U2.DRA
AC78:AD 13 A5      115              LDA  AD.CH0.CTRL   ;SET UP A/D FOR CH0
AC7B:8D D3 C0      116              STA  AD.CTRL
AC7E:AD 0A A5      117              LDA  INT.NUM       ;MULT. INTEGRATION COUNT
AC81:8D 0B A5      118              STA  INT.CNT
AC84:A9 00         119              LDA  #00           ;S/H DATA AVAILABLE
AC86:8D 35 A5      120              STA  SMPL.AVAIL    ;FLAG INITIALLY ZERO
AC89:AD 35 A5      121 WAIT.MS      LDA  SMPL.AVAIL    ;WAIT FOR SAMPLE
AVAILABLE
AC8C:F0 FB   AC89  122              BEQ  WAIT.MS
AC8E:20 6F B4      123              JSR  CONVERT       ;PERFORM A/D CONVERSION
```

```
AC91:AD D1 C0      124              LDA  AD.HIGH       ;RETRIEVE H BYTE RAW DATA
AC94:29 0F         125              AND  #%00001111    ;KEEP ONLY DATA BITS
AC96:8D 3F A5      126              STA  MEAS.TEMP.H
AC99:AD D0 C0      127              LDA  AD.LOW        ;RETRIEVE L BYTE RAW DATA
AC9C:8D 40 A5      128              STA  MEAS.TEMP.L
AC9F:20 83 AE      129              JSR  OF.CHK.CH0    ;CHECK FOR A/D OVERFLOW
ACA2:AD 40 A5      130              LDA  MEAS.TEMP.L
ACA5:38            131              SEC                ;SUBTRACT LOW ORDER BYTE
ACA6:ED 16 A5      132              SBC  CH0.INJ.L     ;INJECTION CURRENT
ACA9:99 01 B9      133              STA  SCRATCH0+1,Y  ;L BYTE CH0 DATA
ACAC:AD 3F A5      134              LDA  MEAS.TEMP.H   ;SUBTRACT HIGH ORDER BYTE
ACAF:ED 15 A5      135              SBC  CH0.INJ.H     ;INJECTION CURRENT
ACB2:99 00 B9      136              STA  SCRATCH0,Y    ;H BYTE CH0 DATA
ACB5:20 C1 AE      137              JSR  UF.CHK.CH0    ;CHECK FOR UNDERFLOW
ACB8:20 03 AF      138              JSR  ZERO.CH0      ;CHECK FOR "ZERO" DATA
ACBB:20 CB AA      139              JSR  SUM.CH0       ;ADD TO PREVIOUS CH0 DATA
ACBE:AD 14 A5      140              LDA  AD.CH1.CTRL   ;SET UP A/D FOR CH1
ACC1:8D D3 C0      141              STA  AD.CTRL
ACC4:20 66 B4      142              JSR  MUX.SETTLE    ;A/D MUX MUST SETTLE
ACC7:20 6F B4      143              JSR  CONVERT       ;PERFORM A/D CONVERSION
ACCA:AD D1 C0      144              LDA  AD.HIGH       ;RETRIEVE H BYTE RAW DATA
ACCD:29 0F         145              AND  #%00001111    ;KEEP ONLY DATA BITS
ACCF:8D 3F A5      146              STA  MEAS.TEMP.H
ACD2:AD D0 C0      147              LDA  AD.LOW        ;RETRIEVE L BYTE RAW DATA
ACD5:8D 40 A5      148              STA  MEAS.TEMP.L
ACD8:20 97 AE      149              JSR  OF.CHK.CH1    ;CHECK FOR A/D OVERFLOW
ACDB:AD 40 A5      150              LDA  MEAS.TEMP.L
ACDE:38            151              SEC                ;SUBTRACT LOW ORDER BYTE
ACDF:ED 18 A5      152              SBC  CH1.INJ.L     ;INJECTION CURRENT
ACE2:99 01 BB      153              STA  SCRATCH1+1,Y  ;L BYTE CH1 DATA
ACE5:AD 3F A5      154              LDA  MEAS.TEMP.H   ;SUBTRACT HIGH ORDER BYTE
ACE8:ED 17 A5      155              SBC  CH1.INJ.H     ;INJECTION CURRENT
ACEB:99 00 BB      156              STA  SCRATCH1,Y    ;H BYTE CH1 DATA
ACEE:20 D7 AE      157              JSR  UF.CHK.CH1    ;CHECK FOR UNDERFLOW
ACF1:20 19 AF      158              JSR  ZERO.CH1      ;CHECK FOR "ZERO" DATA
ACF4:20 E7 AA      159              JSR  SUM.CH1       ;ADD TO PREVIOUS CH1 DATA
ACF7:20 77 B0      160              JSR  RATIO.MS      ;COMPUTE RATIO
ACFA:20 BB B0      161              JSR  SUM.RATIO     ;ADD TO PREVIOUS RATIOS
ACFD:C8            162              INY                ;UPDATE ADDRESS INDEX
ACFE:C8            163              INY
ACFF:AD 13 A5      164              LDA  AD.CH0.CTRL   ;SET UP FOR A/D CH0.CTRL
AD02:8D D3 C0      165              STA  AD.CTRL
AD05:CE 0D A5      166              DEC  SAMPLE.CNT    ;DECREMENT SAMPLE COUNT
AD08:F0 13   AD1D  167              BEQ  COMP.MS       ;CHECK FOR END OF SWEEP
AD0A:A9 31         168              LDA  #%00110001    ;NO, PLACE S/H IN "TRACK"
AD0C:8D 81 C2      169              STA  U2.DRA        ;MODE
AD0F:AD 0A A5      170              LDA  INT.NUM       ;RESET MULTIPLE
AD12:8D 0B A5      171              STA  INT.CNT       ;INTEGRATION COUNT
AD15:A9 00         172              LDA  #00           ;RESET SAMPLE AVAILABLE
AD17:8D 35 A5      173              STA  SMPL.AVAIL    ;FLAG
AD1A:4C 89 AC      174              JMP  WAIT.MS       ;CONTINUE SAME SWEEP
AD1D:A9 00         175 COMP.MS      LDA  #00           ;DISABLE ACTIVE
AD1F:8D 39 A5      176              STA  DATA.ACTIVE   ;DATA MEASUREMENTS
AD22:20 E9 B0      177              JSR  AVG.CH0       ;COMPUTE CH0 DATA AVG
AD25:E8            178              INX                ;UPDATE ADDRESS INDEX
AD26:E8            179              INX
AD27:20 19 B1      180              JSR  AVG.CH1       ;COMPUTE CH1 DATA AVG
AD2A:E8            181              INX                ;UPDATE ADDRESS INDEX
```

```
AD2B:E8              182              INX
AD2C:20 49 B1        183              JSR  AVG.RATIO     ;COMPUTE SWEEP AVG RATIO
AD2F:E8              184              INX
AD30:E8              185              INX                ;UPDATE ADDRESS INDEX
AD31:E8              186              INX
AD32:E8              187              INX
AD33:EE 34 A5        188              INC  SWEEP.CNT     ;SWEEP COMPLETED
AD36:AD 34 A5        189              LDA  SWEEP.CNT
AD39:C9 0B           190              CMP  #11           ;CHECK FOR ALL 10 SWEEPS
AD3B:F0 23   AD60    191              BEQ  FINISH.MS     ;YES
AD3D:20 0F B0        192              JSR  INIT.SUMS     ;INITIALIZE SUM LOCATIONS
AD40:AD 0C A5        193              LDA  SAMPLE.NUM    ;RESET SAMPLE COUNT
AD43:8D 0D A5        194              STA  SAMPLE.CNT
AD46:A0 00           195              LDY  #$00          ;RESET ADDRESS INDEX
AD48:A9 31           196              LDA  #%00110001    ;PLACE S/H IN "TRACK"
MODE
AD4A:8D 81 C2        197              STA  U2.DRA
AD4D:AD 0A A5        198              LDA  INT.NUM       ;RESET MULTIPLE
AD50:8D 0B A5        199              STA  INT.CNT       ;INTEGRATION COUNT
AD53:A9 00           200              LDA  #00           ;RESET SAMPLE AVAILABLE
AD55:8D 35 A5        201              STA  SMPL.AVAIL    ;FLAG
AD58:A9 01           202              LDA  #01           ;ENABLE ACTIVE
AD5A:8D 39 A5        203              STA  DATA.ACTIVE   ;DATA MEASUREMENTS
AD5D:4C 89 AC        204              JMP  WAIT.MS       ;CONTINUE MEASUREMENTS
AD60:20 60 AE        205 FINISH.MS    JSR  POST.MEAS     ;POST-MEASUREMENT
AD63:20 97 B1        206              JSR  SWEEP.AVG     ;AVERAGE SWEEP VALUES
AD66:A9 31           207              LDA  #%00110001    ;PLACE S/H IN "TRACK"
MODE
AD68:8D 81 C2        208              STA  U2.DRA
AD6B:A9 00           209              LDA  #%00000000    ;TRIGGER LEVEL LOW
AD6D:8D 80 C2        210              STA  U2.DRB
AD70:60              211              RTS                ;RETURN FROM BASIC CALL
AD71:                212 ;
AD71:20 2D AE        213 DATA.FILE    JSR  PRE.MEAS      ;PRE-MEASUREMENT
AD74:A9 C8           214              LDA  #200          ;TOTAL SAMPLE COUNT
AD76:8D 0D A5        215              STA  SAMPLE.CNT
AD79:A0 00           216              LDY  #$00          ;ADDRESS INDEX
AD7B:A9 31           217              LDA  #%00110001    ;PLACE S/H IN "TRACK"
MODE
AD7D:8D 81 C2        218              STA  U2.DRA
AD80:AD 13 A5        219              LDA  AD.CH0.CTRL   ;SET UP A/D FOR CH0
AD83:8D D3 C0        220              STA  AD.CTRL
AD86:AD 0A A5        221              LDA  INT.NUM       ;MULT. INTEGRATION COUNT
AD89:8D 0B A5        222              STA  INT.CNT
AD8C:A9 00           223              LDA  #00           ;S/H DATA AVAILABLE
AD8E:8D 35 A5        224              STA  SMPL.AVAIL    ;FLAG INITIALLY ZERO
AD91:AD 35 A5        225 WAIT.DF      LDA  SMPL.AVAIL    ;WAIT FOR SAMPLE
AVAILABLE
AD94:F0 FB   AD91    226              BEQ  WAIT.DF
AD96:20 6F B4        227              JSR  CONVERT       ;PERFORM A/D CONVERSION
AD99:AD D1 C0        228              LDA  AD.HIGH
AD9C:29 0F           229              AND  #%00001111    ;KEEP ONLY DATA BITS
AD9E:99 00 B9        230              STA  SCRATCH0,Y    ;HIGH BYTE CH0
ADA1:AD D0 C0        231              LDA  AD.LOW
ADA4:99 00 BA        232              STA  SCRATCH0.A,Y  ;LOW BYTE CH0
ADA7:AD 14 A5        233              LDA  AD.CH1.CTRL   ;SET UP A/D FOR CH1
ADAA:8D D3 C0        234              STA  AD.CTRL
ADAD:20 66 B4        235              JSR  MUX.SETTLE    ;A/D MUX MUST SETTLE
```

```
ADB0:20 6F B4      236             JSR  CONVERT       ;PERFORM A/D CONVERSION
ADB3:AD D1 C0      237             LDA  AD.HIGH
ADB6:29 0F         238             AND  #%00001111   ;KEEP ONLY DATA BITS
ADB8:99 00 BB      239             STA  SCRATCH1,Y   ;HIGH BYTE CH1
ADBB:AD D0 C0      240             LDA  AD.LOW
ADBE:99 00 BC      241             STA  SCRATCH1.A,Y  ;LOW BYTE CH1
ADC1:C8            242             INY               ;UPDATE ADDRESS INDEX
ADC2:AD 13 A5      243             LDA  AD.CH0.CTRL  ;SET UP A/D FOR CH0
ADC5:8D D3 C0      244             STA  AD.CTRL
ADC8:CE 0D A5      245             DEC  SAMPLE.CNT   ;DECREMENT SAMPLE COUNT
ADCB:F0 13   ADE0  246             BEQ  FINISH.DF    ;CHECK FOR 200 SAMPLES
ADCD:A9 31         247             LDA  #%00110001   ;NO, PLACE S/H IN "TRACK"
ADCF:8D 81 C2      248             STA  U2.DRA       ;MODE
ADD2:AD 0A A5      249             LDA  INT.NUM      ;RESET MULTIPLE
ADD5:8D 0B A5      250             STA  INT.CNT      ;INTEGRATION COUNT
ADD8:A9 00         251             LDA  #00          ;RESET SAMPLE AVAILABLE
ADDA:8D 35 A5      252             STA  SMPL.AVAIL   ;FLAG
ADDD:4C 91 AD      253             JMP  WAIT.DF
ADE0:20 60 AE      254 FINISH.DF   JSR  POST.MEAS    ;YES, POST-MEASUREMENT
ADE3:A9 31         255             LDA  #%00110001   ;PLACE S/H IN "TRACK"
MODE
ADE5:8D 81 C2      256             STA  U2.DRA
ADE8:A9 00         257             LDA  #%00000000   ;TRIGGER LEVEL LOW
ADEA:8D 80 C2      258             STA  U2.DRB
ADED:60            259             RTS               ;RETURN FROM BASIC CALL
ADEE:              260 ;
ADEE:              261 ;*******    DATA ERROR FLAG INITIALIZATION     ********
ADEE:              262 ;
ADEE:A9 00         263 INIT.SWEEP  LDA  #00          ;INITIALIZE OVERFLOW
ADF0:8D 20 A5      264             STA  OF.SW1       ;ERROR FLAGS
ADF3:8D 21 A5      265             STA  OF.SW2
ADF6:8D 22 A5      266             STA  OF.SW3
ADF9:8D 23 A5      267             STA  OF.SW4
ADFC:8D 24 A5      268             STA  OF.SW5
ADFF:8D 25 A5      269             STA  OF.SW6
AE02:8D 26 A5      270             STA  OF.SW7
AE05:8D 27 A5      271             STA  OF.SW8
AE08:8D 28 A5      272             STA  OF.SW9
AE0B:8D 29 A5      273             STA  OF.SW10
AE0E:8D 2A A5      274             STA  UF.SW1       ;INITIALIZE UNDERFLOW
AE11:8D 2B A5      275             STA  UF.SW2       ;ERROR FLAGS
AE14:8D 2C A5      276             STA  UF.SW3
AE17:8D 2D A5      277             STA  UF.SW4
AE1A:8D 2E A5      278             STA  UF.SW5
AE1D:8D 2F A5      279             STA  UF.SW6
AE20:8D 30 A5      280             STA  UF.SW7
AE23:8D 31 A5      281             STA  UF.SW8
AE26:8D 32 A5      282             STA  UF.SW9
AE29:8D 33 A5      283             STA  UF.SW10
AE2C:60            284             RTS
AE2D:              285 ;
AE2D:              286 ;***********     PRE-MEASUREMENT ROUTINE     **********
AE2D:              287 ;
AE2D:A9 00         288 PRE.MEAS    LDA  #00          ;RESET SYNCHRONIZATION
FLAG
AE2F:8D 3A A5      289             STA  SYNC.OK      ;AND DATA MEASUREMENT
FLAG
AE32:8D 39 A5      290             STA  DATA.ACTIVE
```

```
AE35:A9 01        291             LDA  #01          ;BEGIN MEASUREMENT PERIOD
AE37:8D 38 A5     292             STA  MEAS.ACTIVE
AE3A:AD 6D A5     293             LDA  DUMMY.FLASH  ;DUMMY FLASHES TO ALLOW
AE3D:8D 3B A5     294             STA  DATA.SETTLE  ;DATA TO REACH S.S.
AE40:A9 7F        295             LDA  #%01111111   ;CLEAR ANY INTERRUPTS
AE42:8D 8D C2     296             STA  U2.IFR
AE45:A9 C0        297             LDA  #%11000000   ;ENABLE U2 T1 VIA
AE47:8D 8E C2     298             STA  U2.IER       ;INTERRUPTS
AE4A:58           299             CLI               ;ENABLE PROCESSOR IRQ'S
AE4B:AD 3A A5     300 SYNC.MEAS   LDA  SYNC.OK      ;WAIT FOR PROPER
AE4E:F0 FB   AE4B 301             BEQ  SYNC.MEAS    ;SYNCHRONIZATION
AE50:A9 00        302             LDA  #00          ;RESET SYNCHRONIZATION
FLAG
AE52:8D 3A A5     303             STA  SYNC.OK
AE55:CE 3B A5     304             DEC  DATA.SETTLE
AE58:D0 F1   AE4B 305             BNE  SYNC.MEAS    ;CHECK TRANSIENT PERIOD
AE5A:A9 01        306             LDA  #01          ;FINISHED, SET ACTIVE
DATA
AE5C:8D 39 A5     307             STA  DATA.ACTIVE  ;MEASUREMENT FLAG
AE5F:60           308             RTS
AE60:             309 ;
AE60:             310 ;***********     POST-MEASUREMENT ROUTINE    **********
AE60:             311 ;
AE60:78           312 POST.MEAS   SEI               ;DISABLE PROCESSOR IRQ'S
AE61:A9 40        313             LDA  #%01000000   ;DISABLE U2 T1 VIA
AE63:8D 8E C2     314             STA  U2.IER       ;INTERRUPTS
AE66:A9 00        315             LDA  #00          ;RESET MEASUREMENT
AE68:8D 38 A5     316             STA  MEAS.ACTIVE  ;FLAGS
AE6B:8D 39 A5     317             STA  DATA.ACTIVE
AE6E:60           318             RTS
AE6F:             319 ;
AE6F:             320 ;*****     SS DATA OVERFLOW CHECKING ROUTINE     *****
AE6F:             321 ;
AE6F:AD 3F A5     322 OF.CHK.SS   LDA  MEAS.TEMP.H
AE72:C9 0F        323             CMP  #$0F         ;CHECK FOR MAX VALUE
AE74:F0 01   AE77 324             BEQ  CONT.CHK.SS
AE76:60           325             RTS               ;NO
AE77:AD 40 A5     326 CONT.CHK.SS LDA  MEAS.TEMP.L  ;YES
AE7A:C9 FF        327             CMP  #$FF         ;CHECK FOR MAX VALUE
AE7C:F0 01   AE7F 328             BEQ  OVER.SS
AE7E:60           329             RTS               ;NO
AE7F:20 2F AF     330 OVER.SS     JSR  OVERFLOW     ;YES, SET ERROR FLAG
AE82:60           331             RTS
AE83:             332 ;
AE83:             333 ;*****     MS CH0 OVERFLOW CHECKING ROUTINE     *****
AE83:             334 ;
AE83:AD 3F A5     335 OF.CHK.CH0  LDA  MEAS.TEMP.H
AE86:C9 0F        336             CMP  #$0F         ;CHECK FOR MAX VALUE
AE88:F0 01   AE8B 337             BEQ  CONT.CHK.0
AE8A:60           338             RTS               ;NO
AE8B:AD 40 A5     339 CONT.CHK.0  LDA  MEAS.TEMP.L  ;YES
AE8E:C9 FF        340             CMP  #$FF         ;CHECK FOR MAX VALUE
AE90:F0 01   AE93 341             BEQ  OVER.CH0
AE92:60           342             RTS               ;NO
AE93:20 2F AF     343 OVER.CH0    JSR  OVERFLOW     ;YES, SET ERROR FLAG
AE96:60           344             RTS
AE97:             345 ;
AE97:             346 ;*****     MS CH1 OVERFLOW CHECKING ROUTINE     *****
```

```
AE97:                 347 ;
AE97:AD 3F A5         348 OF.CHK.CH1  LDA  MEAS.TEMP.H
AE9A:C9 0F            349             CMP  #$0F          ;CHECK FOR MAX VALUE
AE9C:F0 01    AE9F    350             BEQ  CONT.CHK.1
AE9E:60               351             RTS                ;NO
AE9F:AD 40 A5         352 CONT.CHK.1  LDA  MEAS.TEMP.L   ;YES
AEA2:C9 FF            353             CMP  #$FF          ;CHECK FOR MAX VALUE
AEA4:F0 01    AEA7    354             BEQ  OVER.CH1
AEA6:60               355             RTS                ;NO
AEA7:20 2F AF         356 OVER.CH1    JSR  OVERFLOW      ;YES, SET ERROR FLAG
AEAA:60               357             RTS
AEAB:                 358 ;
AEAB:                 359 ;*****     SS DATA UNDERFLOW CHECKING ROUTINE     *****
AEAB:                 360 ;
AEAB:B9 00 B8         361 UF.CHK.SS   LDA  SCRATCH,Y     ;LOAD HIGH BYTE DATA
AEAE:C9 10            362             CMP  #$10
AEB0:B0 01    AEB3    363             BCS  UNDER.SS      ;CHECK FOR UNDERFLOW
AEB2:60               364             RTS                ;NO
AEB3:A9 00            365 UNDER.SS    LDA  #$00          ;YES, SUBSTITUTE
UNDERFLOW
AEB5:99 00 B8         366             STA  SCRATCH,Y     ;DATA WITH A VALUE OF 1
AEB8:A9 01            367             LDA  #$01
AEBA:99 01 B8         368             STA  SCRATCH+1,Y
AEBD:20 9F AF         369             JSR  UNDERFLOW     ;SET ERROR FLAG
AEC0:60               370             RTS
AEC1:                 371 ;
AEC1:                 372 ;****     MS CH0 DATA UNDERFLOW CHECKING ROUTINE     ****
AEC1:                 373 ;
AEC1:B9 00 B9         374 UF.CHK.CH0  LDA  SCRATCH0,Y    ;LOAD HIGH BYTE DATA
AEC4:C9 10            375             CMP  #$10
AEC6:B0 01    AEC9    376             BCS  UNDER.CH0     ;CHECK FOR UNDERFLOW
AEC8:60               377             RTS                ;NO
AEC9:A9 00            378 UNDER.CH0   LDA  #$00          ;YES, SUBSTITUTE
UNDERFLOW
AECB:99 00 B9         379             STA  SCRATCH0,Y    ;DATA WITH A VALUE OF 1
AECE:A9 01            380             LDA  #$01
AED0:99 01 B9         381             STA  SCRATCH0+1,Y
AED3:20 9F AF         382             JSR  UNDERFLOW     ;SET ERROR FLAG
AED6:60               383             RTS
AED7:                 384 ;
AED7:                 385 ;****     MS CH1 DATA UNDERFLOW CHECKING ROUTINE     ****
AED7:                 386 ;
AED7:B9 00 BB         387 UF.CHK.CH1  LDA  SCRATCH1,Y    ;LOAD HIGH BYTE DATA
AEDA:C9 10            388             CMP  #$10
AEDC:B0 01    AEDF    389             BCS  UNDER.CH1     ;CHECK FOR UNDERFLOW
AEDE:60               390             RTS                ;NO
AEDF:A9 00            391 UNDER.CH1   LDA  #$00          ;YES, SUBSTITUTE
UNDERFLOW
AEE1:99 00 BB         392             STA  SCRATCH1,Y    ;DATA WITH A VALUE OF 1
AEE4:A9 01            393             LDA  #$01
AEE6:99 01 BB         394             STA  SCRATCH1+1,Y
AEE9:20 9F AF         395             JSR  UNDERFLOW     ;SET ERROR FLAG
AEEC:60               396             RTS
AEED:                 397 ;
AEED:                 398 ;******    SS ZERO CHECKING ROUTINE      *****
AEED:                 399 ;
AEED:B9 00 B8         400 ZERO.SS     LDA  SCRATCH,Y
AEF0:C9 00            401             CMP  #$00          ;CHECK FOR ZERO VALUE
```

```
AEF2:F0 01   AEF5  402              BEQ  CONT.Z.SS
AEF4:60            403              RTS              ;NO
AEF5:B9 01 B8      404 CONT.Z.SS    LDA  SCRATCH+1,Y ;YES
AEF8:C9 00         405              CMP  #$00        ;CHECK FOR ZERO VALUE
AEFA:F0 01   AEFD  406              BEQ  SUBST.SS
AEFC:60            407              RTS              ;NO
AEFD:A9 01         408 SUBST.SS     LDA  #01         ;YES SUBSTITUTE A
AEFF:99 01 B8      409              STA  SCRATCH+1,Y ;VALUE OF ONE
AF02:60            410              RTS
AF03:              411 ;
AF03:              412 ;******    MS CH0 ZERO CHECKING ROUTINE     *****
AF03:              413 ;
AF03:B9 00 B9      414 ZERO.CH0     LDA  SCRATCH0,Y
AF06:C9 00         415              CMP  #$00        ;CHECK FOR ZERO VALUE
AF08:F0 01   AF0B  416              BEQ  CONT.Z.CH0
AF0A:60            417              RTS              ;NO
AF0B:B9 01 B9      418 CONT.Z.CH0   LDA  SCRATCH0+1,Y ;YES
AF0E:C9 00         419              CMP  #$00        ;CHECK FOR ZERO VALUE
AF10:F0 01   AF13  420              BEQ  SUBST.CH0
AF12:60            421              RTS              ;NO
AF13:A9 01         422 SUBST.CH0    LDA  #01         ;YES SUBSTITUTE A
AF15:99 01 B9      423              STA  SCRATCH0+1,Y ;VALUE OF ONE
AF18:60            424              RTS
AF19:              425 ;
AF19:              426 ;******    MS CH1 ZERO CHECKING ROUTINE     *****
AF19:              427 ;
AF19:B9 00 BB      428 ZERO.CH1     LDA  SCRATCH1,Y
AF1C:C9 00         429              CMP  #$00        ;CHECK FOR ZERO VALUE
AF1E:F0 01   AF21  430              BEQ  CONT.Z.CH1
AF20:60            431              RTS              ;NO
AF21:B9 01 BB      432 CONT.Z.CH1   LDA  SCRATCH1+1,Y ;YES
AF24:C9 00         433              CMP  #$00        ;CHECK FOR ZERO VALUE
AF26:F0 01   AF29  434              BEQ  SUBST.CH1
AF28:60            435              RTS              ;NO
AF29:A9 01         436 SUBST.CH1    LDA  #01         ;YES SUBSTITUTE A
AF2B:99 01 BB      437              STA  SCRATCH1+1,Y ;VALUE OF ONE
AF2E:60            438              RTS
AF2F:              439 ;
AF2F:              440 ;*******     OVERFLOW ERROR FLAG ROUTINE     ******
AF2F:              441 ;
AF2F:AD 34 A5      442 OVERFLOW     LDA  SWEEP.CNT   ;DETERMINE SWEEP
AF32:C9 01         443              CMP  #01         ;IN WHICH OVERFLOW
AF34:F0 2D   AF63  444              BEQ  OF.ERR.SW1  ;ERROR OCCURED
AF36:C9 02         445              CMP  #02
AF38:F0 2F   AF69  446              BEQ  OF.ERR.SW2
AF3A:C9 03         447              CMP  #03
AF3C:F0 31   AF6F  448              BEQ  OF.ERR.SW3
AF3E:C9 04         449              CMP  #04
AF40:F0 33   AF75  450              BEQ  OF.ERR.SW4
AF42:C9 05         451              CMP  #05
AF44:F0 35   AF7B  452              BEQ  OF.ERR.SW5
AF46:C9 06         453              CMP  #06
AF48:F0 37   AF81  454              BEQ  OF.ERR.SW6
AF4A:C9 07         455              CMP  #07
AF4C:F0 39   AF87  456              BEQ  OF.ERR.SW7
AF4E:C9 08         457              CMP  #08
AF50:F0 3B   AF8D  458              BEQ  OF.ERR.SW8
AF52:C9 09         459              CMP  #09
```

```
AF54:F0 3D   AF93  460              BEQ  OF.ERR.SW9
AF56:C9 0A         461              CMP  #10
AF58:F0 3F   AF99  462              BEQ  OF.ERR.SW10
AF5A:A9 20         463              LDA  #%00100000   ;INVALID SWEEP NUMBER
AF5C:8D 60 A5      464              STA  INVALID      ;SYSTEM ERROR BYE
AF5F:20 7A B4      465              JSR  ERROR        ;SYSTEM ERROR ROUTINE
AF62:60            466              RTS
AF63:A9 01         467 OF.ERR.SW1   LDA  #01
AF65:8D 20 A5      468              STA  OF.SW1
AF68:60            469              RTS
AF69:A9 01         470 OF.ERR.SW2   LDA  #01          ;SET ERROR FLAG
AF6B:8D 21 A5      471              STA  OF.SW2       ;ASSOCIATED WITH SWEEP
AF6E:60            472              RTS               ;NUMBER
AF6F:A9 01         473 OF.ERR.SW3   LDA  #01
AF71:8D 22 A5      474              STA  OF.SW3
AF74:60            475              RTS
AF75:A9 01         476 OF.ERR.SW4   LDA  #01
AF77:8D 23 A5      477              STA  OF.SW4
AF7A:60            478              RTS
AF7B:A9 01         479 OF.ERR.SW5   LDA  #01
AF7D:8D 24 A5      480              STA  OF.SW5
AF80:60            481              RTS
AF81:A9 01         482 OF.ERR.SW6   LDA  #01
AF83:8D 25 A5      483              STA  OF.SW6
AF86:60            484              RTS
AF87:A9 01         485 OF.ERR.SW7   LDA  #01
AF89:8D 26 A5      486              STA  OF.SW7
AF8C:60            487              RTS
AF8D:A9 01         488 OF.ERR.SW8   LDA  #01
AF8F:8D 27 A5      489              STA  OF.SW8
AF92:60            490              RTS
AF93:A9 01         491 OF.ERR.SW9   LDA  #01
AF95:8D 28 A5      492              STA  OF.SW9
AF98:60            493              RTS
AF99:A9 01         494 OF.ERR.SW10  LDA  #01
AF9B:8D 29 A5      495              STA  OF.SW10
AF9E:60            496              RTS
AF9F:              497 ;
AF9F:              498 ;*******     UNDERFLOW ERROR FLAG ROUTINE     ******
AF9F:              499 ;
AF9F:AD 34 A5      500 UNDERFLOW    LDA  SWEEP.CNT    ;DETERMINE SWEEP
AFA2:C9 01         501              CMP  #01          ;IN WHICH UNDERFLOW
AFA4:F0 2D   AFD3  502              BEQ  UF.ERR.SW1   ;ERROR OCCURED
AFA6:C9 02         503              CMP  #02
AFA8:F0 2F   AFD9  504              BEQ  UF.ERR.SW2
AFAA:C9 03         505              CMP  #03
AFAC:F0 31   AFDF  506              BEQ  UF.ERR.SW3
AFAE:C9 04         507              CMP  #04
AFB0:F0 33   AFE5  508              BEQ  UF.ERR.SW4
AFB2:C9 05         509              CMP  #05
AFB4:F0 35   AFEB  510              BEQ  UF.ERR.SW5
AFB6:C9 06         511              CMP  #06
AFB8:F0 37   AFF1  512              BEQ  UF.ERR.SW6
AFBA:C9 07         513              CMP  #07
AFBC:F0 39   AFF7  514              BEQ  UF.ERR.SW7
AFBE:C9 08         515              CMP  #08
AFC0:F0 3B   AFFD  516              BEQ  UF.ERR.SW8
AFC2:C9 09         517              CMP  #09
```

```
AFC4:F0 3D   B003  518              BEQ  UF.ERR.SW9
AFC6:C9 0A         519              CMP  #10
AFC8:F0 3F   B009  520              BEQ  UF.ERR.SW10
AFCA:A9 20         521              LDA  #%00100000   ;INVALID SWEEP NUMBER
AFCC:8D 60 A5      522              STA  INVALID      ;SYSTEM ERROR BYTE
AFCF:20 7A B4      523              JSR  ERROR        ;SYSTEM ERROR ROUTINE
AFD2:60            524              RTS
AFD3:A9 01         525 UF.ERR.SW1   LDA  #01          ;SET ERROR FLAG
AFD5:8D 2A A5      526              STA  UF.SW1       ;ASSOCIATED WITH SWEEP
AFD8:60            527              RTS               ;NUMBER
AFD9:A9 01         528 UF.ERR.SW2   LDA  #01
AFDB:8D 2B A5      529              STA  UF.SW2
AFDE:60            530              RTS
AFDF:A9 01         531 UF.ERR.SW3   LDA  #01
AFE1:8D 2C A5      532              STA  UF.SW3
AFE4:60            533              RTS
AFE5:A9 01         534 UF.ERR.SW4   LDA  #01
AFE7:8D 2D A5      535              STA  UF.SW4
AFEA:60            536              RTS
AFEB:A9 01         537 UF.ERR.SW5   LDA  #01
AFED:8D 2E A5      538              STA  UF.SW5
AFF0:60            539              RTS
AFF1:A9 01         540 UF.ERR.SW6   LDA  #01
AFF3:8D 2F A5      541              STA  UF.SW6
AFF6:60            542              RTS
AFF7:A9 01         543 UF.ERR.SW7   LDA  #01
AFF9:8D 30 A5      544              STA  UF.SW7
AFFC:60            545              RTS
AFFD:A9 01         546 UF.ERR.SW8   LDA  #01
AFFF:8D 31 A5      547              STA  UF.SW8
B002:60            548              RTS
B003:A9 01         549 UF.ERR.SW9   LDA  #01
B005:8D 32 A5      550              STA  UF.SW9
B008:60            551              RTS
B009:A9 01         552 UF.ERR.SW10  LDA  #01
B00B:8D 33 A5      553              STA  UF.SW10
B00E:60            554              RTS
B00F:              555 ;
B00F:              556              CHN  JMC1.2       ;CHAIN IN NEXT SOURCE
FILE
B00F:                1 ;
B00F:                2 ;*********     SYSTEM SUM INITIALIZATIONS     *********
B00F:                3 ;
B00F:A9 00           4 INIT.SUMS      LDA  #$00         ;INITIALIZE ALL SUM
B011:8D 55 A5        5                STA  CH0.SUM.H    ;LOCATIONS TO ZERO
B014:8D 56 A5        6                STA  CH0.SUM.M    ;VALUES
B017:8D 57 A5        7                STA  CH0.SUM.L
B01A:8D 58 A5        8                STA  CH1.SUM.H
B01D:8D 59 A5        9                STA  CH1.SUM.M
B020:8D 5A A5       10                STA  CH1.SUM.L
B023:8D 5B A5       11                STA  RAT.SUM.H
B026:8D 5C A5       12                STA  RAT.SUM.MH
B029:8D 5D A5       13                STA  RAT.SUM.M
B02C:8D 5E A5       14                STA  RAT.SUM.ML
B02F:8D 5F A5       15                STA  RAT.SUM.L
B032:60             16                RTS
B033:               17 ;
B033:               18 ;*****     SINGLE SWEEP RATIO COMPUTATION     *****
```

```
B033:                   19 ;
B033:B9 FC B7           20 RATIO.SS     LDA  SCRATCH-4,Y  ;LOAD DIVIDEND LOCATIONS
B036:8D 47 A5           21              STA  DIV.QUOT.MH  ;WITH CH0 CORRECTED DATA
B039:B9 FD B7           22              LDA  SCRATCH-3,Y
B03C:8D 48 A5           23              STA  DIV.QUOT.M
B03F:A9 00              24              LDA  #$00
B041:8D 49 A5           25              STA  DIV.QUOT.ML
B044:8D 4A A5           26              STA  DIV.QUOT.L
B047:A9 00              27              LDA  #$00         ;LOAD DIVISOR LOCATIONS
B049:8D 4C A5           28              STA  DIVISOR.MH   ;WITH CH1 CORRECTED DATA
B04C:8D 4D A5           29              STA  DIVISOR.M
B04F:B9 FE B7           30              LDA  SCRATCH-2,Y
B052:8D 4E A5           31              STA  DIVISOR.ML
B055:B9 FF B7           32              LDA  SCRATCH-1,Y
B058:8D 4F A5           33              STA  DIVISOR.L
B05B:20 30 B3           34              JSR  DIVIDE.32
B05E:AD 47 A5           35              LDA  DIV.QUOT.MH  ;RETRIEVE QUOTIENT AS
B061:99 00 B8           36              STA  SCRATCH,Y    ;INTEGER PART OF RATIO
B064:AD 48 A5           37              LDA  DIV.QUOT.M
B067:99 01 B8           38              STA  SCRATCH+1,Y
B06A:AD 49 A5           39              LDA  DIV.QUOT.ML  ;RETRIEVE QUOTIENT AS
B06D:99 02 B8           40              STA  SCRATCH+2,Y  ;FRACTIONAL PART OF RATIO
B070:AD 4A A5           41              LDA  DIV.QUOT.L
B073:99 03 B8           42              STA  SCRATCH+3,Y
B076:60                 43              RTS
B077:                   44 ;
B077:                   45 ;*****     MULTIPLE SWEEP RATIO COMPUTATION     *****
B077:                   46 ;
B077:B9 00 B9           47 RATIO.MS     LDA  SCRATCH0,Y   ;LOAD DIVIDEND LOCATIONS
B07A:8D 47 A5           48              STA  DIV.QUOT.MH  ;WITH CH0 CORRECTED DATA
B07D:B9 01 B9           49              LDA  SCRATCH0+1,Y
B080:8D 48 A5           50              STA  DIV.QUOT.M
B083:A9 00              51              LDA  #$00
B085:8D 49 A5           52              STA  DIV.QUOT.ML
B088:8D 4A A5           53              STA  DIV.QUOT.L
B08B:A9 00              54              LDA  #$00         ;LOAD DIVISOR LOCATIONS
B08D:8D 4C A5           55              STA  DIVISOR.MH   ;WITH CH1 CORRECTED DATA
B090:8D 4D A5           56              STA  DIVISOR.M
B093:B9 00 BB           57              LDA  SCRATCH1,Y
B096:8D 4E A5           58              STA  DIVISOR.ML
B099:B9 01 BB           59              LDA  SCRATCH1+1,Y
B09C:8D 4F A5           60              STA  DIVISOR.L
B09F:20 30 B3           61              JSR  DIVIDE.32
B0A2:AD 47 A5           62              LDA  DIV.QUOT.MH  ;RETRIEVE QUOTIENT AS
B0A5:99 00 BD           63              STA  RAT.INT,Y    ;INTEGER PART OF RATIO
B0A8:AD 48 A5           64              LDA  DIV.QUOT.M
B0AB:99 01 BD           65              STA  RAT.INT+1,Y
B0AE:AD 49 A5           66              LDA  DIV.QUOT.ML  ;RETRIEVE QUOTIENT AS
B0B1:99 00 BE           67              STA  RAT.FRAC,Y   ;FRACTIONAL PART OF RATIO
B0B4:AD 4A A5           68              LDA  DIV.QUOT.L
B0B7:99 01 BE           69              STA  RAT.FRAC+1,Y
B0BA:60                 70              RTS
B0BB:                   71 ;
B0BB:                   72 ;**********     RATIO SUMMATION ROUTINE     ********
B0BB:                   73 ;
B0BB:18                 74 SUM.RATIO    CLC               ;SUM TOGETHER WITH
B0BC:AD 5F A5           75              LDA  RAT.SUM.L    ;PREVIOUS RATIOS
B0BF:79 01 BE           76              ADC  RAT.FRAC+1,Y ;L BYTE FRACTIONAL PART
```

```
B0C2:8D 5F A5      77             STA  RAT.SUM.L
B0C5:AD 5E A5      78             LDA  RAT.SUM.ML
B0C8:79 00 BE      79             ADC  RAT.FRAC,Y  ;H BYTE FRACTIONAL PART
B0CB:8D 5E A5      80             STA  RAT.SUM.ML
B0CE:AD 5D A5      81             LDA  RAT.SUM.M
B0D1:79 01 BD      82             ADC  RAT.INT+1,Y ;L BYTE INTEGER PART
B0D4:8D 5D A5      83             STA  RAT.SUM.M
B0D7:AD 5C A5      84             LDA  RAT.SUM.MH
B0DA:79 00 BD      85             ADC  RAT.INT,Y   ;H BYTE INTEGER PART
B0DD:8D 5C A5      86             STA  RAT.SUM.MH
B0E0:AD 5B A5      87             LDA  RAT.SUM.H
B0E3:69 00         88             ADC  #00         ;ALLOW FOR PROPAGATION
B0E5:8D 5B A5      89             STA  RAT.SUM.H
B0E8:60            90             RTS
B0E9:              91 ;
B0E9:              92 ;******     CHANNEL 0 DATA SWEEP COMPUTATION     ******
B0E9:              93 ;
B0E9:AD 55 A5      94 AVG.CH0     LDA  CH0.SUM.H   ;COMPUTE AVERAGE VALUE
B0EC:8D 46 A5      95             STA  DIV.QUOT.H  ;FOR CHANNEL 0 DATA
B0EF:AD 56 A5      96             LDA  CH0.SUM.M
B0F2:8D 48 A5      97             STA  DIV.QUOT.M  ;LOAD DIVIDEND LOCATIONS
B0F5:AD 57 A5      98             LDA  CH0.SUM.L   ;WITH SUM OF CH0 DATA
B0F8:8D 4A A5      99             STA  DIV.QUOT.L
B0FB:A9 00        100             LDA  #$00        ;LOAD DIVIDEND LOCATIONS
B0FD:8D 4B A5     101             STA  DIVISOR.H   ;WITH TOTAL SAMPLE COUNT
B100:8D 4D A5     102             STA  DIVISOR.M
B103:AD 0C A5     103             LDA  SAMPLE.NUM
B106:8D 4F A5     104             STA  DIVISOR.L
B109:20 DA B2     105             JSR  DIVIDE.24
B10C:AD 48 A5     106             LDA  DIV.QUOT.M  ;RETRIEVE QUOTIENT TERMS
B10F:9D 00 B8     107             STA  SCRATCH,X   ;CORRESPONDING TO AVG
B112:AD 4A A5     108             LDA  DIV.QUOT.L  ;VALUE
B115:9D 01 B8     109             STA  SCRATCH+1,X
B118:60           110             RTS
B119:             111 ;
B119:             112 ;******     CHANNEL 1 DATA SWEEP COMPUTATION     ******
B119:             113 ;
B119:AD 58 A5     114 AVG.CH1     LDA  CH1.SUM.H   ;COMPUTE AVERAGE VALUE
B11C:8D 46 A5     115             STA  DIV.QUOT.H  ;FOR CHANNEL 1 DATA
B11F:AD 59 A5     116             LDA  CH1.SUM.M
B122:8D 48 A5     117             STA  DIV.QUOT.M  ;LOAD DIVIDEND LOCATIONS
B125:AD 5A A5     118             LDA  CH1.SUM.L   ;WITH SUM OF CH1 DATA
B128:8D 4A A5     119             STA  DIV.QUOT.L
B12B:A9 00        120             LDA  #$00        ;LOAD DIVISOR LOCATIONS
B12D:8D 4B A5     121             STA  DIVISOR.H   ;WITH TOTAL SAMPLE COUNT
B130:8D 4D A5     122             STA  DIVISOR.M
B133:AD 0C A5     123             LDA  SAMPLE.NUM
B136:8D 4F A5     124             STA  DIVISOR.L
B139:20 DA B2     125             JSR  DIVIDE.24
B13C:AD 48 A5     126             LDA  DIV.QUOT.M  ;RETRIEVE QUOTIENT TERMS
B13F:9D 00 B8     127             STA  SCRATCH,X   ;CORRESPONDING TO AVG
B142:AD 4A A5     128             LDA  DIV.QUOT.L  ;VALUE
B145:9D 01 B8     129             STA  SCRATCH+1,X
B148:60           130             RTS
B149:             131 ;
B149:             132 ;*****    AVERAGE RATIO SWEEP COMPUTATION     *****
B149:             133 ;
B149:AD 5B A5     134 AVG.RATIO   LDA  RAT.SUM.H   ;COMPUTE AVERAGE VALUE
```

```
B14C:8D 46 A5      135              STA  DIV.QUOT.H   ;FOR CH0/CH1 RATIO
B14F:AD 5C A5      136              LDA  RAT.SUM.MH
B152:8D 47 A5      137              STA  DIV.QUOT.MH
B155:AD 5D A5      138              LDA  RAT.SUM.M    ;LOAD DIVIDEND LOCATIONS
B158:8D 48 A5      139              STA  DIV.QUOT.M   ;WITH SUM OF RATIOS
B15B:AD 5E A5      140              LDA  RAT.SUM.ML
B15E:8D 49 A5      141              STA  DIV.QUOT.ML
B161:AD 5F A5      142              LDA  RAT.SUM.L
B164:8D 4A A5      143              STA  DIV.QUOT.L
B167:A9 00         144              LDA  #$00         ;LOAD DIVISOR LOCATIONS
B169:8D 4B A5      145              STA  DIVISOR.H    ;WITH TOTAL SAMPLE COUNT
B16C:8D 4C A5      146              STA  DIVISOR.MH
B16F:8D 4D A5      147              STA  DIVISOR.M
B172:8D 4E A5      148              STA  DIVISOR.ML
B175:AD 0C A5      149              LDA  SAMPLE.NUM
B178:8D 4F A5      150              STA  DIVISOR.L
B17B:20 9E B3      151              JSR  DIVIDE.40
B17E:AD 47 A5      152              LDA  DIV.QUOT.MH  ;RETRIEVE QUOTIENT TERMS
B181:9D 00 B8      153              STA  SCRATCH,X    ;CORRESPONDING TO AVG
B184:AD 48 A5      154              LDA  DIV.QUOT.M   ;INTEGER PART OF RATIO
B187:9D 01 B8      155              STA  SCRATCH+1,X
B18A:AD 49 A5      156              LDA  DIV.QUOT.ML  ;RETRIEVE QUOTIENT TERMS
B18D:9D 02 B8      157              STA  SCRATCH+2,X  ;CORRESPONDING TO AVG
B190:AD 4A A5      158              LDA  DIV.QUOT.L   ;FRACTIONAL PART OF RATIO
B193:9D 03 B8      159              STA  SCRATCH+3,X
B196:60            160              RTS
B197:              161 ;
B197:              162 ;*******     AVERAGE MEASUREMENT COMPUTATIONS
******
B197:              163 ;
B197:20 0F B0      164 SWEEP.AVG    JSR  INIT.SUMS    ;INITIALIZE SUM LOCATIONS
B19A:A0 00         165              LDY  #$00         ;ADDRESS INDEX
B19C:A9 0A         166              LDA  #10
B19E:8D 34 A5      167              STA  SWEEP.CNT
B1A1:18            168 NEXT.AVG     CLC
B1A2:AD 57 A5      169              LDA  CH0.SUM.L    ;ADD CH0 SWEEP AVG TO
B1A5:79 01 B8      170              ADC  SCRATCH+1,Y  ;CURRENT CH0 SWEEP SUM
B1A8:8D 57 A5      171              STA  CH0.SUM.L
B1AB:AD 55 A5      172              LDA  CH0.SUM.H
B1AE:79 00 B8      173              ADC  SCRATCH,Y
B1B1:8D 55 A5      174              STA  CH0.SUM.H
B1B4:C8            175              INY               ;UPDATE ADDRESS INDEX
B1B5:C8            176              INY
B1B6:18            177              CLC
B1B7:AD 5A A5      178              LDA  CH1.SUM.L    ;ADD CH1 SWEEP AVG TO
B1BA:79 01 B8      179              ADC  SCRATCH+1,Y  ;CURRENT CH1 SWEEP SUM
B1BD:8D 5A A5      180              STA  CH1.SUM.L
B1C0:AD 58 A5      181              LDA  CH1.SUM.H
B1C3:79 00 B8      182              ADC  SCRATCH,Y
B1C6:8D 58 A5      183              STA  CH1.SUM.H
B1C9:C8            184              INY               ;UPDATE ADDRESS INDEX
B1CA:C8            185              INY
B1CB:18            186              CLC
B1CC:AD 5F A5      187              LDA  RAT.SUM.L    ;ADD RATIO SWEEP AVG
B1CF:79 03 B8      188              ADC  SCRATCH+3,Y  ;TO CURRENT RATIO
B1D2:8D 5F A5      189              STA  RAT.SUM.L    ;SWEEP SUM
B1D5:AD 5E A5      190              LDA  RAT.SUM.ML
B1D8:79 02 B8      191              ADC  SCRATCH+2,Y
```

```
B1DB:8D 5E A5      192          STA  RAT.SUM.ML
B1DE:AD 5D A5      193          LDA  RAT.SUM.M
B1E1:79 01 B8      194          ADC  SCRATCH+1,Y
B1E4:8D 5D A5      195          STA  RAT.SUM.M
B1E7:AD 5C A5      196          LDA  RAT.SUM.MH
B1EA:79 00 B8      197          ADC  SCRATCH,Y
B1ED:8D 5C A5      198          STA  RAT.SUM.MH
B1F0:AD 5B A5      199          LDA  RAT.SUM.H
B1F3:69 00         200          ADC  #00          ;ALLOW FOR PROPAGATION
B1F5:8D 5B A5      201          STA  RAT.SUM.H
B1F8:C8            202          INY
B1F9:C8            203          INY               ;UPDATE ADDRESS INDEX
B1FA:C8            204          INY
B1FB:C8            205          INY
B1FC:CE 34 A5      206          DEC  SWEEP.CNT
B1FF:D0 A0   B1A1  207          BNE  NEXT.AVG     ;CHECK FOR 10 SWEEPS
B201:AD 55 A5      208          LDA  CH0.SUM.H    ;YES, LOAD DIVIDEND
B204:8D 46 A5      209          STA  DIV.QUOT.H   ;LOCATIONS WITH SUM OF
B207:AD 57 A5      210          LDA  CH0.SUM.L    ;CH0 AVERAGE VALUES
B20A:8D 4A A5      211          STA  DIV.QUOT.L
B20D:A9 00         212          LDA  #$00         ;LOAD DIVISOR LOCATIONS
B20F:8D 4B A5      213          STA  DIVISOR.H    ;FOR TOTAL SWEEP COUNT
B212:A9 0A         214          LDA  #10          ;EQUAL TO 10
B214:8D 4F A5      215          STA  DIVISOR.L
B217:20 9C B2      216          JSR  DIVIDE.16
B21A:AD 46 A5      217          LDA  DIV.QUOT.H   ;RETRIEVE QUOTIENT AND
B21D:99 00 B8      218          STA  SCRATCH,Y    ;SAVE AS OVERALL CH0
B220:AD 4A A5      219          LDA  DIV.QUOT.L   ;AVERAGE VALUE
B223:99 01 B8      220          STA  SCRATCH+1,Y
B226:C8            221          INY               ;UPDATE ADDRESS INDEX
B227:C8            222          INY
B228:AD 58 A5      223          LDA  CH1.SUM.H    ;LOAD DIVIDEND LOCATIONS
B22B:8D 46 A5      224          STA  DIV.QUOT.H   ;WITH SUM OF CH1 AVERAGE
B22E:AD 5A A5      225          LDA  CH1.SUM.L    ;VALUES
B231:8D 4A A5      226          STA  DIV.QUOT.L
B234:A9 00         227          LDA  #$00         ;LOAD DIVISOR LOCATIONS
B236:8D 4B A5      228          STA  DIVISOR.H    ;FOR TOTAL SWEEP COUNT
B239:A9 0A         229          LDA  #10          ;EQUAL TO 10
B23B:8D 4F A5      230          STA  DIVISOR.L
B23E:20 9C B2      231          JSR  DIVIDE.16
B241:AD 46 A5      232          LDA  DIV.QUOT.H   ;RETRIEVE QUOTIENT AND
B244:99 00 B8      233          STA  SCRATCH,Y    ;SAVE AS OVERALL CH1
B247:AD 4A A5      234          LDA  DIV.QUOT.L   ;AVERAGE VALUE
B24A:99 01 B8      235          STA  SCRATCH+1,Y
B24D:C8            236          INY               ;UPDATE ADDRESS INDEX
B24E:C8            237          INY
B24F:AD 5B A5      238          LDA  RAT.SUM.H    ;LOAD DIVIDEND LOCATIONS
B252:8D 46 A5      239          STA  DIV.QUOT.H   ;WITH SUM OF AVERAGE
B255:AD 5C A5      240          LDA  RAT.SUM.MH   ;RATIOS
B258:8D 47 A5      241          STA  DIV.QUOT.MH
B25B:AD 5D A5      242          LDA  RAT.SUM.M
B25E:8D 48 A5      243          STA  DIV.QUOT.M
B261:AD 5E A5      244          LDA  RAT.SUM.ML
B264:8D 49 A5      245          STA  DIV.QUOT.ML
B267:AD 5F A5      246          LDA  RAT.SUM.L
B26A:8D 4A A5      247          STA  DIV.QUOT.L
B26D:A9 00         248          LDA  #$00         ;LOAD DIVISOR LOCATIONS
B26F:8D 4B A5      249          STA  DIVISOR.H    ;FOR TOTAL SWEEP COUNT
```

```
B272:8D 4C A5      250             STA  DIVISOR.MH   ;EQUAL TO 10
B275:8D 4D A5      251             STA  DIVISOR.M
B278:8D 4E A5      252             STA  DIVISOR.ML
B27B:A9 0A         253             LDA  #10
B27D:8D 4F A5      254             STA  DIVISOR.L
B280:20 9E B3      255             JSR  DIVIDE.40
B283:AD 47 A5      256             LDA  DIV.QUOT.MH  ;RETRIEVE QUOTIENT AS
B286:99 00 B8      257             STA  SCRATCH,Y    ;OVERALL AVG INTEGER
B289:AD 48 A5      258             LDA  DIV.QUOT.M   ;PART OF RATIO
B28C:99 01 B8      259             STA  SCRATCH+1,Y
B28F:AD 49 A5      260             LDA  DIV.QUOT.ML  ;RETRIEVE QUOTIENT AS
B292:99 02 B8      261             STA  SCRATCH+2,Y  ;OVERALL AVG FRACTIONAL
B295:AD 4A A5      262             LDA  DIV.QUOT.L   ;PART OF RATIO
B298:99 03 B8      263             STA  SCRATCH+3,Y
B29B:60            264             RTS
B29C:              265 ;
B29C:              266 ;**********     16 BIT UNSIGNED DIVISION     **********
B29C:              267 ;
B29C:8E 50 A5      268 DIVIDE.16   STX  DIV.TEMPX    ;SAVE X REGISTER
B29F:A9 00         269             LDA  #$00         ;CLEAR PARTIAL DIVIDEND
B2A1:8D 41 A5      270             STA  REMAIN.H
B2A4:8D 45 A5      271             STA  REMAIN.L
B2A7:A2 10         272             LDX  #16          ;DIVIDEND BIT COUNT = 16
B2A9:0E 4A A5      273 DNXTBT.16   ASL  DIV.QUOT.L   ;SHIFT DIVIDEND/QUOTIENT
B2AC:2E 46 A5      274             ROL  DIV.QUOT.H
B2AF:2E 45 A5      275             ROL  REMAIN.L     ;SHIFT PARTIAL DIVIDEND
B2B2:2E 41 A5      276             ROL  REMAIN.H
B2B5:AD 45 A5      277             LDA  REMAIN.L
B2B8:38            278             SEC               ;SUBTRACT LOW BYTES
B2B9:ED 4F A5      279             SBC  DIVISOR.L
B2BC:8D 54 A5      280             STA  DIV.TEMP.L   ;SAVE LOW BYTE RESULT
B2BF:AD 41 A5      281             LDA  REMAIN.H
B2C2:ED 4B A5      282             SBC  DIVISOR.H    ;SUBTRACT HIGH BYTES
B2C5:90 0C   B2D3  283             BCC  CNTDN.16     ;DIVISOR > DIVIDEND ?
B2C7:EE 4A A5      284             INC  DIV.QUOT.L   ;NO, SET BIT IN QUOTIENT
B2CA:8D 41 A5      285             STA  REMAIN.H     ;AND ENTER SUBTRACT
RESULT
B2CD:AD 54 A5      286             LDA  DIV.TEMP.L   ;INTO PARTIAL DIVIDEND
B2D0:8D 45 A5      287             STA  REMAIN.L
B2D3:CA            288 CNTDN.16    DEX               ;DECREMENT BIT COUNT
B2D4:D0 D3   B2A9  289             BNE  DNXTBT.16    ;LOOP UNTIL ALL 16 BITS
B2D6:AE 50 A5      290             LDX  DIV.TEMPX    ;RESTORE X REGISTER
B2D9:60            291             RTS
B2DA:              292 ;
B2DA:              293 ;**********     24 BIT UNSIGNED DIVISION     **********
B2DA:              294 ;
B2DA:8E 50 A5      295 DIVIDE.24   STX  DIV.TEMPX    ;SAVE X REGISTER
B2DD:A9 00         296             LDA  #$00         ;CLEAR PARTIAL DIVIDEND
B2DF:8D 41 A5      297             STA  REMAIN.H
B2E2:8D 43 A5      298             STA  REMAIN.M
B2E5:8D 45 A5      299             STA  REMAIN.L
B2E8:A2 18         300             LDX  #24          ;DIVIDEND BIT COUNT = 24
B2EA:0E 4A A5      301 DNXTBT.24   ASL  DIV.QUOT.L   ;SHIFT DIVIDEND/QUOTIENT
B2ED:2E 48 A5      302             ROL  DIV.QUOT.M
B2F0:2E 46 A5      303             ROL  DIV.QUOT.H
B2F3:2E 45 A5      304             ROL  REMAIN.L     ;SHIFT PARTIAL DIVIDEND
B2F6:2E 43 A5      305             ROL  REMAIN.M
B2F9:2E 41 A5      306             ROL  REMAIN.H
```

```
B2FC:AD 45 A5      307             LDA  REMAIN.L
B2FF:38            308             SEC                ;SUBTRACT LOW BYTES
B300:ED 4F A5      309             SBC  DIVISOR.L
B303:8D 54 A5      310             STA  DIV.TEMP.L    ;SAVE LOW BYTE RESULT
B306:AD 43 A5      311             LDA  REMAIN.M
B309:ED 4D A5      312             SBC  DIVISOR.M     ;SUBTRACT MIDDLE BYTES
B30C:8D 52 A5      313             STA  DIV.TEMP.M    ;SAVE MIDDLE BYTE RESULT
B30F:AD 41 A5      314             LDA  REMAIN.H
B312:ED 4B A5      315             SBC  DIVISOR.H     ;SUBTRACT HIGH BYTES
B315:90 12   B329  316             BCC  CNTDN.24      ;DIVISOR > DIVIDEND ?
B317:EE 4A A5      317             INC  DIV.QUOT.L    ;NO, SET BIT IN QUOTIENT
B31A:8D 41 A5      318             STA  REMAIN.H      ;AND ENTER SUBTRACT
RESULT
B31D:AD 52 A5      319             LDA  DIV.TEMP.M    ;INTO PARTIAL DIVIDEND
B320:8D 43 A5      320             STA  REMAIN.M
B323:AD 54 A5      321             LDA  DIV.TEMP.L
B326:8D 45 A5      322             STA  REMAIN.L
B329:CA            323 CNTDN.24    DEX                ;DECREMENT BIT COUNT
B32A:D0 BE   B2EA  324             BNE  DNXTBT.24     ;LOOP UNTIL ALL 24 BITS
B32C:AE 50 A5      325             LDX  DIV.TEMPX     ;RESTORE X REGISTER
B32F:60            326             RTS
B330:              327 ;
B330:              328 ;**********      32 BIT UNSIGNED DIVISION      **********
B330:              329 ;
B330:8E 50 A5      330 DIVIDE.32   STX  DIV.TEMPX     ;SAVE X REGISTER
B333:A9 00         331             LDA  #$00          ;CLEAR PARTIAL DIVIDEND
B335:8D 42 A5      332             STA  REMAIN.MH
B338:8D 43 A5      333             STA  REMAIN.M
B33B:8D 44 A5      334             STA  REMAIN.ML
B33E:8D 45 A5      335             STA  REMAIN.L
B341:A2 20         336             LDX  #32           ;DIVIDEND BIT COUNT = 32
B343:0E 4A A5      337 DNXTBT.32   ASL  DIV.QUOT.L    ;SHIFT DIVIDEND/QUOTIENT
B346:2E 49 A5      338             ROL  DIV.QUOT.ML
B349:2E 48 A5      339             ROL  DIV.QUOT.M
B34C:2E 47 A5      340             ROL  DIV.QUOT.MH
B34F:2E 45 A5      341             ROL  REMAIN.L      ;SHIFT PARTIAL DIVIDEND
B352:2E 44 A5      342             ROL  REMAIN.ML
B355:2E 43 A5      343             ROL  REMAIN.M
B358:2E 42 A5      344             ROL  REMAIN.MH
B35B:AD 45 A5      345             LDA  REMAIN.L
B35E:38            346             SEC                ;SUBTRACT LOW BYTES
B35F:ED 4F A5      347             SBC  DIVISOR.L
B362:8D 54 A5      348             STA  DIV.TEMP.L    ;SAVE LOW BYTE RESULT
B365:AD 44 A5      349             LDA  REMAIN.ML
B368:ED 4E A5      350             SBC  DIVISOR.ML    ;SUBTRACT M/L BYTES
B36B:8D 53 A5      351             STA  DIV.TEMP.ML   ;SAVE M/L BYTE RESULT
B36E:AD 43 A5      352             LDA  REMAIN.M
B371:ED 4D A5      353             SBC  DIVISOR.M     ;SUBTRACT MIDDLE BYTES
B374:8D 52 A5      354             STA  DIV.TEMP.M    ;SAVE MIDDLE BYTE RESULT
B377:AD 42 A5      355             LDA  REMAIN.MH
B37A:ED 4C A5      356             SBC  DIVISOR.MH    ;SUBTRACT M/H BYTES
B37D:90 18   B397  357             BCC  CNTDN.32      ;DIVISOR > DIVIDEND ?
B37F:EE 4A A5      358             INC  DIV.QUOT.L    ;NO, SET BIT IN QUOTIENT
B382:8D 42 A5      359             STA  REMAIN.MH     ;AND ENTER SUBTRACT
RESULT
B385:AD 52 A5      360             LDA  DIV.TEMP.M    ;INTO PARTIAL DIVIDEND
B388:8D 43 A5      361             STA  REMAIN.M
B38B:AD 53 A5      362             LDA  DIV.TEMP.ML
```

```
B38E:8D 44 A5      363              STA  REMAIN.ML
B391:AD 54 A5      364              LDA  DIV.TEMP.L
B394:8D 45 A5      365              STA  REMAIN.L
B397:CA            366 CNTDN.32     DEX                ;DECREMENT BIT COUNT
B398:D0 A9   B343  367              BNE  DNXTBT.32     ;LOOP UNTIL ALL 32 BITS
B39A:AE 50 A5      368              LDX  DIV.TEMPX     ;RESTORE X REGISTER
B39D:60            369              RTS
B39E:              370 ;
B39E:              371 ;**********     40 BIT UNSIGNED DIVISION     **********
B39E:              372 ;
B39E:8E 50 A5      373 DIVIDE.40    STX  DIV.TEMPX     ;SAVE X REGISTER
B3A1:A9 00         374              LDA  #$00          ;CLEAR PARTIAL DIVIDEND
B3A3:8D 41 A5      375              STA  REMAIN.H
B3A6:8D 42 A5      376              STA  REMAIN.MH
B3A9:8D 43 A5      377              STA  REMAIN.M
B3AC:8D 44 A5      378              STA  REMAIN.ML
B3AF:8D 45 A5      379              STA  REMAIN.L
B3B2:A2 28         380              LDX  #40           ;DIVIDEND BIT COUNT = 40
B3B4:0E 4A A5      381 DNXTBT.40    ASL  DIV.QUOT.L    ;SHIFT DIVIDEND/QUOTIENT
B3B7:2E 49 A5      382              ROL  DIV.QUOT.ML
B3BA:2E 48 A5      383              ROL  DIV.QUOT.M
B3BD:2E 47 A5      384              ROL  DIV.QUOT.MH
B3C0:2E 46 A5      385              ROL  DIV.QUOT.H
B3C3:2E 45 A5      386              ROL  REMAIN.L      ;SHIFT PARTIAL DIVIDEND
B3C6:2E 44 A5      387              ROL  REMAIN.ML
B3C9:2E 43 A5      388              ROL  REMAIN.M
B3CC:2E 42 A5      389              ROL  REMAIN.MH
B3CF:2E 41 A5      390              ROL  REMAIN.H
B3D2:AD 45 A5      391              LDA  REMAIN.L
B3D5:38            392              SEC                ;SUBTRACT LOW BYTES
B3D6:ED 4F A5      393              SBC  DIVISOR.L
B3D9:8D 54 A5      394              STA  DIV.TEMP.L    ;SAVE LOW BYTE RESULT
B3DC:AD 44 A5      395              LDA  REMAIN.ML
B3DF:ED 4E A5      396              SBC  DIVISOR.ML    ;SUBTRACT M/L BYTES
B3E2:8D 53 A5      397              STA  DIV.TEMP.ML   ;SAVE M/L BYTE RESULT
B3E5:AD 43 A5      398              LDA  REMAIN.M
B3E8:ED 4D A5      399              SBC  DIVISOR.M     ;SUBTRACT MIDDLE BYTES
B3EB:8D 52 A5      400              STA  DIV.TEMP.M    ;SAVE MIDDLE BYTE RESULT
B3EE:AD 42 A5      401              LDA  REMAIN.MH
B3F1:ED 4C A5      402              SBC  DIVISOR.MH    ;SUBTRACT M/H BYTES
B3F4:8D 51 A5      403              STA  DIV.TEMP.MH   ;SAVE M/H BYTE RESULT
B3F7:AD 41 A5      404              LDA  REMAIN.H
B3FA:ED 4B A5      405              SBC  DIVISOR.H     ;SUBTRACT HIGH BYTES
B3FD:90 1E   B41D  406              BCC  CNTDN.40      ;DIVISOR > DIVIDEND ?
B3FF:EE 4A A5      407              INC  DIV.QUOT.L    ;NO, SET BIT IN QUOTIENT
B402:8D 41 A5      408              STA  REMAIN.H      ;AND ENTER SUBTRACT
RESULT
B405:AD 51 A5      409              LDA  DIV.TEMP.MH   ;INTO PARTIAL DIVIDEND
B408:8D 42 A5      410              STA  REMAIN.MH
B40B:AD 52 A5      411              LDA  DIV.TEMP.M
B40E:8D 43 A5      412              STA  REMAIN.M
B411:AD 53 A5      413              LDA  DIV.TEMP.ML
B414:8D 44 A5      414              STA  REMAIN.ML
B417:AD 54 A5      415              LDA  DIV.TEMP.L
B41A:8D 45 A5      416              STA  REMAIN.L
B41D:CA            417 CNTDN.40     DEX                ;DECREMENT BIT COUNT
B41E:D0 94   B3B4  418              BNE  DNXTBT.40     ;LOOP UNTIL ALL 40 BITS
B420:AE 50 A5      419              LDX  DIV.TEMPX     ;RESTORE X REGISTER
```

```
B423:60             420             RTS
B424:               421 ;
B424:               422 ;**********     SOFTWARE DELAY ROUTINE #1    **********
B424:               423 ;
B424:8E 61 A5       424 SW.DELAY1   STX  DLY.TEMPX    ;SAVE X & Y REGISTERS
B427:8C 62 A5       425             STY  DLY.TEMPY
B42A:AD 63 A5       426             LDA  DELAY        ;LOAD TIMING BYTE
B42D:A2 A5          427 GEN.DLY1    LDX  #$A5         ;LOAD X AND Y FOR A
B42F:A0 EA          428             LDY  #$EA         ;300 MSEC TIME DELAY
B431:CA             429 WAIT.DLY1   DEX
B432:D0 FD   B431   430             BNE  WAIT.DLY1    ;LOOP UNTIL X=0
B434:88             431             DEY
B435:D0 FA   B431   432             BNE  WAIT.DLY1    ;LOOP UNTIL X=Y=0
B437:38             433             SEC
B438:E9 01          434             SBC  #01          ;DECREMENT TIMING BYTE
B43A:D0 F1   B42D   435             BNE  GEN.DLY1     ;LOOP UNTIL ACC=0
B43C:AE 61 A5       436             LDX  DLY.TEMPX    ;RESTORE X & Y REGISTERS
B43F:AC 62 A5       437             LDY  DLY.TEMPY
B442:60             438             RTS
B443:               439 ;
B443:               440 ;**********     SOFTWARE DELAY ROUTINE #2    **********
B443:               441 ;
B443:8E 61 A5       442 SW.DELAY2   STX  DLY.TEMPX    ;SAVE X REGISTER
B446:AD 63 A5       443             LDA  DELAY        ;LOAD TIMING BYTE
B449:A2 12          444 GEN.DLY2    LDX  #$12         ;LOAD X FOR 100 USEC
B44B:CA             445 WAIT.DLY2   DEX               ;TIME DELAY
B44C:D0 FD   B44B   446             BNE  WAIT.DLY2    ;LOOP UNTIL X = 0
B44E:EA             447             NOP
B44F:38             448             SEC
B450:E9 01          449             SBC  #01          ;DECREMENT TIMING BYTE
B452:D0 F5   B449   450             BNE  GEN.DLY2     ;LOOP UNTIL ACC = 0
B454:AE 61 A5       451             LDX  DLY.TEMPX    ;RESTORE X REGISTER
B457:60             452             RTS
B458:               453 ;
B458:               454 ;**********     OUTPUT SETTLING ROUTINE     **********
B458:               455 ;
B458:A9 05          456 OUT.SETTLE  LDA  #05          ;SET FOR 1.5 SEC
B45A:8D 63 A5       457             STA  DELAY
B45D:20 24 B4       458             JSR  SW.DELAY1    ;OUTPUT SETTLING TIME
B460:A9 7F          459             LDA  #%01111111   ;CLEAR ANY INTERRUPTS
B462:8D 8D C2       460             STA  U2.IFR       ;BEFORE RETURNING
B465:60             461             RTS
B466:               462 ;
B466:               463 ;******     A/D MULTIPLEXOR SETTLING ROUTINE     ******
B466:               464 ;
B466:A9 01          465 MUX.SETTLE  LDA  #01          ;SET FOR 100 USEC
B468:8D 63 A5       466             STA  DELAY
B46B:20 43 B4       467             JSR  SW.DELAY2
B46E:60             468             RTS
B46F:               469 ;
B46F:               470 ;***********     A/D CONVERSION ROUTINE     **********
B46F:               471 ;
B46F:AD D2 C0       472 CONVERT     LDA  START.CONV   ;START CONVERSION
B472:AD D1 C0       473 WAIT.CONV   LDA  AD.HIGH      ;CHECK FOR CONVERSION
B475:2A             474             ROL               ;STATUS BIT SET
B476:2A             475             ROL
B477:B0 F9   B472   476             BCS  WAIT.CONV    ;RETURN WHEN CONVERSION
B479:60             477             RTS               ;COMPLETED
```

```
B47A:                  478 ;
B47A:                  479 ;***************      ERROR ROUTINE     ***************
B47A:                  480 ;
B47A:A9 C5             481 ERROR       LDA  #$C5          ;LETTER E
B47C:20 ED FD          482             JSR  COUT
B47F:A9 D2             483             LDA  #$D2          ;LETTER R
B481:20 ED FD          484             JSR  COUT
B484:20 ED FD          485             JSR  COUT
B487:A9 CF             486             LDA  #$CF          ;LETTER O
B489:20 ED FD          487             JSR  COUT
B48C:A9 D2             488             LDA  #$D2          ;LETTER R
B48E:20 ED FD          489             JSR  COUT
B491:A9 A3             490             LDA  #$A3          ;POUND SIGN
B493:20 ED FD          491             JSR  COUT
B496:A9 A0             492             LDA  #$A0          ;SPACE
B498:20 ED FD          493             JSR  COUT
B49B:AD 60 A5          494             LDA  INVALID       ;DETERMINE WHICH ERROR
B49E:2A                495             ROL
B49F:B0 14   B4B5      496             BCS  NEXT1
B4A1:2A                497             ROL
B4A2:B0 1C   B4C0      498             BCS  NEXT2
B4A4:2A                499             ROL
B4A5:B0 24   B4CB      500             BCS  NEXT3
B4A7:2A                501             ROL
B4A8:B0 2C   B4D6      502             BCS  NEXT4
B4AA:A9 B0             503             LDA  #$B0          ;NUMBER ZERO
B4AC:20 ED FD          504             JSR  COUT          ;UNKNOWN ERROR
B4AF:A9 8D             505             LDA  #$8D          ;CARRIAGE RETURN
B4B1:20 ED FD          506             JSR  COUT
B4B4:60                507             RTS
B4B5:A9 B1             508 NEXT1       LDA  #$B1          ;NUMBER 1
B4B7:20 ED FD          509             JSR  COUT          ;ERRONEOUS CALL TO PHASE
2
B4BA:A9 8D             510             LDA  #$8D          ;CARRIAGE RETURN
B4BC:20 ED FD          511             JSR  COUT
B4BF:60                512             RTS
B4C0:A9 B2             513 NEXT2       LDA  #$B2          ;NUMBER 2
B4C2:20 ED FD          514             JSR  COUT          ;ERRONEOUS CALL TO PHASE
4
B4C5:A9 8D             515             LDA  #$8D          ;CARRIAGE RETURN
B4C7:20 ED FD          516             JSR  COUT
B4CA:60                517             RTS
B4CB:A9 B3             518 NEXT3       LDA  #$B3          ;NUMBER 3
B4CD:20 ED FD          519             JSR  COUT          ;INVALID SWEEP NUMBER
B4D0:A9 8D             520             LDA  #$8D          ;CARRIAGE RETURN
B4D2:20 ED FD          521             JSR  COUT
B4D5:60                522             RTS
B4D6:A9 B4             523 NEXT4       LDA  #$B4          ;NUMBER 4
B4D8:20 ED FD          524             JSR  COUT          ;UNKNOWN INTERRUPT
B4DB:A9 8D             525             LDA  #$8D          ;CARRIAGE RETURN
B4DD:20 ED FD          526             JSR  COUT
B4E0:60                527             RTS
B4E1:                  528 ;
B4E1:                  529 ;********* CLOCK START ROUTINE *********
B4E1:                  530 ;
B4E1:AD 64 A5          531 CLKSTART    LDA  CLK.CNTRL.A ;SET UP SELECTED INTERRUPT
INTERVAL
B4E4:8D C1 C0          532             STA  CRA.CLK
```

```
B4E7:AD 65 A5      533             LDA  CLK.CNTRL.B
B4EA:8D C3 C0      534             STA  CRB.CLK
B4ED:AD C0 C0      535             LDA  DRA.CLK     ;CLEAR PREVIOUS INTERRUPT
FLAGS
B4F0:AD C2 C0      536             LDA  DRB.CLK
B4F3:A9 2F         537             LDA  #$2F        ;ENABLE INTERRUPTS OUT OF
PIA
B4F5:8D C2 C0      538             STA  DRB.CLK
B4F8:58            539             CLI               ;ENABLE PROCESSOR
INTERRUPTS
B4F9:60            540             RTS
B4FA:              541 ;
B4FA:              542 ;********* CLOCK STOP ROUTINE *********
B4FA:              543 ;
B4FA:78            544 CLKSTOP     SEI               ;DISABLE PROCESSOR
INTERRUPTS
B4FB:A9 04         545             LDA  #$04        ;DISABLE CLOCK INTERRUPTS
B4FD:8D 64 A5      546             STA  CLK.CNTRL.A
B500:8D 65 A5      547             STA  CLK.CNTRL.B
B503:AD 64 A5      548             LDA  CLK.CNTRL.A
B506:8D C1 C0      549             STA  CRA.CLK
B509:AD 65 A5      550             LDA  CLK.CNTRL.B
B50C:8D C3 C0      551             STA  CRB.CLK
B50F:AD C0 C0      552             LDA  DRA.CLK     ;CLEAR PREVIOUS CLOCK
INTERRUPT FLAGS
B512:AD C2 C0      553             LDA  DRB.CLK
B515:60            554             RTS
B516:              555 ;
B516:              556 ;********* ENABLE PROCESSOR INTERRUPT ROUTINE *********
B516:              557 ;
B516:58            558 ENABLE      CLI
B517:60            559             RTS
B518:              560 ;
B518:              561 ;*********     INTERRUPT SERVICE ROUTINE     **********
B518:              562 ;
B518:A5 45         563 ISR         LDA  $45         ;RESTORE ACCUMULATOR
B51A:48            564             PHA               ;PUSH ACCUMULATOR
B51B:8A            565             TXA               ;PUSH X REGISTER
B51C:48            566             PHA
B51D:98            567             TYA               ;PUSH Y REGISTER
B51E:48            568             PHA
B51F:AD 8D C2      569             LDA  U2.IFR       ;INSPECT INTERRUPTS
B522:2D 8E C2      570             AND  U2.IER
B525:2A            571             ROL
B526:2A            572             ROL
B527:B0 22   B54B  573             BCS  TIMER1       ;CHECK FOR T1 IRQ
B529:AD C1 C0      574             LDA  CRA.CLK     ;CHECK FOR IRQ FROM CLOCK
PORT A
B52C:29 40         575             AND  #%01000000
B52E:2A            576             ROL
B52F:2A            577             ROL
B530:B0 16   B548  578             BCS  CLOCK       ;IF YES THEN SERVICE CLOCK
INTERRUPT
B532:AD C3 C0      579             LDA  CRB.CLK     ;CHECK FOR IRQ FROM CLOCK
PORT B
B535:29 C0         580             AND  #%11000000
B537:2A            581             ROL
```

```
B538:B0 0E   B548  582             BCS  CLOCK        ;IF YES THEN SERVICE CLOCK
INTERRUPT
B53A:2A            583             ROL
B53B:B0 0B   B548  584             BCS  CLOCK        ;IF YES THEN SERVICE CLOCK
INTERRUPT
B53D:A9 10         585             LDA  #%00010000   ;NO, ERRONEOUS INTERRUPT
B53F:8D 60 A5      586             STA  INVALID      ;SYSTEM ERROR BYTE
B542:20 7A B4      587             JSR  ERROR        ;SYSTEM ERROR ROUTINE
B545:4C FF B5      588             JMP  RETURN
B548:4C F6 B5      589 CLOCK       JMP  CLK.SERV     ;JUMP TO CLOCK SERVICE
ROUTINE
B54B:A9 01         590 TIMFR1      LDA  #01          ;YES, SET SYNC FLAG
B54D:8D 3A A5      591             STA  SYNC.OK
B550:AD 36 A5      592             LDA  INJ.ACTIVE   ;CHECK FOR INJECTION
B553:C9 01         593             CMP  #$01
B555:F0 20   B577  594             BEQ  INJ.CHK      ;CURRENT MEASUREMENT
B557:AD 38 A5      595             LDA  MEAS.ACTIVE  ;CHECK FOR ACTIVE
B55A:D0 08   B564  596             BNE  CONT.MEAS    ;MEASUREMENT PERIOD
B55C:A9 40         597             LDA  #%01000000   ;CLEAR IRQ FLAG
B55E:8D 8D C2      598             STA  U2.IFR
B561:4C FF B5      599             JMP  RETURN       ;SYNCHRONIZATION ONLY
B564:AD 80 C2      600 CONT.MEAS   LDA  U2.DRB       ;NO, DATA MEASUREMENT
B567:2A            601             ROL               ;INSPECT TRIGGER LEVEL
B568:90 41   B5AB  602             BCC  DATA.CHK     ;PRESENTLY LOW ?
B56A:A9 00         603             LDA  #%00000000   ;NO, FALLING TRANSITION
B56C:8D 80 C2      604             STA  U2.DRB       ;FOR FLASH TRIGGER
B56F:A9 40         605             LDA  #%01000000   ;CLEAR IRQ FLAG
B571:8D 8D C2      606             STA  U2.IFR
B574:4C FF B5      607             JMP  RETURN       ;AND RETURN
B577:AD 37 A5      608 INJ.CHK     LDA  INJ.STATUS   ;YES, CHECK STATUS
B57A:D0 22   B59E  609             BNE  SKIP.INJ     ;PRESENTLY HIGH ?
B57C:A9 01         610             LDA  #01          ;NO, SET STATUS HIGH
B57E:8D 37 A5      611             STA  INJ.STATUS
B581:A9 32         612             LDA  #%00110010   ;START INTEGRATION FOR
B583:8D 81 C2      613             STA  U2.DRA       ;INJECTION CURRENT
B586:AE 3E A5      614             LDX  INT.LOOP
B589:CA            615 INT.INJ     DEX               ;INTEGRATION LOOP
B58A:D0 FD   B589  616             BNE  INT.INJ
B58C:A9 30         617             LDA  #%00110000   ;CEASE INTEGRATION
B58E:8D 81 C2      618             STA  U2.DRA
B591:A9 40         619             LDA  #%01000000   ;CLEAR IRQ FLAG
B593:8D 8D C2      620             STA  U2.IFR
B596:CE 0B A5      621             DEC  INT.CNT      ;INTEGRATION COUNT
B599:D0 64   B5FF  622             BNE  RETURN       ;FINISHED ?
B59B:4C CF B5      623             JMP  INT.FINISH   ;YES
B59E:A9 00         624 SKIP.INJ    LDA  #00          ;SET STATUS LOW
B5A0:8D 37 A5      625             STA  INJ.STATUS
B5A3:A9 40         626             LDA  #%01000000   ;CLEAR IRQ FLAG
B5A5:8D 8D C2      627             STA  U2.IFR
B5A8:4C FF B5      628             JMP  RETURN
B5AB:AD 39 A5      629 DATA.CHK    LDA  DATA.ACTIVE  ;CHECK FOR ACTIVE
B5AE:F0 39   B5E9  630             BEQ  SKIP.DATA    ;DATA MEASUREMENT
B5B0:A9 80         631             LDA  #%10000000   ;YES, RISING TRANS.
B5B2:A2 3A         632             LDX  #%00111010   ;INTEGRATOR CONTROL
B5B4:8D 80 C2      633             STA  U2.DRB       ;FLASH TRIGGER
B5B7:8E 81 C2      634             STX  U2.DRA       ;BEGIN INTEGRATION
B5BA:AE 3E A5      635             LDX  INT.LOOP
B5BD:CA            636 INT.DATA    DEX               ;INTEGRATION LOOP
```

```
B5BE:D0 FD   B5BD  637              BNE  INT.DATA
B5C0:A9 30         638              LDA  #%00110000   ;CEASE INTEGRATION
B5C2:8D 81 C2      639              STA  U2.DRA
B5C5:A9 40         640              LDA  #%01000000   ;CLEAR IRQ FLAG
B5C7:8D 8D C2      641              STA  U2.IFR
B5CA:CE 0B A5      642              DEC  INT.CNT      ;INTEGRATION COUNT
B5CD:D0 30   B5FF  643              BNE  RETURN
B5CF:A9 20         644 INT.FINISH   LDA  #%00100000   ;PLACE S/H IN "HOLD"
B5D1:8D 81 C2      645              STA  U2.DRA
B5D4:A9 01         646              LDA  #01          ;S/H CIRCUITRY MUST
B5D6:8D 63 A5      647              STA  DELAY        ;SETTLE
B5D9:20 43 B4      648              JSR  SW.DELAY2
B5DC:A9 21         649              LDA  #%00100001   ;DISCHARGE INTEGRATORS
B5DE:8D 81 C2      650              STA  U2.DRA
B5E1:A9 01         651              LDA  #01          ;SET SAMPLE AVAILABLE
B5E3:8D 35 A5      652              STA  SMPL.AVAIL   ;FLAG
B5E6:4C FF B5      653              JMP  RETURN
B5E9:A9 80         654 SKIP.DATA    LDA  #%10000000   ;NO, RISING TRANSITION
B5EB:8D 80 C2      655              STA  U2.DRB       ;FOR FLASH TRIGGER
B5EE:A9 40         656              LDA  #%01000000   ;CLEAR IRQ FLAG
B5F0:8D 8D C2      657              STA  U2.IFR
B5F3:4C FF B5      658              JMP  RETURN
B5F6:EE 66 A5      659 CLK.SERV     INC  TIME.OUT    ;INCREMENT TIME.OUT COUNT
FOR BASIC
B5F9:AD C0 C0      660              LDA  DRA.CLK     ;CLEAR PREVIOUS INTERRUPT
FLAGS
B5FC:AD C2 C0      661              LDA  DRB.CLK
B5FF:68            662 RETURN       PLA               ;PULL Y REGISTER
B600:A8            663              TAY
B601:68            664              PLA               ;PULL X REGISTER
B602:AA            665              TAX
B603:68            666              PLA               ;PULL ACCUMULATOR
B604:40            667              RTI               ;RETURN FROM IRQ
```

```
A513 AD.CH0.CTRL    A514 AD.CH1.CTRL    C0D3 AD.CTRL        C0D1 AD.HIGH
C0D0 AD.LOW         A843 AUTO           A87C AUTO.CAL0      A93E AUTO.CAL1
B0E9 AVG.CH0        B119 AVG.CH1        AB03 AVG.INJ0       AB32 AVG.INJ1
B149 AVG.RATIO      A510 CH0.AD.GAIN    A515 CH0.INJ.H      A516 CH0.INJ.L
A50F CH0.PGAIN      A555 CH0.SUM.H      A557 CH0.SUM.L      A556 CH0.SUM.M
A512 CH1.AD.GAIN    A517 CH1.INJ.H      A518 CH1.INJ.L      A511 CH1.PGAIN
A558 CH1.SUM.H      A55A CH1.SUM.L      A559 CH1.SUM.M      AB79 CHOICE.1
AB7C CHOICE.2       AB7F CHOICE.3       A564 CLK.CNTRL.A    A565 CLK.CNTRL.B
B5F6 CLK.SERV       A567 CLKSTART.H     A568 CLKSTART.L     B4E1 CLKSTART
A569 CLKSTOP.H      B4FA CLKSTOP        A56A CLKSTOP.L      B548 CLOCK
B2D3 CNTDN.16       B329 CNTDN.24       B397 CNTDN.32       B41D CNTDN.40
AD1D COMP.MS        A658 CONFIG         A8B7 CONT.CAL0      A979 CONT.CAL1
AE8B CONT.CHK.0     AE9F CONT.CHK.1     AE77 CONT.CHK.SS    B564 CONT.MEAS
AF0B CONT.Z.CH0     AF21 CONT.Z.CH1     AEF5 CONT.Z.SS      B46F CONVERT
FDED COUT           C0C1 CRA.CLK        C0C3 CRB.CLK        A51B DA.COPY1
A51C DA.COPY2       A51D DA.COPY3       A51E DA.COPY4       A51F DA.COPY5
A802 DA.CTRL        C0B8 DA.CTRL1       C0B9 DA.CTRL2       C0BA DA.CTRL3
C0BB DA.CTRL4       C0BC DA.CTRL5       A539 DATA.ACTIVE    B5AB DATA.CHK
AD71 DATA.FILE      A53B DATA.SETTLE    A563 DELAY          A546 DIV.QUOT.H
A54A DIV.QUOT.L     A548 DIV.QUOT.M     A547 DIV.QUOT.MH    A549 DIV.QUOT.ML
A554 DIV.TEMP.L     A551 DIV.TEMP.MH    A552 DIV.TEMP.M     A553 DIV.TEMP.ML
A550 DIV.TEMPX      B29C DIVIDE.16      B2DA DIVIDE.24      B330 DIVIDE.32
B39E DIVIDE.40      A54B DIVISOR.H      A54F DIVISOR.L      A54D DIVISOR.M
A54C DIVISOR.MH     A54E DIVISOR.ML     A561 DLY.TEMPX      A562 DLY.TEMPY
B2A9 DNXTBT.16      B2EA DNXTBT.24      B343 DNXTBT.32      B3B4 DNXTBT.40
C0C0 DRA.CLK        C0C2 DRB.CLK        A56D DUMMY.FLASH    B516 ENABLE
A56B ENABLE.H       A56C ENABLE.L       B47A ERROR          A914 EXIT.CAL0
A9D6 EXIT.CAL1      A92A FINAL.CAL0     A9EC FINAL.CAL1     ADE0 FINISH.DF
AABE FINISH.DK      AD60 FINISH.MS      AC4A FINISH.SS      A508 FLASH.F
A53C FLASH.H        AA1A FLASH.INJ      A53D FLASH.L        B42D GEN.DLY1
B449 GEN.DLY2       B00F INIT.SUMS      ADEE INIT.SWEEP     A536 INJ.ACTIVE
B577 INJ.CHK        A537 INJ.STATUS     A821 INT.CAL        A50B INT.CNT
B5BD INT.DATA       B5CF INT.FINISH     B589 INT.INJ        A53E INT.LOOP
A50A INT.NUM        A509 INT.PERIOD     A560 INVALID        B518 ISR
AC5B M.SWEEP        A858 MAN.CAL        A50E MANUAL         A83F MAN
A538 MEAS.ACTIVE    AA4B MEAS.INJ       A519 MEAS.MODE      A53F MEAS.TEMP.H
A540 MEAS.TEMP.L    B466 MUX.SETTLE     B1A1 NEXT.AVG       B4B5 NEXT1
B4C0 NEXT2          B4CB NEXT3          B4D6 NEXT4          AE83 OF.CHK.CH0
AE97 OF.CHK.CH1     AE6F OF.CHK.SS      AF99 OF.ERR.SW10    AF63 OF.ERR.SW1
AF69 OF.ERR.SW2     AF6F OF.ERR.SW3     AF75 OF.ERR.SW4     AF7B OF.ERR.SW5
AF81 OF.ERR.SW6     AF87 OF.ERR.SW7     AF8D OF.ERR.SW8     AF93 OF.ERR.SW9
A520 OF.SW1         A529 OF.SW10        A521 OF.SW2         A522 OF.SW3
A523 OF.SW4         A524 OF.SW5         A525 OF.SW6         A526 OF.SW7
A527 OF.SW8         A528 OF.SW9         A51A OFFSET.ADJ     B458 OUT.SETTLE
AE93 OVER.CH0       AEA7 OVER.CH1       AE7F OVER.SS        AF2F OVERFLOW
A8E5 PGAIN.CAL0     A9A7 PGAIN.CAL1     A8DA PGAIN.FIX0     A99C PGAIN.FIX1
A501 PHASE1.L       A6B4 PHASE1         A500 PHASE1.H       A82D PHASE2
A502 PHASE2.H       A503 PHASE2.L       AA00 PHASE3         A504 PHASE3.H
A505 PHASE3.L       A506 PHASE4.H       A507 PHASE4.L       AB61 PHASE4
AABF POST.INJ       AE60 POST.MEAS      AA2A PRE.INJ        AE2D PRE.MEAS
A892 RANGE.CAL0     A954 RANGE.CAL1     BE00 RAT.FRAC       BD00 RAT.INT
A55B RAT.SUM.H      A55F RAT.SUM.L      A55C RAT.SUM.MH     A55D RAT.SUM.M
A55E RAT.SUM.ML     B077 RATIO.MS       B033 RATIO.SS       A541 REMAIN.H
A545 REMAIN.L       A543 REMAIN.M       A542 REMAIN.MH      A544 REMAIN.ML
B5FF RETURN         AB82 S.SWEEP        A50D SAMPLE.CNT     A50C SAMPLE.NUM
B900 SCRATCH0       B800 SCRATCH        BA00 SCRATCH0.A     BB00 SCRATCH1
BC00 SCRATCH1.A     B5E9 SKIP.DATA      B59E SKIP.INJ       AC23 SKIP.RATIO
ABDC SKIP.Z.CH0     AC19 SKIP.Z.CH1     A535 SMPL.AVAIL     C0D2 START.CONV
```

```
 AF13 SUBST.CH0      AF29 SUBST.CH1      AEFD SUBST.SS       AACB SUM.CH0
 AAE7 SUM.CH1        B0BB SUM.RATIO      B424 SW.DELAY1      B443 SW.DELAY2
 B197 SWEEP.AVG      A534 SWEEP.CNT      AA40 SYNC.INJ       AE4B SYNC.MEAS
 A53A SYNC.OK        A7CB SYS.INIT       A6C4 TABLE          A566 TIME.OUT
 B54B TIMER1         A7B5 TIMER          A689 TMASTER        C20B U1.ACR
 C203 U1.DDRA        C202 U1.DDRB        C201 U1.DRA        ?C200 U1.DRB
 C20E U1.IER         C20D U1.IFR         C20C U1.PCR        ?C205 U1.T1C.H
?C204 U1.T1C.L      ?C207 U1.T1L.H      ?C206 U1.T1L.L      ?C209 U1.T2C.H
?C208 U1.T2C.L       C28B U2.ACR         C283 U2.DDRA        C282 U2.DDRB
 C281 U2.DRA         C280 U2.DRB         C28E U2.IER         C28D U2.IFR
 C28C U2.PCR         C285 U2.T1C.H       C284 U2.T1C.L      ?C287 U2.T1L.H
?C286 U2.T1L.L      ?C289 U2.T2C.H      ?C288 U2.T2C.L       AEC1 UF.CHK.CH0
 AED7 UF.CHK.CH1     AEAB UF.CHK.SS      AFD3 UF.ERR.SW1     B009 UF.ERR.SW10
 AFD9 UF.ERR.SW2     AFDF UF.ERR.SW3     AFE5 UF.ERR.SW4     AFEB UF.ERR.SW5
 AFF1 UF.ERR.SW6     AFF7 UF.ERR.SW7     AFFD UF.ERR.SW8     B003 UF.ERR.SW9
 A52A UF.SW1         A533 UF.SW10        A52B UF.SW2         A52C UF.SW3
 A52D UF.SW4         A52E UF.SW5         A52F UF.SW6         A530 UF.SW7
 A531 UF.SW8         A532 UF.SW9         AEC9 UNDER.CH0      AEDF UNDER.CH1
 AEB3 UNDER.SS       AF9F UNDERFLOW      B472 WAIT.CONV      AD91 WAIT.DF
 B431 WAIT.DLY1      B44B WAIT.DLY2      AA68 WAIT.INJ       AC89 WAIT.MS
 ABA5 WAIT.SS        A89F WAIT1.CAL0     A961 WAIT1.CAL1     AF03 ZERO.CH0
 AF19 ZERO.CH1       AEED ZERO.SS
** SUCCESSFUL ASSEMBLY := NO ERRORS
** ASSEMBLER CREATED ON 21-MAY-83 REL-07
** TOTAL LINES ASSEMBLED  2033
** FREE SPACE PAGE COUNT   62
    2  JMC1.1
    3  JMC1.2
```

BIBLIOGRAPHY

1. *Flashlamp Applications Manual.* 1983 EG&G Electro-Optics. Arlington Heights, IL.

2. Adams, G. E., Stratford, I. J. and Rajaratnam, S. "Interaction of Cytoxic and Sensitizing Effects of Electron-Affinic Drugs and Hyperthermia." Third *International Symposium: Cancer Therapy by Hyperthermia, Drugs, and Radiation.* Dethlefsen, L. A. ed.1982 NCI. Bethesda.

3. Alcala, R. J., Gratton, E. and Jameson, D. M. "A Multifrequency Phase Fluorometer Using the Harmonic Content of a Mode-Locked Laser." Anal. Instrum. **14**(3&4): 225-250, 1985.

4. Angel, S. M. "Optrodes: Chemically Selective Fiber-Optic Sensors." Spectroscopy. **2**(4): 38-48, 1988.

5. Atkins, P. W. *Physical Chemistry.* 1982 W. H. Freeman and Company. New York.

6. Bamberg, E. and Lauger, P. "Blocking of the Gramicidin Channel by Divalent Cations." J. Membrane Biol. **35**: 351-375, 1977.

7. Baratt, G. M. and Wills, E. D. "The Effect of Hyperthermia and Radiation on Lysosomal Enzyme Activity of Mouse Mammary Tumors." Eur. J. Cancer. **15**: 243-250, 1979.

8. Bass, H., Moore, J. L. and Coakely, W. T. "Lethality in Mammalian Cells Due to Hyperthermia Under Oxic and Hypoxic Conditions." Inter. J. Radiat. Biol. **33**: 57-67, 1978.

9. Bicher, H. I. "The Physiological Effects of Hyperthermia." Radiology. **137**: 511-513, 1980.

10. Bicher, H. I., Hetzel, F. W., Sandu, T. S., Frinak, S., Vaupel, P., O'Hara, M. D. and O'Brien, T. "Effects of Hyperthermia on Normal and Tumor Microenvironments." Radiology. **137**: 523-530, 1980.

11. Bicher, H. I., Sandhu, T. S. and Hetzel, F. W. "Inhomogeneities in Oxygen and pH Distribution in Tumors." Radiation Research. **83**: 376, 1980.

12. Biegel, C. M. and Gould, J. M. "Kinetics of Hydrogen Ion Diffusion across Phospholipid Vesicle Membranes." Biochemistry. **20**: 3474-3479, 1981.

13. Bierman, H. R., Kelly, K. H. and Singer, G. "Studies on the Blood Supply of Tumors in Man. IV. The Increased Oxygen Content of Venous Blood Draining Neoplasms." Journal of the National Cancer Institute. **12**: 701-707, 1952.

14. Brown, R. G. and Porter, G. "Effect of pH on the Emission and Absorption Characteristics of 2,3-Dicyano-p-hydroquinone." J. Chem. Soc. Faraday Trans. I. **73**: 1281-1285, 1977.

15. Cavaliere, R., Ciocatto, E. C., Giovanella, B. C., Heidelberger, C., Johnson, R. O., Moricca, G. and Rossi-Fanelli, A. "Selective Heat Sensitivity of Cancer Cells (Biochemical and Clinical Studies)." Cancer. **20**: 1351-1381, 1967.

16. Chen, T. T. and Heidelberger, C. "Quantitative Studies on the Malignant Transformation of Mouse Prostate Cells by Carcinogenic Hydrocarbons In-Vitro." Int. J. Cancer. **4**: 166-178, 1969.

17. Clement, N. R. and Gould, J. M. "Kinetics for Development of Gramicidin-Induced Permeability in Unilamellar Phospholipid Vesicles." Biochemistry. **20**: 1544-1548, 1981.

18. Creighton, A. M. and Jackman, L. M. "Hydrogen Transfer. Part XIV. The Quinone Cyclodehydrogenation of Acids and Alcohols." J. Chem. Soc. 3138-3144, 1960.

19. Cress, A. E. and Gerner, E. W. "Cholesterol Levels Inversely Reflect the Thermal Sensitivity of Mammalian Cells In Culture." Nature. **283**: 677, 1980.

20. Crile, G. J. "The Effects of Heat and Radiation on Cancers Implanted into the Feet of Mice." Cancer Research. **23**: 372-380, 1963.

21. Deamer, D. W. and Nicholos, J. W. "Proton-Hydroxide Permeability of Liposomes." Proc. Natl. Acad. Sci. USA. **80**: 165-168, 1983.

22. Dereniak, E. L. and Crowe, D. G. *Optical Radiation Detectors.* Pure and Applied Optics. Goodman, J. W. ed. 1984 John Wiley & Sons. New York.

23. Dickson , J. A. and Calderwood, S. K. "Thermosensitivity of Neoplastic Tissues In-Vivo." *Hyperthermia in Cancer Therapy*. Storm, F. K. ed. 1983 G. K. Hall Medical Publishers. Boston.

24. Dickson, J. A. and Calderwood, S. K. "Effects of Hyperglycemia and Hyperthermia on the pH, Glycolysis, and Respiration of the Yoshida Sarcoma In-Vivo." Journal of the National Cancer Institute. **63**: 1371-1381, 1979.

25. Eden, M., Haines, B. and Kahler, H. "The pH of Rat Tumors Measured In-Vivo." Journal of the National Cancer Institute. **16**: 541-556, 1955.

26. Ehlert, K. S. *System Design and Development for Control, Acquisition, and Analysis of Signals from Fiber Optic Sensors*. M.S. thesis, Department of Electrical and Computer Engineering, University of Illinois at Urbana-Champaign, 1988.

27. Fritz, J. S. and Schenk, G. H. *Quantitative Analytical Chemistry*. 1969 Allyn and Bacon, Inc. Boston.

28. Fugate, R. D. "Fluorescence Duration Gives New Dimension to Chemical Analysis." R & D. **27**(4): 120-124, 1985.

29. Gerweck, L. E. "Modification of Cell Lethality at Elevated Temperatures: The pH Effect." Radiat. Res. **70**: 224-235, 1977.

30. Gerweck, L. E. "Influence of Microenvironmental Conditions on Sensitivity to Hyperthermia or Radiation for Cancer Therapy." *Clinical Prospects for Hypoxic Cell Sensitizers and Hyperthermia.* 1978 University of Wisconsin. Madison.

31. Gerweck, L. E. "Hyperthermia in Cancer Therapy: The Biological Basis and Unresolved Questions." Cancer Res. **45**: 3408-3414, 1985.

32. Gerweck, L. E., Nygaard, T. G. and Burlett, M. "Response of Cells to Hyperthermia Under Acute and Chronic Hypoxic Conditions." Cancer Research. **39**: 966-972, 1979.

33. Gillies, R. J., Cook, J., Fox, M. H. and Giuliano, K. A. "Flow Cytometric Analysis of Intracellular pH in 3T3 Cells." Amer. J. Physiol. **253**: C121-C125, 1987.

34. Gratton, E., Jameson, D. M. and Hall, R. D. "Multifrequency Phase and Modulation Fluoremetry." Ann. Rev. Biophys. Bioeng. **13**: 105-124, 1984.

35. Gratton, E. and Limkeman, M. "Microprocessor-Controlled Photon-Counting Spectrofluorometer." Rev. Sci. Instrum. **54**(3): 294-299, 1983.

36. Gratton, E., Linkeman, M., Lacowicz, J. R., Maliwal, B. P., Cherek, H. and Laczko, G. "Resolution of Mixtures of Fluorophores Using Variable-Frequency Phase and Modulation Data." Biophys. J. **46**: 479-486, 1984.

37. Hahn, G. M. "Metabolic Aspects of the Role of Hyperthermia in Mammalian Cell Inactivation and Their Possible Relevance to Cancer Treatment." Cancer Research. **34**: 3117-3123, 1974.

38. Hahn, G. M. "Mammalian Cell Survival Responses After Exposure to Elevated Temperatures." *Hyperthermia and Cancer.* 1982 Plenum Press. New York.

39. Hahn, G. M. "Technical Aspects of Hyperthermia." *Hyperthermia and Cancer.* 1982 Plenum Press. New York.

40. Hahn, G. M. and Shiu, E. C. "Effect of pH and Elevated Temperature on the Cytotoxicity of Some Chemotherapeutic Agents on Chinese Hamster Cells In-Vitro." Cancer Research. **43**: 5789-5791, 1983.

41. Hall, E. J. "Hyperthermia: An Overview." *Third International Symposium: Cancer Therapy by Hyperthermia, Drugs and Radiation.* Dethlefsen, L. A. ed. 1982 NCI. Bethesda.

42. Harisiadis, L., Hall, E. J., Kraljevic, U. and Borek, C. "Hyperthermia: Biological Studies at the Cellular Level." Radiology. **117**: 447-452, 1975.

43. Hladky, S. B., Haydon, D. A. and Myers, V. B. "Ion Transfer Across Lipid Membranes in the Presence of Gramicidin A. " Biochim. Biophys. Acta. **274**: 294-322, 1972.

44. Hofer, K. G., Brizzard, B. and Hofer, M. G. "The Effects of Lysosome Modification on the Heat Potentiation of Radiation Damage and Direct Heat Death of BP-8 Sarcoma Cells." Eur. J. Cancer. **15**: 1449-1457, 1979.

45. Hume, S. P., Rogers, M. A. and Field, S. B. "Heat-induced Thermal Resistance and Its Relationship to Lysosomal Response." Int. J. Radiat. Biol. **34**: 503, 1978.

46. Jahde, E. and Rajewsky, M. F. "Sensitization of Clonogenic Malignant Cells to Hyperthermia by Glucose-Mediated, Tumor-selective pH Reduction." J. Cancer Res. Clin. Oncology. **104**: 23-30, 1982.

47. Janata, J. "Do Optical Sensors Really Measure pH." Anal. Chem. **59**: 1351-1356, 1987.

48. Janata, J. and Bezegh, A. "Chemical Sensors." Anal. Chem. **60**: 62R-74R, 1988.

49. Kang, M. S., Song, C. W. and Levitt, S. H. "Role of Vascular Function in Response of Tumors In-Vivo to Hyperthermia." Cancer Research. **40**: 1130-1135, 1980.

50. Kim, S. H., Kim, J. H. and Hahn, E. W. "Enhanced Killing of Hypoxic Tumor Cells by Hyperthermia." Br. J. Radiol. **48**: 872-874, 1975.

51. Kim, S. H., Kim, J. H. and Hahn, E. W. "Selective Potentiation of Hyperthermia Killing of Hypoxic Cells by 5-thio-D-Glucose." Cancer Res. **38**: 2935-2938, 1978.

52. Klein, E., Autian, J., Bower, J. D., Buffaloe, G., Centella, L. J., Colton, C. K., Darby, T. D., Farrell, P. C., Holland, F. F., Kennedy, R. S., Lipps, B., Mason, R., Nolph, K. D., Villarroel, F., Wathen, R. L. and . "Evaluation of Hemodialyzers and Dialysis Membranes." Artifical Organs. **1**(2): 59-77, 1977.

53. Kolthoff, I. M. and Lingane, J. J. *Polarography*. 1952 Interscience Publishers. New York.

54. Kurtz, I. and Balaban, R. S. "Fluorescence Emission Spectroscopy of 1,4-Dihydroxyphthalonitrile: A Method for Determining Intracellular pH in Cultured Cells." Biophys. J. **48**: 499-508, 1985.

55. Lehmann, J. F. *Therapeutic Heat and Cold.* 1982 Williams &Wilkins. Baltimore.

56. LeVeen, H. H., Wapnick, S. and Piccone, V. "Tumor Erradication by Radiofrequency Therapy. Response in 21 Patients." JAMA. **235**: 2198-2200, 1976.

57. Li, G. C. and Hahn, G. M. "Ethanol-induced Tolerance to Heat and to Adriamycin." Nature. **274**: 699-701, 1978.

58. Magin, R. L. and Weinstein, J. "The Design and Characterization of Temperature-Sensitive Liposomes." *Liposome Technology*. Gregoriadis, G. ed. 1984 CRC Press. Boca Raton.

59. Mondovi, B., Strom, R. and Rotilio, G. "The Biochemical Mechanism of Selective Heat Sensitivity of Cancer Cells. I. Studies on Cellular Respiration." Eur J. Cancer. **5**: 129-136, 1969.

60. Morrison, R. T. and Boyd, R. N. *Organic Chemistry*. 1973 Allyn and Bacon, Inc. Boston.

61. Munkholm, C., Walt, D. R., Milanovich, F. P. and Klainer, S. M. "Polymer Modification of Fiber Optic Chemical Sensors as a Method of Enhancing Fluorescence Signal for pH Measurement." Anal. Chem. **58**: 1427-1430, 1986.

62. Musgrove, E., Rugg, C. and Hedley, D. "Flow Cytometric Measurement of Cytoplasmic pH: A Critical Evaluation of Available Fluorochromes." Cytometry. **7**: 347-355, 1986.

63. Narayanaswamy, R. "Optical Fibre Sensors in Chemical Analysis." Analytical Proceedings. **22**: 204-206, 1985.

64. Offenbacher, H., Wolfbeis, O. S. and Furlinger, E. "Fluorescence Optical Sensors for Continuous Determination of Near-Neutral pH Values." Sensors and Actuators. **9**: 73-84, 1986.

65. Overgaard, J. "Effect of Hyperthermia on Cytochrome C Oxidase Activity in Tumor Cells." IRCS Med. Sci. Biochem. Cancer. **3**: 225, 1975.

66. Overgaard, J. "Ultrastructure of a Murine Mammary Carcinoma Exposed to Hyperthermia In-Vivo." Cancer Research. **36**: 983-995, 1976.

67. Overgaard, J. "Effects of Hyperthermia on Malignant Cells In-Vivo: A Review and Hypothesis." Cancer. **39**: 2637, 1977.

68. Overgaard, K. and Overgaard, J. "Inverstigations on the Possibility for a Thermic Tumor Therapy." Eur. J. Cancer. **8**: 65, 1972.

69. Overgaard, K. and Overgaard, J. "Investigations on the Possibility of a Thermic Tumour Therapy: II. Action of Combined Heat-Roetgen Treatment on a Transplanted Mouse Mammary Carcinoma." Eur. J. Cancer. **8**: 573, 1972.

70. Paliwal, B. R. *Basic Physics Parameters and Instrumentation of Hyperthermia. A Categorical Course in Radiation Therapy*. 57-70, 1987.

71. Parke, T. V. and Davis, W. W. "Use of Apparent Dissociation Constants in Qualitative Organic Analysis." Anal. Chem. **26**(4): 642-645, 1954.

72. Pease, J. S. and Wang, J. C. "Gated Photon Counting Can Improve Optical Measurements." Laser Focus/Electro-Optics. **24**(2): 102-105, 1988.

73. Peterson, J. I., Goldstein, S. R., Fitzgerald, R. V. and Buckhold, D. W. "Fiber-Optic pH Probe for Physiological Use." Anal. Chem. **52**: 864-869, 1980.

74. Peterson, J. I. and Sullivan, J. V. "Method of Making Small-Diameter Tubing from Porous Film." Rev. Sci. Instrum. **54**(12): 1792, 1983.

75. Prosser, C. L. "Inorganic Ions." *Comparative Animal Physiology*. Prosser, C. L. ed. 1973 Saunders College Publishing. Philadelphia.

76. Roti-Roti, J. L. and Winward, R. T. "The Effects of Hyperthermia on the Protein-to-DNA Ratio of Isolated HeLa Cell Chromatin." Radiat. Res. **74**: 159-169, 1978.

77. Saari, L. and Seitz, W. R. "pH Sensor Based on Immobilized Fluoresceinamine." Anal. Chem. **54**: 821-823, 1982.

78. Sapareto, S. A. "The Biology Of Hyperthermia In-Vitro." *Physical Aspects of Hyperthermia*. Nussbaum, G. H. ed. 1982 American Institute of Physics. New York.

79. Scheggi, A. M. and Baldini, F. "pH Sensing by Fibre Optics." Optica Acta. **33**: 1587-1597, 1986.

80. Scott, J. "Lock-Ins Handle Ratioed Optics Measurements." Laser Focus/Electro-Optics. **24**(6): 104-112, 1988.

81. Shimonaka, H. and Noazawa, Y. "Subcellular Distribution and Thermally Induced Transition of Adenylate Cyclase Activity in Thermotolerant Tetrahymena Surface Membranes." Cell Struct. Funct. **2**: 81-89, 1977.

82. Song, C. W. "Physiological Factors in Hyperthermia." *Third International Symposium: Cancer Therapy By Hyperthermia, Drugs, and Radiation.* Dethlefsen, L. A. ed. 1982 NCI. Bethesda.

83. Song, C. W. "Physiological Factors in Hyperthermia of Tumors." *Physical Aspects of Hyperthermia.* Nussbaum, G. H. ed. 1982 American Institute of Physics. New York.

84. Song, C. W., Clement, S. S. and Levitt, S. H. "Cytoxic and Radiosensitizing Effects of 5-thio-D- Glucose on Hypoxic Cells." Radiology. **123**: 201-205, 1977.

85. Song, C. W., Kang, M. S., Rhee, J. G. and Levitt, S. H. "The Effect of Hyperthermia on Vascular Function, pH, and Cell Survival." Radiology. **137**: 795-803, 1980.

86. Song, C. W., Lokshina, A., Rhee, J. G., Patten, M. and Levitt, S. H. "Implication of Blood Flow in Hyperthermic Treatment of Tumors." IEEE Transactions on Biomedical Engineering. **31**(1): 9-16, 1984.

87. Steffer, C. "Aspects of Biochemical Hyperthermia." *Third International Symposium: Cancer Therapy by Hyperthermia, Drugs, and Radiation.* Dethlefsen, L. A. ed. 1982 NCI. Bethesda.

88. Strom, R., Crifo, C., Rossi-Fanelli, A. and Mondovi, B. "Biochemical Aspects of Heat Sensitivity of Tumor Cells." *Selective Heat Sensitivity of Cancer Cells.* 1977 Springer-Verlag. New York.

89. Suit, H. D. "Hyperthermia in the Treatment of Tumors." *First International Symposium on Cancer Therapy By Hyperthermia and Radiation.* 1976 American College of Radiology. Chicago.

90. Suit, H. D. "Hyperthermia Effects on Animal Tissues." Radiology. **123**: 483-487, 1977.

91. Suit, H. D. and Shwayder, M. "Hyperthermia: Potential as an Anti-Tumor Agent." Cancer. **34**: 122-129, 1974.

92. Thistlethwaite, A. J., Leeper, D. B., Moylan, D. J. and Nerlinger, R. E. "pH Distrubtion in Human Tumors." Int. J. Radiation Oncology Biol. Phys. **11**: 1647-1652, 1985.

93. Tomasovic, S. P., Turner, G. N. and Dewey, W. C. "Effects of Hyperthermia on Non-histone Protiens Isolated with DNA." Radiat. Res. **73**: 535-552, 1978.

94. Valet, G., Raffael, A., Moroder, L., Wunsch, E. and Ruhenstroth-Bauer, G. "Fast Intracellular pH Determination in Single Cells by Flow-Cytometry." Naturwissenschaften. **68**: 265-266, 1981.

95. Von Ardenne, M. M., Bohme, G. and Kell, E. "On the Optimization of Local Hyperthermy in Tumors Based on a New Radio Frequency Procedure." Cancer Res. Clin. Oncol. **94**: 163-184, 1979.

96. Weast, R. C. *CRC Handbook of Chemistry and Physics*. 1968 The Chemical Rubber Company. Cleveland.

97. Westcott, C. C. *pH Measurements*. 1978 Academic Press, Inc. Orlando.

98. White, T. G. *Design and Noise Analysis of an Operational Amplifier-Photodiode Pair for Use in Fiber Optic Sensors*. M.S. thesis, Department of Electrical and Computer Engineering, University of Illinois at Urbana-Champaign, 1987.

99. Wickershiem, K. J. "Recent Advances in Optical Temperature Measurements." Ind Res Dev. **21**: 82-89, 1979.

100. Willard, H. H., Merritt, L. L. and Dean, J. A. *Instrumental Methods of Analysis*. 1974 D. Van Nostrand Company. New York.

101. Wright, J. C. "You Can Find Treasure Hidden in the Trash." R & D. **29**(2): 140-143, 1987.

102. Yatvin, M. B. "The Influence of Membrane Lipid Composition and Procaine on Hyperthermic Death of Mice Cells." Int. J. Radiat. Biol. **32**: 513-521, 1977.

103. Zhujun, Z. and Seitz, R. "A Fluorescence Sensor for Quantifying pH in the Range form 6.5-8.5." Analytica Chimica Acta. **160**: 47-55, 1984.

VITA

John F. McCarthy was born in Brockton, Massachusetts on April 25,1952. He received his B.A. degree with a joint concentration in Physics and Chemistry from Boston University in 1976. He then attended the University of Connecticut where he graduated with an M.S. in Electrical Engineering in 1978. From 1978 to 1979 he worked as a development engineer in the field of audiometric instrumentation for Grason-Stadler, Inc., in Littleton, Ma. Since coming to the University of Illinois in 1979, he has held teaching and research assistantships in many different departments. While at Illinois, he has also acted as a technical consultant on a wide variety of projects. Mr. McCarthy is currently enrolled as a Medical Scholar at the University of Illinois and is working on his M.D. degree in the College of Medicine at Urbana-Champaign.